UNIVERSITY OF CALIFORNIA

Los Angeles

The ecological impacts of leaf drought tolerance

A dissertation submitted in partial satisfaction of

the requirements for the degree Doctor of

Philosophy in Biology

by

Megan Kathleen Bartlett

2016

ABSTRACT OF THE DISSERTATION

The ecological impacts of leaf drought tolerance

by

Megan Kathleen Bartlett

Doctor of Philosophy in Biology

University of California, Los Angeles, 2016

Professor Lawren Sack, Chair

Climate change is expected to exacerbate drought for many plants, making drought tolerance a key driver of species and ecosystem responses. However, predicting responses from traits requires greater understanding of how physiological processes impact ecology. I developed new theory and methods and applied meta-analyses to characterize the ecological impacts of leaf drought tolerance. I compared the predictive ability of several traits for ecological drought tolerance and showed that the leaf water potential at turgor loss point, or wilting (π_{tlp}), was the strongest predictor of species' habitat water supply. I then showed that the main driver of π_{tlp} was the osmotic potential at full hydration (π_o), or the solute concentration of a hydrated cell. Thus, plants achieve greater leaf drought tolerance by accumulating solutes in the leaf cells. I then developed a new method to rapidly estimate π_{tlp} from measurements of π_o. This method is 30x

faster than the standard, making it feasible to characterize drought tolerance for many species within diverse clades and communities. Plasticity - the ability of individual plants to change trait values - is expected to strongly influence species' responses to climate change. I meta-analyzed plasticity in π_{tlp} and showed that, while most species became more drought tolerant under dry conditions, π_{tlp} from wet or dry conditions and not plasticity predicted species distributions. Thus, π_{tlp} measured in one season can reliably characterize most species' ecological drought tolerances. Drought tolerance traits are also expected to impact species distributions within ecosystems through effects on habitat associations and competition. I showed that π_{tlp} was a strong driver of habitat associations in a tropical community, and that drought tolerant species were significantly spatially clustered, suggesting drought tolerant species exclude sensitive species through hierarchical competition. Finally, plant drought tolerance is determined by multiple traits. I applied meta-analyses to evaluate general patterns in the relationships among hydraulic, stomatal, and wilting traits, and produce a framework for predicting plant responses to a wide range of water stress from one or two sampled traits. Overall, these findings provide insight into the impacts of leaf drought tolerance on plant ecology at community and global scales.

The dissertation of Megan Kathleen Bartlett is approved.

Philip Rundel

Priyanga Amarasekare

H. Jochen Schenk

Stephen Hubbell

Lawren Sack, Committee Chair

University of California, Los Angeles

2016

TABLE OF CONTENTS

LIST OF TABLES

LIST OF SUPPLEMENTARY TABLES

LIST OF FIGURES

CHAPTER 2

CHAPTER 3

CHAPTER 4

CHAPTER 5

LIST OF SUPPLEMENTARY FIGURES

ACKNOWLEGEMENTS

I am grateful to so many people who made it possible for me to be where I am today.

First and foremost, I want to thank my advisor, Lawren Sack. You've taught me everything I know about being a scientist, from the big (everything in the next 350 pages!) to the small (every project really does need a good acronym). You have created so many opportunities for me in the last six years, and made it possible for me to be a part of so much incredible science. Thank you for your countless hours of support, mentorship, and guidance. I am forever grateful to have been your student.

I would also like to thank my collaborators, from whom I have learned so much. From our work at the Xishuangbanna Tropical Botanical Garden, I am grateful to Dr. Kunfang Cao for our enriching collaboration and for hosting me as a visiting student, and to Ya Zhang, Shanwen Sun, Rico Ardy, and Nissa Kreidler for working 8am to midnight day after day in the lab with me for our data (and special thanks to Nissa and Zhangya for invaluable help in the field). From Project WILT, thank you to Jerome Chave, Isabelle Maréchaux, Philippe Gaucher, and Emilie Joetzjer for a truly awesome collaboration.

I'm also very grateful to my committee members Phil Rundel, Steve Hubbell, Jochen Schenk, and Priyanga Amarasekare for their feedback and encouragement. EEB has been an amazing place to be a grad student, and I feel so lucky to have received so much support and genuine interest in my growth as a scientist. Also, thank you to Jocelyn Yamadera for your help navigating grad school. You are the patron saint of EEB!

Before grad school, many people helped me discover research as a career. I want to thank Craig Gates for putting me on the path to becoming a scientist. To Missy Holbrook, thank you for introducing me to plant physiology. Thanks also to Cam Webb for creating the Biodiversity

of Borneo field course- it is still amazing to me that a career in tropical ecology isn't too good to be true.

There are no words for how lucky I have been to have such fantastic labmates. Thank you for years of inspiration, support, cake, and smash-it. To Christine, thank you for always having the best animal videos, and for knowing where everything is. Grace, I'm so grateful that you're here with me and I'm here with you. Marissa, thank you for being a ray of sunshine. Leila, thank you for catching the bugs and taking them outside. Camila, thank you for sharing your charisma, uniqueness, nerve, and talent. Christian, thank you for making sure there's still some Florida in the lab. And thank you to the rest of my wonderful friends inside and outside of EEB, who made grad school a joy.

I'm also so grateful for my mom and my sister. Mom, thank you for always encouraging me- from letting me keep my onions in the dark in the laundry room (that paper is coming out any day now) to driving hours to pick up phosphate waste for my science fair project to reading my press releases now. And thanks for always reminding me how amazing plants are- there's nothing like opening "Flora of the Silk Road" after a long day to make plants magical again.

And finally, thank you to Scott, for always supporting and encouraging me, and sharing years, adventures, and tacos.

Co-authored work: **Chapter 2** is from Bartlett, M. K., Scoffoni, C. & Sack, L. (2012). The determinants of leaf turgor loss point and prediction of drought tolerance of species and biomes: a global meta-analysis. *Ecology Letters,* 15, 393-405. C. Scoffoni contributed data and to writing the manuscript, L. Sack mentored at all stages of the project. **Chapter 3** is from Bartlett, M. K., Scoffoni, C., Ardy, R., Zhang, Y., Sun, S-w., Cao, K-f. & Sack, L. (2012). Rapid determination

of comparative drought tolerance traits: using an osmometer to predict turgor loss point. *Methods in Ecology and Evolution,* 3, 880-888. C. Scoffoni, R. Ardy, Y. Zhang, S-w. Sun, and K-f. Cao helped with data collection and provided feedback on the manuscript, L. Sack mentored at all stages of the project. **Chapter 4** is from Bartlett, M. K., Zhang, Y., Kreidler, N., Sun, S-w., Ardy, R., Cao, K-f. & Sack, L. (2014). Global analysis of plasticity in turgor loss point, a key drought tolerance trait. *Ecology Letters,* 17, 1580-1590. Y. Zhang, N. Kreidler, S-w. Sun, R. Ardy, and K-f. Cao helped collect data and provided feedback on the manuscript, L. Sack mentored at all stages of the project. **Chapter 5** is from Bartlett, M. K., Zhang, Y., Kreidler, N., Sun, S-w., Lin, L., Hu, Y-h., Cao, K-f. & Sack, L. (2016). Drought tolerance as a driver of tropical forest assembly: resolving spatial signatures for multiple processes. *Ecology,* 97(2), 503-514. Y. Zhang, N. Kreidler, S-w. Sun, L. Lin, Y-h. Hu and K-f. Cao contributed data and provided feedback on the manuscript, L. Sack mentored at all stages of the project. **Chapter 6** is from Bartlett, M. K., Klein, T., Jansen, S., Choat, B. & Sack, L. (*in review*) Resolving the temporal sequence and correlations of plant drought responses: coordination among stomatal, hydraulic, and wilting traits. T. Klein, S. Jansen, and B. Choat contributed data, helped design analyses, and provided feedback on the manuscript, L. Sack mentored at all stages of the project.

Funding: This work was generously supported by Vavra Fellowships and research grants, the UCLA Pauley Fellowship, the UCLA Regent's Stipend, the UCLA Dissertation Year Fellowship, the Charles E. and Sue K. Young student award, the Center for Tropical Forest Science- Forest Global Earth Observatory of the Smithsonian Institution, the National Science Foundation (#1108534, #DGE-0707424, #10-591, #IOS-0546784 (to L. Sack), and #DEB-1046113 (to S. J. Davies)), and the National Key Basic Research Program of China (#2014CB954100).

BIOGRAPHICAL SKETCH

PROFESSIONAL PREPARATION

2009 B.A. in Organismic and Evolutionary Biology (Harvard University)

PUBLICATIONS

Published work

Anderegg, W. R. L., Klein, T., **Bartlett, M. K.,** Sack, L., Pellegrini, A. F. A., Choat, B. & Jansen, S. 2016. Meta-analysis reveals that hydraulic traits explain cross-species patterns of drought-induced tree mortality across the globe. Proceedings of the National Academy of Sciences, *in press.*

Maréchaux, I., **Bartlett, M. K.**, Gaucher, P., Sack, L. & Chave, J. 2016. Causes of variation in leaf-level drought tolerance within an Amazonian forest. Journal of Plant Hydraulics, 3.

Chu, C-j., **Bartlett, M. K.**, Wang, Y., He, F-l., Weiner, J., Chave, J. & Sack, L. 2016. Does climate directly influence NPP globally? Global Change Biology, 22(1), 12-24.

Bartlett, M. K., Zhang, Y., Yang, J., Kreidler, N., Sun, S-w., Lin, L., Hu, Y-H., Cao, K-F. & Sack, L. 2016. Drought tolerance as a driver of tropical forest assembly: resolving spatial signatures for multiple processes. Ecology, 97(2), 503-514.

Maréchaux, I., **Bartlett, M. K.**, Sack, L., Baraloto, C., Engel, J., Joetzjer, E. & Chave, J. 2015. Drought tolerance as predicted by leaf water potential at turgor loss point varies strongly across species within an Amazonian forest. Functional Ecology, 29, 1268-1277.

Bartlett, M. K., Zhang, Y., Kreidler, N., Sun, S-w., Cao, K-F. & Sack, L. 2014. Global meta-analysis of plasticity in turgor loss point, a key drought tolerance trait. Ecology Letters, 17(12), 1580-1590.

Bartlett, M. K., Scoffoni, C., Ardy, R., Zhang, Y. Sun, S-w., Cao, K-F. & Sack, L. 2012. Rapid determination of comparative drought tolerance traits: using an osmometer to predict turgor loss point. Methods in Ecology and Evolution, 3(5), 880-888.

Bartlett, M. K., Scoffoni, C. & Sack, L. 2012. The determinants of leaf turgor loss point and prediction of drought tolerance of species and biomes: a global meta-analysis. Ecology Letters, 15(5), 393-405.

Wicklein, H. F., Ollinger, S. V., Martin, M. E., Hollinger, D. Y., Lepine, L. C., Day, M. C., **Bartlett, M. K.**, Richardson, A. D. & Norby, R. J. 2012. Variation in foliar nitrogen and albedo in response to nitrogen fertilization and elevated CO_2. Oecologia, 169(4), 915-925.

Bartlett, M. K., Ollinger, S. V., Hollinger, D. Y., Wicklein, H. F. & Richardson, A. D. 2011. Canopy-scale relationships between foliar nitrogen and albedo are not observed in leaf reflectance and transmittance within temperate deciduous tree species. Botany, 89(7), 491-497.

Papers in review or in revision

Bartlett, M. K., Klein, T., Jansen, S., Choat, B. & Sack, L. Resolving the temporal sequence and correlations of plant drought responses: coordination among stomatal, hydraulic, and wilting traits. Proceedings of the National Academy of Sciences, *in review.*

Scoffoni, C., Albuquerque, C., Brodersen, C. R., Townes, S. V., John, G., **Bartlett, M. K.,** Buckley, T. N., McElrone, A. J. & Sack, L. Outside-xylem pathways, not xylem

embolism, drive leaf hydraulic decline with dehydration. Nature Communications, *in review.*

Méndez-Alonzo, R., López-Portillo, J., Moctezuma, C., **Bartlett, M. K.** & Sack, L. Osmotic and hydraulic adjustment of mangrove saplings to extreme salinity. Tree Physiology, *submitted.*

Méndez-Alonzo, R., Ewers, F., Jacobsen, A., Pratt, B., Scoffoni, C., **Bartlett, M. K.** & Sack, L. How do functional traits combine across ecosystems? Phenotypic integration of structure and physiology of leaves and stems of 17 shrub species of Southern California. Journal of Ecology, *submitted.*

SYNERGISTIC ACTIVITIES

- Member of the National Institute for Mathematical and Biological Synthesis (NIMBioS) working group "A mechanistic dynamic energy budget model of tree performance to predict functional trait drivers, species distributions, and responses to global change," led by Sabrina Russo and Glen Ledder (2014-2016)
- Conference presentations at the Association for Tropical Biology and Conservation (2015), Ecological Society of America (2012, 2014, 2015), Southern California Academy of Sciences (2011-12), and UCLA's Ecolunch (2011) and EcoEvoPub (2015) series
- Dissemination of research articles as press releases written for a popular science audience
- Reviewer of 11 papers for: Ecology (1), Functional Ecology (4), American Journal of Botany (1), Conservation Physiology (1), Tree Physiology (4)
- Graduate student liaison for the department plant evolutionary biologist search committee (January – April 2016)
- Member of the Ecological Society of America and the Association for Tropical Biology and Conservation

CHAPTER 1

PREMISE OF THE DISSERTATION

Many plant species are expected to face increasing drought under climate change (Sheffield & Wood 2008), making drought tolerance integral to predicting climate change impacts on species and ecosystems (McDowell et al. 2013). Plant drought tolerance is generally quantified as the water potentials that induce declines in key physiological functions, such as stomatal conductance (Brodribb et al. 2003), leaf, stem, and root hydraulic conductivity (Alder et al. 1996, Maherali et al. 2004, Brodribb & Holbrook 2004, Scoffoni et al. 2011), and leaf cell turgor (Cheung et al. 1975). Applying biophysical principles to mechanistically scale up from these organ-level traits has been increasingly recognized as an especially powerful approach to predicting water uptake and gas exchange at the whole-plant and ecosystem levels (Powell et al. 2013, Rowland et al. 2015, Sperry & Love 2015). Indeed, soil-plant-atmosphere models, which explicitly simulate stomatal conductance and hydraulic conductivity from environmental water supply, have been shown to reasonably approximate observed transpiration (Fisher et al. 2007) and mortality rates (McDowell et al. 2013), and even to outperform less physiologically realistic models (Bonan et al. 2014).

However, despite these advances at the plant level, scaling from drought tolerance traits to ecosystem responses has been limited by several fundamental knowledge gaps. My PhD thesis seeks to address these gaps by characterizing the ecological impacts of leaf drought tolerance.

First, at the beginning of my PhD work, relatively few drought tolerance traits had been assessed as predictors of species distributions relative to environmental water supply (Maherali et al. 2004), which had fueled decades of controversy in the ecophysiology literature over which traits most strongly determine ecological drought tolerance, or the ability to persist in drier

habitats (e.g., Sinclair & Ludlow 1985, Kramer 1988). I developed new equations expressing the leaf drought tolerance traits the turgor loss point (π_{tlp}), or the leaf water potential that induces wilting, and the relative water content in the cells at turgor loss point (RWC_{tlp}), as a function of cellular anatomy and chemical composition traits. I compared the predictive ability of these drought tolerance traits for species distributions relative to ecosystem water supply, and then applied these equations to a trait dataset compiled from the literature to determine the cellular drivers of variation in π_{tlp} and $RWC_{tlp,}$ both across species and within species in response to environmental variation.

Identifying the cellular chemical composition trait osmotic potential at full hydration (π_o), or the solute concentration of a hydrated leaf cell, as the strongest driver of π_{tlp} allowed me to then develop a rapid method for measuring π_{tlp} by calibrating π_{tlp} values with measurements from an established rapid method for $\pi_{o.}$ This method, presented in Chapter 3, made the assessment of π_{tlp} across diverse species 30-fold faster than the standard pressure-volume curve method. This reduction in effort makes feasible sampling across diverse clades and communities.

Plasticity, or the ability of individual plants to change trait values, is expected to strongly affect species responses to climate change by widening their range of tolerable climatic conditions (Dormann 2007; Nicotra et al. 2010; Anderegg 2015), but the ecological impacts of plasticity in drought tolerance traits have rarely been studied. To address this gap, in Chapter 4, I compared the importance of π_{tlp} and intraspecific plasticity in π_{tlp} ($\Delta\pi_{tlp}$) to species distributions relative to water supply worldwide. I compiled wet and dry season values for π_{tlp} from the literature, and compared the ability of wet season π_{tlp} and seasonal plasticity ($\Delta\pi_{tlp}$) to predict both π_{tlp} under water-stressed conditions and species distributions across global variation in water supply.

Chapters 2 and 4 established π_{tlp} as a significant driver of species distributions at a global scale. However, the effect of drought tolerance traits on species' distributions within ecosystems is a complex, unresolved question. Drought tolerance traits are expected to impact species' habitat associations and competitive interactions (Becker 1998; Rodríguez-Iturbe et al. 1999), but these effects have not been quantified, or compared with the impact of other leaf nutrient and structural traits that have been demonstrated to affect species distributions within communities (Kraft et al. 2008). In Chapter 5, I quantified the impact of leaf drought tolerance on species' spatial distributions within a community, and inferred the effect of π_{tlp} on community assembly from hypothesized relationships between spatial patterns in trait variation and key community assembly processes. I applied the rapid method I developed in Chapter 3 to measure π_{tlp} and leaf nutrient and structural investment traits for 43 species in the Xishuangbanna Tropical Botanical Garden (XTBG) research plot, a seasonally dry tropical forest in Yunnan, China. I then compared the ability of π_{tlp} and the other commonly measured leaf functional traits to predict species distributions across topographic variation within the forest, as well as the ability of species differences in these traits to predict spatial clustering among heterospecific neighbors, in order to assess the relative importance of these traits to habitat association and competition processes.

The weak impact of these traits on spatial associations between species suggested that quantifying the impact of traits on competitive interactions could require moving beyond individual traits to integrate the effects of multiple traits on plant performance and resource demand. While previous studies have compared values and tested correlations for some drought tolerance traits across small species sets (Brodribb et al. 2003; Hao et al. 2010; Johnson et al. 2011; Guyot et al. 2012; Bucci et al. 2013), the covariance among drought tolerance traits has

not been tested for general patterns across plant diversity. In Chapter 6, I compiled published data for the water potential thresholds inducing stomatal closure, π_{tlp}, declines in hydraulic conductivity in the leaves, stems, and roots, and plant mortality. I used the sequence of these traits to address several key controversies in the literature concerning the relative drought tolerance of hydraulic, stomatal, and turgor responses. The correlations across species to provided a framework for predicting plant responses to a wide range of water stress from one or two sampled traits, increasing the ability to rapidly characterize drought tolerance across diverse species.

REFERENCES

Alder, N. N., Sperry, J. S. & Pockman, W. T. (1996). Root and stem xylem embolism, stomatal conductance, and leaf turgor in *Acer grandidentatum* populations along a soil moisture gradient. *Oecologia*, 105, 293-301.

Anderegg, W. R. L. (2014). Spatial and temporal variation in plant hydraulic traits and their relevance for climate change impacts on vegetation. *New Phytol.,* 205, 1008-1014.

Becker, P., Rabenold, P. E., Idol, J. R. & Smith, A. P. (1988). Water potential gradients for gaps and slopes in a Panamanian tropical moist forest's dry season. *J. Trop. Ecol.,* 4, 173-184.

Bonan, G. B., Williams, M., Fisher, R. A. & Oleson, K. W. (2014). Modeling stomatal conductance in the earth system: linking leaf water-use efficiency and water transport along the soil–plant–atmosphere continuum. *Geosci. Model Dev.,* 7, 2193-2222.

Brodribb, T. J., Holbrook, N. M., Edwards, E. J. & Gutiérrez, M. V. (2003). Relations between stomatal closure, leaf turgor and xylem vulnerability in eight tropical dry forest trees. *Plant Cell Environ*., 26, 443-450.

Brodribb, T.J. & Holbrook, N. M. (2004). Stomatal protection against hydraulic failure: a comparison of coexisting ferns and angiosperms. *New Phytol.*, 162, 663-670.

Bucci, S.J., *et al.* (2013). The stem xylem of Patagonian shrubs operates far from the point of catastrophic dysfunction and is additionally protected from drought-induced embolism by leaves and roots. *Plant Cell Environ.,* 36(12), 2163-2174

Cheung, Y. N. S., Tyree, M. T. & Dainty, J. (1975). Water relations parameters on single leaves obtained in a pressure bomb and some ecological interpretations. *Can. J. Bot.*, 53, 1342-1346.

Dormann, C.F. (2007). Promising the future? Global change projections of species distributions.

Basic Appl. Ecol., 8, 387–397.

Fisher, R. A., *et al.* (2007). The response of an Eastern Amazonian rain forest to drought stress: results and modelling analyses from a throughfall exclusion experiment. *Global Change Biol.,* 13, 2361-2378.

Guyot, G., Scoffoni, C. & Sack, L. (2012). Combined impacts of irradiance and dehydration on leaf hydraulic conductance: insights into vulnerability and stomatal control. *Plant Cell Environ*, 35(5), 857-871.

Hao, G. Y., *et al.* (2010). Differentiation of leaf water flux and drought tolerance traits in hemiepiphytic and non-hemiepiphytic Ficus tree species. *Func. Ecol.,* 24, 731-740.

Johnson, D. M., McCulloh, K.A., Meinzer, F. C., Woodruff D. R. & Eissenstat, D. M. (2011). Hydraulic patterns and safety margins, from stem to stomata, in three eastern U.S. tree species. *Tree Physiol*., 31(6), 659-668.

Kraft, N. J. B., Valencia, R. & Ackerly, D. A. (2008). Functional traits and niche-based tree community assembly in an Amazonian forest. *Science,* 322, 580 – 582.

Kramer, P. J. (1988). Changing concepts regarding plant water relations. *Plant Cell Environ.,* 11, 565-568.

Maherali, H., Pockman, W. T. & Jackson, R. B. (2004). Adaptive variation in the vulnerability of woody plants to xylem cavitation. *Ecology*, 85, 2184-2199.

McDowell, N. G., *et al.* (2013). Evaluating theories of drought-induced vegetation mortality using a multimodel–experiment framework. *New Phytol*., 200, 304-321.

Nicotra, A.B., Atkin, O.K., Bonser, S.P., Davidson, A.M., Finnegan, E.J., Mathesius, U. et al. (2010). Plant phenotypic plasticity in a changing climate. *Trends Plant Sci.,* 15, 684–692.

Powell, T. L. *et al.* (2013). Confronting model predictions of carbon fluxes with measurements

of Amazon forests subjected to experimental drought. *New Phytol.*, 200, 350-365.

Rodriguez-Iturbe, I., D'Odorico, P., Porporato, A. & Ridolfi, L. (1999). Tree-grass coexistence in savannas: the role of spatial dynamics and climate fluctuations. *Geophys Res Lets*., 26, 247-250.

Rowland, L. *et al.* (2015). Modelling climate change responses in tropical forests: similar productivity estimates across five models, but different mechanisms and responses. *Geosci. Model Dev.,*8, 1097-1110.

Scoffoni, C., Rawls, M., McKown, A., Cochard, H. & Sack, L. (2011). Decline of leaf hydraulic conductance with dehydration: relationship to leaf size and venation architecture. *Plant Physiol.,* 156, 832-843.

Sheffield, J. & Wood, E.F. (2008). Global trends and variability in soil moisture and drought characteristics, 1950–2000, from observation-driven simulations of the terrestrial hydrologic cycle. *J. Clim.,* 21, 432–458.

Sinclair, T. R. & Ludlow, M. M. (1985). Who taught plants thermodynamics? The unfulfilled potential of plant water potential. *Aust. J. Plant Physiol.,* 12, 213-217.

Sperry, J. S. & Love, D. M. (2015). What plant hydraulics can tell us about responses to climate-change droughts. *New Phytol.,* 207, 14-27.

CHAPTER 2

THE DETERMINANTS OF LEAF TURGOR LOSS POINT AND PREDICTION OF DROUGHT TOLERANCE OF SPECIES AND BIOMES: A GLOBAL META-ANALYSIS

ABSTRACT

Increasing drought is one of the most critical challenges facing species and ecosystems worldwide, and improved theory and practices are needed for quantification of species tolerances. Leaf water potential at turgor loss, or wilting (π_{tlp}), is classically recognized as a major physiological determinant of plant water stress response. However, the cellular basis of π_{tlp} and its importance for predicting ecological drought tolerance have been controversial. A meta-analysis of 317 species from 72 studies showed that π_{tlp} was strongly correlated with water availability within and across biomes, indicating power for anticipating drought responses. We derived new equations giving both π_{tlp} and relative water content at turgor loss point (RWC_{tlp}) as explicit functions of osmotic potential at full turgor (π_o) and bulk modulus of elasticity (ε). Sensitivity analyses and meta-analyses showed that π_o is the major driver of π_{tlp}. By contrast, ε plays no direct role in driving drought tolerance within or across species, but sclerophylly and elastic adjustments act to maintain RWC_{tlp}, preventing cell dehydration, and additionally protect against nutrient, mechanical, and herbivory stresses independently of drought tolerance. These findings clarify biogeographic trends and the underlying basis of drought tolerance parameters with applications in comparative assessments of species and ecosystems worldwide.

Key words: Biogeography, biomes, climate, plant hydraulics, plant traits

INTRODUCTION

Climate change is predicted to increase the incidence and severity of droughts in ecosystems worldwide (Sheffield & Wood 2008). Species differences in drought tolerance are integral determinants not only of present distributions but also of future scenarios, including the probability of extinctions (Engelbrecht *et al.* 2007; Bonan 2008; Feeley *et al.* 2011). Predicting the impact of climate change on plant performance and survival is a major challenge facing plant science and ecology (Grierson *et al.* 2011). However, there remain fundamental gaps in our knowledge of which traits can be used to assess ecological drought tolerance. Cell turgor loss is arguably the best recognized classical indicator of plant water stress, having impacts on cellular structural integrity, metabolism and whole-plant performance (Kramer & Boyer 1995; McDowell 2011). Consequently, the leaf water potential at turgor loss, or bulk turgor loss point (π_{tlp}, units MPa) has been used to assess physiological drought tolerance for decades. Despite its potential use for quantifying ecological drought tolerance (Niinemets 2001; Brodribb & Holbrook 2003; Lenz *et al.* 2006; Blackman *et al.* 2010), no study to our knowledge has tested the relationship between π_{tlp} and water supply within or across biomes, or its performance as an indicator of drought tolerance relative to other plant traits. Additionally, significant ambiguities concerning the underlying physiological and anatomical determinants of π_{tlp} are featured prominently in textbooks of physiological and whole plant ecology (e.g., Jones 1992; Larcher 2003; Nobel 2009). We undertook new analyses to clarify this topic and its importance, given the critical need for physiological measures that can be used to assess species' drought tolerances and thus their likely sensitivity to ongoing climate change.

The π_{tlp} is classically measured in assessments of drought tolerance, one of six key bulk leaf parameters relating to cellular composition and structural properties typically calculated

from a plot of leaf water potential (Ψ_{leaf}) against water volume in drying leaves, known as the pressure-volume (p-v) curve (see primer in Fig. 2.1 and Table 2.1). The π_{tlp} is often recognized as the "higher-level" trait that quantifies leaf and plant drought tolerance most directly, because a more negative π_{tlp} extends the range of Ψ_{leaf} at which the leaf remains turgid and maintains function (Sack *et al.* 2003; Lenz *et al.* 2006). Plants with low π_{tlp} tend to maintain stomatal conductance, hydraulic conductance, photosynthetic gas exchange and growth at lower soil water potential (Ψ_{soil}), which is especially important when droughts occur during the growing season (Abrams & Kubiske 1990; Sack *et al.* 2003; Baltzer *et al.* 2008; Mitchell *et al.* 2008; Blackman *et al.* 2010). The π_{tlp} is thus a trait quantifying the ability to "tolerate" drought, rather than to "avoid" drought by ceasing gas exchange and surviving on stored water, shedding leaves, or dying back to below-ground parts or to seeds (e.g., as done by annuals, deep-rooted perennials, or phreatophytes, CAM succulents or drought-dormant species; Chaves *et al.* 2002; Brodribb & Holbrook 2005; Ogburn & Edwards 2010). The π_{tlp} also defines the Ψ_{soil} below which the plant cannot take up sufficient water to recover from wilting. Known as the "permanent wilting point", this was previously thought to correspond to a Ψ_{soil} of -1.5 MPa (Veihmeyer & Hendrickson 1928), but the π_{tlp} is now known to vary across species, and thus may influence ecological distributions with respect to water availability. Some have focused on a second p-v curve parameter as a possible determinant of drought tolerance, the relative water content at π_{tlp} (RWC_{tlp}). The other four parameters, i.e., the apoplastic water fraction (a_f), modulus of elasticity (ε), osmotic potential at full hydration (π_o), and the tissue capacitance (C; see Table 2.1 and Fig. 2.1 for their derivation and significance) have also been correlated with various aspects of drought tolerance (Niinemets 2001; Brodribb & Holbrook 2003; Lenz *et al.* 2006; Baltzer *et al.* 2008). Indeed, numerous studies have evaluated ε, π_o and a_f as functional determinants, or

"drivers" of π_{tlp} within species, as plants adjust π_{tlp} in response to drought, and across species according to habitat water supply (e.g., Joly & Zaerr 1987; Niinemets 2001; Lenz *et al.* 2006).

Decades of research have improved p-v curve analysis and clarified its biological meaning (Höfler 1920; Tyree & Hammel 1972; Richter 1978; Tyree 1981; Abrams & Kubiske 1990; Niinemets 2001; Brodribb & Holbrook 2003; Lenz *et al.* 2006; Baltzer *et al.* 2008). However, in our view the application of π_{tlp} as an ecological drought tolerance trait has been slowed by four inter-related major controversies concerning its mechanistic basis and interpretation that have confused generations of students in physiology and ecology. By "controversy" we mean problems that engendered debate among two or more scientific points of view and that remain unresolved because of a lack of a theoretical framework or information for decision. We developed new theory and meta-analyses to resolve these controversies:

(1) *How are p-v parameters related to water supply within and across biomes?* We need improved means for rapidly assessing species' drought tolerances. The π_{tlp} and other p-v parameters, especially RWC_{tlp}, ε and $\pi_{o,}$ have been alternatively proposed as predictors of physiological drought tolerance, and possibly of realized ecological drought tolerance, though without a global test to our knowledge. Meanwhile, leaf mass per area (LMA) has been proposed as a correlate or predictor of drought tolerance in many species sets, partly because it is associated with ε (e.g., Niinemets 2001; Wright *et al.* 2005; Poorter *et al.* 2009; Markesteijn *et al.* 2011a), but to our knowledge there have been no comparative tests of the correlation of p-v parameters and LMA with water availability within or across biomes.

(2) *What traits underlie π_{tlp} adjustment during drought within species and π_{tlp} differences across species?* The importance of other p-v traits in determining the higher-level trait π_{tlp} within and across species has remained controversial. Plants of given species improve their drought

tolerance by making their π_{tlp} more negative, and this might be done in three possible ways (Fig. 2.2): accumulating solutes (decreasing π_o), reducing symplastic water content by redistributing more water outside of the cell walls (increasing a_f), and/or increasing cell wall flexibility (decreasing ε), known as osmotic, apoplastic and elastic "adjustments", respectively. Osmotic adjustment has been observed in numerous species to enable the maintenance of growth and yield during drought (e.g., Gonzalez *et al.* 1999; Merchant *et al.* 2007) but strong arguments have also been made for the importance of elastic and apoplastic adjustments (Joly & Zaerr 1987; Iraki *et al.* 1989; Chimenti & Hall 1994; Kozlowski & Pallardy 2002; Moore *et al.* 2008), though ε and a_f have been observed to increase (Bowman & Roberts 1985; Joly & Zaerr 1987; Chimenti & Hall 1994; Kozlowski & Pallardy 2002) or decrease (Kubiske & Abrams 1991; Kozlowski & Pallardy 2002) during drought. Because these parameters are typically adjusted simultaneously, their relative importance in influencing π_{tlp} has remained unclear.

An analogous controversy has surrounded the role of π_o, a_f and ε in determining *interspecific* differences in π_{tlp}. A study of compiled data for 51 shrub and tree species reported a 10-fold variation across species in ε but only 4-fold in π_o, and concluded that ε has greater potential to influence π_{tlp} and drought tolerance (Niinemets 2001). In contrast, three studies that examined fewer species found π_o but not ε to predict differences in π_{tlp} (Lenz *et al.* 2006; Baltzer *et al.* 2008; Mitchell *et al.* 2008).

(3) *How exactly are π_{tlp} and/or RWC_{tlp} important in plant water relations?* While most have considered that a more negative π_{tlp} benefits drought tolerance, as described above, a counter-argument has been made that a *less* negative π_{tlp} may be beneficial. According to this view, a *less* negative π_{tlp} enables leaves to quickly lose turgor and close their stomata as Ψ_{leaf} declines and thereby maintain a high RWC_{tlp} (Walter & Stadelmann 1968; Read *et al.* 2006).

Indeed, some have argued that maintaining cell hydration is more important than turgor, as dehydration can induce shrinkage, wall structural damage, and potentially osmotic stress due to very strong ion concentration, all of which could disrupt metabolic processes. Indeed, a total cell relative water content below 75% severely inhibits ATP, RuBP, and protein production (Lawlor & Cornic 2002). The importance of π_{tlp} and RWC_{tlp} as drought tolerance predictors has been frequently debated without resolution (e.g., Sinclair & Ludlow 1985; Kramer 1988; Schulte 1992).

(4) *What are the roles of the modulus of elasticity, sclerophylly and malacophylly in drought tolerance?* The convergent evolution of sclerophyllous plants, with mechanically tough leaves and stiff cell walls, in mediterranean and semi-desert systems was classically interpreted as indicating an importance in drought tolerance, though a number of other conditions may select for tough evergreen leaves, such as low nutrients or evergreen shade (Grubb 1986; Sack 2004; Markesteijn *et al.* 2011b). While sclerophylly can be defined in several ways, such as a high leaf mass per area (LMA) or lignin concentration (Read & Sanson 2003), the feature most closely related to water relations is ε, and several have hypothesized that a high ε contributes critically to species-differences in drought tolerance (Salleo & Nardini 2000; Niinemets 2001; Read *et al.* 2006). The relationship between high ε, $\pi_{tlp,}$ and drought tolerance has been termed "one of the oldest controversies in ecology" (Lamont *et al.* 2002) and has given rise to numerous hypotheses. A first hypothesis is that a high ε causes Ψ_{leaf} to decline rapidly as leaves dehydrate, allowing sustained water uptake from drying soil (Bowman & Roberts 1985). A second hypothesis considers high ε to actually *lower* π_{tlp}, contrary to the mechanisms in Fig 2.2 (Larcher 2003; Lenz *et al.* 2006). A third hypothesis is that, consistent with Fig. 2.2, a high ε contributes to a less negative π_{tlp} and this would enable stomata to close quickly with turgor loss and maintain a

high RWC_{tlp}, which would benefit drought tolerance as described for controversy (2) (Walter & Stadelmann 1968; Read *et al.* 2006). A fourth hypothesis considers a high ε to provide mechanical support for cells with very negative π_o and π_{tlp}, to prevent bursting due to excessive turgor pressure when they are fully hydrated (Jones 1992). A fifth hypothesis is that a higher ε could mechanically constrain shrinkage in cells with very negative π_o and π_{tlp}, allowing RWC_{tlp} to remain high, the so-called "cell water conservation hypothesis" (Cheung *et al.* 1975; Jones 1992). Finally, a sixth hypothesis is that a high ε and sclerophylly might in fact play no direct role in drought tolerance, and instead improve carbon and/or nutrient balance by contributing to longer leaf lifespans (Grubb 1986; Sack 2004; Markesteijn *et al.* 2011b). Indeed, a number of species persist in arid-zones despite having relatively low ε, i.e., the malacophylls, or soft-leaved species of dry areas (Walter 1985). No study to our knowledge has investigated these hypotheses in detail, though the contradictions have slowed interpretation of p-v parameters and sclerophylly.

Here, we provide a unique perspective to resolve controversies 1-4 from the fundamental cellular relationships to the biome scale. We first determined new mathematical relationships among p-v parameters. We then applied these relationships in sensitivity analyses and meta-analyses of a new global database, and related p-v parameters to aridity within and across biomes. We compiled data for π_{tlp}, π_o, ε, a_f, RWC_{tlp} and LMA for species of a wide range of growth forms and habitat preferences in the global literature. These p-v data were originally generated with the bench-drying method (using a pressure chamber; Koide *et al.* 2000) (n = 317 species from 72 studies; see Supplemental Data file "SupplementalData2.1.csv"). For species from studies that did not include LMA, we compiled mean values from the Global Plant Network (GLOPNET) dataset (Wright *et al.* 2004).

METHODS

Derivation of new equations for π_{tlp} and RWC_{tlp} as functions of other p-v parameters

We present two equations summarizing the p-v curve as a function of its parameters, given classical assumptions based on the structure and physiology of the leaf (e.g. Tyree & Hammel 1972; Baltzer *et al.* 2008; Mitchell *et al.* 2008; see Appendix section Supplemental Methods 2.1). Solving these equations for π_{tlp} and RWC_{tlp} gave the following novel relationships:

$$\pi_{tlp} = \frac{\pi_o \varepsilon}{\pi_o + \varepsilon} \quad \text{Eqn 2.1}$$

$$RWC_{tlp} = \frac{\pi_o + \varepsilon}{\varepsilon} \quad \text{Eqn 2.2}$$

Previous studies have used statistical regression to relate π_{tlp} differences to the other p-v parameters (e.g., Schulte & Hinckley 1985), but there has been little basis for favoring any particular model, without knowledge of the underlying relationships among parameters. Despite their elegance and usefulness, this is the first presentation to our knowledge of eqns 2.1 and 2.2.

Notably, in eqn 2.2 and elsewhere, RWC_{tlp} refers to the symplastic relative water content at turgor loss point, i.e., that within the leaf cells, unless specified otherwise as the total RWC_{tlp}, which includes the water in the apoplast. The two are inter-related as:

$$\text{total } RWC_{tlp} = (100 - a_f) \times RWC_{tlp} + a_f \quad \text{Eqn 2.3}$$

Further, in deriving eqns 2.1 and 2.2, we followed the classical method (e.g. Tyree & Hammel 1972; Koide *et al.* 2000) of defining ε as the slope of Ψ_P against symplastic rather than total relative water content, correcting for a_f (Fig. 2.1; Table 2.1). Thus, the a_f was considered implicitly in the calculation of ε (Fig. 2.1; Table 2.1). However in some studies, when the data did not allow clear estimation of the a_f, modulus of elasticity was calculated as the slope of Ψ_P

against *total* rather than symplastic relative water content (ε*; e.g. Sack *et al.* 2003; Lenz *et al.* 2006; Baltzer *et al.* 2008); the two measures are inter-related as $\varepsilon^* = \frac{\varepsilon}{(100-a_f)}$. If using ε*, the analogous equations for π_{tlp} and RWC_{tlp} are:

$$\pi_{tlp} = \frac{\pi_o \varepsilon^*}{\frac{\pi_o}{100-a_f}+\varepsilon^*} \quad \text{Eqn 2.1a}$$

$$RWC_{tlp} = \frac{\frac{\pi_o}{100-a_f}+\varepsilon^*}{\varepsilon^*} \quad \text{Eqn 2.2a}$$

We additionally considered each of the analyses described below using eqns 2.1a and 2.2a, as this allowed the separate consideration of a_f. Those analyses confirmed the findings below, and are presented in the Appendix section Supplemental Results and Discussion 2.1.

The application of eqns 2.1 and 2.2 in combination with global meta-analyses enabled the resolution of all four major controversies.

RESULTS AND DISCUSSION

Resolution of controversy (1): The π_{tlp} and π_o correspond with ecological drought tolerance

Given the inter-relationship among p-v parameters in eqns 2.1 and 2.2, multiple parameters may be predictive of ecological drought tolerance. Thus, we tested the relationship of each p-v parameter with moisture gradients within and across biomes, and additionally tested leaf mass per area (LMA), a functional trait commonly measured as an indicator of drought tolerance. These analyses showed that π_{tlp} and π_o are excellent indicators of drought tolerance, and much more powerful than LMA.

First, we compared species among biome categories: semi-desert, mediterranean-climate/dry temperate, temperate forest (conifers and angiosperms), coastal vegetation, mangrove, crop herb, and wet and dry tropical forest (n= 20-30 species per biome), using

ANOVAs. We first tested differences within each biome in each p-v parameter and in LMA between woody and herbaceous species, and between evergreen and deciduous species, and when no differences were found, those categories were pooled for an overall biome mean (Sokal & Rohlf 1995). Additionally, for each variable, we tested biome means for correlation with Priestly-Taylor coefficients of biome water availability (α; Prentice *et al.* 1992).

While all traits varied significantly among biomes (ANOVA; Table S2.1), only π_{tlp} and π_o showed separation of moist from dry biomes (Fig. 2.3, dark and light blue bars). Additionally, the biome means for π_{tlp} and π_o correlated tightly with biome water availability as quantified by Priestly-Taylor coefficients (α; r = 0.90, p = 0.03-0.006; Fig. 2.3, inset panels). No other traits correlated with water availability.

Second, to test traits in their ability to predict drought tolerance *within* biomes, we conducted two analyses. We compared LMA and π_{tlp} values of wet- and dry-forest species compiled from studies of temperate and tropical systems (Baltzer *et al.* 2008; Baltzer *et al.* 2009; Blackman *et al.* 2010), using t-tests. LMA did not reflect differences in forest water availability (Fig. S2.1A-C), whereas π_{tlp} shifted strongly to more negative values from wet to dry forests ($p \leq 0.05$, Fig. S2.1D). Next, we used stepwise regression to test the relationship of LMA to a published drought tolerance index for tropical woody species (Sokal & Rohlf 1995; Engelbrecht & Kursar 2003; Poorter & Markesteijn 2008), and the relationship of both LMA and p-v parameters to a drought tolerance index for temperate woody species (Niinemets & Valladares 2006). LMA was poorly correlated with the drought tolerance index for tropical woody species ($r^2 < 0.001$; Fig. S2.1A, B). However, for the temperate forest species, LMA correlated as well as p-v parameters with the drought index. The π_{tlp} and π_o were negatively correlated with species' drought tolerance index (r = -0.51 and -0.42, $p < 0.01$) whereas ε and log-transformed LMA

were positively correlated with the index (r = 0.24 and r = 0.63 respectively, p < 0.001); neither total RWC_{tlp} nor a_f related to drought tolerance. Using both LMA and π_{tlp} improved prediction of drought tolerance in this species set (Fig. S2.2; r^2 increased from 0.40 and 0.26 respectively for the traits individually, to 0.47), as these traits were uncorrelated ($r^2 < 0.1$).

We conclude that π_{tlp} and π_o are reliable indicators of species drought tolerance within and across biomes, in contrast with other p-v parameters. The evidence did not support a mechanistic linkage of LMA with drought tolerance; high LMA values were found in moist as well as dry biomes and tropical forests. Notably, LMA can be related to drought tolerance in given species sets, especially when drought stress coincides with other environmental conditions for which high LMA confers a benefit. For example, among deciduous species LMA tends to be higher for species adapted to more exposed areas, whereas among evergreen species LMA tends to be higher for species adapted to deep shade, nutrient shortage and/or herbivore pressure (Walters & Reich 1999; Sack 2004; Lusk *et al.* 2008; Markesteijn *et al.* 2011b). By contrast, as expected from their more direct physiological role, the π_{tlp} and π_o showed far stronger correspondence with ecological distribution with respect to water supply.

Resolution of controversy (2): π_o determines differences in π_{tlp} within- and across-species

Given the importance of π_{tlp}, clarifying its underlying basis is critical. Using eqn 2.1, which showed that the π_{tlp} is a function of π_o and ε, we tested the theoretical sensitivity of π_{tlp} to other p-v parameters, and then applied the equation and meta-analyses of the global dataset to determine which parameters drove actual differences in π_{tlp} within and among species. These analyses all indicated that π_{tlp} is influenced by π_o with a negligible direct role for ε.

The structure of eqn 2.1 indicated that the sensitivity of π_{tlp} to a given parameter may vary widely depending on the value of the other parameter. We used simulations to characterize the relationship of π_{tlp} to changes in π_o and ε values across ranges of realistic parameter values (Fig. 2.4A and B; we performed analogous analyses for RWC_{tlp} using eqn 2.2 in "*Resolution of Controversy (4)*"; Fig. 2.4C and D). Simulations that held one parameter constant demonstrated the effect of shifts in the other parameter on π_{tlp}. Several new principles emerged. The decline of π_{tlp} as π_o becomes more negative is very strong at all values of π_o and any value of ε, though increasingly rapid at low ε (Fig. 2.4A). However, the π_{tlp} is not sensitive to ε in the same way; reducing ε can in principle make π_{tlp} values more negative, but only within a narrow range of low ε values, and depends on π_o (Fig. 2.4B). The π_o defines the possible range of covariation in π_{tlp} and ε: the π_o sets not only the highest π_{tlp} attainable, but also the lowest ε attainable, because the relationship of π_{tlp} to ε is asymptotic, and biologically infeasible values of π_{tlp} occur when $\varepsilon \leq -\pi_o$ (Fig. 2.4B). Thus, the range of ε that impacts π_{tlp} depends on π_o: a more negative value of π_o results in sensitivity of π_{tlp} to ε over a greater range of ε values (Fig. 2.4B). Indeed, variation in ε has little influence on π_{tlp} under most local conditions, but theoretically, in extreme parameter spaces (i.e., low ε, low π_o), ε might be strongly influential.

The strong sensitivity of π_{tlp} to π_o was borne out in the global dataset for changes in given species during drought. Drought treatments led to a reduction of π_{tlp} for plants of given species by 0.44 ± 0.10 MPa on average (paired *t*-test, $p < 0.001$, $n = 25$). To determine the importance of π_o and ε in driving shifts of π_{tlp} within species during drought (Fig. 2.2), we used eqn 2.1 to partition the role of the different parameters. We determined the "post-drought π_{tlp}" that would be attained with the shift of each parameter singly, by applying eqn 2.1 using the post-drought value for that parameter while fixing the other parameter at its pre-drought value. The post-

drought π_{tlp} achieved by shifting each parameter was tested for significance by comparing with the pre-drought π_{tlp} (*t*-tests across all taxa, n = 25 species or varieties), and considering separately the taxa that increased (n = 14) and decreased in ε (n = 11) during drought (Fig. 2.5). We found that shifts to more negative π_o, i.e., osmotic adjustment, accounted almost entirely for the observed decreases in π_{tlp}. By contrast, shifts in ε had negligible in impact on π_{tlp}. In fact, on average, ε shifted upward, which would have made π_{tlp} *less* negative by 0.1 MPa considering all taxa, and by 0.2 MPa considering only taxa that increased ε (all $p < 0.05$). In those taxa that did decrease ε, however, this did not occur in the range of parameter values in which π_{tlp} was sensitive to ε, and this shift accounted for a decrease in π_{tlp} of on average 0.01 MPa. Thus, osmotic adjustment was the only mechanism employed by plants to render π_{tlp} more negative during drought.

To comprehensively determine the importance of π_o and ε to *interspecific* differences in π_{tlp}, we conducted three analyses. All analyses showed that, despite the mathematical sensitivity of π_{tlp} to ε at certain values, there is no evidence that variation in ε drives functional variation in π_{tlp}. First, we used correlations to determine pairwise relationships between variables. Consistent with the previous analysis, across the global dataset, π_{tlp} was strongly correlated with π_o (Fig. 2.6A). There was a notable inverse correlation of π_{tlp} and ε (Fig. 2.6B), contrary to the mechanistic relationship expected from eqn 2.1. A partial correlation analysis of π_{tlp}, ε and π_o allowed considering the correlations among parameters while holding another "fixed", i.e., testing the correlation between two variables after removing the influence of a third variable (Sokal & Rohlf 1995). While controlling for the variation in ε did not affect the partial correlation of π_{tlp} and π_o across the global dataset (log-transformed data; $r_{partial} = 0.95$; $p < 0.001$), controlling for the variation in π_o changed the direction of the correlation of π_{tlp} and ε to positive

($r_{partial}$ = 0.40; $p < 0.001$), as expected from eqn 2.1. Thus, any ability of a lower ε to directly drive a more negative π_{tlp} (Fig. 2.2) was reversed by a strong negative correlation of π_o and ε, a relationship previously reported in smaller species sets (Niinemets 2001; Sack *et al.* 2003; Lenz *et al.* 2006). The π_{tlp} is actually insensitive to ε, and the apparent association of low π_{tlp} with high ε across species arises secondarily from the negative correlation of ε with π_o, a general relationship further discussed in "*Resolution of controversy (4)*". This analysis indicated no direct role for ε in directly driving species-differences in π_{tlp}.

Second, to determine the degree that species' π_{tlp} values individually would be sensitive to changes in π_o and ε, we calculated partial derivatives $\partial\pi_{tlp}/\partial\varepsilon$ and $\partial\pi_{tlp}/\partial\pi_o$ from eqn 2.1 using the parameter values for each species in the global dataset. The partial derivatives, i.e., the slope of the relationship between π_{tlp} and each parameter at each observed parameter value, indicated how π_{tlp} would change with actual shifts in each variable. To test the importance of shifts in the two parameters, we compared mean partial derivative values across species using paired *t*-tests (n = 89) and the equations:

$$\frac{\partial \pi_{tlp}}{\partial \varepsilon} = \frac{\pi_o^2}{(\varepsilon + \pi_o)^2} \qquad \text{Eqn 2.4}$$

$$\frac{\partial \pi_{tlp}}{\partial \pi_o} = \frac{\varepsilon^2}{(\varepsilon + \pi_o)^2} \qquad \text{Eqn 2.5}$$

Consistent with the previous analyses, the π_{tlp} was far more responsive to changes in π_o than ε: across all species, the mean value for $\partial\pi_{tlp}/\partial\pi_o$ was 30-fold greater than $\partial\pi_{tlp}/\partial\varepsilon$ ($t = 41.1$, $p < 2.2 \times 10^{-16}$; paired *t*-test; Fig. 2.7). We also graphically compared the observed partial derivative values to those calculated from randomly generated p-v parameters, to determine whether plants preferentially occupied parameter spaces that made them more sensitive to a given parameter, or evenly occupied all the theoretically feasible parameter combinations and

would thus be sensitive to changes in both π_o and ε. The observed values of $\partial\pi_{tlp}/\partial\varepsilon$ did not enter the theoretically plausible parameter space wherein π_{tlp} is more sensitive to ε than π_o (Fig. 2.7).

Finally, given that eqn 2.1 showed a stronger sensitivity of π_{tlp} to ε at low values of ε, we determined the sensitivity of π_{tlp} in those species with lowest ε values, and even here found stronger sensitivity to π_o. We identified the 25 observations in the global dataset with lowest ε, and, using eqn 2.1, tested the amount that π_{tlp} was made more negative by reducing ε or by increasing π_o by 20%. For these species, the π_o and π_{tlp} values were relatively high; mean values ± SE (MPa) were respectively 3.5 ± 0.15, -1.0 ± 0.07 and -1.4 ± 0.07. Reducing ε by 20%, without change in π_o, led to an average decrease of π_{tlp} by 0.28 MPa ± 0.07 whereas making π_o more negative by 20% had twice the effect, decreasing π_{tlp} by 0.56 MPa ± 0.098 (paired *t*-test; $p < 0.001$).

Our analyses demonstrated that shifts in π_{tlp} for plants of given species are driven by osmotic and not elastic adjustment, and that differences within and across species in π_{tlp} are attributable entirely to π_o. Although lower values of ε may in principle result in lower π_{tlp}, that only can occur in a limited range of parameter values (i.e., when ε is very low, especially when π_o is high). Within species on average, and across species, this effect was completely overcome by the general inverse correlation of ε and π_o, such that higher ε was associated with a more negative π_{tlp}. Although numerous studies had concluded that ε had a strong role in driving π_{tlp} reductions within species or differences in π_{tlp} across species, based on finding substantial variation in ε values, π_o was the important factor due to the far greater sensitivity of π_{tlp} to π_o.

Resolution of controversy (3): a low π_{tlp} but not low RWC_{tlp} is associated with drought tolerance

Previous researchers have debated the importance of π_{tlp} versus RWC_{tlp} as traits predictive of drought tolerance (Sinclair & Ludlow 1985; Kramer 1988; Schulte 1992). The analysis of species across biomes indicated that π_{tlp} and not total RWC_{tlp} was correlated with habitat moisture (Fig. 2.3). This conclusion was supported by additional analyses within and across species. Whereas within species π_{tlp} declined strongly during drought (see "Controversy (2)" above), RWC_{tlp} showed a nonsignificant decline of only 1.2% (paired t-test, $p = 0.08$; $n = 13$). Indeed, across species globally, RWC_{tlp} showed relatively narrow variation, with a coefficient of variation (cv) of 11%, compared to π_{tlp} with a cv of 34%. There was only an empirically weak and statistically nonsignificant tendency for RWC_{tlp} to decline as π_{tlp} become more negative ($p = 0.06$; $r^2 = 0.03$; slope = 1.9; $n = 76$, indicating a decline of ~2% in RWC_{tlp} per MPa of π_{tlp}). The RWC_{tlp} appears to be conserved above 60% in all species, corresponding to a total RWC_{tlp} of 75%, consistent with previous demonstrations that dehydration below this level severely inhibits metabolism (Lawlor & Cornic 2002). These data indicate that variation in π_{tlp} is considerably more significant to physiological and ecological drought tolerance.

Resolution of controversy (4): Sclerophylly (high ε) has no direct role in drought tolerance, but plays supporting roles

The above analyses indicated no primary contribution of ε to drought tolerance through lowering π_{tlp}. However, we considered six additional hypotheses for a role of ε in drought tolerance. We found strong evidence to support an indirect role in cell water conservation, and further benefits for tolerance of other resource shortages and/or mechanical and herbivory stresses.

The first and second hypotheses could be rejected based on theory. The idea that a higher ε confers drought tolerance by inducing steep declines in Ψ_{leaf} below Ψ_{soil} as leaves lose water,

enabling water to be taken up from the roots (Bowman & Roberts 1985; Niinemets 2001) can be rejected according to the Ohm's Law analogy for the soil-plant-atmosphere continuum. While for excised leaves a higher ε will lead to a more rapid decline of Ψ_{leaf} with loss of a given volume of water, in intact plants it is not ε, but plant hydraulic conductance (K_{plant}) that will determine Ψ_{leaf} and its difference from Ψ_{soil} for a given transpiration rate (E): ($\Psi_{leaf} = \Psi_{soil} - E/K_{plant}$; Tyree & Zimmermann 2002). The Ψ_{leaf} will thus always be below Ψ_{soil} regardless of ε. Likewise, the second hypothesis, that a high ε actually *lowers* π_{tlp}, contrary to the mechanisms in Fig. 2.2, can be rejected from the graphical analysis of the p-v curve (Fig. 2.2) and the analysis of eqn 2.1 (Fig. 2.4). Proposed a number of times, including in textbooks (e.g., Larcher 2003), this fallacy apparently arises from a misleading plot of the p-v relationship (Fig. S2.3).

The third and fourth hypotheses could be rejected based on our analyses. The idea that a high ε would confer drought tolerance by driving a less negative π_{tlp} and thereby rapid turgor loss such that stomata to close quickly to conserve leaf water at a high RWC_{tlp} (Walter & Stadelmann 1968; Read *et al.* 2006) was not supported because π_{tlp} is very insensitive to ε at high values of ε (Figs 2.4 and 2.7). Additionally, a more negative, rather than less negative π_{tlp} was related to greater drought tolerance, within and across species and biomes (Figs 2.3, 2.5). Finally, early stomatal closure can be developed independently of π_{tlp}. While across species the Ψ_{leaf} at stomatal closure correlates with π_{tlp}, the stomata close in response to a low water potential in or near the guard cells and/or to chemical signals, which can be decoupled from bulk leaf π_{tlp} (Davies & Zhang 1991; Brodribb & Holbrook 2003). Thus, several species close their stomata at Ψ_{leaf} values less negative than their π_{tlp}, enabling survival on stored water which is lost slowly given low minimum epidermal conductance after stomatal closure (Guyot *et al.* 2012).

The fourth hypothesis was the idea that a high ε and stiffer cell walls might be required mechanically for cells with very negative π_o, to withstand high turgor pressures at full hydration (Jones 1992). However, cell walls do not apparently need such high ε to sustain turgor pressure. Cell walls can withstand experimental pressures many times higher than their turgor pressure before rupture (Carpita 1985; Blewett *et al.* 2000).

Indeed, the data strongly supported the fifth hypothesis, a role of high ε allowing cells to prevent dehydration below a dangerous threshold RWC_{tlp}. The idea that a high ε allows cells to maintain a higher RWC_{tlp} despite very negative π_o and π_{tlp}— the "cell water conservation hypothesis" (Cheung *et al.* 1975; Jones 1992) is depicted in Fig. 2.8, wherein illustrative values of ε = 18 MPa and π_o = -0.95 MPa were shifted by 50% to increase or decrease ε, or to decrease π_o, or to simultaneously increase ε and decrease π_o. As expected, ε reduction only slightly decreased π_{tlp}, whereas π_o reduction was considerably more effective in lowering π_{tlp}. However, reductions of ε and π_o both resulted in RWC_{tlp} declines (Fig. 2.4C and D). In contrast, a coordinated reduction of π_o and *increase* of ε lowered π_{tlp} while maintaining a constant RWC_{tlp}, which would achieve both tolerance of lower Ψ_{soil} and prevention of dangerous cell dehydration and shrinkage.

Given the potential importance of this mechanism, to test its theoretical effectiveness we used eqn 2.2 to apply the sensitivity analyses previously applied for π_{tlp} to determine the sensitivity of RWC_{tlp} to its underlying parameters within and among species. First, we used eqn 2.2 to calculate how shifts in ε and π_o in response to drought affected RWC_{tlp} for given species from the global database (for n = 13 taxa overall, and for the 5 taxa that decreased ε, and for the 8 taxa that increased ε). As discussed above, droughted plants exhibited a nonsignificant decrease in their RWC_{tlp} values (paired t-test, p = 0.09). However, for the 8 taxa that increased ε

during drought, the adjustments made in π_o alone, to reduce π_{tlp}, would have caused a 6.1% decline in post-drought RWC_{tlp} to 79.4 $\pm$ 3.5%, while adjustments in ε alone would have caused a 4.6% increase in post-drought RWC_{tlp} to 88.4 $\pm$ 2.2%, and these coordinated adjustments allowed RWC_{tlp} to be maintained even as π_{tlp} was lowered. For the 5 taxa that decreased ε during drought, adjustments in π_o alone would have caused only a non-significant 0.04% decline in post-drought $RWC_{tlp,}$ while adjustments in ε would have caused a 0.4% increase. Overall, these data indicate that plants in both groups reduced π_o to drive a lower π_{tlp} (both $p < 0.01$), and species underwent elastic adjustment if needed to maintain a high $RWC_{tlp.}$

We also tested whether differences across species in ε likewise counteracted low π_o to maintain RWC_{tlp}. We conducted a partial derivative sensitivity analysis for RWC_{tlp} as for π_{tlp} above. The partial derivatives $\partial RWC_{tlp}/\partial\varepsilon$ and $\partial RWC_{tlp}/\partial\pi_o$ were calculated for species in the global database and compared with paired t-tests (n = 76 species) using the equations:

$$\frac{\partial \mathrm{RWC_{tlp}}}{\partial \varepsilon} = \frac{-\pi_o}{\varepsilon^2} \qquad \text{Eqn 2.7}$$

$$\frac{\partial \mathrm{RWC_{tlp}}}{\partial \pi_o} = \frac{1}{\varepsilon} \qquad \text{Eqn 2.8}$$

Across species, RWC_{tlp} was significantly more sensitive to adjustments in π_o than ε, with $\partial RWC_{tlp}/\partial\pi_o$ nearly 7-fold greater than $\partial RWC_{tlp}/\partial\varepsilon$ (paired t-test, $p < 2 \times 10^{-16}$, n = 76). These analyses indicate that the decreases in π_o necessary to generate a very negative π_{tlp} also would drive a strong decline in RWC_{tlp}, requiring a higher ε to prevent decreases in RWC_{tlp}. As previously discussed, none of the species in our global database had a total RWC_{tlp} of less than 75% (corresponding here to a 60% symplastic RWC_{tlp}), which would significantly impair metabolic function, suggesting that plants favor the adjustment of ε to maintain sufficient RWC_{tlp} (Lawlor & Cornic 2002).

The mechanistic feasibility of cell water conservation explains very well the correspondence of ε with drought adaptation which had been at first sight ambiguous, i.e., its negative correlation across species with π_{tlp}, with high values in many plants of dry biomes, and its frequent increase in droughted plants. We note that other effects may also contribute to these trends. For example, a higher ε may be directly linked with the reduction of π_o, if carbon is redirected from cell wall extensin for osmotic adjustment, resulting in a less flexible cell wall (Iraki *et al.* 1989; Moore *et al.* 2008). Further, a low π_o and high ε may be coordinated with other structural features that benefit drought tolerance, such as the general trend for dry-adapted plants to exhibit a higher density of smaller cells, which increases wall investment and makes solute accumulation more efficient in lower cell volumes (Cutler *et al.* 1977). Some have proposed that a high ε may also enable more rapid refilling of embolisms in leaf xylem (Salleo *et al.* 1997) but recent studies did show that even species with low ε can have strong refilling capacity (Trifilo *et al.* 2003; Scoffoni *et al.* 2012).

The sixth hypothesis was also supported by our review of the literature and meta-analyses. Sclerophylly and high ε would have additional benefits for plants in arid areas that are not directly linked to water relations, e.g., via a high LMA and high leaf density, conferring leaf longevity (Loveless 1961; Groom & Lamont 1999; Chaves *et al.* 2002; Wright & Westoby 2002). Higher leaf longevity provides an economic advantage, especially given low nutrient supply and/or a short dry season or winter, allowing greater total photosynthetic returns when leaf replacement costs exceed maintenance costs (Orians & Solbrig 1977; Mooney *et al.* 1983; Salleo *et al.* 1997). Indeed, many sclerophyllous species in semi-arid climates evolved tough leaves in response to nutrient or mechanical stress under moister climate regimes, and numerous species that currently inhabit wet zones exhibit sclerophylly (Buckley *et al.* 1980; Ackerly 2004).

Conversely, sclerophylly is not necessary for drought adaptation; numerous species of dry areas exhibit soft leaves (malacophylly), including succulent and semi-deciduous species (Walter 1985). Because these species have high π_o, their π_{tlp} would be unresponsive to ε (Fig. 2.4). Thus, these species would not gain any direct advantage from having a low ε with respect to lowering their π_{tlp}. The low ε of deciduous malacophylls may simply reflect low cell wall investment in short-lived leaves (Fig. 2.4; Goldstein & Nobel 1991; Loik & Nobel 1991). Additionally, in dry-habitat plants with soft leaves and water storage tissues, flexible cell walls may further contribute to greater water storage capacitance after stomatal closure, given an impermeable cuticle (Ogburn & Edwards 2010). Such a low ε in water storage tissues would contribute to succulence, a drought avoidance mechanism independent of low π_{tlp}, which contributes to an ability to survive water shortage, though not allowing the maintenance of gas exchange and growth (see Appendix section Supplemental Results and Discussion 2.2).

Scales of drought tolerance

Our analyses supported a strong association of π_{tlp} with not only physiological but also ecological drought tolerance. The π_{tlp} reflects the ability of the bulk leaf tissue to maintain function during drought, and is also correlated with other leaf drought tolerance traits, including the Ψ_{leaf} values at which growth ceases, stomatal conductance or leaf hydraulic conductance decline by 50%, and leaves desiccate irreversibly (Abrams & Kubiske 1990; Sack *et al.* 2003; Baltzer *et al.* 2008; Mitchell *et al.* 2008; Blackman *et al.* 2010). However, as for other functional traits, π_{tlp} must be understood as one factor in leaf and whole-plant water relations and species distributions with respect to water supply, as there are cases where other factors would become equally or more significant. At the leaf level, the π_{tlp} is an average characteristic of all cells, and it is usually

robust to heterogeneity in cell anatomy, structure, and function across the leaf (Tyree & Hammel 1972; Tyree 1981). However, for some taxa this average may not well represent the turgor loss point of the photosynthetic mesophyll cells, or bundle sheath cells that contribute to hydraulic conductance, or epidermal cells or guard cells that control stomata, and thus in cases may not be a good predictor of these cells' loss of function.

Further, while leaf and whole-plant drought tolerance are generally coordinated, as shown by the relationships between π_{tlp} and water availability in this study, some plants with relatively tolerant leaves may be drought-sensitive at the whole-plant level (e.g., *Magnolia grandiflora* due to its shallow roots; Scoffoni *et al.* 2011). Conversely, as mentioned above, species with sensitive leaves may have excellent drought survival—especially succulent species, when π_{tlp} is likely to be less important than the capacitance of water storage cells (Chaves *et al.* 2002; Ogburn & Edwards 2010). Other species may go dormant, shed leaves or whole shoots during the drought season, or persist in episodically very dry habitats through desiccation tolerance of vegetative parts and/or seeds (Jenks & Wood 2007).

Even beyond whole-plant drought tolerance, at ecological scales, the interplay between drought tolerance and competitive and trophic interactions will contribute to species distributions and population dynamics (Chesson *et al.* 2004). Even so, recent work has provided strong evidence that drought tolerance indeed scales up in many cases to determine communities and their dynamics in dry as well as typically wet systems (e.g., Engelbrecht *et al.* 2007; McDowell 2011; Blackman *et al.* 2012).

CONCLUSIONS

We are in strong need of traits for rapidly assessing species' drought tolerances. Prediction of drought tolerance and distributions for diverse species and vegetation types based on traits is increasingly necessary given climate change. A direct role of π_{tlp} and π_o in determining physiological drought tolerance is well established but and the lack of demonstration of a role in realized ecological drought tolerance and the controversies of their interpretation slowed their application in comparative and community level trait studies. In our global meta-analysis, π_{tlp} showed a strong association with water availability within and across biomes, and was typically more effective than LMA and other p-v parameters as a functional trait representing drought tolerance.

Beyond establishing the importance of π_{tlp} as a functional trait at species and biome levels, we resolved long-standing controversies surrounding its interpretation. The derivation and application of eqns 2.1 and 2.2 clarified the mechanistic bases for π_{tlp} and RWC_{tlp} and provided a novel mathematical framework to resolve questions of their significance and their determination. These analyses showed that variation in π_{tlp} within and across species is due virtually entirely to shifts in π_o, with coordinated adjustments in ε having no direct impact on π_{tlp}, but acting to compensate for variation in π_o and allowing maintenance of a high $RWC_{tlp,}$ thereby preventing dangerous levels of cell dehydration and shrinkage.

These findings also clarified species-level drought responses and biogeographic trends in sclerophylly. A high ε has an indirect role in drought adaptation, including maintaining RWC_{tlp} and thereby, cell hydration, when π_o is low, which provides a benefit for sclerophylly in many arid-adapted species, given the strong relationship of π_o with drought tolerance. However, not all arid-zone species have high ε; malacophyllous species that avoid drought with water storing or deciduous leaves and low solute concentrations can have low ε. Further, sclerophylly would also

be selected in leaves without a low π_o and thus poor drought tolerance, to extend leaf lifespan during other resource shortages or stresses.

The new perspective presented here points to a renewed value of π_{tlp}, and a clear framework for the importance of its underlying parameters. Given the remarkable degree that π_o and π_{tlp} scale up, cell water relations has previously unappreciated predictive power at the levels of leaf, whole plant and even the biome. Given additional consideration of other factors that can contribute to tolerance or avoidance of drought, the π_{tlp} has strong value as a functional trait for species and ecosystem analyses, to allow increasing assessment of their comparative drought tolerance and their potential sensitivity to climate change.

ACKNOWLEDGEMENTS

We thank Steven Diep and Christine Vuong for assistance with analysis and John Boyer, Erika Edwards, Michele Holbrook, Park Nobel, and anonymous reviewers for insightful and helpful discussion and comments on the manuscript; we are particularly grateful to John Sperry for first explaining the role of ε in cell water conservation, so well supported by our analyses. This work was supported by National Science Foundation Grants #IOS-0546784 and the Department of Ecology and Evolutionary Biology, University of California, Los Angeles.

Table 2.1 A primer of terms and symbols used in leaf pressure-volume (p-v) analysis of water relations and drought tolerance, including measured metrics and parameters derived from p-v analysis, units, derivation, and biological significance. See Fig. 2.1 for graphical depiction of parameters. For the derivation and significance of capacitance, see Appendix section Supplemental Results and Discussion 2.2.

Symbol	Variables	Unit	Derivation	Significance
Measured metrics				
Ψ_W	Bulk leaf water potential	MPa	Volume-weighted average of water potentials (forces acting on water) in the leaf	Index of leaf hydration and demand for water
Ψ_S	Osmotic potential	MPa	The portion of the p-v curve following turgor loss point gives $\Psi_W = \Psi_S$	A lower water potential caused by concentration of cell solute
Ψ_P	Pressure potential	MPa	In the portion of the p-v curve before turgor loss point, $\Psi_W - \Psi_S = \Psi_P$	A higher water potential caused by turgor pressure against the cell walls
RWC	Relative water content	%	Fraction of saturated water mass present in leaf	Leaf hydration
R	100- RWC	%	-	-
Parameters derived from pressure-volume curve analysis				
π_{tlp}	Turgor loss point	MPa	Point at which $\Psi_P = 0$ and $\Psi_W = \Psi_S$	Point at which leaf cells become flaccid, on average
ε	Modulus of elasticity	MPa	$\frac{\Delta \Psi_P}{\Delta RWC_{symplastic}}$	Wall stiffness, calculated from symplastic water content
ε^*	Modulus of elasticity	MPa	$\frac{\Delta \Psi_P}{\Delta RWC_{total}}$	Wall stiffness, calculated from total water content
π_o	Osmotic potential at full rehydration	MPa	Ψ_S at full hydration ($R = 0$)	Solute concentration in cells
a_f	Apoplastic fraction	%	*RWC* at $\Psi_S = -\infty$	Extracellular water content
Total RWC_{tlp}	Relative water content at turgor loss point	%	Total *RWC* at which $\Psi_W = \pi_{tlp}$	Leaf hydration at which cells become flaccid
Symplastic RWC_{tlp}	Relative symplastic water content at turgor loss point	%	Symplastic *RWC* at which $\Psi_W = \pi_{tlp}$	Symplastic leaf hydration at which cells become flaccid

FIGURE CAPTIONS

Figure 2.1 A primer of pressure-volume curve construction. **A.** plot of water potential versus 100-total relative water content (100 - *RWC* = *R*, units %); the leaf water potential (Ψ_{leaf}, units MPa) is the sum of the pressure potential (Ψ_P) and solute potential (Ψ_S). The slope of Ψ_P between *R*=0 and turgor loss point (R = 100- RWC_{tlp}) is the modulus of elasticity (ε, units MPa). The *y*-intercept of the Ψ_S curve is the osmotic potential at full turgor (π_o), and when Ψ_P =0, Ψ_{leaf} = the water potential at turgor loss point (π_{tlp}). The apoplastic fraction (a_f) is the *R* at which Ψ_{leaf} trends toward -∞. **B.** A plot of -1/Ψ versus *R* facilitates parameter estimation.

Figure 2.2 Graphical illustration of the impacts on π_{tlp} of changing given pressure-volume (p-v) curve parameters in a plot of Ψ_{leaf}, Ψ_P and Ψ_S against *R* (symbols as in Fig 2.1 and Table 2.1) **A.** The p-v curve of Fig. 2.1A. **B.** When π_o is more negative but ε and a_f are fixed, the RWC_{tlp} decreases, and the π_{tlp} is shifted to more negative. **C.** When ε is higher, but π_o and a_f are fixed, the RWC_{tlp} increases, the π_{tlp} is shifted to less negative. **D.** When a_f is higher, the π_{tlp} is shifted to more negative, via a reduction of ε (see formula for ε in Table 2.1).

Figure 2.3 Global data for pressure-volume parameters (symbols as in Table 2.1) and leaf mass per area (LMA), with mean ± standard error across biome categories, with inset plots of biome category means against the Priestly-Taylor coefficient of annual moisture availability (α). Biome categories: semi-desert, mediterranean-type vegetation/dry temperate woodland, tropical dry and wet forest, temperate forest angiosperm and conifer, coastal vegetation, mangrove and crop herb. Data within biomes were separated into herb (H) versus woody (W), or evergreen (E) versus deciduous (D) when significantly different (Table S2.1). Only π_o and π_{tlp} showed separation of

moist and dry biomes (light and dark blue bars respectively), and correlated with α across biomes (both $r^2 = 0.81$, $p = 0.03$ to 0.006).

Figure 2.4 Simulations based on equations 2.1 and 2.22, demonstrating the implications of the relationships among the pressure-volume parameters (symbols as in Fig 2.1 and Table 2.1). Each point would represent parameters determined in a single p-v curve. **A.** The π_{tlp} is sensitive to π_o across the full range of values, and especially at lower ε. **B.** Decreases in ε result in more negative π_{tlp} only within a narrow range of low ε values. The range of values of ε values with an influence on π_{tlp} increases as π_o becomes more negative. **C.** and **D.** The RWC_{tlp} is also sensitive to π_o and shows a considerably stronger response to ε.

Figure 2.5 The impact of shifts in pressure-volume parameters on turgor loss point (π_{tlp}) for given species during drought. Mean values ± standard error for the adjustment of π_{tlp} observed in response to drought for given species from a global dataset, and that driven by the change in each component pressure-volume parameter alone, using eqn 2.1. White bars represent all taxa (n = 25 species and varieties), gray bars those taxa that decreased in the modulus of elasticity (ε) in response to drought (n = 14), and black bars those taxa that increased in ε in response to drought (n = 11).

Figure 2.6 The relationship of turgor loss point (π_{tlp}) to other pressure volume parameters (osmotic potential at full turgor, π_o; modulus of elasticity, ε) across species in a global dataset. Note that this analysis alone, though previously the most comprehensive analysis of variation in pressure-volume curve parameters across species (Niinemets 2001; Lenz *et al.* 2006) cannot

elucidate the non-linear relationships among parameters or partition the sensitivity of π_{tlp} to individual parameters, but this analysis still indicates a strong, direct impact of π_o in determining variation in π_{tlp} and no direct determining role for ε. **A.** π_{tlp} vs. π_o; $r = 0.96$, $p < 1 \times 10^{-15}$ **B.** π_{tlp} vs. ε; $r = 0.28$, $p < 0.001$.

Figure 2.7 The sensitivity of π_{tlp} to shifts in π_o and ε in a global dataset, characterized as the partial derivative of π_{tlp} with respect to each parameter. The contour surface shows the partial derivatives calculated from 1000 randomly generated parameter values across the range of parameter space, indicating the theoretically possible π_{tlp} responsiveness. The black points are partial derivatives of the observed values (89 total; excluding the 2% of partial derivative values >10, for visual clarity). While it was theoretically possible for $\partial\pi_{tlp}/\partial\varepsilon > \partial\pi_{tlp}/\partial\pi_o$, as seen in the rapid contour rise at low ε and π_o, all species occupied the spaces where $\partial\pi_{tlp}/\partial\pi_o > \partial\pi_{tlp}/\partial\varepsilon$ (the points were higher in the left than the right panel as emphasized by the darker color of the plane and its higher position, made clearer by the rotation of the plots).

Figure 2.8 The mechanism for cell water conservation (symbols as in Table 2.1). A. From initial values (black point), decreasing π_o strongly reduced π_{tlp} and RWC_{tlp} (blue), whereas increases or decreases in ε raised or lowered RWC_{tlp} with slight impact on π_{tlp} (green and red respectively). Coordinated π_o and ε adjustments reduced π_{tlp} and maintained RWC_{tlp} (purple). **B.** In the global dataset, π_o and ε were inversely correlated ($r = 0.42$; $p < 1 \times 10^{-14}$), and π_{tlp} decreased with π_o but not ε (darker red = more negative values), consistent with cell water conservation. All values of symplastic RWC_{tlp} were above 60%, corresponding to total RWC_{tlp} of 75%, a threshold for metabolic inhibition (solid line).

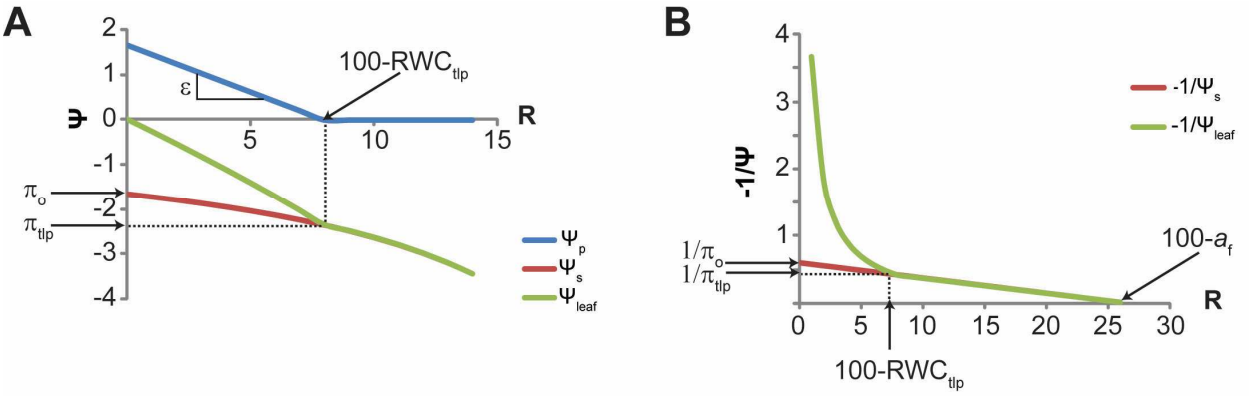
A
2
1
0
-1
-2
-3
-4
Ψ
ε
100-RWC$_{tlp}$
5
10
15
R
π$_o$
π$_{tlp}$
Ψ$_p$
Ψ$_s$
Ψ$_{leaf}$
B
4
3
2
1
-1/Ψ
-1/Ψ$_s$
-1/Ψ$_{leaf}$
1/π$_o$
1/π$_{tlp}$
100-a_f
0
5
10
15
20
25
30
R
100-RWC$_{tlp}$

Figure 2.1

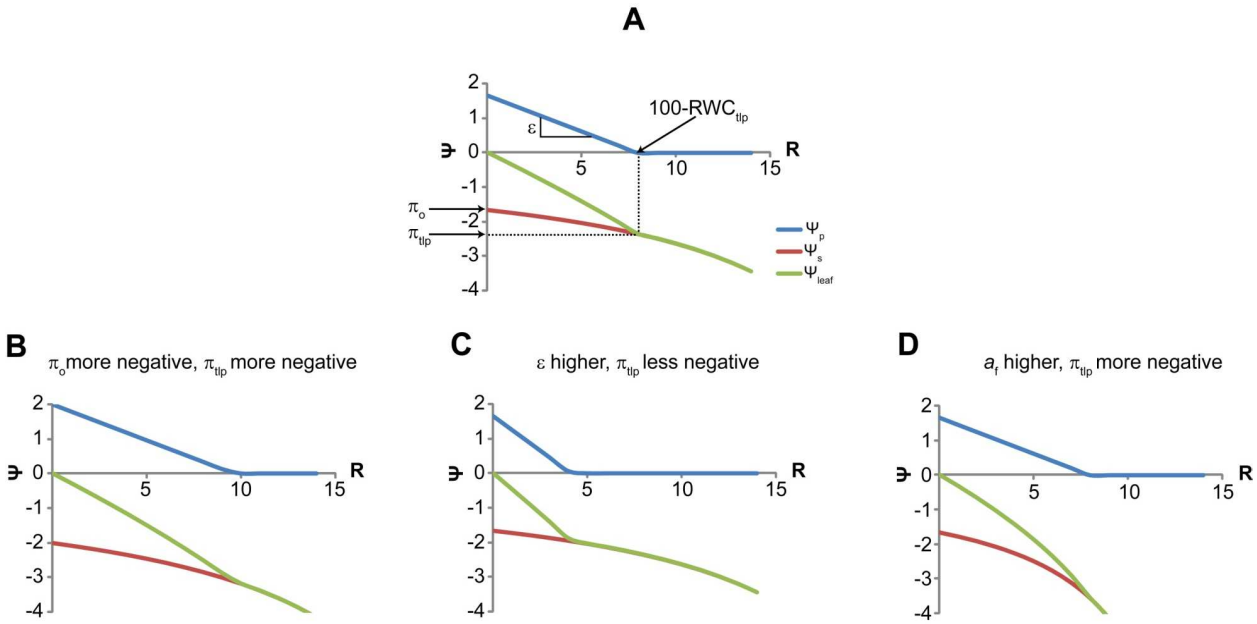
A
100-RWC$_{tlp}$
ε
Ψ
R
5
10
15
2
1
0
-1
-2
-3
-4
π$_o$
π$_{tlp}$
Ψ$_p$
Ψ$_s$
Ψ$_{leaf}$
B
π$_o$ more negative, π$_{tlp}$ more negative
C
ε higher, π$_{tlp}$ less negative
D
a_f higher, π$_{tlp}$ more negative

Figure 2.2

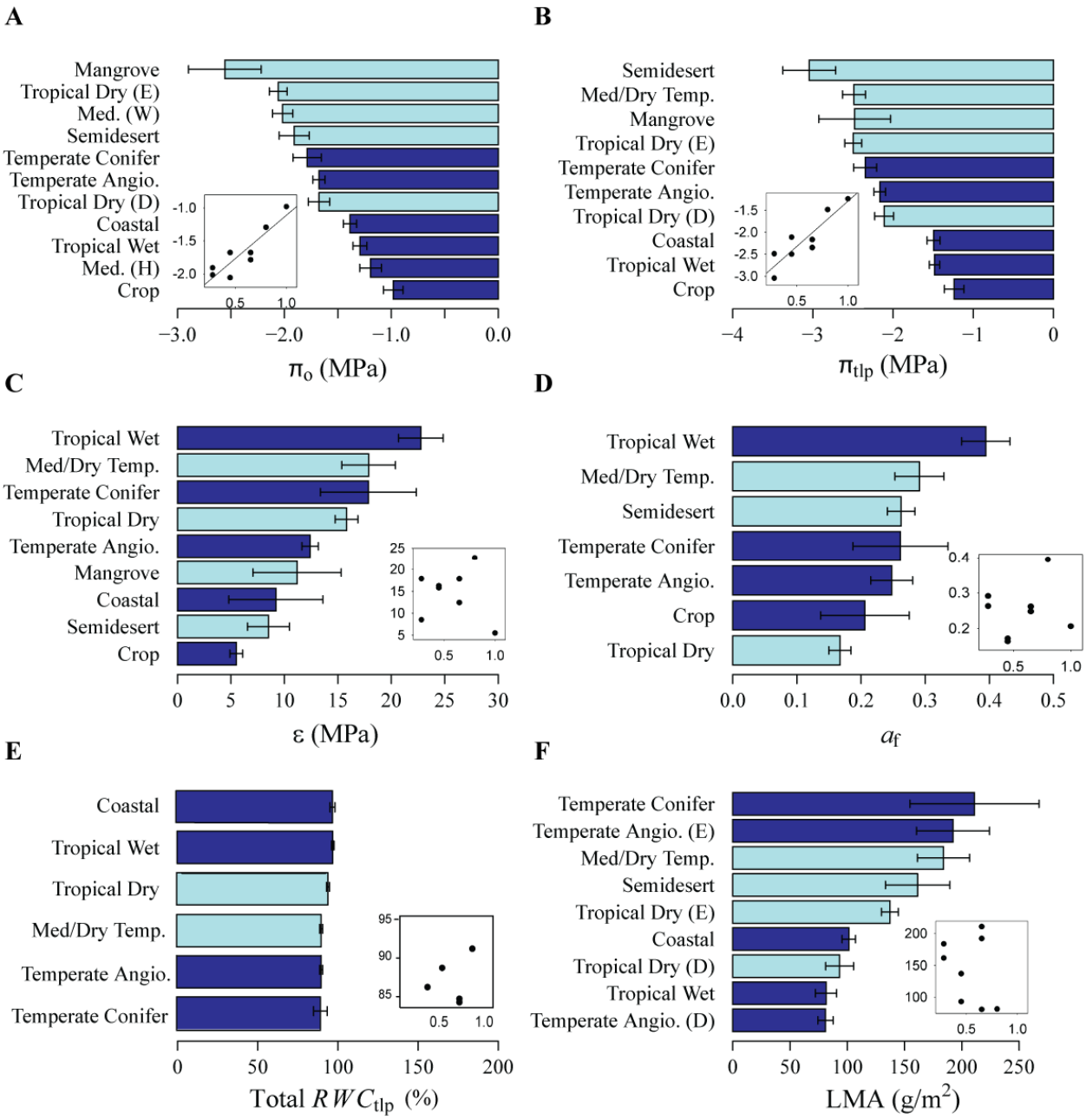
A
Mangrove
Tropical Dry (E)
Med. (W)
Semidesert
Temperate Conifer
Temperate Angio.
Tropical Dry (D)
Coastal
Tropical Wet
Med. (H)
Crop
−3.0
−2.0
−1.0
0.0
π_o (MPa)
B
Semidesert
Med/Dry Temp.
Mangrove
Tropical Dry (E)
Temperate Conifer
Temperate Angio.
Tropical Dry (D)
Coastal
Tropical Wet
Crop
−4
−3
−2
−1
0
π_{tlp} (MPa)
C
Tropical Wet
Med/Dry Temp.
Temperate Conifer
Tropical Dry
Temperate Angio.
Mangrove
Coastal
Semidesert
Crop
0
5
10
15
20
25
30
ε (MPa)
D
Tropical Wet
Med/Dry Temp.
Semidesert
Temperate Conifer
Temperate Angio.
Crop
Tropical Dry
0.0
0.1
0.2
0.3
0.4
0.5
a_f
E
Coastal
Tropical Wet
Tropical Dry
Med/Dry Temp.
Temperate Angio.
Temperate Conifer
0
50
100
150
200
Total RWC_{tlp} (%)
F
Temperate Conifer
Temperate Angio. (E)
Med/Dry Temp.
Semidesert
Tropical Dry (E)
Coastal
Tropical Dry (D)
Tropical Wet
Temperate Angio. (D)
0
50
100
150
200
250
LMA (g/m^2)

Figure 2.3

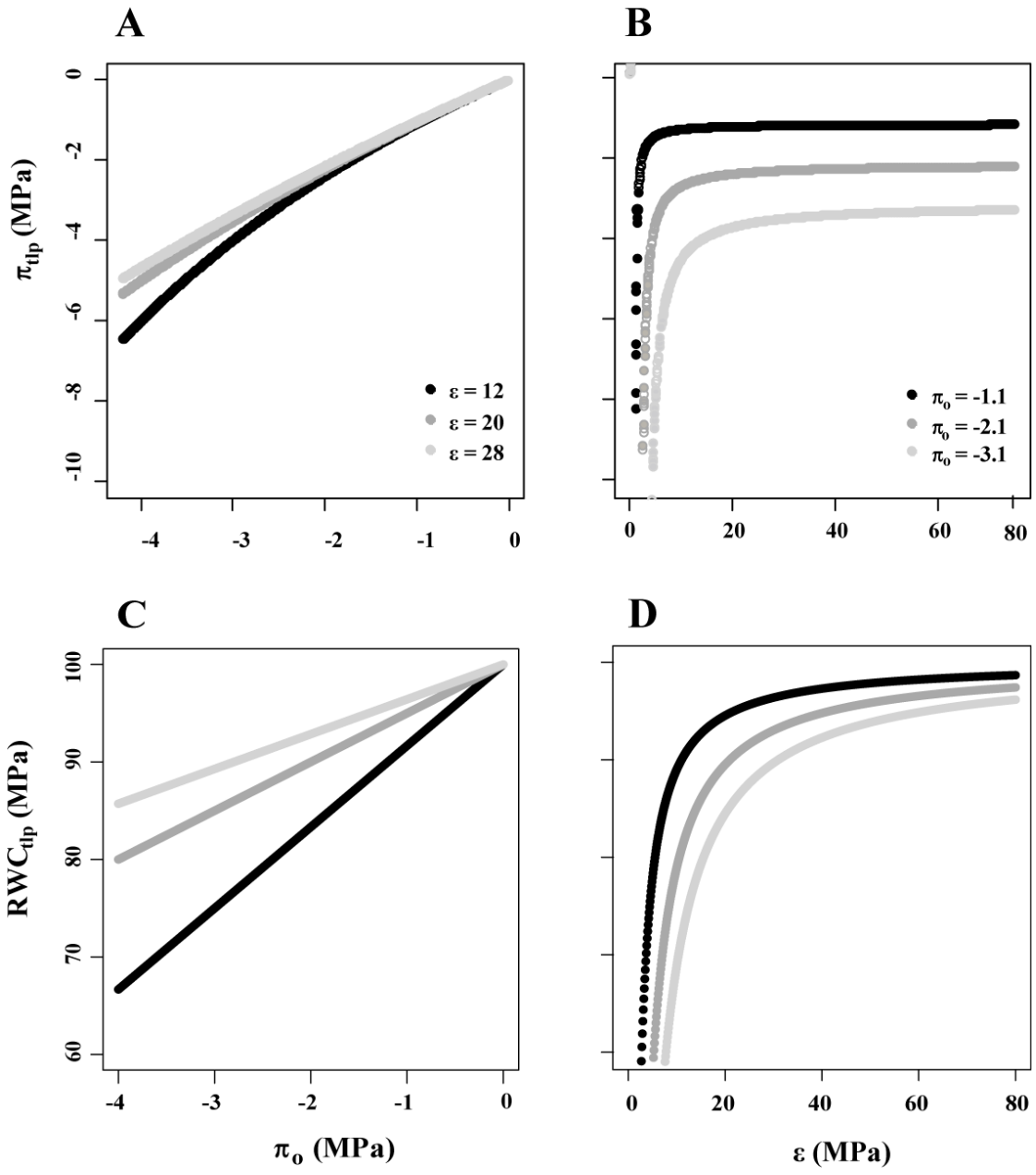
A
B
C
D
π_{tlp} (MPa)
0
-2
-4
-6
-8
-10
-4
-3
-2
-1
0
ε = 12
ε = 20
ε = 28
π_o = -1.1
π_o = -2.1
π_o = -3.1
0
20
40
60
80
RWC_{tlp} (MPa)
100
90
80
70
60
π_o (MPa)
ε (MPa)

Figure 2.4

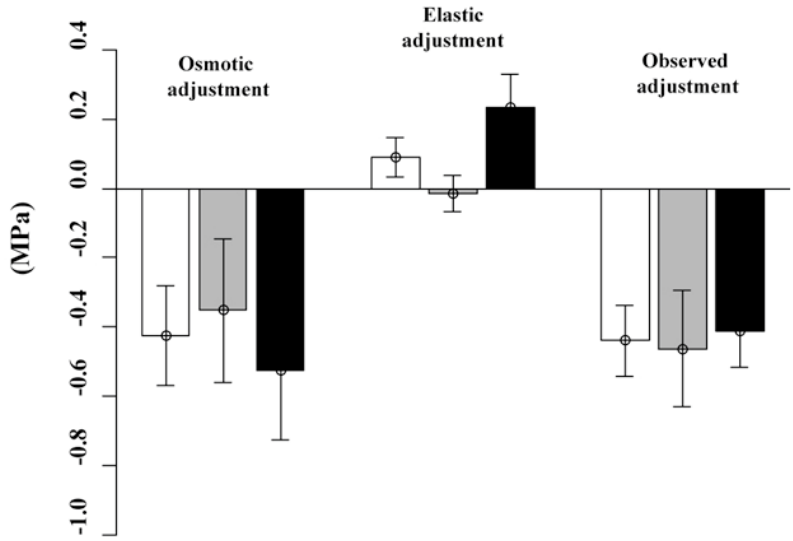
Osmotic adjustment
Elastic adjustment
Observed adjustment
(MPa)
0.4
0.2
0.0
-0.2
-0.4
-0.6
-0.8
-1.0

Figure 2.5

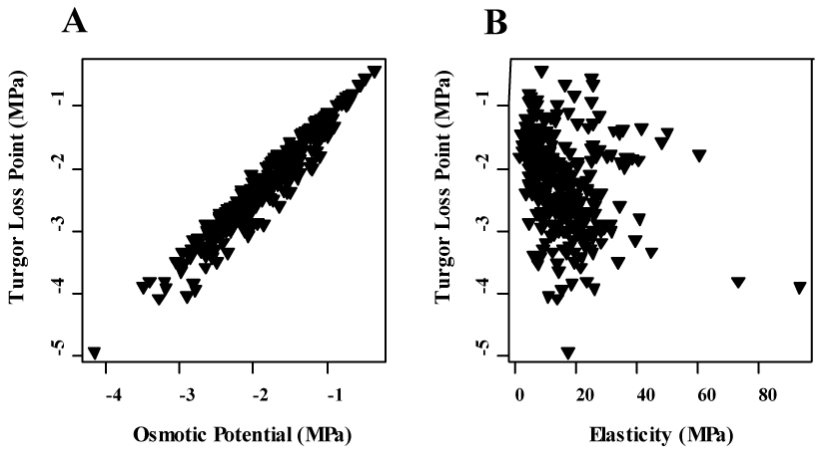
A
B
Turgor Loss Point (MPa)
-1
-2
-3
-4
-5
-4
-3
-2
-1
Osmotic Potential (MPa)
Turgor Loss Point (MPa)
-1
-2
-3
-4
-5
0
20
40
60
80
Elasticity (MPa)

Figure 2.6

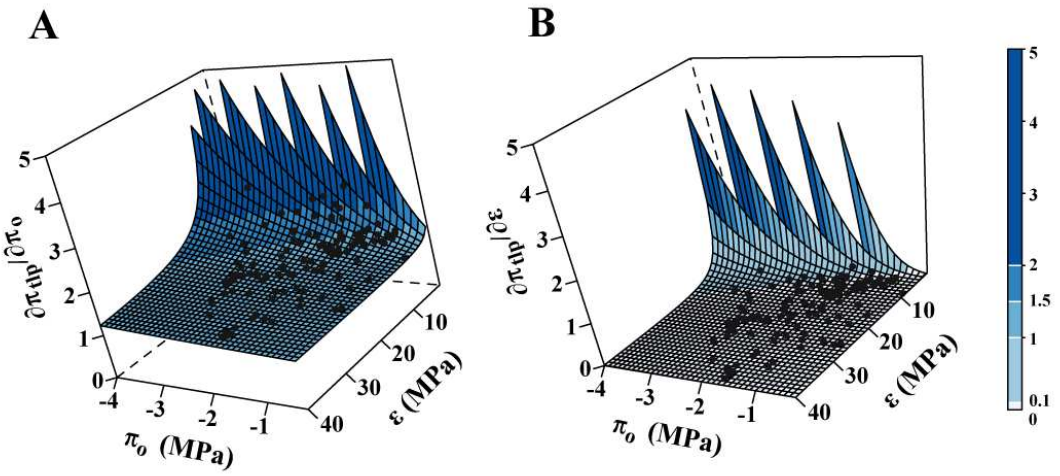
A
B
$\partial\pi_{tlp}/\partial\pi_o$
$\partial\pi_{tlp}/\partial\varepsilon$
π_o (MPa)
ε (MPa)
5
4
3
2
1
0
-4
-3
-2
-1
10
20
30
40
0.1

Figure 2.7

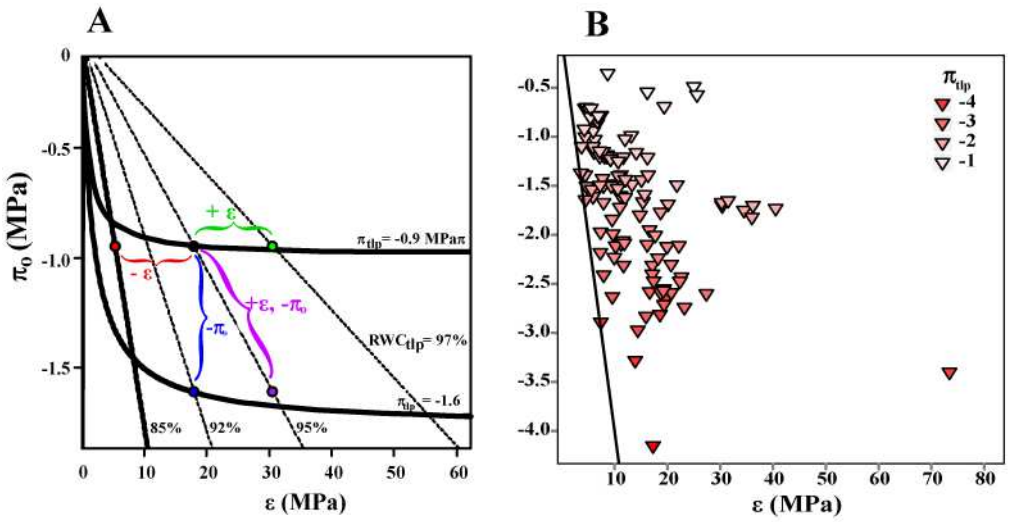
A
B
π_0 (MPa)
ε (MPa)
π_{tlp}= -0.9 MPaπ
RWC$_{tlp}$= 97%
π_{tlp} = -1.6
85%
92%
95%
+ ε
- ε
-π_o
+ε, -π_o
π_{tlp}
-4
-3
-2
-1

Figure 2.8

SUPPLEMENTAL MATERIAL

Table S2.1. Summary of mean values ± standard error from a global database for pressure-volume parameters (see Table 2.1) and for leaf mass per area (LMA).

Figure S2.1. The turgor loss point (π_{tlp}) showed greater value than leaf mass per area (LMA) as predictor of drought tolerance between vegetation types. The presence of numerous soft-leaved deciduous species in tropical dry forests and of high-LMA species in tropical wet forests suggested that LMA is likely to be a poor predictor of drought tolerance between tropical forest sites (Prior *et al.* 2003; Poorter *et al.* 2009). **a.** Plot showing no relationship ($r^2 < 0.001$) between LMA and drought tolerance (based on species' relative abundances in dry forest sites) for 38 seedlings of Bolivian rainforest species (new plot of data of Poorter & Markesteijn 2008). **b.** Plot showing no relationship ($r^2 < 0.001$) between LMA and drought tolerance for 11 Panamanian rainforest species (based on relative survival in drought versus normal rainfall conditions, new plot of data of Engelbrecht & Kursar 2003; Wright *et al.* 2010). **c. and d.** Plots showing no significant differences in LMA ($p = 0.52, 0.86$) but significantly lower π_{tlp} ($p \leq 0.05$) in dry forests than wet forests of southeast Asia (black bars; Baltzer *et al.* 2008; Baltzer *et al.* 2009; n = 18, 7) and Australia (white bars; Blackman *et al.* 2010; n = 14, 5).

Figure S2.2. Plots showing that turgor loss point (π_{tlp}) and leaf mass per area (LMA) are equally good predictors of drought tolerance index (DI) in temperate woody species (n = 33 for LMA, n = 47 for π_{tlp}). The observed drought index was based on a 1-5 ranking (1 = least tolerant) of the annual precipitation, seasonality, ratio of precipitation to potential evapotranspiration, and the duration of and soil water potential during the dry season of each species' habitat (Niinemets &

Valladares 2006; Hallik *et al.* 2009). For these plots the DI was predicted from regressions of observed DI against LMA, π_{tlp} and both in combination: DI = 2.045 log(LMA) -0.874 $r^2 = 0.39$, $p < 0.01$; DI = $-0.78\pi_{tlp} + 1.36$; $r^2 = 0.26$, $p < 0.01$; DI = $1.650\log(LMA) - 0.473\ \pi_{tlp}$ -1.150; $r^2 = 0.47$, $p < 0.01$. **A.** DI as predicted by LMA plotted against observed DI; $r = 0.63$, $p < 0.001$ **B.** DI as predicted by π_{tlp} plotted against observed DI; $r = 0.51$, $p < 0.001$. **C.** DI as predicted by a multiple regression of both LMA and π_{tlp} plotted against observed DI; $r = 0.68$, $p < 0.001$ ($n = 31$). We plotted data only for species for which both LMA and π_{tlp} were available; a previous analysis of a larger dataset for northern hemisphere woody species for the correlation of LMA with this DI ($n = 339$) resulted in worse performance by LMA, with a lower correlation than in our smaller dataset; r = 0.09 (Hallik *et al.* 2009). The correlation of drought tolerance with LMA in these data and not other species sets (e.g., Fig. S2.1) may reflect the gradient of nutrient availability coinciding with that of water availability across North American ecosystems, which is not a universal trend across other biomes or continents (Grubb 1989).

Figure S2.3. Fallacious graphical suggestion that a higher modulus of elasticity (ε) can result in a more negative turgor loss point (π_{tlp}); in fact, a higher ε leads to a less negative π_{tlp} (see Figs 2.2C and 2.5B). **A.** Pressure volume curve as in Fig. 2.1, showing only the trajectories of leaf water potential and solute potential (Ψ_{leaf} and Ψ_S respectively) against R = 100-relative water content, with RWC_{tlp} = relative water content at turgor loss point. **B.** Fallacious curves supposedly showing a shift to lower π_{tlp} caused by a higher ε. This plot is based on the mistaken assumptions that (1) a higher ε leads to a steeper slope of solute potential (Ψ_S); in fact, a higher ε, which corresponds to a steeper slope of pressure potential (Ψ_P, not shown), would not affect that of Ψ_S (see Fig. 2.2C) and (2) that RWC_{tlp} would be fixed; in fact RWC_{tlp} would increase as ε

increases (see Fig. 2.2C). This misleading graphical analysis has led several to conclude that a higher ε can drive a more negative π_{tlp}, providing one of the putative mechanisms for sclerophylly to result in greater drought tolerance.

Figure S2.4. Verifying eqns 2.1 and 2.2 (symbols as in Fig 2.1 and Table 2.1). **A.** Observed π_{tlp} compared with values predicted by applying eqn 2.1 to p-v parameters from a global compiled dataset ($\hat{\pi}_{tlp} = 0.986\pi_{tlp}$, $r^2 = 0.99$, $p < 2 \times 10^{-16}$, n = 89 species). **B.** Observed RWC_{tlp} compared with values predicted by applying eqn 2.2 to p-v parameters ($\widehat{RWC}_{tlp} = 1.03\text{RWC}_{tlp}$, $r^2 = 0.57$, $p < 2 \times 10^{-7}$, n = 74 species). The equations applied to data of studies that determined ε as the slope of Ψ_P against R between full turgor and turgor loss point (blue points) or those that recognized a variable ε and presented the value at full turgor (black points).

Figure S2.5. Validating the predictive power of the alternative eqns 2.1a and 2.2a, based on a modulus of elasticity (ε*) calculated from total leaf relative water content, rather than from symplastic leaf relative water content. **A**. Observed turgor loss point (π_{tlp}) compared with values for turgor loss point predicted by applying eqn 2.1a to pressure volume parameters ($\hat{\pi}_{tlp}$) from a global compiled dataset (n = 89 species). In this model form, π_{tlp} is a function of osmotic potential at full turgor (π_o), apoplastic fraction (a_f), and ε*. $\hat{\pi}_{tlp} = 0.986\pi_{tlp}$, with standard error = 0.029, $r^2 = 0.99$, $p < 2 \times 10^{-16}$. **B.** Observed values of relative water content at turgor loss point (RWC_{tlp}) compared to values calculated from eqn 2.2a and a global database of π_o, a_f, and ε* from n = 74 species. $\widehat{RWC}_{tlp} = 0.992\text{RWC}_{tlp}$, with standard error = 0.011, $r^2 = 0.35$, $p < 2 \times 10^{-16}$. The better fit for π_{tlp} than for RWC_{tlp} can be explained by its lower sensitivity to a_f and ε* in simulations based on eqns 2.1a and 2.2a; these parameters are estimated through linear

approximations in the p-v plot and thus subject to greater measurement error than π_o (Sack *et al.* 2003; Scoffoni *et al.* 2011).

Figure S2.6. Simulations demonstrating the implications of the relationships among the pressure-volume parameters based on the alternative eqns 2.1a and 2.2a. As with Eqns 2.1 and 2.2, the sensivity of turgor loss point (π_{tlp}) and relative water content at turgor loss point (RWC_{tlp}) to a particular parameter has a non-linear dependency on the value of the other parameter. The π_{tlp} showed the greatest response to π_o (see also Fig. 2.5). **A.** A lower π_o drives a more negative π_{tlp} at any ε*, and a higher ε* results in more negative π_{tlp} only within a narrow range of low ε values. The range of values of ε* values with an influence on π_{tlp} increases as π_o becomes more negative. **B.** Increasing a_f shifts the curve slightly to the right by increasing the value of ε* at which the π_{tlp} and ε* relationship shows a vertical asymptote (at $\varepsilon^* = -\frac{\pi_o}{100-a_f}$). **C.** The RWC_{tlp} shows the same relationships as the π_{tlp} with ε* and π_o, increasing to an asymptote with increasing ε*, with the curve shifting to the right at more negative π_o resulting in lower RWC_{tlp} values. **D.** The relationship of RWC_{tlp} to elasticity shifts to the left at higher a_f, producing higher values of RWC_{tlp}.

Figure S2.7. The impact of shifts in pressure-volume parameters on turgor loss point (π_{tlp}) for given species during drought based on the alternative eqns 2.1 and 2.1a. Mean values ± standard error for the adjustment of π_{tlp} observed in response to drought for given species from a global dataset, and that driven by the change in each component pressure-volume parameter alone, using the alternative eqn 2.1a. White bars represent all taxa (n = 25 species and varieties), gray

bars those taxa that decreased in the modulus of elasticity (ε*) in response to drought (n = 14), and black bars those taxa that increased in ε* in response to drought (n = 11).

Supplemental Methods 2.1. Derivation and verification of new fundamental equations

Supplemental Results and Discussion 2.1. Alternative formulation of ε and the impact of apoplastic fraction

Supplemental Results and Discussion 2.2. The role of capacitance and elasticity in drought survival

Table S2.1 Summary of mean values ± standard error from a global database for pressure-volume parameters (see Table 2.1) and for leaf mass per area (LMA) within biome categories, with number of species from each biome represented for each variable, and the p-values for ANOVAs determining the differences among biomes for each variable. Within biomes, tests were made between woody/herbaceous and evergreen/deciduous species, and means for these categories are presented when they showed significant differences in a given parameter.

	π_o (MPa)	π_{tlp} (MPa)	ε (MPa)	a_f	RWC_{tlp} (%)	LMA (g/m^2)
Semidesert	-1.91 ± 0.14 18	-3.05 ± 0.33 10	8.5 ± 1.9 6	0.26 ± 0.02 5	74.4 ± 1.4 8	161 ± 28 5
Med./Temp. Dry	-	-2.49 ± 0.14 27	17.9 ± 2.5 28	0.29 ± 0.04 15	84.0 ± 1.4 15	184 ± 23 25
(Herb)	-1.19 ± 0.11 10	-	-	-	-	-
(Woody)	-2.02 ± 0.09 47	-	-	-	-	-
Mangrove	-2.55 ± 0.34 7	-2.48 ± 0.44 5	11.2 ± 4.1 4	-	-	-
Coastal	-1.39 ± 0.06 24	-1.5 ± 0.08 4	9.2 ± 4.4 2	-	91.7 ± 1.4 2	101 ± 6 3
Temperate Conifer	-1.79 ± 0.13 9	-2.35 ± 0.14 9	17.9 ± 4.5 9	0.26 ± 0.07 5	84.6 ± 3.1 5	211 ± 56 5
Temperate Angio.	-1.68 ± 0.06 61	-2.17 ± 0.07 59	12.4 ± 0.8 60	0.25 ± 0.03 24	83.3 ± 0.8 35	-
(Evergreen)	-	-	-	-	-	192 ± 32 25
(Deciduous)	-	-	-	-	-	81 ± 7 17
Tropical Dry	-	-	15.8 ± 1.1 53	0.17 ± 0.02 8	88.7 ± 0.9 35	-
(Evergreen)	-2.06 ± 0.08 41	-2.50 ± 0.11 40	-	-	-	137 ± 7 27
(Deciduous)	-1.68 ± 0.10 27	-2.11 ± 0.12 27	-	-	-	93 ± 12 17
Tropical Moist	-1.29 ± 0.06 40	-1.48 ± 0.06 50	22.8 ± 2.1 39	0.39 ± 0.04 24	78.6 ± 2.5 36	81 ± 9 11
Crop Herbs	-0.98 ± 0.09 11	-1.24 ± 0.12 10	5.5 ± 0.6 6	0.21 ± 0.07 2	82 ± 7.5 2	-
p (ANOVA)	$< 1 \times 10^{-13}$	$< 1 \times 10^{-15}$	< 0.0001	0.009	< 0.0001	0.008

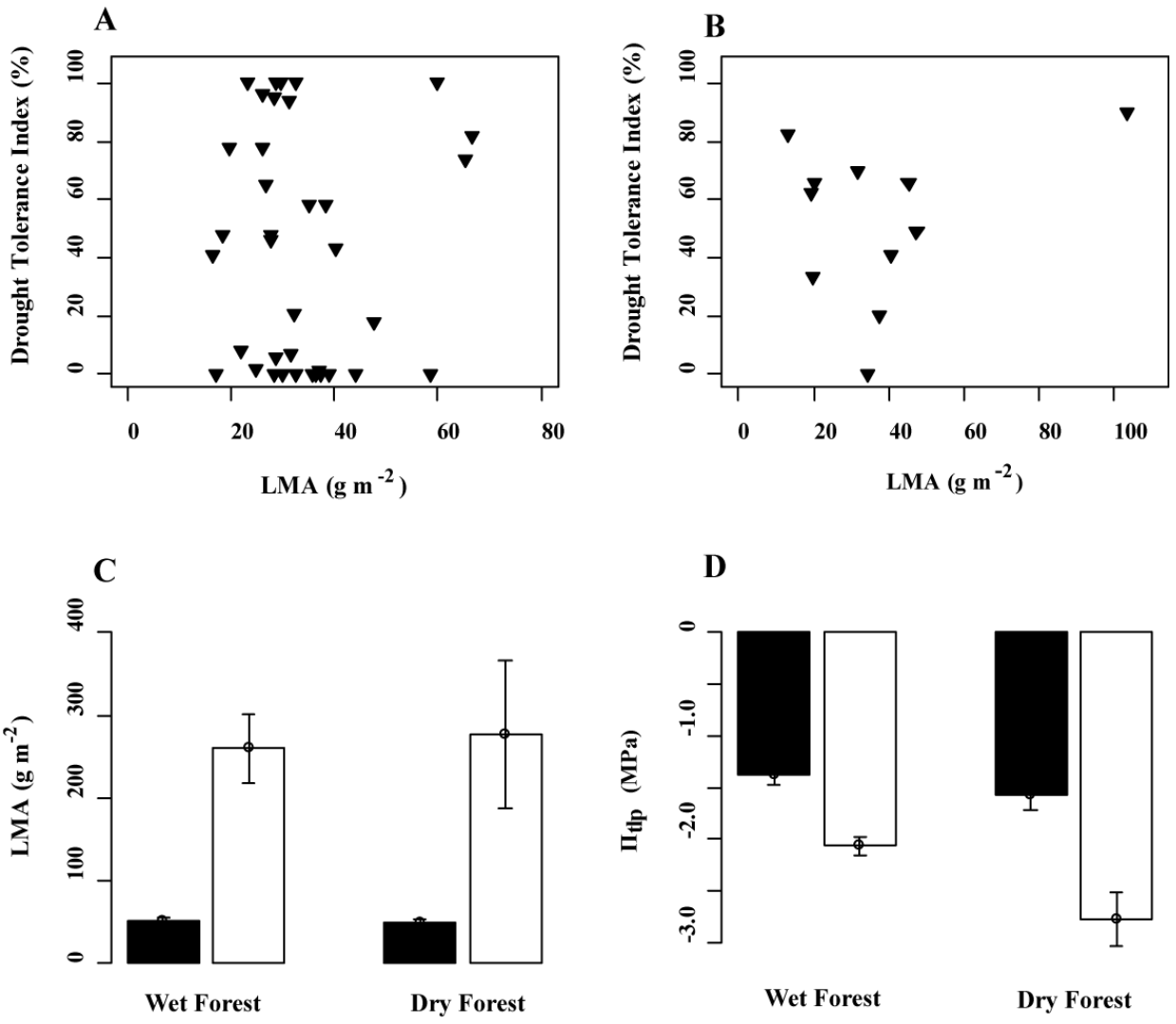
A
Drought Tolerance Index (%)
0
20
40
60
80
100
0
20
40
60
80
LMA (g m -2)
B
Drought Tolerance Index (%)
0
20
40
60
80
100
0
20
40
60
80
100
LMA (g m -2)
C
LMA (g m-2)
0
100
200
300
400
Wet Forest
Dry Forest
D
Πtlp (MPa)
0
-1.0
-2.0
-3.0
Wet Forest
Dry Forest

Figure S2.1

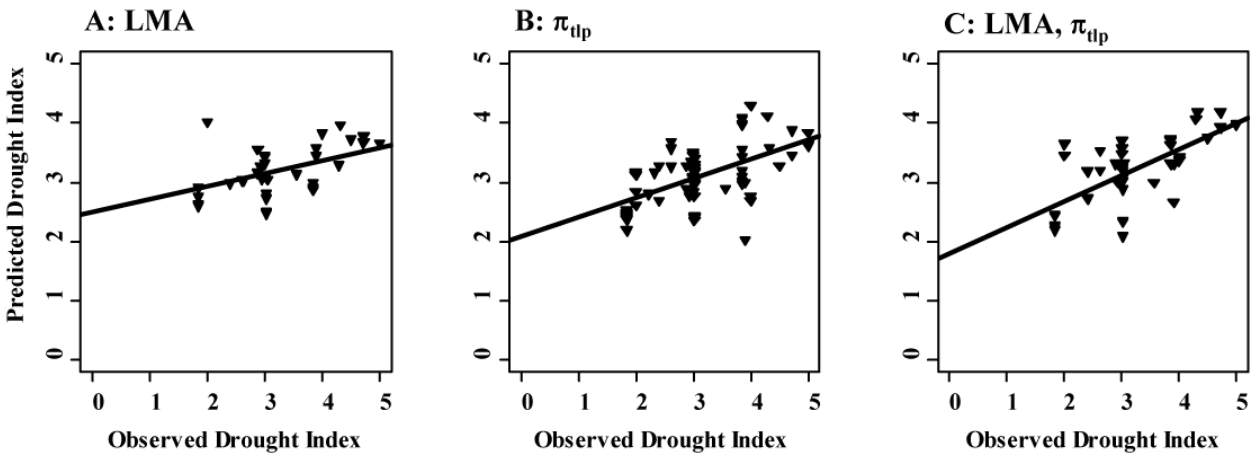
A: LMA
B: π_{tlp}
C: LMA, π_{tlp}
Predicted Drought Index
Observed Drought Index
Observed Drought Index
Observed Drought Index
0
1
2
3
4
5

Figure S2.2

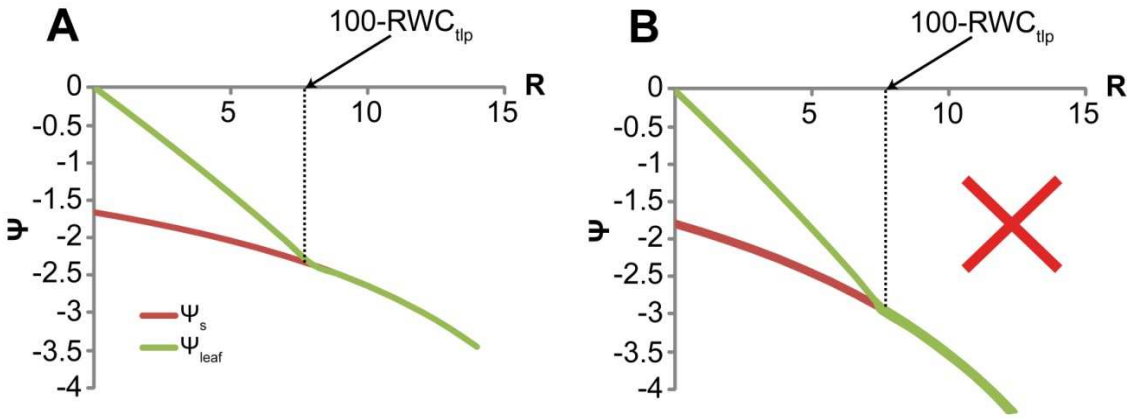

Figure S2.3

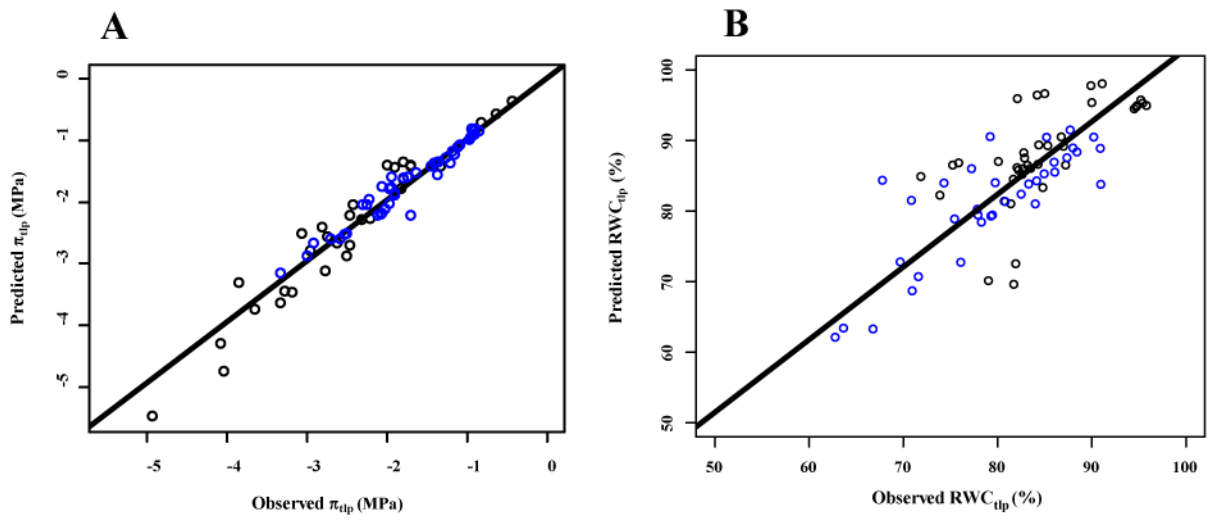
A
Predicted π_{tlp} (MPa)
Observed π_{tlp} (MPa)
0
-1
-2
-3
-4
-5
B
Predicted RWC_{tlp} (%)
Observed RWC_{tlp} (%)
100
90
80
70
60
50

Figure S2.4

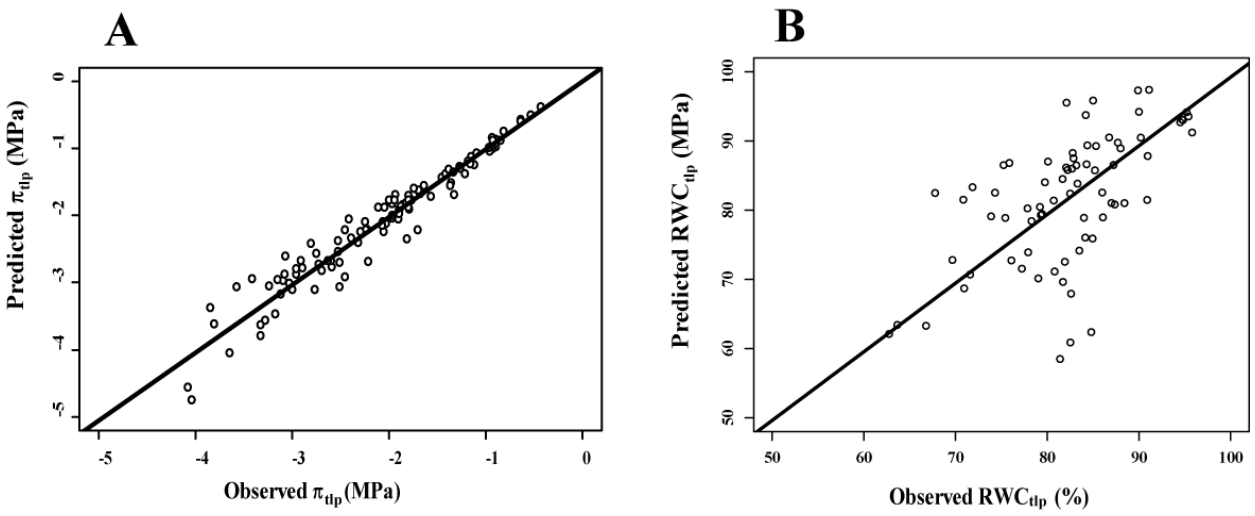
A
Predicted π_{tlp} (MPa)
Observed π_{tlp}(MPa)
B
Predicted RWC_{tlp} (MPa)
Observed RWC_{tlp} (%)

Figure S2.5

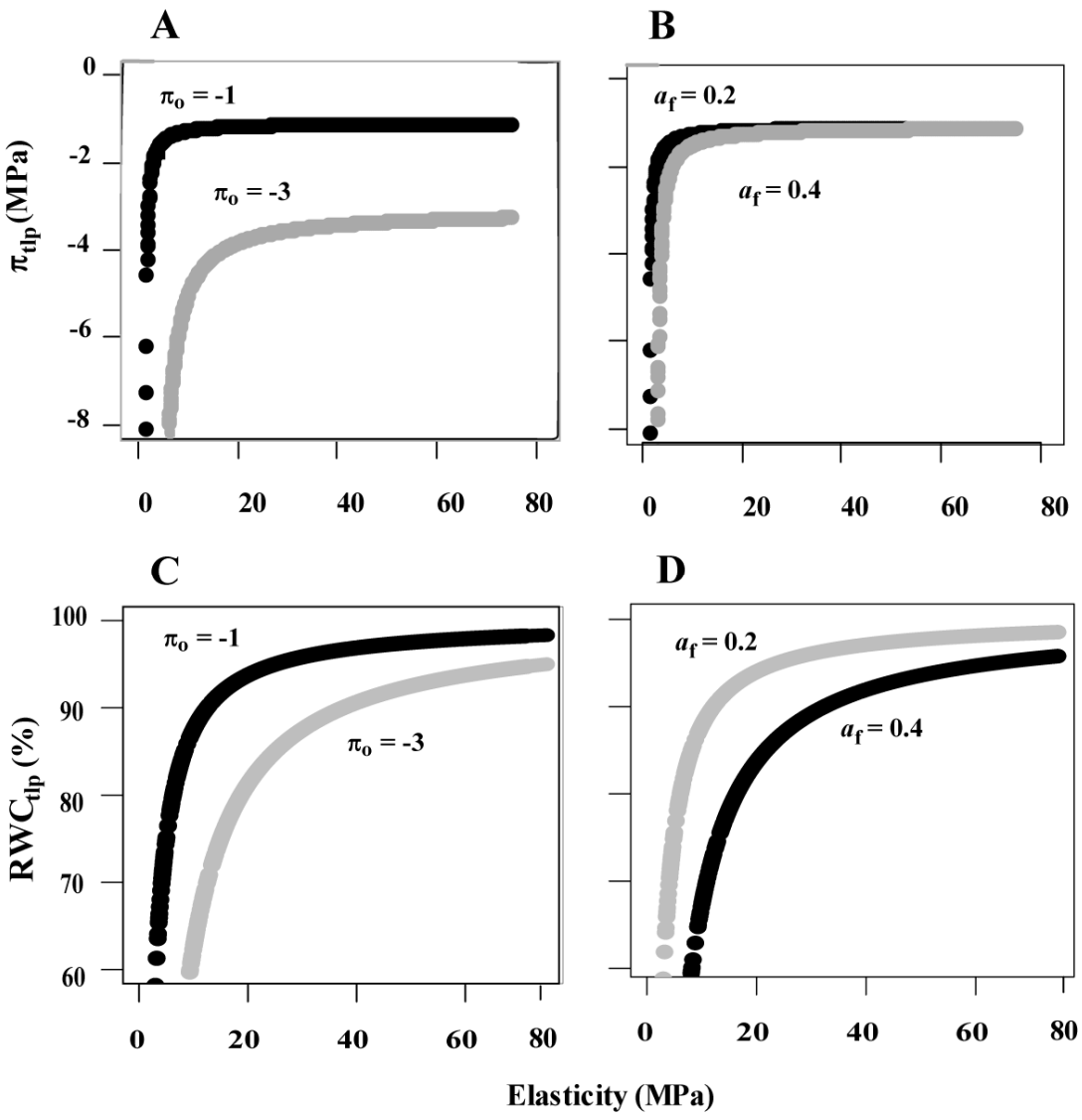
A
B
C
D
π_o = -1
π_o = -3
a_f = 0.2
a_f = 0.4
π_{tlp} (MPa)
RWC_{tlp} (%)
Elasticity (MPa)
0
-2
-4
-6
-8
100
90
80
70
60
0
20
40
60
80

Figure S2.6.

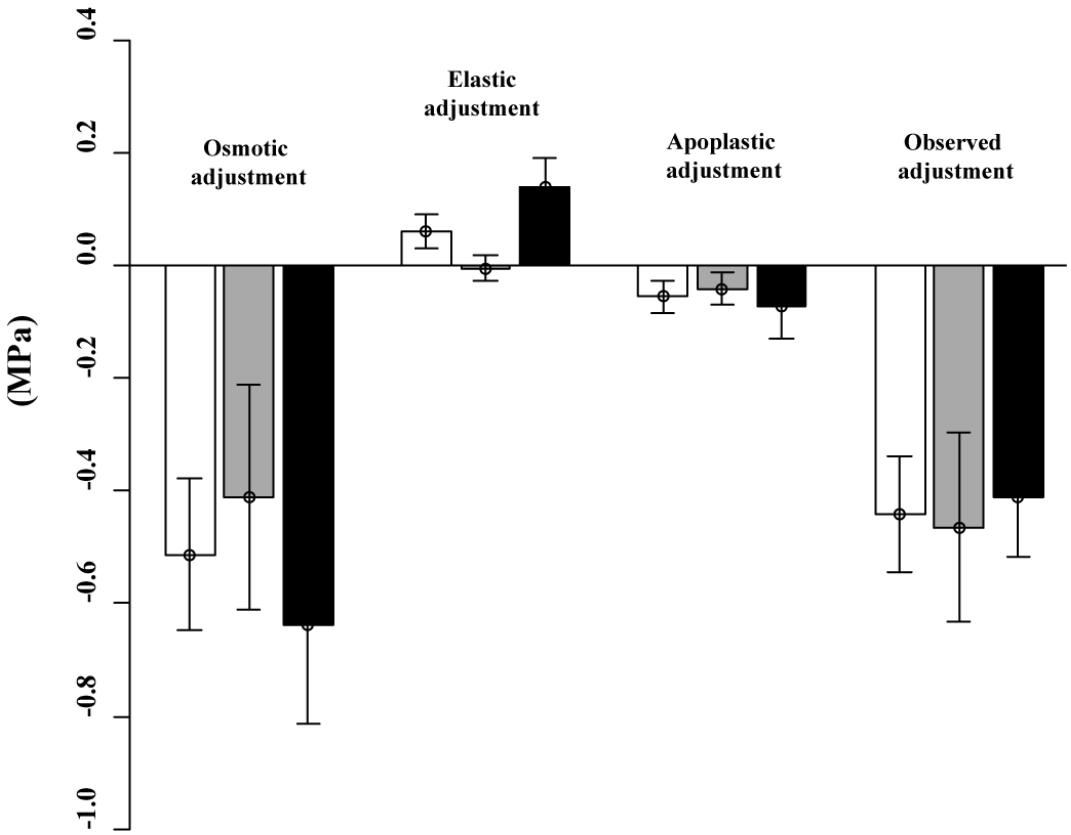
Osmotic adjustment
Elastic adjustment
Apoplastic adjustment
Observed adjustment
(MPa)
0.4
0.2
0.0
-0.2
-0.4
-0.6
-0.8
-1.0

Figure S2.7

REFERENCES

META-ANALYSIS DATA REFERENCES

Abrams MD, Kubiske ME (1990) Photosynthesis and water relations during drought in *Acer rubrum* L. genotypes from contrasting sites in central Pennsylvania. *Funct Ecol* 4: 727-733.

Abrams MD, Kubiske ME, Steiner KC (1990) Drought adaptations and responses in five genotypes of *Fraxinus pennsylvanica* Marsh.: photosynthesis, water relations, and leaf morphology. *Tree Physiol* 6: 305-315.

Abrams MD, Kloeppel BD, Kubiske ME (1992) Ecophysiological and morphological responses to shade and drought in two contrasting ecotypes of *Prunus serotina*. *Tree Physiol* 10: 343-355.

Alsina MM, De Herralde F, Aranda X, Save R, Biel C (2007) Water relations and vulnerability to embolism are not related: Experiments with eight grapevine cultivars. *Vitis* 46: 1-6

Aranda I, Gil L, Pardos J (1996) Seasonal water relations of three broadleaved species (*Fagus sylvatica* L., *Quercus petraea* (Mattuschka) Liebl. and *Quercus pyrenaica* Willd.) in a mixed stand in the centre of the Iberian Peninsula. *Forest Ecol Manage* 84: 219-229.

Bacelar EA et al. (2006) Immediate responses and adaptive strategies of three olive cultivars under contrasting water availability regimes: Changes on structure and chemical composition of foliage and oxidative damage. *Plant Science* 170: 596-605.

Badalotti A, Anfodillo T, Grace J (2000) Evidence of osmoregulation in *Larix decidua* at alpine treeline and comparative responses to water availability of two co-occurring evergreen species. *Ann For Sci* 57: 623-633.

Bakul MRA, Akter MS, Islam MN, Chowdhury MMAA, Roy MC (2010) Effect of water stress on physiological characters and yield in some mutants T-Aman rice lines. Bangladesh Res. Pub. J. 3(3): 1095-1106

Baltzer JL, Davies SJ, Bunyavejchewin S, Noor NSM (2008) The role of desiccation tolerance in determining tree species distributions along the Malay-Thai Peninsula. *Funct Ecol* 22: 221-231.

Baltzer JL, Gregoire DM, Bunyavejchewin S, Noor NSM, Davies SJ (2009) Coordination of foliar and wood anatomical traits contributes to tropical tree distributions and productivity along the Malay-Thai Peninsula. American Journal of Botany 96(12): 2214-2223.

Barnes PW (1985) Adaptation to water stress in the big bluestem-sand bluestem complex. *Ecology* 66: 1908-1920.

Blackman C.J., Brodribb T.J. & Jordan G.J. (2010). Leaf hydraulic vulnerability is related to conduit dimensions and drought resistance across a diverse range of woody angiosperms. *New Phytol.*, 188, 1113-1123.

Blake TJ, Li J (2003) Hydraulic adjustment in jack pine and black spruce seedlings under controlled cycles of dehydration and rehydration. *Physiol Plant* 117 (4): 532-539.

Bowman WD, Strain BR (1988) Physiological responses in two populations of *Andropogon glomeratus* to short-term salinity. *Oecologia* 75: 78-82.

Burghardt M, Riederer M (2003) Ecophysiological relevance of cuticular transpiration of deciduous and evergreen plants in relation to stomatal closure and leaf water potential. *J Exp Bot* 54: 1941-1949.

Castell C, Terradas J (1995) Water relations, gas exchange and growth of dominant and suppressed shoots of *Arbutus unedo* L. *Tree Physiol* 15: 405-409.

Castro-Diez P, Navarro J (2007) Water relations of seedlings of three *Quercus* species: variations across and within species grown in contrasting light and water regimes. *Tree Physiol* 27: 1011-1018.

Chimenti CA, Hall AJ (1994) Responses to water stress of apoplastic water fraction and bulk modulus of elasticity in sunflower (*Helianthus annus* L.) genotypes of contrasting capacity for osmotic adjustment. *Plant Soil* 166: 101-107.

Choat B, Sack L, Holbrook NM (2007) Diversity of hydraulic traits in nine *Cordia* species growing in tropical forests with contrasting precipitation. *New Phytol* 175(4): 686-698.

Clifford SC et al. (1998) The role of solute accumulation, osmotic adjustment, and changes in cell wall elasticity in drought tolerance in *Ziziphus mauritiana* (Lamk.). *J Exp Bot* 49: 967-977.

Correia MJ, Coelho D, David MM (2001) Response to seasonal drought in three cultivars of *Ceratonia siliqua*: leaf growth and water relations. *Tree Physiol* 21: 645-653.

Corcuera L, Camero JJ, Gil-Pelegrin E (2002) Functional groups in *Quercus* species derived from the analysis of pressure-volume curves. *Trees* 16: 465-472.

Dawson TE, Bliss LC (1989) Patterns of water use and the tissue water relations in the dioecious shrub, *Salix arctica*: the physiological basis for habitat partitioning between the sexes. *Oecologia* 79(3): 332-343.

Dichio B et al. (2003) Drought-induced variations of water relations parameters in *Olea europaea. Plant Soil* 257: 381-389.

Downton WJS (1982) Growth and osmotic relations of the mangrove *Avicennia marina*, as influenced by salinity. *Aust J Plant Physiol* 9: 519-528.

Foreseth IN, Erhleringer JR (1982) Ecophysiology of two solar tracking desert winter annuals. *Oecologia* 54: 41-49.

Gonzalez- Rodriguez AM, Jimenez MS, Morales D, Aschan G, Losch R (1999) Physiological responses of *Laurus azorica* and *Viburnum rigidum* to drought stress: osmotic adjustment and tissue elasticity. *Phyton* 39: 251-263.

Groom PK, Lamont BB (1997) Xerophytic implications of increased sclerophylly: interactions with water and light in *Hakea psilorrhyncha* seedlings. *New Phytol* 136: 231-237.

Guarnaschelli AB, Prystupa P, Lemcoff JH (2006) Drought conditioning improves water status, stomatal conductance and survival of Eucalyptus globulus subsp. bicostata seedlings. *Am Forest Sci* 63: 941-950.

Hao GY et al. (2008) Stem and leaf hydraulics of congeneric tree species from adjacent tropical savanna and forest ecosystems. *Oecologia* 155: 405-415

Hao GY, Sack L, Wang AY, Cao KF, Guillermo G (2010) Differentiation of leaf water flux and drought tolerance traits in hemiepiphytic and non-hemiepiphytic *Ficus* tree species. *Funct Ecol* 24: 731-740.

Henson IE (1984) Effects of atmospheric humidity on abscisic-acid accumulation and water status in leaves of rice (*Oryza sativa*). *Annals of Botany* 54: 569-582

Herppich WB, von Willert DJ (1995) Dynamic changes in leaf bulk water relations during stomatal oscillations in mangrove species. Continuous analysis using a dewpoint hygrometer. *Physiol Plant* 94: 479-485.

Hietz P, Briones O (1998) Correlation between water relations and within-canopy distribution of epiphytic ferns in a Mexican cloud forest. *Oecologia* 114: 305-316.

Holbrook NM, Sinclair TR (1992) Water balance in the arborescent palm, *Sabal palmetto.* I. Stem structure, tissue water release properties and leaf epidermal conductance. *Plant Cell Environ* 15: 393-399.

Hunt ER, Nobel PS (1987) Non-steady-state water flow for three desert perennials with different capacitances. *Aust J Plant Physiol* 14(4): 363-375.

Jackson PA, Spomer GG (1979) Biophysical adaptations of four western conifers to habitat water conditions. *Botanical Gazette* 140: 428-432.

Joly JJ, Zaerr JB (1987) Alteration of cell-wall elastic content and elasticity in Douglas fir during periods of water deficit. *Plant Physiol* 83: 418-442.

Kissel RM, Wilson TB, Bannister P, Mark AF (1987) Water relations of some native and exotic shrubs of New Zealand. *New Phytol* 107: 29-37.

Kubiske ME, Abrams MD (1991) Seasonal, diurnal, and rehydration-induced variation of pressure-volume relationships in *Psuedotsuga menziesii*. *Physiol Plant* 83: 107-116.

Kubiske ME, Pregitzer KS (1997) Ecophysiological responses to simulated canopy gaps of two tree species of contrasting shade tolerance in elevated CO_2. *Funct Ecol* 11: 24-32.

Lemcoff JH, Guarnachelli AB, Garau AM, Prystupa P (2002) Elastic and osmotic adjustments in rooted cuttings of several clones of *Eucalyptus camadulensis* Dehn. From southeastern Australia after a drought. *Flora* 197: 134-142.

Le Roux X, Bariac T (1998) Seasonal variations in soil, grass and shrub water status in a West African humid savanna. *Oecologia* 113: 456-466.

Lo Gullo MA, Salleo S (1988) Different strategies of drought resistance in three Mediterranean sclerophyllous trees growing in the same environmental conditions. *New Phytol* 108: 267-276.

Loveless, AR (1962) Further evidence to support a nutritional interpretation of sclerophylly. *Ann Bot* 26: 551-561.

Maatallah S, Ghanem ME, Albouchi A, Bizid E, Lutts S (2010) A greenhouse investigation of responses to different water stress regimes of *Laurus nobilis* trees from two climatic regions. *J Arid Environ* 74(3): 327-337.

Ma CC et al. (2008) Physiological adaptations of four dominant *Caragana* species in the desert region of the Inner Mongolia Plateau. *J Arid Environ* 72: 247-254.

Major JE, Johnsen KH (1999) Shoot water relations of mature black spruce families displaying a genotype × environment interaction in growth rate. II. Temporal trends and response to varying soil water conditions. *Tree Physiol* 19: 375-382.

Maury P, Berger M, Mojayad F, Planchon C (2000) Leaf water characteristics and drought acclimation in sunflower genotypes. *Plant Soil 223*: 153-160.

Meinzer FC, Grantz DA, Goldstein G, Saliendra NZ (1990) Leaf water relations and maintenance of gas-exchange in coffee cultivars grown in drying soil. *Plant Physiol* 94: 1781-1787.

Merchant A, Callister A, Arndt S, Tausz M, Adams M (2007) Contrasting physiological responses of six *Eucalyptus* species to water deficit. *Ann Bot* 100: 1507-1515.

Miller PC, Hom J, Poole DK (1975) Water relations of three mangrove species in South Florida. *Oecologia Plantarum* 10(4): 355-367.

Morant-Manceau A, Pradier E, Tremblin G (2004) Osmotic adjustment, gas exchanges and chlorophyll fluorescence of a hexaploid triticale and its parental species under salt stress. *J Plant Physiol* 161: 25-33.

Nardini A, Gortan E, Ramani M, Salleo S (2008) Heterogeneity of gas exchange rates over the leaf surface in tobacco: an effect of hydraulic architecture? *Plant Cell Environ* 31: 804-812.

Ngugi MR, Doley D, Hunt MA, Dart P, Ryan P (2003) Leaf water relations of *Eucalyptus cloeziana* and *Eucalyptus argophloia* in response to water deficit. *Tree Physiol* 23: 335-343.

Nilsen ET, Sharifi MR, Rundel PW (1984) Comparative water relations of phreatophytes in the Sonoran Desert of California. *Ecology* 65: 767-778.

Olivares E, Medina E (1992) Water and nutrient relations of woody perennials from tropical dry forests. *J Veg Sci* 3(3): 383-392.

Pardos A, Gil L, Aranda I (2004) Osmotic adjustment in two temperate oak species [*Quercus pyrenaica* Willd and *Quercus petraea* (Matt.) Liebl] of the Iberian Peninsula in response to drought. *Sistemas y recursos forestales* 13: 339-346.

Parker WC, Colombo SJ (1995) A critical re-examination of pressure-volume analysis of conifer shoots: comparison of three procedures for generating PV curves on shoots of *Pinus resinosa* Ait. seedlings. *J Exp Bot* 46: 1701-1709.

Rada F et al. (1989) Osmotic and turgor relations of three mangrove ecosystem species. *Aust J Plant Physiol* 16: 477-486.

Reekie JY, Struik PC, Hicklenton PR, Duval JR (2007) Prohexadione-calcium changes morphological and physiological traits in strawberry plants and preconditions transplants to water stress. *Eur J Hort Sci* 72: 158-163

Ripley BS, Pammenter NW (2004) Do low standing biomass and leaf area index of sub-tropical coastal dunes ensure that plants have an adequate supply of water? *Oecologia* 139: 535-544.

Rodrigues ML, Pacheco CMA, Chaves MM (1995) Soil-plant water relations, root distribution and biomass partitioning in *Lupinus albus* L. under drought conditions. *J Exp Bot* 289: 947-956.

Rosado BHP, De Mattos EA (2010) Interspecific variation of functional traits in a CAM-tree dominated sandy coastal plain. *J Veg Sci* 21: 43-54.

Saito T, Terashima I (2004) Reversible decreases in the bulk elastic modulus of mature leaves of deciduous *Quercus* species subjected to two drought treatments. *Plant Cell Environ* 27: 863-875.

Sanchez FJ, de Andres EF, Tenorio JL, Ayerbe L (2004) Growth of epicotyls, turgor maintenance and osmotic adjustment in pea plants (*Pisum sativum* L.) subjected to water stress. *Field Crops R* 86: 81-90

Sanchez-Blanco MJ, Morales MA, Torrecillas A, Alarcon JJ (1998) Diurnal and seasonal osmotic potential changes in *Lotus creticus creticus* plants grown under saline stress. *Plant Sci* 136: 1-10.

Sanchez-Blanco MJ, Alvarez S, Navarro A, Banon S (2009) Changes in leaf water relations, gas exchange, growth and flowering quality in potted geranium plants irrigated with different water regimes. *J Plant Physiol* 166: 467-476

Scoffoni C, Pou A, Aasamaa K, Sack L (2008) The rapid light response of leaf hydraulic conductance: new evidence from two experimental methods. *Plant Cell Environ* 13: 1803-1812.

Scoffoni C, Rawls M, McKown A, Cochard H, Sack L (2011) Decline of leaf hydraulic conductance with dehydration: relationship to leaf size and venation architecture. *Plant Physiol* 156: 832-843.

Shrestha BB, Uprety Y, Nepal K, Tripathi S, Jha PK (2007) Phenology and water relations of eight woody species in the Coronation Garden of Kirtipur, central Nepal. *Himalayan J Sci* 4(6): 49-56.

Sinclair R (1983) Water relations of tropical epiphytes. *J Exp Bot* 34(149): 1652-1663.

Sobrado MA (1986) Tissue water relations and leaf growth of tropical corn cultivars under water deficits. *Plant Cell Environ* 9: 451-457

Storey R, Ahmad N, Wyn Jones RG (1977) Taxonomic and ecological aspects of the distribution of glycinebetaine and related compounds in plants. *Oecologia* 27: 319-332.

Suarez N, Sobrado MA, Medina E (1998) Salinity effects on the leaf water relations components and ion accumulation patterns *in Avicennia germinans* (L.) L. seedlings. *Oecologia* 114: 299-304.

Torrecillas A, Alarcon JJ, Sanchezblanco MJ, Bolarin MC (1994) Osmotic adjustment in leaves of *Lycopersicon esculentum* and *L. pennellii* in response to saline water irrigation. Biologia Plantarum 36: 247-254

Wan C, Sosebee RE, McMichael BL (1993) Drought-induced changes in water relations in broom snakeweed (*Gutierrezia sarothrae*) under greenhouse- and field-grown conditions. *Environm Ex Bot* 33(2): 323-330.

Wenhui Z (1998) Water relations balance parameters of 30 woody species from Cerrado vegetation in the wet and dry season. *J Forest Res* 9: 233-239.

White DA, Turner NC, Galbraith JH(2000) Leaf water relations and stomatal behavior of four allopatric *Eucalyptus* species planted in Mediterranean southwestern Australia. *Tree Physiol* 20: 1157-1165.

Whitfield, CJ (1932) Osmotic concentrations of chaparral, coastal sagebrush, and dune species of Southern California. *Ecology* 13: 279-285.

TEXT REFERENCES

Abrams M.D. & Kubiske M.E. (1990). Photosynthesis and water relations during drought in *Acer rubrum* L genotypes from contrasting sites in central Pennsylvania. *Funct. Ecol.*, 4, 727-733.

Ackerly D.D. (2004). Adaptation, niche conservatism, and convergence: Comparative studies of leaf evolution in the California chaparral. *Am. Nat.*, 163, 654-671.

Baltzer J.L., Davies S.J., Bunyavejchewin S. & Noor N.S.M. (2008). The role of desiccation tolerance in determining tree species distributions along the Malay-Thai Peninsula. *Funct. Ecol.*, 22, 221-231.

Baltzer J.L., Gregoire D.M., Bunyavejchewin S., Noor N.S.M. & Davies S.J. (2009). Coordination of foliar and wood anatomical traits contributes to tropical tree distributions and productivity along the Malay-Thai peninsula. *Am. J. Bot.*, 96, 2214-2223.

Blackman C.J., Brodribb T.J. & Jordan G.J. (2010). Leaf hydraulic vulnerability is related to conduit dimensions and drought resistance across a diverse range of woody angiosperms. *New Phytol.*, 188, 1113-1123.

Blackman C.J., Brodribb T.J. & Jordan G.J. (2012). Leaf hydraulic vulnerability influences species' bioclimatic limits in a diverse group of woody angiosperms. *Oecologia*, in press, Early Access Online.

Blewett J., Burrows K. & Thomas C. (2000). A micromanipulation method to measure the mechanical properties of single tomato suspension cells. *Biotechnology Letters*, 22, 1877-1883.

Bonan G.B. (2008). Forests and climate change: forcings, feedbacks, and the climate benefits of forests. *Science*, 320, 1444-1449.

Bowman W.D. & Roberts S.W. (1985). Seasonal changes in tissue elasticity in chaparral shrubs. *Physiol. Plant.*, 65, 233-236.

Brodribb T.J. & Holbrook N.M. (2003). Stomatal closure during leaf dehydration, correlation with other leaf physiological traits. *Plant Physiol.*, 132, 2166-2173.

Brodribb T.J. & Holbrook N.M. (2005). Leaf physiology does not predict leaf habit; examples from tropical dry forest. *Trees-- Structure and Function*, 19, 290-295.

Buckley R.C., Corlett R.T. & Grubb P.J. (1980). Are the xeromorphic trees of tropical upper montane rain forests drought-resistant? *Biotropica*, 12, 124-136.

Carpita N.C. (1985). Tensile strength of cell walls of living cells. *Plant Physiol.*, 79, 485-488.

Chaves M.M., Pereira J.S., Maroco J., Rodrigues M.L., Ricardo C.P.P., Osorio M.L., Carvalho I., Faria T. & Pinheiro C. (2002). How plants cope with water stress in the field: photosynthesis and growth. *Ann. Bot.*, 89, 907-916.

Chesson P., Gebauer R.L.E., Schwinning S., Huntly N., Wiegand K., Ernest M.S.K., Sher A., Novoplansky A. & Weltzin J.F. (2004). Resource pulses, species interactions, and diversity maintenance in arid and semi-arid environments. *Oecologia*, 141, 236-253.

Cheung Y.N.S., Tyree M.T. & Dainty J. (1975). Water relations parameters on single leaves obtained in a pressure bomb and some ecological interpretations. *Canadian Journal of Botany*, 53, 1342-1346.

Chimenti C.A. & Hall A.J. (1994). Responses to water stress of apoplastic water fraction and bulk modulus of elasticity in sunflower (*Helianthus annuus* L) genotypes of contrasting capacity for osmotic adjustment. *Plant Soil*, 166, 101-107.

Cutler J.M., Rains D.W. & Loomis R.S. (1977). The importance of cell size in the water relations of plants. *Physiologia Plantarum*, 40, 255-260.

Davies W.J. & Zhang J.H. (1991). Root signals and the regulation of growth and development of plants in drying soil. *Annu. Rev. Plant Physiol. Plant Molec. Biol.*, 42, 55-76.

Engelbrecht B.M.J., Comita L.S., Condit R., Kursar T.A., Tyree M.T., Turner B.L. & Hubbell S.P. (2007). Drought sensitivity shapes species distribution patterns in tropical forests. *Nature*, 447, 80-U2.

Engelbrecht B.M.J. & Kursar T.A. (2003). Comparative drought-resistance of seedlings of 28 species of co-occurring tropical woody plants. *Oecologia*, 136, 383-393.

Feeley K.J., Davies S.J., Perez R., Hubbell S.P. & Foster R.B. (2011). Directional changes in the species composition of a tropical forest. *Ecology*, 92, 871-882.

Goldstein G. & Nobel P.S. (1991). Changes in osmotic pressure and mucilage during low temperature acclimation of *Opuntia ficus-indica*. *Plant Physiol.*, 97, 954-961.

Gonzalez A., Martin I. & Ayerbe L. (1999). Barley yield in water-stress conditions. The influence of precocity, osmotic adjustment and stomatal conductance. *Field Crop. Res.*, 62, 23-34.

Grierson C.S., Barnes S.R., Chase M.W., Clarke M., Grierson D., Edwards K.J., Jellis G.J., Jones J.D., Knapp S., Oldroyd G., Poppy G., Temple P., Williams R. & Bastow R. (2011). One hundred important questions facing plant science research. *New Phytol.*, 192, 6-12.

Groom P.K. & Lamont B.B. (1999). Which common indices of sclerophylly best reflect differences in leaf structure? *Ecoscience*, 6, 471-474.

Grubb P.J. (1986). Sclerophylls, pachyphylls and pycnophylls: nature and significance of hard leaf surfaces. In: *Insects and the Plant Surface* (eds. Juniper B & Southwood SR). Arnold London, pp. 137-150.

Guyot G., Scoffoni C. & Sack L. (2012). Combined impacts of irradiance and dehydration on leaf hydraulic conductance: insights into vulnerability and stomatal control. *Plant, Cell & Environment*, in press.

Höfler K. (1920). Ein schema für die osmotiche leistung der pflanzenzelle. (A graph for the osmotic potential of plant cells.). *Berichte der deutschen botanishen Gesellschaft. (Journal of the German Botanical Society).* 26, 414-422.

Iraki N.M., Bressan R.A., Hasegawa P.M. & Carpita N.C. (1989). Alteration of the physical and chemical structure of the primary cell wall of growth-limied plant cells adapted to osmotic stress. *Plant Physiol.*, 91, 39-47.

Jenks M.A. & Wood A.J. (2007). *Plant Desiccation Tolerance*. Wiley, New York.

Joly R.J. & Zaerr J.B. (1987). Alteration of cell wall water content and elasticity in Douglas fir during periods of water deficit. *Plant Physiol.*, 83, 418-422.

Jones H.G. (1992). *Plants and Microclimate, 2nd ed.* Cambridge University Press, Cambridge.

Koide R.T., Robichaux R.H., Morse S.R. & Smith C.M. (2000). Plant water status, hydraulic resistance and capacitance. In: *Plant Physiological Ecology: Field Methods and Instrumentation* (eds. Pearcy RW, Ehleringer JR, Mooney HA & Rundel PW). Kluwer Dordrecht, the Netherlands, pp. 161-183.

Kozlowski T.T. & Pallardy S.G. (2002). Acclimation and adaptive responses of woody plants to environmental stresses. *Bot. Rev.*, 68, 270-334.

Kramer P.J. (1988). Changing concepts regarding plant water relations: opinon. *Plant Cell Environ.*, 11, 565-568.

Kramer P.J. & Boyer J.S. (1995). *Water relations of plants and soils*. Academic Press, San Diego, California.

Kubiske M.E. & Abrams M.D. (1991). Seasonal, diurnal and rehydration-induced variation of pressure-volume relationships in *Pseudotsuga menziesii*. *Physiol. Plant.*, 83, 107-116.

Lamont B.B., Groom P.K. & Cowling R.M. (2002). High leaf mass per area of related species assemblages may reflect low rainfall and carbon isotope discrimination rather than low phosphorus and nitrogen concentrations. *Funct. Ecol.*, 16, 403-412.

Larcher W. (2003). *Physiological Plant Ecology, 4th ed.* Springer, Berlin.

Lawlor D.W. & Cornic G. (2002). Photosynthetic carbon assimilation and associated metabolism in relation to water deficits in higher plants. *Plant Cell Environ.*, 25, 275-294.

Lenz T.I., Wright I.J. & Westoby M. (2006). Interrelations among pressure-volume curve traits across species and water availability gradients. *Physiol. Plant.*, 127, 423-433.

Loik M.E. & Nobel P.S. (1991). Water relations and mucopolysaccharide increases for a winter hardy cactus during acclimation to subzero temperatures. *Oecologia*, 88, 340-346.

Loveless A.R. (1961). A nutritional interpretation of sclerophylly based on differences in the chemical composition of sclerophyllous and mesophytic leaves. *Annals of Botany*, 25, 168-&.

Lusk C.H., Reich P.B., Montgomery R.A., Ackerly D.D. & Cavender-Bares J. (2008). Why are evergreen leaves so contrary about shade? *Trends Ecol. Evol.*, 23, 299-303.

Markesteijn L., Poorter L., Paz H., Sack L., Paz H. & Bongers L. (2011a). Ecological differentiation in xylem cavitation resistance is associated with stem and leaf structural traits. *Plant, Cell & Environment*, 34, 137-148.

Markesteijn L., Poorter L., Paz H., Sack L., Paz H. & Bongers L. (2011b). Hydraulic niche partitioning among saplings of tropical dry forest species: coordination of species moisture and light requirements. *New Phytol.*, in press.

McDowell N.G. (2011). Mechanisms linking drought, hydraulics, carbon metabolism, and vegetation mortality. *Plant Physiol.*, 155, 1051-1059.

Merchant A., Callister A., Arndt S., Tausz M. & Adams M. (2007). Contrasting physiological responses of six Eucalyptus species to water deficit. *Ann. Bot.*, 100, 1507-1515.

Mitchell P.J., Veneklaas E.J., Lambers H. & Burgess S.S.O. (2008). Leaf water relations during summer water deficit: differential responses in turgor maintenance and variation in leaf structure among different plant communities in south-western Australia. *Plant Cell Environ.*, 31, 1791-1802.

Mooney H.A., Field C., Gulmon S.L., Rundel P. & Kruger F.J. (1983). Photosynthetic Characteristic of South-African Sclerophylls. *Oecologia*, 58, 398-401.

Moore J.P., Vicre-Gibouin M., Farrant J.M. & Driouich A. (2008). Adaptations of higher plant cell walls to water loss: drought vs desiccation. *Physiol. Plant.*, 134, 237-245.

Niinemets U. (2001). Global-scale climatic controls of leaf dry mass per area, density, and thickness in trees and shrubs. *Ecology*, 82, 453-469.

Niinemets U. & Valladares F. (2006). Tolerance to shade, drought, and waterlogging of temperate Northern Hemisphere trees and shrubs. *Ecol. Monogr.*, 76, 521-547.

Nobel P.S. (2009). *Physicochemical and Environmental Plant Physiology, 5th edition*. Academic Press, San Diego.

Ogburn R.M. & Edwards E.J. (2010). The ecological water-use strategies of succulent plants. In: *Advances in Botanical Research, Vol 55* (ed. Kader JCDM), pp. 179-225.

Orians G.H. & Solbrig O.T. (1977). Cost-income model of leaves and roots with special reference to arid and semiarid areas. *Am. Nat.*, 111, 677-690.

Poorter H., Niinemets U., Poorter L., Wright I.J. & Villar R. (2009). Causes and consequences of variation in leaf mass per area (LMA): a meta-analysis. *New Phytol.*, 182, 565-588.

Poorter L. & Markesteijn L. (2008). Seedling traits determine drought tolerance of tropical tree species. *Biotropica*, 40, 321-331.

Prentice I.C., Cramer W., Harrison S.P., Leemans R., Monserud R.A. & Solomon A.M. (1992). A global biome model based on plant physiology and dominance, soil properties and climate. *Journal of Biogeography*, 19, 117-134.

Read J. & Sanson G.D. (2003). Characterizing sclerophylly: the mechanical properties of a diverse range of leaf types. *New Phytol.*, 160, 81-99.

Read J., Sanson G.D., de Garine-Wichatitsky M. & Jaffre T. (2006). Sclerophylly in two contrasting tropical environments: Low nutrients vs. low rainfall. *Am. J. Bot.*, 93, 1601-1614.

Richter H. (1978). Diagram for description of water relations in plant cells and organs. *J. Exp. Bot.*, 29, 1197-1203.

Sack L. (2004). Responses of temperate woody seedlings to shade and drought: do trade-offs limit potential niche differentiation? *Oikos*, 107, 110-127.

Sack L., Cowan P.D., Jaikumar N. & Holbrook N.M. (2003). The 'hydrology' of leaves: co-ordination of structure and function in temperate woody species. *Plant, Cell and Environment*, 26, 1343-1356.

Salleo S. & Nardini A. (2000). Sclerophylly: evolutionary advantage or mere epiphenomenon? *Plant Biosyst.*, 134, 247-259.

Salleo S., Nardini A. & LoGullo M.A. (1997). Is sclerophylly of Mediterranean evergreens an adaptation to drought? *New Phytol.*, 135, 603-612.

Schulte P.J. (1992). The units of currency for plant water status. *Plant Cell Environ.*, 15, 7-10.

Schulte P.J. & Hinckley T.M. (1985). A comparison of pressure-volume curve data analysis techniques. *J. Exp. Bot.*, 36, 1590-1602.

Scoffoni C., McKown A.D., Rawls M. & Sack L. (2012). Dynamics of leaf hydraulic conductance with water status: quantification and analysis of species differences under steady-state. *J. Exp. Bot.*, in press.

Scoffoni C., Rawls M., McKown A., Cochard H. & Sack L. (2011). Decline of leaf hydraulic conductance with dehydration: relationship to leaf size and venation architecture. *Plant Physiol.*, 156, 832-843.

Sheffield J. & Wood E.F. (2008). Global trends and variability in soil moisture and drought characteristics, 1950-2000, from observation-driven simulations of the terrestrial hydrologic cycle. *Journal of Climate*, 21, 432-458.

Sinclair T.R. & Ludlow M.M. (1985). Who taught plants thermodynamics? The unfulfilled potential of plant water potential. *Aust. J. Plant Physiol.*, 12, 213-217.

Sokal R.R. & Rohlf F.J. (1995). *Biometry, 3rd ed.* W.H. Freeman, New York.

Trifilo P., Gasco A., Raimondo F., Nardini A. & Salleo S. (2003). Kinetics of recovery of leaf hydraulic conductance and vein functionality from cavitation-induced embolism in sunflower. *J. Exp. Bot.*, 54, 2323-2330.

Tyree M.T. (1981). The relationship between the bulk modulus of elasticity of a complex tissue and the mean modulus of its cells. *Ann. Bot.*, 47, 547-559.

Tyree M.T. & Hammel H.T. (1972). Measurement of turgor pressure and water relations of plants by pressure bomb technique. *J. Exp. Bot.*, 23, 267-282.

Veihmeyer F.J. & Hendrickson A.H. (1928). Soil moisture at permanent wilting of plants. *Plant Physiol.*, 3, 355-357.

Walter H. (1985). *Vegetation of the Earth*. 3rd edn. Springer-Verlag, Berlin.

Walter H. & Stadelmann E.J. (1968). The physiological prerequisites for the transition of autotrophic plants from water to terrestrial life. *Bioscience*, 18, 694-701.

Walters M.B. & Reich P.B. (1999). Low-light carbon balance and shade tolerance in the seedlings of woody plants: do winter deciduous and broad-leaved evergreen species differ? *New Phytol.*, 143, 143-154.

Wright I.J., Reich P.B., Cornelissen J.H.C., Falster D.S., Groom P.K., Hikosaka K., Lee W., Lusk C.H., Niinemets U., Oleksyn J., Osada N., Poorter H., Warton D.I. & Westoby M. (2005). Modulation of leaf economic traits and trait relationships by climate. *Glob. Ecol. Biogeogr.*, 14, 411-421.

Wright I.J., Reich P.B., Westoby M., Ackerly D.D., Baruch Z., Bongers F., Cavender-Bares J., Chapin T., Cornelissen J.H.C., Diemer M., Flexas J., Garnier E., Groom P.K., Gulias J., Hikosaka K., Lamont B.B., Lee T., Lee W., Lusk C., Midgley J.J., Navas M.L., Niinemets U., Oleksyn J., Osada N., Poorter H., Poot P., Prior L., Pyankov V.I., Roumet C., Thomas S.C., Tjoelker M.G., Veneklaas E.J. & Villar R. (2004). The worldwide leaf economics spectrum. *Nature*, 428, 821-827.

Wright I.J. & Westoby M. (2002). Leaves at low versus high rainfall: coordination of structure, lifespan and physiology. *New Phytol.*, 155, 403-416.

CHAPTER 3

RAPID DETERMINATION OF COMPARATIVE DROUGHT TOLERANCE TRAITS: USING AN OSMOMETER TO PREDICT TURGOR LOSS POINT

ABSTRACT

Across plant species, drought tolerance and distributions with respect to water availability are strongly correlated with physiological traits, the leaf water potential at wilting, i.e, turgor loss point (π_{tlp}), and the cell solute potential at full hydration, i.e., osmotic potential (π_o). We present methods to determine these parameters 30 times more rapidly than the standard pressure-volume (p-v) curve approach, making feasible community-scale studies of plant drought tolerance. We optimized existing methods for measurements of π_o using vapor-pressure osmometry of freeze-thawed leaf discs from 30 species growing in two precipitation regimes, and developed the first regression relationships to accurately estimate pressure-volume curve values of both π_o and π_{tlp} from osmometer values. The π_o determined with the osmometer (π_{osm}) was an excellent predictor of the π_o determined from the p-v curve (π_{pv}, r^2= 0.80). While the correlation of π_{osm} and π_{pv} enabled prediction, the relationship departed from the 1:1 line. The discrepancy between the methods could be quantitatively accounted for by known sources of error in osmometer measurements, i.e., dilution by the apoplastic water, and solute dissolution from destroyed cell walls. An even stronger prediction of π_{pv} could be made using π_{osm}, leaf density (ρ), and their interaction (r^2= 0.85, all $p < 2 \times 10^{-10}$). The π_{osm} could also be used to predict π_{tlp} (r^2= 0.86). Indeed, π_{osm} was a better predictor of π_{tlp} than leaf mass per unit area (LMA; r^2= 0.54), leaf thickness (T; r^2= 0.12), ρ (r^2= 0.63), and leaf dry matter content (LDMC; r^2= 0.60), which have been previously proposed as drought tolerance indicators. Models combining π_{osm} with LMA, T,

ρ, or LDMC or other p-v curve parameters (i.e., elasticity and apoplastic fraction) did not significantly improve prediction of π_{tlp}. This osmometer method enables accurate measurements of drought tolerance traits across a wide range of leaf types and for plants with diverse habitat preferences, with a fraction of effort of previous methods. We expect it to have wide application for predicting species responses to climate variability, and to assess ecological and evolutionary variation in drought tolerance in natural populations and agricultural cultivars.

Keywords: climate change, functional traits, leaf traits, survival, water deficit, water relations

INTRODUCTION

The bulk leaf turgor loss point (π_{tlp}), the water potential at which wilting occurs, is typically strongly related to plant drought tolerance and, therefore, species distributions with respect to water supply (Abrams & Kubiske 1990; Engelbrecht *et al.* 2000; Baltzer *et al.* 2008; Bartlett *et al.* 2012). This parameter is generally estimated from a pressure-volume (p-v) curve, which measures the decline of leaf water potential (Ψ_{leaf}) with leaf dehydration (Koide *et al.* 1989). Physiologically, the π_{tlp} is the Ψ_{leaf} at which the average cell turgor pressure is lost; at this point, Ψ_{leaf} equals osmotic potential and subsequent Ψ_{leaf} declines are due to increasing osmotic concentration (with π the symbol for osmotic potential). Across species, π_{tlp} is correlated with other important drought tolerance parameters, including Ψ_{leaf} at 50% loss of hydraulic and stomatal conductances and the lethal Ψ_{leaf} (Auge *et al.* 1998; Brodribb & Holbrook 2003; Sack *et al.* 2003; Bucci *et al.* 2004; Lenz *et al.* 2006; Scoffoni *et al.* 2012). Recent analyses have shown that osmotic potential at full hydration (π_o) is the most important trait predicting π_{tlp} across species, and the shifts in π_{tlp} for given species during seasonal and experimental droughts, and

thus that π_o and π_{tlp} are powerful traits for predicting drought tolerance and distributions with respect to water supply (Bartlett *et al.* 2012). However, the standard p-v curve method for determining π_o and π_{tlp} is highly time-consuming for measuring large species sets. We present a method for rapid π_{tlp} and π_o determination, based on osmometer measurement of π_o.

The p-v curve has been the most commonly used method for measuring π_o because it allows estimation of a number of physiological parameters, including π_{tlp} (Tyree & Hammel 1972; Turner 1988; Koide *et al.* 1989). Methods have been described for measuring π_o using a thermocouple psychrometer or osmometer (i.e., a psychrometer with Peltier cooling) (Turner 1981) for samples of extracted (expressed) sap from crushed leaf tissue (Wenkert 1980; Eldredge & Shock 1990; Morgan 1992), hot water extractions from dried leaf tissue (Kohl 1996; 1997), or for discs of leaf tissue that have been rapidly frozen and thawed to break cell walls and release protoplasmic contents (Kikuta & Richter 1992a; Ball & Oosterhuis 2005; Callister *et al.* 2006). Previous work toward cross-validating π_o measurement methods found correlations between measurements made with the p-v curve and estimates based on psychrometry measurements of vacuolar fluid (Shackel 1987), and osmometer measurements of freeze-thawed tissue, wherein leaf tissue is frozen to rupture cells and allow vapor pressure measurements based on evaporation from the cytoplasm (Nonami & Schulze 1989), although the choice of method influenced π_o values (Ball & Oosterhuis 2005). At least two sources of error have been proposed to influence osmometer methods: (1) *apoplastic dilution*, wherein symplastic fluid released from crushed cells is diluted by apoplastic water with low solute concentration, resulting in less negative π_o values; and (2) *dissolution of cell wall solutes* from destroyed cell walls, which makes π_o more negative (Shepherd 1975; Turner 1981; Grange 1983; Kikuta & Richter 1992a). Among osmometer methods, measurement of freeze-thaw discs is most robust to these errors, especially

when first- and second-order veins are excluded (Kikuta & Richter 1992a; Callister *et al.* 2006), though values for π_o may be more negative (Grange 1983; Kikuta *et al.* 1985; Callister *et al.* 2006), less negative (Meinzer *et al.* 1986; Ball & Oosterhuis 2005), or equal to (Auge *et al.* 1989) those from the p-v curve. Notably, there have been no standard protocols and experimental techniques, which may have contributed to discrepancies.

The first purpose of this study was to develop an osmometry method for prediction of p-v curve values of π_o and π_{tlp}. Because previous studies showed a strong relationship across species between p-v curve values of π_{tlp} and π_o (Sack *et al.* 2003; Blackman *et al.* 2010; Scoffoni *et al.* 2011) we aimed to estimate π_{tlp} from π_o values determined from osmometry for diverse species varying strongly in leaf construction and physiology. We used freeze-thaw discs because of their lower susceptibility to error and easier processing than expressed sap and hot water extractions (Kikuta & Richter 1992a). We also tested whether including other leaf functional traits would improve π_{pv} and π_{tlp} prediction. The second purpose of this study was to evaluate the sources of method discrepancies. We estimated cell wall investment using functional traits to determine the relative contribution of cell wall dissolution and apoplastic dilution to differences between the two methods. We thus provide an efficient and accurate alternative to the p-v curve for determining π_o and π_{tlp} for comparative studies at scales from physiology to community ecology.

METHODS

Experiments to optimize osmometer measurements

Osmotic potential was measured with a VAPRO 5520 vapor pressure osmometer (Wescor, Logan, UT), a newer model of the VAPRO 5500, shown to be accurate and precise in previous studies of expressed sap osmotic potential (Ball & Oosterhuis 2005). Because there is no

published standard method, we first conducted several experiments to optimize methodology. One sun-exposed branch was collected from each of 9 *Hedera canariensis* (Araliaceae) and 14 *Heteromeles arbutifolia* (Rosaceae) individuals growing adjacent to the University of California, Los Angeles campus. Excised branches were kept in humid, opaque bags, then recut underwater at least two nodes distal to the original cut and rehydrated overnight in bags. One leaf disc was sampled from one mature, fully expanded leaf per branch, centrally between the midrib and margin, using an 8 mm diameter cork borer.

Tests were made of the potential impacts on π_o measurement of (1) disc freezing time, (2) thawing time, and (3) reduction of evaporation during thawing. All discs were tightly wrapped in foil to limit condensation or frost after freezing and evaporation prior to processing. To test for an effect of disc freezing time, discs were submerged in liquid nitrogen (LN_2) for 2, 5, or 15 min. To test for an effect of thawing time, upon removal from the LN_2 the disc was either immediately measured or allowed to thaw for 1 h. To test the effectiveness of reducing evaporation during thawing, foil-wrapped discs were thawed either exposed on a lab bench, or placed inside a sealed plastic bag humidified with moist paper, and compared to discs measured immediately after freezing. After each treatment the disc was punctured 10-15 times with sharp-tipped forceps to facilitate evaporation through the cuticle and decrease equilibration time (Kikuta & Richter 1992b) immediately before sealing in the osmometer chamber, using the standard 10 μL chamber well. A measurement was recorded approximately every 2 min without opening the chamber, until equilibrium was indicated by an increase between measurements of <0.01 MPa. If a given set of treatments did not affect the equilibration time or the final π_o value, data were pooled for subsequent comparisons. Thus, for example, given no effect of LN_2 exposure time, the π_o data for different exposure times were pooled before testing for the effect of thawing time.

Species and method comparison

To evaluate the utility of the osmometer method in determining π_o and $\pi_{tlp,}$ for comparative studies, we tested 30 woody species that varied strongly in their drought tolerance, at two locations with different precipitation regimes. First, we selected 15 diverse tree and shrub species cultivated in gardens adjacent to the University of California, Los Angeles campus, including the two used in the optimization experiments (Table 3.1). These species originate from a range of native habitats, from chaparral to tropical wet forest, and currently experience a mean annual temperature of 17.3 ºC and annual precipitation of 450 mm (National Weather Service). We also selected 15 forest tree species at the Center for Tropical Forest Science long term research plot in Xishuangbanna, Yunnan, China, a tropical rainforest with a mean annual temperature of 21.0ºC, and annual precipitation of 1532 mm, with over 80% of annual precipitation occurring from May to October (Cao *et al.* 2006). Trees in this forest show strong topographic habitat associations, which are hypothesized to reflect variation in soil preferences (Lan *et al.* 2009). Our sampling was conducted during the wet season.

One branch from each of three to six individuals was collected for osmometer measurements as described above. Leaf discs were treated with a 2 min submersion time in LN_2, 10 min equilibration time, and no thawing time outside of the osmometer chamber, given the results of the optimization experiments (see *Result*s). P-v curves were produced and analyzed according to the bench drying method (Sack *et al.* 2010) with a pressure chamber (Plant Moisture Stress Model 1000, Corvallis, Oregon), and turgor loss point (π_{tlp}), osmotic potential (π_{pv}), apoplastic fraction (a_f), and modulus of elasticity (ε) were determined according to standard methods (Turner 1988; Koide *et al.* 1989; Sack *et al.* 2010). P-v curve data were

determined within 4 weeks of the osmometer data from the same individuals of *Bauhinia galpinii* at UCLA and all the XTBG species; for the remaining 14 species at UCLA, previously published p-v data were used that had been determined for the same individuals within the previous two years (Scoffoni *et al.* 2008; 2011; 2012). We selected individuals at UCLA that are irrigated year-round and collected leaves for both approaches during the same times of year to minimize potential differences in seasonal osmotic adjustment.

Prior to measurement, leaves were rehydrated overnight, which is a standard pre-treatment in the literature for p-v curve determination to ensure all measurements are made at full hydration and are therefore comparable across studies with differences in water availability. Failing to rehydrate may instead produce Ψ_{leaf} values at arbitrary relative water contents below saturation. We note that rehydration before measurement can lead to hydration of the airspaces by capillarity uptake and/or exudation of water from cells. During p-v curve determination, we used the standard correction method to remove data points representing an oversaturated symplastic water content; these points appear in the curve as a 'plateau' of points with constant Ψ_{leaf} despite a decreasing relative water content (Kubiske & Abrams 1990, 1991a, b; Sack *et al.* 2010). Additionally, rehydration prior to measurement can cause solute leakage from cells into the apoplast, such that p-v curve analyses find less negative values of π_{tlp} and π_o, and lower values of a_f (Kubiske & Abrams 1990, 1991a, b). Such effects can reduce resolution for determining seasonal shifts in p-v parameters for given species (Kubiske & Abrams 1990; 1991a, b). Even so, using a standard rehydration treatment does not preclude species-comparisons, and is arguably necessary to produce comparable measurements. Our analysis of data from previous studies indicated that species-differences in p-v parameters are largely robust to rehydration effects after one corrects data for the plateau effect; p-v parameters determined with and without

rehydration were strongly correlated across species, though the relationships were not 1:1, and measurements on rehydrated material underestimated the most negative osmotic potentials (r^2= 0.61 for π_o, and 0.77 for π_{tlp}; $p < 0.001$; data from Kubiske & Abrams 1990; 1991a, b; Fig. S3.1). These potential effects on solute concentration and p-v parameters, as well as the need for standardization, warrant further consideration to develop best measurement practices. However, explicitly recommending a pre-measurement rehydration method is outside the scope of our study, as it would not affect the method proposed here. A rehydration pre-treatement should not affect the relationship between osmometer and p-v curve estimates of osmotic potential, as long as the pre-treatment is consistent between the two methods, as was applied here.

Leaf fresh mass, leaf area (LI-COR 3000C area meter), thickness (T; mm), and dry mass after oven drying for 72 hours at 70ºC were determined for calculation of leaf dry mass per unit area (LMA; g m^{-2}), leaf dry matter content (LDMC; dry mass/fresh mass), and leaf density (ρ; LMA/T; g cm^{-3}). Thickness was averaged from the top, middle, and bottom of each leaf.

Statistics

We first tested the π_o values determined using the osmometer (π_{osm}) against those from p-v curve analysis (π_{pv}) using a paired *t*-test. Next, we used regression analysis to test how well π_{pv} and π_{tlp} could be predicted from π_{osm} (R; version 2.12.0). We additionally tested a range of linear models for predicting π_{pv} and π_{tlp} from π_{osm} when including additional p-v parameters and leaf functional traits (a_f, ε, LMA, T, ρ, and LDMC; Table S3.1). We also tested the ability to predict π_{tlp} from $\widehat{\pi_{tlp}}$, an estimate based on a previously derived analytical solution for the p-v equations giving π_{tlp} as a function of π_o and ε (Bartlett *et al.* 2012):

$$\widehat{\pi_{tlp}} = \frac{\pi_{osm} \times \varepsilon}{\pi_{osm} + \varepsilon} \qquad \text{eqn 3.1}$$

Model selection was performed within a maximum likelihood framework. Maximum likelihood parameters were determined for each model applied to the data for all species; the R^2 and slope of expected vs. observed values, forced through the origin was used as an index of goodness of fit. Models were compared using the Akaike information criterion corrected for low n (AICc); the model with the lowest AICc value has best support, and differences > 2 in AICc values are considered meaningful (Burnham & Anderson 2002, 2004). Parameters were estimated using the Simulated Annealing procedure for global optimization, then used as the initial values in Nelder– Mead simplex search procedure for local optimization; standard errors for the parameters were generated from the Hessian matrix (R version 2.14.0; RDCT, 2005; code available on request). For the best-fit models we calculated the 95% confidence intervals, and 95% prediction intervals assuming sample sizes of 3, 6, or 10 leaves per species (Sokal & Rohlf 1995; Royer *et al.* 2007).

To determine whether prediction of drought tolerance parameters would differ between the two sampled locations, the two datasets (UCLA and Xishuangbanna) were compared in their parameter values, and in the best-fit relationship of π_{pv} and π_{tlp} against predictor variables, using analysis of covariance to compare the slopes and intercepts (SMATR software; (Falster *et al.* 2006; Warton *et al.* 2006).

The second purpose of our study was to investigate the source of discrepancies between osmometer and p-v curve measurements of π_o. We tested the influence of the opposing biases of apoplastic dilution and cell wall dissolution, considered the most significant biases in osmometer methods (see *Introduction*). We compared the measured π_{osm} with an estimated value ($\widehat{\pi}_{osm}$), determined from π_{pv} and adjusted for these effects. We assumed that the amount of apoplastic dilution would be proportional to a_f, and assumed an apoplastic solute concentration of 0 for

non-halophytic species (Gabriel & Kesselmeier 1999; James *et al.* 2006), and that additional solute from the cell walls would be proportional to wall investment. Thus, we fitted the following equation, which includes both the apoplastic dilution effect and the cell wall dissolution effect, and their interaction:

$$\hat{\pi}_{osm} = \underbrace{a \times \pi_{pv} \times (1 - a_f)}_{\substack{apoplastic \\ dilution}} + \underbrace{b \times wall\ investment}_{\substack{wall \\ dissolution}} + \underbrace{c \times wall\ investment \times \pi_{pv} \times (1 - a_f)}_{interaction} + d \quad \text{eqn 3.2}$$

We used LMA, T, ρ, ε, and LDMC as estimates of cell wall investment. In particular, ε, ρ and LDMC should be strongly related to the proportion of leaf tissue occupied by cell walls (Garnier & Laurent 1994; Lenz *et al.* 2006).

The determination of a_f by p-v analysis involves extrapolation beyond the range of data and thus can be imprecise (Andersen *et al.* 1991; Wardlaw 2005), and 11 species measured here had a_f values not significantly different from 0, including 10 species with negative a_f values (t-test; $p > 0.10$). The apoplastic dilution and cell wall investment analyses were conducted including all species, setting to 0 those a_f values that did not differ significantly from 0 (see Table 3.1). Notably, determination of other p-v parameters is robust to uncertainty in a_f (Andersen *et al.* 1991).

RESULTS

Optimizing the osmometer method for π_o determination

The method optimization experiments indicated reliable approaches to rapidly determine osmotic potential from leaf discs in the osmometer. First, there was no effect of freezing time for *Hedera canariensis* or *Heteromeles arbutifolia*. The minimum time used, 2 minutes, was adequate to completely freeze leaf tissue and fracture the cell walls (Fig. 3.1a). Notably, Kikuta and Richter (1992) allowed discs to thaw for 1 hour before measuring, but we found complete thawing

occurs within chamber equilibration time and additional thawing time was unnecessary (Fig. 3.1b).

Leaf discs must be shielded from evaporation prior to measurement. Discs exposed on the bench for one hour had inaccurate low π_o values, whereas discs could be stored in humidified bags for one hour with no change in measured π_o (Fig. 3.1b). The equilibration time of approximately 10 minutes varied little among individuals, treatments, or species.

Prediction of π_{pv} from osmometry measurements

Across the 30 measured species, the values of π_o measured by osmometry (π_{osm}) and p-v curves (π_{pv}) were equivalent on average (species-mean ± standard error were -1.38 ± 0.10 and -1.41 ± 0.07 MPa respectively; paired t-test; p= 0.31). Further, we found strong correlation between π_{osm} and π_{pv}. However, while the 1:1 line forced through the origin fitted the data with statistical significance ($p < 1\times10^{-5}$), it had low goodness of fit (r^2= 0.47), such that the π_{osm} overestimated π_{pv} at less negative values and underestimated π_{pv} at more negative values. The best-fit model for predicting π_{pv} included both π_{osm} and ε (Table S3.1), and eliminated this bias (r^2 for predicted value against observed value, forced through the origin= 0.86; $p < 2\times10^{-11}$). The second most strongly supported model for predicting π_{pv} included $\pi_{osm,}$ the easily measured functional trait ρ, and their interaction term (r^2= 0.85; $p < 2\times10^{-12}$) (Table S3.1). Notably, π_{osm} alone was also an excellent predictor of π_{pv} (r^2= 0.80; $p < 2\times10^{-10}$; Fig. 3.2). The 95% prediction intervals were ±18%, ±13.5%, and ±11% for the univariate model, if estimating species values from sample sizes of 3, 6 and 10 leaves, respectively, compared to ±14.5%, ±10.7%, and ±9% for the model incorporating ρ and ±14%, ±10.5%, and ±9% for the best-fit model based on π_{osm} and ε. Thus, π_{pv} can be estimated accurately from osmometry measurements alone, or from π_{osm} and ρ.

Identifying the traits that affect method comparison for osmotic potential

We tested whether the deviation of the π_{osm} versus π_{pv} relationship from the 1:1 line could be accounted for by the opposing effects of apoplastic dilution and cell wall dissolution by fitting eqn 3.2. This model eliminated the bias in the π_{osm} versus π_{pv} relationship; $\widehat{\pi}_{osm}$ was correlated with π_{pv} with a slope statistically indistinguishable from 1 (slope ± standard error = 0.954 ± 0.14; r^2= 0.65; p <2×10^{-4}; Table S3.1; Fig. 3.3). In applying eqn 3.2, LDMC and LMA were significantly better metrics for cell wall investment than ρ, T, or ε (ΔAICc > 2; Table S3.1). The bias in the original relationship, wherein π_{osm} becomes increasingly more negative relative to π_{pv} as both decrease, and vice versa as they approach 0, is thus associated with the negative correlations of LDMC and LMA with π_{pv} (r^2= 0.56, 0.49; both p <1×10^{-4}, respectively); species with higher osmotic concentrations tend to have greater cell wall investment. For species with π_o values closer to zero, cell wall dissolution only weakly offsets apoplastic dilution, whereas for species with more negative π_o, cell wall dissolution increasingly offsets dilution, accounting for the method discrepancy across π_o values.

Prediction of π_{tlp} from osmometry measurements

Osmometer measurements enabled accurate prediction of the turgor loss point (Fig. 3.4). The π_{tlp} was strongly correlated with π_{osm} (r^2= 0.86; p <1×10^{-12}), as expected, given the close correlation of π_{tlp} with π_{pv} (r^2= 0.91; p <2×10^{-12}) (Fig. 3.2; Table S3.1).

We tested whether π_{tlp} could be predicted from other leaf functional traits alone, or whether these improved the prediction from π_{osm}. We considered physiological traits a_f and ε, and ρ, T, LMA and LDMC, frequently measured traits representing structural investment (Sack

et al. 2003). Across species, the π_{tlp} was significantly negatively correlated with ε (r^2= 0.57; p <2×10^{-8}), LMA (r^2= 0.56; p <2×10^{-5}), LDMC (r^2= 0.61; p <2×10^{-5}), ρ (r^2= 0.63; p <2×10^{-5}), T (r^2= 0.12; p= 0.03), and a_f (r^2= 0.22; p= 0.02). The best-fit models from the osmometer method, i.e., those with AICc values within 2 units of the most negative value, predicted π_{tlp} from π_{osm} alone and from both π_{osm} and ρ (Table S1; p <2×10^{-12}, r^2= 0.86-0.89). The observed π_{tlp} was also correlated, though not as strongly, with π_{tlp} predicted from equation 3.1, $\widehat{\pi_{tlp}}$, calculated from ε and π_{osm} (p <2×10^{-10}, r^2= 0.78). The leaf construction traits thus did not add significant predictive power to the relationship between π_{tlp} and π_{osm}, and the univariate relationship is more parsimonious. The 95% prediction intervals of the univariate relationship of π_{tlp} to π_{osm} were ±23%, ±17.4%, and ±14.8%, if estimating species values from sample sizes of 3, 6, and 10 leaves, respectively. The π_{tlp} can therefore be reliably predicted from osmometer measurements, even given wide variation in other pressure-volume parameters and leaf construction traits.

As expected, the values of π_o and π_{tlp} for species from the wetter XTBG site (-1.19 and -1.51 MPa, respectively) were significantly less negative than those for the UCLA site (-1.55 and -2.09, respectively; t-tests; both p <0.001). The recommended models for π_{pv} and π_{tlp} gave excellent predictions for these mean parameters at each site (predicted π_o= -1.20 for XTBG and -1.55 for UCLA; predicted π_{tlp}= -1.59 and -2.02, respectively). Further, there were no statistically significant differences between the regression lines for the two sites, relating observed π_{tlp} to π_{tlp} predicted from π_{osm}; observed π_{pv} to π_{pv} predicted from π_{osm}; observed π_{pv} to π_{pv} predicted from ρ, π_{osm}, and their interaction; or observed π_{pv} to π_{pv} predicted from π_{osm} and ε (SMATR ANCOVA, all p >0.3). These regression relationships and the osmometer measurements themselves are therefore robust across ecosystems with different water availabilities.

DISCUSSION

This study provides an approach to estimating key water relations parameters rapidly, which should enable the standardized assessment of many species for drought tolerance. The optimized freeze-thaw disc osmometer measurements (π_{osm}) were tightly correlated with p-v curve estimates of π_o (π_{pv}) and also π_{tlp}, with the π_{pv} estimation improved by including leaf density as a predictor, whereas the π_{tlp} estimation was independent of both leaf structure and habitat preferences. We propose our optimized osmometer method for determining π_o as a standard method. The minimum equilibration time, however, should be confirmed for instruments with different well sizes.

Earlier studies have used osmometer methods for measuring π_o and compared them with expressed-sap and p-v curve methods, but the largest previous study showed relationships of π_{osm} and π_{pv} for 5 species (Callister *et al.* 2006). We expanded on that work, refining the methodology by evaluating the effects of freezing time, thawing time, and thawing conditions, and providing equations for the relationship of π_{osm} and π_{pv} for 30 species. Additionally, while previous studies have shown a correlation of π_{pv} with π_{tlp} (Sack *et al.* 2003; Lenz *et al.* 2006; Scoffoni *et al.* 2011; Bartlett *et al.* 2012) we are the first to our knowledge to show that π_{osm} can be used to predict π_{tlp} as a rapid alternative to p-v curves.

Notably, π_{osm} and π_{pv} were tightly correlated but not equal. The π_{osm} was higher than π_{pv} for species with less negative values and lower than π_{pv} for species with more negative values. Our analysis indicated that this discrepancy may relate to both apoplastic dilution and wall solute enrichment. A high LDMC, which reflects the proportion of cell wall material in the leaf tissue, correlates across species with more negative π_o values, possibly because greater cell wall investment enables maintenance of a high relative water content at π_{tlp}, and/or because drought

tolerant plants construct leaf tissue with a high density of relatively smaller cells to increase the efficiency of osmotic adjustment (Cutler *et al.* 1977; Bartlett *et al.* 2012). Therefore, for species with more negative π_o, wall solute enrichment would play a more important role than apoplastic dilution, increasing the discrepancy between the two methods. However, the π_{osm} and π_{pv} were equivalent on average across species, and the discrepancies between the two methods were accounted for in our regression model

$$\pi_{pv} = 0.587\pi_{osm} - 0.546 \qquad \text{eqn 3.3}$$

which can be used to reliably estimate π_{pv} (r^2= 0.80). We recommend this regression approach to estimate and present π_{pv} rather than simply determining π_{osm}, because π_{pv} values are most common in the literature. However, the regression equation

$$\pi_{pv} = 0.466\pi_{osm} - 9.31 \times 10^{-5}\pi_{osm}\rho - 9.26 \times 10^{-4}\rho - 0.455 \qquad \text{eqn 3.4}$$

provided the most accurate estimate from the osmometer method (r^2= 0.87). We recommend further validation of these models in species with closely spaced large veins that cannot be avoided when sampling leaf discs.

To our knowledge, this is the first study to produce a regression equation allowing prediction of π_{tlp} from osmometer measurements:

$$\pi_{tlp} = 0.832\pi_{osm} - 0.631 \qquad \text{eqn 3.5}$$

This approach can be applied in other systems. This regression equation was highly significant (r^2= 0.86; $p < 2\times10^{-12}$) for diverse species with a wide range of drought tolerances, leaf characteristics, and p-v parameter values (Table 3.1, Fig. 3.4). The prediction intervals for the estimation of π_{tlp} and π_{pv} were reasonably narrow, <15% given sampling of 10 leaves per species, or 14-17% for sampling of 6 leaves. We propose that the osmometer method and regressions developed here are an accurate proxy for p-v curve measurements of π_o and π_{tlp}. This approach

will continue to improve as comparative data become available for more species and a wider range of p-v parameter values. However, this species set already encompasses 40%, 48%, 52%, and 78% of the total range of π_o, ε, π_{tlp}, and a_f, respectively, found in a global meta-analysis of p-v data, suggesting that these regressions will be robust across the range of p-v parameter variation (Bartlett *et al.* 2012).

The method presented here for determining π_o and π_{tlp} has several advantages over generating p-v curves. Osmometer measurements require approximately 10-15 minutes per individual leaf and an hour for six, which is typically sufficient replication for reliable determination of species means (Sack *et al.* 2003; Hulshof & Swenson 2010), compared to the approximately one or two days required to generate a p-v curve for 4-6 leaves. Thus, this method involves a thirty to fifty-fold increase in measuring speed, or reduction of effort by >95 %. This reduction of effort makes feasible sampling across a wide range of taxa, even potentially an entire community. Indeed, for communities experiencing strongly seasonal climates, repeated sampling for given species may be necessary to determine the role of π_o and π_{tlp} adjustment in conferring ecological drought tolerance. Notably, osmometer measurements had similar or lower standard errors for estimates of π_o for given species than p-v curves (paired t-test; p= 0.08; n= 30). The osmometer is likely to have greater precision because it directly measures π_o, whereas p-v curve determination requires extrapolation from the solute potential versus relative water content relationship. Osmometer measurements are also more feasible than p-v analysis for fragile, large, or succulent leaves, or leaves with short or no petioles.

Given the significance of π_{tlp} and π_o in estimating drought adaptation and acclimation, and thus potentially for predicting species' distribution across soil moisture gradients, rapid surveys would be useful for community-level studies of this functional trait and drought tolerance

screening of agricultural cultivars (cf. (Kraft *et al.* 2008). Notably, π_o and π_{tlp} are much better predictors of leaf drought tolerance than LMA, ρ, and LDMC (Poorter & Markesteijn 2008; Bartlett *et al.* 2012), leaf traits that have been frequently suggested as proxies for the p-v curve parameters or as indices for drought tolerance mainly due to the convenience with which they can be determined (e.g., (Niinemets 2001; Kraft *et al.* 2008; Violle & Jiang 2009). However, the method described here is equally rapid and convenient, given access to the instrument, and, having greater predictive power and mechanistic relevance, should have considerable value for study of the comparative physiology and ecology of drought tolerance.

ACKNOWLEDGEMENTS

We thank Weimin Dang, Park Nobel, Jessica Pasquet-Kok, Christine Vuong, Xuewei Fu, and the XTBG Center for Tropical Forest Science plot directors and staff for logistical assistance and discussion. We are also grateful to anonymous reviewers for comments that significantly improved this manuscript. This work was supported by National Science Foundation Grants #0546784, #DGE-0707424, #10-591.

Table 3.1. Woody species tested, origin, leaf type (evergreen or deciduous, E or D respectively) and pressure-volume curve parameters and osmotic potential at full turgor measured using osmometry, with mean ± standard error values for each parameter. Species nomenclature and biomes and continents of origin from Scoffoni et al. (2008; 2011) and (Fang *et al.* 2011). Species of the Xishuangbanna Botanic Garden (XTBG) were from native forest plots.

	Family	Biome, continent of origin	Leaf type	Turgor loss point (MPa	Osmotic potential (MPa)	Elasticity (MPa)	Apoplastic fraction	Osmometer osmotic potential (MPa)
UCLA species								
Alberta magna	Rubiaceae	Temperate Forest, Africa	E	-1.97±0.07	-1.39±0.05	8.08±0.17	0.45±0.02	-1.45±0.01
Bauhinia galpinii	Fabaceae	Temperate Forest, Africa	D	-1.41±0.07	-1.15±0.08	7.81±1.61	0.08±0.04	-0.95±0.05
Camelia sasanqua	Theaceae	Temperate Forest, Asia	E	-2.12±0.18	-1.61±0.13	7.71±1.11	0.23±0.17	-1.39±0.08
Cercocarpus betuloides	Rosaceae	Mediterranean, N. Am.	E	-2.59±0.02	-1.64±0.04	11.0±0.70	0.59±0.08	-2.08±0.07
Comarostaphylis diversifolia	Ericaceae	Mediterranean, N. Am.	E	-2.60±0.14	-2.23±0.12	34.1±9.77	0.47±0.10	-2.66±0.06
Eucalyptus erythrocorys	Myrtaceae	Temperate Forest, Austral.	E	-2.24±0.10	-1.67±0.06	21.5±2.48	0.63±0.05	-1.54±0.05
Hedera canariensis	Araliaceae	Temperate Forest, Africa	E	-2.06±0.09	-1.16±0.07	12.8±0.79	0.43±0.07	-1.54±0.05
Heteromeles arbutifolia	Rosaceae	Mediterranean, N. Am.	E	-2.34±0.10	-1.89±0.10	16.4±0.49	0.28±0.06	-1.96±0.04
Hymenosporum flavum	Pittosporaceae	Tropical Rainforest, Austral.	D	-2.06±0.05	-1.38±0.04	5.88±0.48	0.36±0.03	-1.75±0.007
Lantana camara	Verbenaceae	Tropical Dry Forest, Pantropical	E	-1.37±0.04	-1.10±0.04	4.85±0.33	0.23±0.12	-0.64±0.01
Magnolia grandiflora	Magnoliaceae	Temperate Forest, N. Am.	E	-2.06±0.05	-1.43±0.02	9.14±1.31	0.16±0.01	-1.68±0.04
Platanus racemosa	Platanaceae	Temperate Riparian, N. Am.	D	-2.03±0.06	-1.54±0.04	8.81±0.53	0.36±0.04	-1.55±0.06
Quercus agrifolia	Fagaceae	Mediterranean, N. America	E	-3.00±0.12	-2.31±0.12	20.8±1.28	0.44±0.09	-3.03±0.12
Raphiolepis indica	Rosaceae	Temperate Forest, Asia	E	-2.07±0.18	-1.37±0.15	11.5±0.79	0.69±0.05	-1.99±0.14
Salvia canariensis	Lamiaceae	Temperate Forest, Africa	E	-1.18±0.07	-0.92±0.05	5.49±0.21	0.22±0.02	-0.79±0.02
XTBG species								
Baccaurea ramiflora	Euphorbiaceae	Tropical Rainforest	E	-1.11±0.10	-0.83±0.07	2.53±0.20	-0.34±0.20*	-0.70±0.007
Barringtonia pendula	Lecythidaceae	Tropical Rainforest	E	-1.02±0.09	-0.77±0.02	3.28±0.72	-0.15±0.12*	-0.74±0.02
Diospyros nigrocortex	Ebenaceae	Tropical Rainforest	E	-1.63±0.09	-1.42±0.06	9.94±0.37	-0.50±0.39*	-1.61±0.04
Eurya austroyunnanensis	Theaceae	Tropical Rainforest	E	-1.51±0.05	-1.31±0.04	9.69±0.90	-0.08±0.08*	-1.04±0.11

Harpullia cupaniodes	Sapindaceae	Tropical Rainforest	E	-1.70±0.38	-1.19±0.34	6.35±1.96	-0.23±0.23*	-1.58±0.08
Knema globularia	Myristicaceae	Tropical Rainforest	E	-1.39±0.13	-1.10±0.08	8.14±0.90	0.28±0.10	-0.98±0.08
Macropanax dispermus	Araliaceae	Tropical Rainforest	E	-1.49±0.15	-1.25±0.08	7.94±0.40	-0.20±0.20*	-1.18±0.06
Mallotus garrettii	Euphorbiaceae	Tropical Rainforest	E	-1.62±0.31	-1.27±0.20	12.0±1.11	0.42±0.04	-1.01±0.09
Mezzettiopsis creaghii	Annonaceae	Tropical Rainforest	E	-1.82±0.14	-1.46±0.12	17.7±5.48	0.42±0.08	-1.24±0.04
Pterospermum menglunen	Acanthaceae	Tropical Rainforest	E	-1.82±0.25	-1.43±0.20	11.2±3.92	0.20±0.28*	-1.26±0.14
Saprosma ternata	Rubiaceae	Tropical Rainforest	E	-1.25±0.06	-1.07±0.05	6.91±0.94	-0.24±0.14*	-0.91±0.12
Parashorea chinensis	Dipterocarpac	Tropical Rainforest	E	-1.52±0.04	-1.12±0.03	4.19±1.17	-0.12±0.13*	-1.36±0.10
Sloanea tomentosa	Elaeocarpacea	Tropical Rainforest	E	-1.45±0.05	-1.12±0.05	6.72±0.96	0.21±0.07	-1.14±0.12
Sumbaviopsis albicans	Euphorbiaceae	Tropical Rainforest	E	-2.18±0.22	-1.52±0.23	4.84±1.87	-0.06±0.12*	-1.70±0.18
Trigonostemon thrysoideu	Euphorbiaceae	Tropical Rainforest	E	-1.19±0.19	-0.99±0.19	6.95±1.84	-0.32±0.14*	-0.82±0.005

* = species marked with an asterisk had an extrapolated apoplastic fraction not significantly different from 0 (t-test, $p > 0.1$)

FIGURE CAPTIONS

Figure 3.1. Effects of different treatments on the measurement of osmotic potential at full turgor by osmometry (π_{osm}) of freeze-thawed leaf discs for *Hedera canariensis* and *Heteromeles arbutifolia*. The π_{osm} was repeatedly measured approximately every 2 minutes once the disc was sealed in the chamber, with stability (i.e., equilibrium) achieved when the change between two sequential measurements was <0.01 MPa. Equilibration required 10 minutes or less for all individuals across species. (3.1a). Providing leaf discs with a 1 hour thawing time did not affect their equilibration pattern or π_{osm} relative to a control sample measured immediately after freezing, as long as the discs were prevented from dehydrating (bars= standard errors). (3.1b). Varying the immersion time in liquid nitrogen between 2, 5, and 15 minutes did not affect π_{osm} at equilibrium for *Heteromeles arbutifolia*.

Figure 3.2. Measurements of osmotic potential at full turgor from pressure-volume (π_{pv}) curve analysis plotted against measurements made with the osmometer (π_{osm}) for species of a wide range of leaf structure and drought tolerances (circles= Xishuangbanna Tropical Botanical Garden species, triangles= University of California, Los Angeles species; see Table S3.1). Results from the two methods were strongly correlated (r^2= 0.80; $p < 2\times10^{-10}$); fitted line is $\pi_{pv} = 0.587\pi_{osm} - 0.546$. Black solid lines are 95% confidence intervals, gray dashed lines are 95% prediction intervals, error bars represent standard errors.

Figure 3.3. Accounting for the discrepancy between measurement of osmotic potential at full turgor with a pressure-volume curve (π_{pv}) and that measured with osmometry (π_{osm}), as was seen in the departure of the data in Fig. 3.2 from the 1:1 line. This bias could be accounted for by the

effects of apoplastic dilution and cell wall dissolution in the osmometry measurement. Here π_{osm} predicted from π_{pv} using eqn 3.2, with leaf dry matter content as a proxy for cell wall investment, was tightly correlated with measured π_{osm} with no bias (slope ± standard error = 0.954 ± 0.14; r^2= 0.65; $p < 2\times10^{-4}$). For this analysis, apoplastic fraction values not significantly different from 0 were set as 0 (see Table 3.1), and data for species from both locations were pooled (n = 30).

Figure 3.4. The prediction of turgor loss point of pressure-volume curve analysis (π_{tlp}) using the osmotic potential at full turgor determined using an osmometer (π_{osm}) for species of a wide range of leaf structure and drought tolerance (circles= Xishuangbanna Tropical Botanical Garden species, triangles= University of California, Los Angeles species; see Table S3.1). The π_{osm} and π_{tlp} were strongly correlated (r^2= 0.86; $p < 1\times10^{-12}$); fitted line is eqn 3.4. Black solid lines are 95% confidence intervals, gray dashed lines are 95% prediction intervals, error bars represent standard errors.

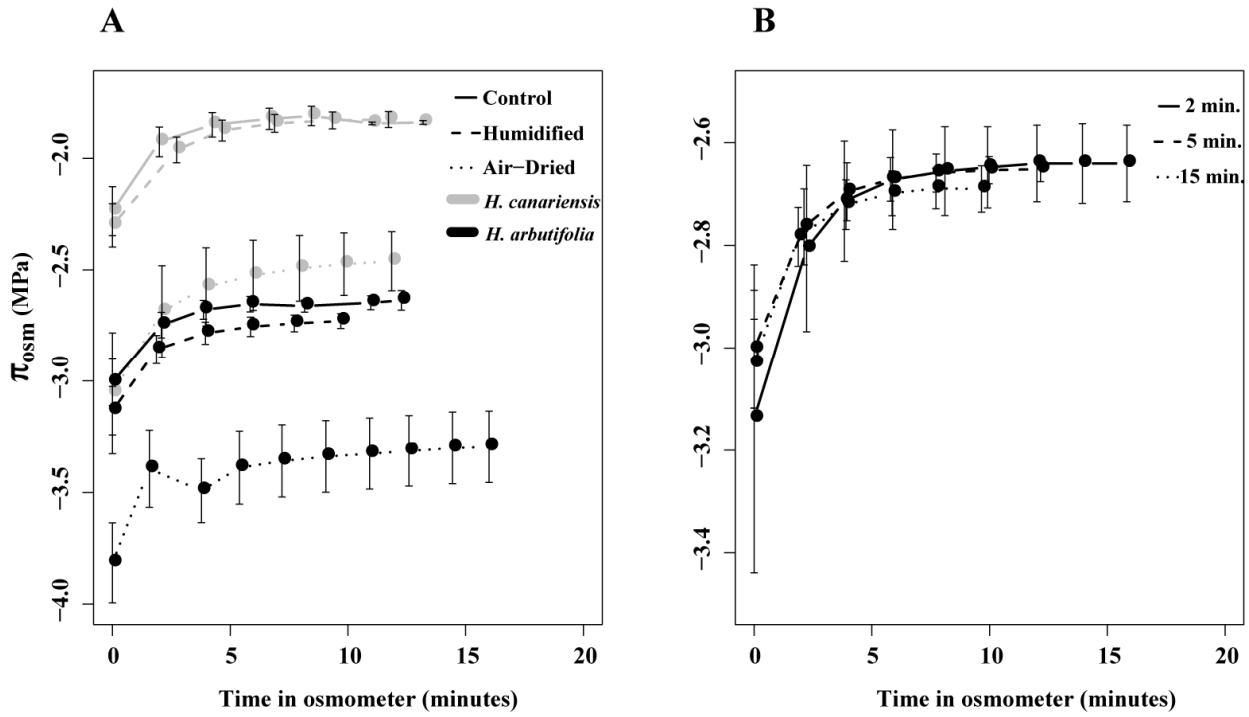
A
B
Control
Humidified
Air−Dried
H. canariensis
H. arbutifolia
2 min.
5 min.
15 min.
π_{osm} (MPa)
−2.0
−2.5
−3.0
−3.5
−4.0
−2.6
−2.8
−3.0
−3.2
−3.4
0
5
10
15
20
Time in osmometer (minutes)
Time in osmometer (minutes)

Figure 3.1

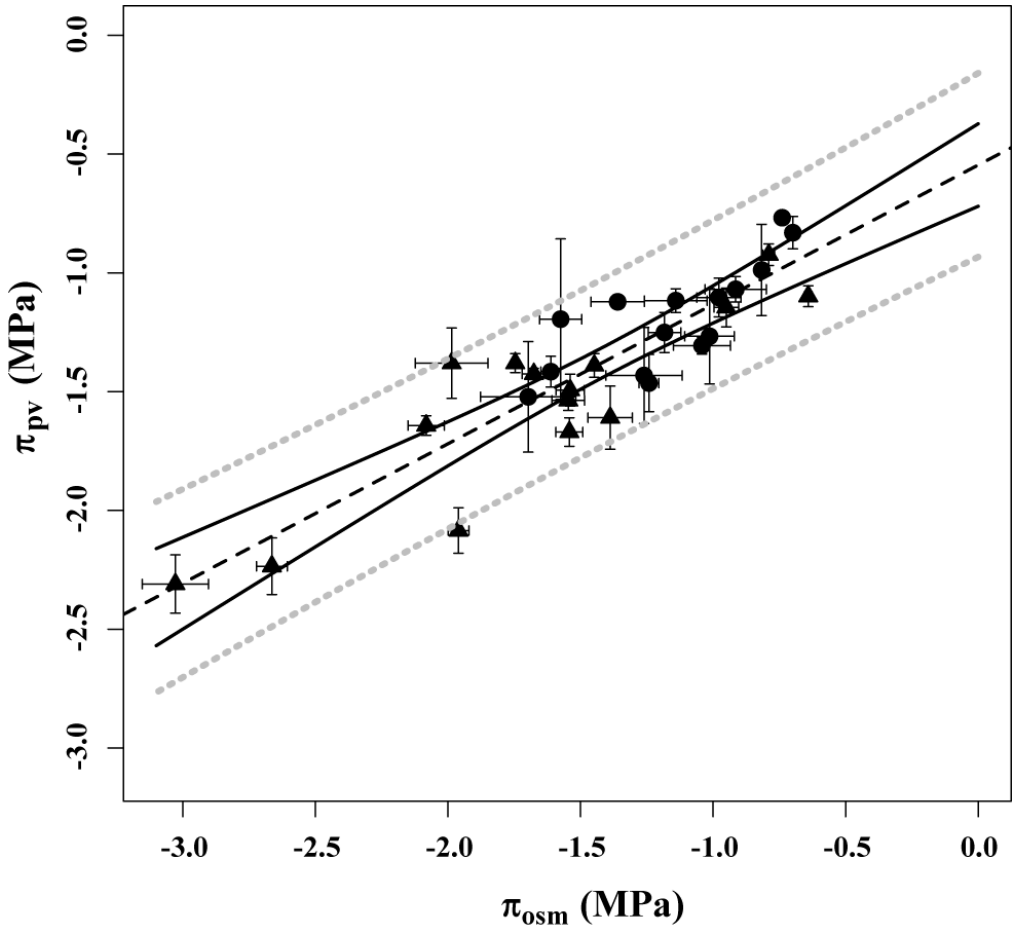

Figure 3.2

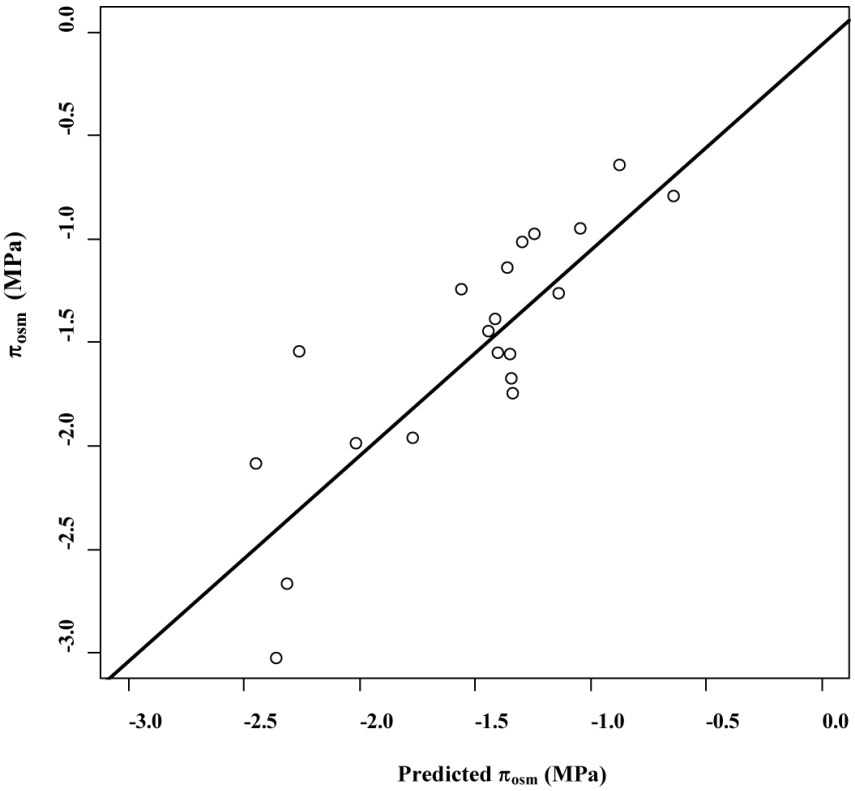
0.0
-0.5
-1.0
-1.5
-2.0
-2.5
-3.0
π_{osm} (MPa)
-3.0
-2.5
-2.0
-1.5
-1.0
-0.5
0.0
Predicted π_{osm} (MPa)

Figure 3.3

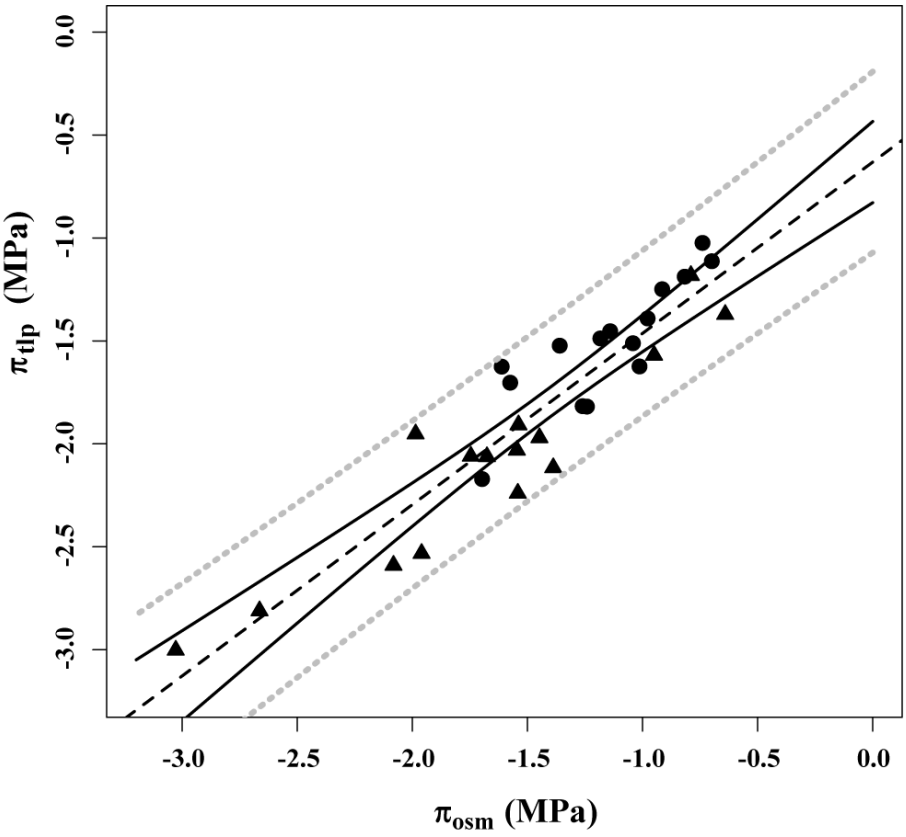

Figure 3.4

SUPPLEMENTAL MATERIALS

Table S3.1 Regression equations predicting pressure-volume curve measurements of osmotic potential (π_{pv}) and turgor loss point (π_{tlp}) from osmometry measurements of osmotic potential (π_{osm}) alone and also including additional pressure-volume curve parameters (elasticity, or cell wall stiffness (ε), and apoplastic fraction (a_f)), and leaf structural and compositional traits (leaf dry matter content (LDMC), leaf thickness (T), leaf density (ρ) and leaf mass per unit area (LMA)).

Figure S3.1. Testing the robustness of species values for osmotic potential at full turgor (π_o) and at turgor loss point (π_{tlp}) as estimated with the pressure-volume curves (p-v curves) to standard rehydration treatment, based on published data. The π_o (A) and π_{tlp} (B) were measured from non-hydrated leaves and leaves rehydrated overnight and p-v curves were corrected for plateau effects. Values for non-rehydrated leaves and for leaves rehydrated for 12h before p-v curve determination were are highly correlated (r^2 = 0.61, 0.77, respectively). Data are seasonal mean values for *Fraxinus americana, Quercus illicifolia, Quercus prius, Quercus rubra, and Pseudostuga menziesii* (Kubiske & Abrams 1991a, b).

Table S3.1. Regression equations predicting pressure-volume curve measurements of osmotic potential (π_{pv}) and turgor loss point (π_{tlp}) from osmometry measurements of osmotic potential (π_{osm}) alone and also including additional pressure-volume curve parameters (elasticity, or cell wall stiffness (ε), and apoplastic fraction (a_f)), and leaf structural and compositional traits (leaf dry matter content (LDMC) , leaf thickness (T), leaf density (ρ) and leaf mass per unit area (LMA)). For estimation of π_{tlp}, models were included using the term $\widehat{\pi_{tlp}}$, wherein eqn 3.1 was used to calculate π_{tlp} from π_{osm} and ε, and $\widehat{\pi_{pv}}$, which was predicted using the best-fit regression of π_{pv} from π_{osm} and ρ. * = Models containing a_f were obtained from only the 20 species with positive a_f values, so AICc values for these models were not comparable with the rest. SE = standard error, given as ± after each coefficient; SD = standard deviation of the random error term, slope = slope of the relationship between the observed values and the values predicted from the regressions, forced through the origin. Best-fit models with lowest AICc values are in bold.

Equation	a	b	c	d	SD	slope	R^2	p	AICc
Prediction of π_{pv}									
$a \times \pi_{osm} + b$	0.587 ± 0.054	-0.546 ± 0.082			0.163	0.988	0.80	$<2x10^{-10}$	-20.22
$a \times \pi_{osm} + b \times \varepsilon + c \times \pi_{osm} \times \varepsilon + d$	**0.436 ± 0.109**	**-0.031 ± 0.014**	**-0.002 ± 0.007**	**-0.513 ± 0.140**	**0.133**	**0.991**	**0.86**	**$<2x10^{-10}$**	**-25.86**
$a \times \pi_{osm} + b \times \varepsilon + c$	**0.407 ± 0.065**	**-0.027 ± 0.007**	**-0.636 ± 0.089**		**0.134**	**0.991**	**0.86**	**$<2x10^{-11}$**	**-25.75**
$a \times \pi_{osm} + b \times \rho + c \times \pi_{osm} \times \rho + d$	0.466 ± 0.128	-0.927 ± 0.519	-0.094 ± 0.258	-0.455 ± 0.186	0.139	0.990	0.85	$<2x10^{-12}$	-23.61
$a \times \pi_{osm} + b \times LMA + c$	0.523 ± 0.076	$(-7.8 \pm 6.6) \times 10^{-4}$	-0.562 ± 0.081		0.159	0.987	0.81	$<2x10^{-9}$	-15.43
$a \times \pi_{osm} + b \times LDMC + c$	0.525 ± 0.082	-0.491 ± 0.492	-0.468 ± 0.113		0.160	0.987	0.80	$<2x10^{-9}$	-15.06
$a \times \pi_{osm} + b \times T + c \times \pi_{osm} \times T + d$	0.538 ± 0.205	0.397 ± 1.10	-0.192 ± 0.655	-0.646 ± 0.311	0.163	0.987	0.80	$<2x10^{-9}$	-14.26
$a \times \rho + b$	-1.81 ± 0.243	-0.766 ± 0.090			0.214	0.977	0.65	$<2x10^{-7}$	-3.88
$a \times LDMC + b$	-2.88 ± 0.491	-0.396 ± 0.172			0.247	0.970	0.53	$<2x10^{-5}$	4.58
$a \times LMA + b$	$-0.004 \pm 7 \times 10^{-4}$	-0.991 ± 0.085			0.257	0.967	0.49	$<2\times10^{-5}$	7.11
$a \times \varepsilon + b$	-0.073 ± 0.012	-1.13 ± 0.120			0.325	0.970	0.57	$<2\times10^{-8}$	21.16
$a \times T + b$	-1.21 ± 0.513	-1.02 ± 0.160			0.332	0.945	0.16	0.03	22.41
Prediction of π_{osm} (testing sources of discrepancy from π_{pv})									
$a \times \pi_{PV}(1 - a_f) + b \times LDMC + c \times \pi_{PV}(1 - a_f)LDMC + d$	**0.993 ± 1.09**	**-2.67± 1.67**	**-0.171± 2.54**	**-0.052 ± 0.598**	**0.316**	**0.963**	**0.71**	**$<2\times10^{-4}$**	**21.14***
$a \times \pi_{PV}(1 - a_f) + b \times \varepsilon + c \times \pi_{PV}(1 - a_f)\varepsilon + d$	-0.737 ± 0.923	0.0073 ± 0.06	0.089 ± 0.061	-1.37 ± 0.876	0.349	0.955	0.65	$<2\times10^{-4}$	25.26*
$a \times \pi_{PV}(1 - a_f) + b \times \rho + b \times \pi_{PV}(1 - a_f)\rho + d$	-0.456 ± 1.09	-1.54 ± 2.35	1.08 ± 2.21	-0.962 ± 1.06	0.351	0.954	0.64	$<2\times10^{-4}$	25.54*
$a \times \pi_{PV}(1 - a_f) + b \times LMA + c \times \pi_{PV}(1 - a_f)LMA + d$	1.95 ± 1.25	$(-8.7 \pm 5.1) \times 10^{-4}$	-0.011 ± 0.008	-2.14 ± 0.897	0.370	0.949	0.60	$<2\times10^{-4}$	27.68*
$a \times \pi_{PV}(1 - a_f) + b \times T + c \times \pi_{PV}(1 - a_f)T + d$	2.23 ± 1.50	-5.61 ± 3.55	-4.07± 3.69	1.10 ± 1.40	0.486	0.912	0.31	$<2\times10^{-4}$	38.56*
Prediction of π_{tlp}									
$a \times \pi_{osm} + b$	0.832 ± 0.006	-0.631 ± 0.024			0.185	0.990	0.86	$<2\times10^{-12}$	-12.58
$a \times \pi_{pv} + b$	**1.31 ± 0.073**	**-0.012 ± 0.104**			**0.144**	**0.994**	**0.91**	**$<2\times10^{-16}$**	**-27.48**
$a \times \widehat{\pi_{pv}} + b$	1.38 ± 0.099	0.086 ± 0.140			0.181	0.991	0.87	$<2\times10^{-11}$	-13.91
$a \times \pi_{osm} + b \times \rho + c \times \pi_{osm} \times \rho + d$	0.933 ± 0.152	-1.55 ± 0.616	-0.532 ± 0.307	-0.254 ± 0.221	0.165	0.992	0.89	$<2\times10^{-11}$	-13.30
$a \times \pi_{osm} + b \times LMA + c \times \pi_{osm} \times LMA + d$	0.907 ± 0.134	-0.004 ± 0.002	$-0.002 \pm 9 \times 10^{-4}$	-0.388 ± 0.177	0.166	0.992	0.89	$<2\times10^{-11}$	-12.95
$a \times \pi_{osm} + b \times T + c \times \pi_{osm} \times T + d$	1.10 ± 0.224	-1.86 ± 1.20	-0.982 ± 0.715	-0.148 ± 0.339	0.178	0.991	0.87	$<2\times10^{-11}$	-8.94

$a \times \widehat{\pi_{tlp}} + b$	0.646 ± 0.063	-0.692 ± 0.116	0.232	0.984	0.78	$<2\times10^{-10}$	0.98
$a \times LDMC + b$	-4.21 ± 0.613	-0.377 ± 0.215	0.308	0.973	0.61	$<2\times10^{-6}$	17.84
$a \times \rho + b$	-2.33 ± 0.363	-1.02 ± 0.135	0.321	0.971	0.58	$<2\times10^{-6}$	20.34
$a \times LMA + b$	$-0.006 \pm 9 \times 10^{-4}$	-1.25 ± 0.108	0.327	0.969	0.56	$<2\times10^{-6}$	21.48
$a \times \varepsilon + b$	-0.073 ± 0.012	-1.13 ± 0.123	0.325	0.970	0.57	$<2\times10^{-6}$	21.17
$a \times T + b$	-2.01 ± 0.668	-1.22 ± 0.208	0.431	0.947	0.23	<0.01	38.21

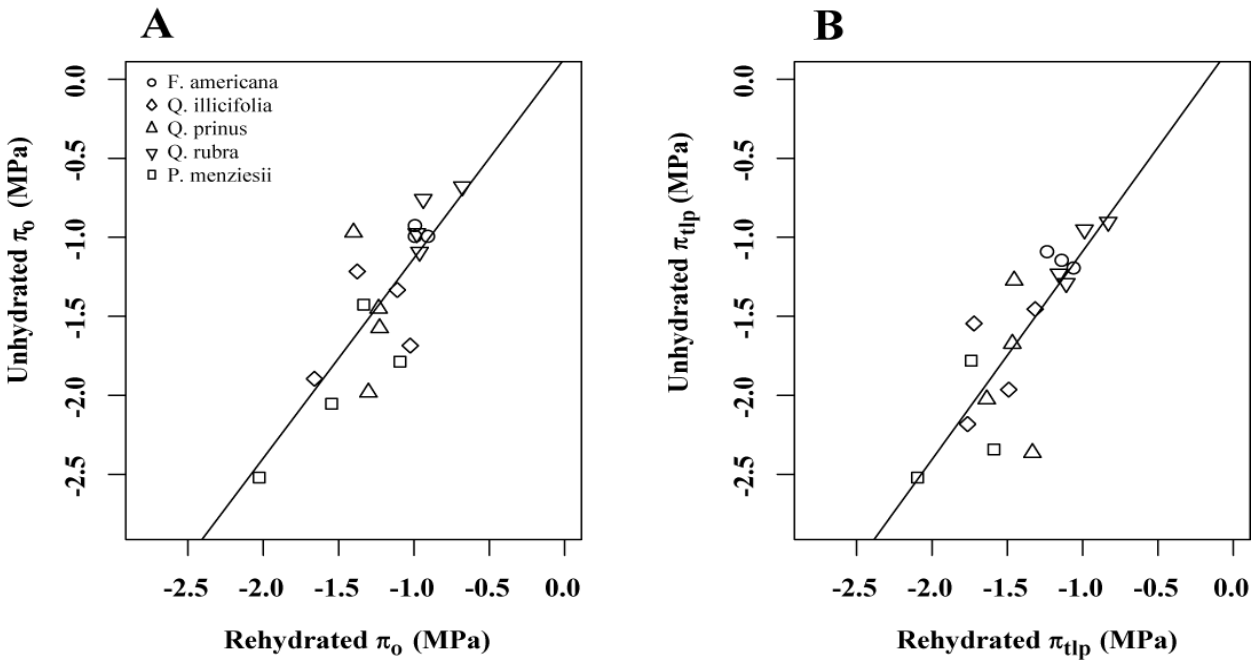
A
F. americana
Q. illicifolia
Q. prinus
Q. rubra
P. menziesii
Unhydrated π_o (MPa)
Rehydrated π_o (MPa)
-2.5
-2.0
-1.5
-1.0
-0.5
0.0
B
Unhydrated π_{tlp} (MPa)
Rehydrated π_{tlp} (MPa)

Figure S3.1

REFERENCES

Abrams, M.D. & Kubiske, M.E. (1990) Photosynthesis and water relations during drought in *Acer rubrum* L. genotypes from contrasting sites in central Pennsylvania. *Functional Ecology,* **4,** 727-733.

Andersen, M.N., Jensen, C.R. & Losch, R. (1991) Derivation of pressure-volume curves by a nonlinear regression procedure and determination of apoplastic water. *Journal of Experimental Botany,* **42,** 159-165.

Auge, R.M., Duan, X.G., Croker, J.L., Witte, W.T. & Green, C.D. (1998) Foliar dehydration tolerance of twelve deciduous tree species. *Journal of Experimental Botany,* **49,** 753-759.

Auge, R.M., Hickok, L.G. & Stodola, A.J.W. (1989) Psychrometric pressure-volume analysis of osmoregulation in roots, shoots, and whole sporophytes of salinized *Ceratopteris*. *Plant Physiology,* **91,** 322-330.

Ball, R.A. & Oosterhuis, D.M. (2005) Measurement of root and leaf osmotic potential using the vapor-pressure osmometer. *Environmental and Experimental Botany,* **53,** 77-84.

Baltzer, J.L., Davies, S.J., Bunyavejchewin, S. & Noor, N.S.M. (2008) The role of desiccation tolerance in determining tree species distributions along the Malay-Thai Peninsula. *Functional Ecology,* **22,** 221-231.

Bartlett, M., Scoffoni, C. & Sack, L. (2012) The determinants of leaf turgor loss point and prediction of drought tolerance of species and biomes: a global meta-analysis. *Ecology Letters,* **in press**.

Blackman, C.J., Brodribb, T.J. & Jordan, G.J. (2010) Leaf hydraulic vulnerability is related to conduit dimensions and drought resistance across a diverse range of woody angiosperms. *New Phytologist,* **188,** 1113-1123.

Brodribb, T.J. & Holbrook, N.M. (2003) Stomatal closure during leaf dehydration, correlation with other leaf physiological traits. *Plant Physiology,* **132,** 2166-2173.

Bucci, S.J., Goldstein, G., Meinzer, F.C., Scholz, F.G., Franco, A.C. & Bustamante, M. (2004) Functional convergence in hydraulic architecture and water relations of tropical savanna trees: from leaf to whole plant. *Tree Physiology,* **24,** 891-899.

Burnham, K.P. & Anderson, D.R. (2002) *Model selection and multimodel inference, 2nd ed*. Springer, New York, New York, USA. .

Burnham, K.P. & Anderson, D.R. (2004) Multimodel inference - understanding AIC and BIC in model selection. *Sociological Methods & Research,* **33,** 261-304.

Callister, A.N., Arndt, S.K. & Adams, M.A. (2006) Comparison of four methods for measuring osmotic potential of tree leaves. *Physiologia Plantarum,* **127,** 383-392.

Cao, M., Zou, X.M., Warren, M. & Zhu, H. (2006) Tropical forests of Xishuangbanna, China. *Biotropica,* **38,** 306-309.

Cutler, J.M., Rains, D.W. & Loomis, R.S. (1977) Importance of cell size in water relations of plants. *Physiologia Plantarum,* **40,** 255-260.

Eldredge, E.P. & Shock, C.C. (1990) Comparison of hydraulic press and pressure chamber estimates of potato leaf water potential. *American Potato Journal,* **67,** 307-312.

Engelbrecht, B.M.J., Velez, V. & Tyree, M.T. (2000) Hydraulic conductance of two co-occuring neotropical understory shrubs with different habitat preferences. *Annals of Forest Science,* **57,** 201-208.

Falster, D.S., Warton, D.I. & Wright, I. (2006) SMATR: Standardised major axis tests and routines, ver 2.0. http://www.bio.mq.edu.au/ecology/SMATR/.

Fang, J., Wang, Z. & Tang, Z. (2011) *Atlas of Woody Plants in China: Distribution and Climate*. Springer, Beijing.

Gabriel, R. & Kesselmeier, J. (1999) Apoplastic solute concentrations of organic acids and mineral nutrients in the leaves of several fagaceae. *Plant and Cell Physiology,* **40,** 604-612.

Garnier, E. & Laurent, G. (1994) Leaf anatomy, specific mass and water-content in congeneric annual and perennial grass species. *New Phytologist,* **128,** 725-736.

Grange, R.I. (1983) Solute production during the measurement of solute potential on disrupted tissue. *Journal of Experimental Botany,* **34,** 757-764.

Hulshof, C.M. & Swenson, N.G. (2010) Variation in leaf functional trait values within and across individuals and species: an example from a Costa Rican dry forest. *Functional Ecology,* **24,** 217-223.

James, J.J., Alder, N.N., Muhling, K.H., Lauchli, A.E., Shackel, K.A., Donovan, L.A. & Richards, J.H. (2006) High apoplastic solute concentrations in leaves alter water relations of the halophytic shrub, Sarcobatus vermiculatus. *Journal of Experimental Botany,* **57,** 139-147.

Kikuta, S.B., Kyriakopoulous, E. & Richter, H. (1985) Leaf hygrometer v. pressure chamber: a comparison of pressure-volume curve data obtained on single leaves by alternating measurements. *Plant Cell and Environment,* **8,** 363-367.

Kikuta, S.B. & Richter, H. (1992a) Leaf disks or press saps? a comparison of techniques for the determination of osmotic potentials in freeze thawed leaf material. *Journal of Experimental Botany,* **43,** 1039-1044.

Kikuta, S.B. & Richter, H. (1992b) A simplified pressure-volume method for the estimation of osmotic adjustement with the pressure chamber. *Bodenkultur,* **43,** 307-318.

Kohl, K. (1996) Population-specific traits and their implication for the evolution of a drought-adapted ecotype in *Armeria maritima*. *Botanica Acta,* **109,** 206-215.

Kohl, K.I. (1997) NaCl homoeostasis as a factor for the survival of the evergreen halophyte *Armeria maritima* (Mill.) Willd. under salt stress in winter. *Plant Cell and Environment,* **20,** 1253-1263.

Koide, R.T., Robichaux, R.H., Morse, S.R. & Smith, C.M. (1989) Plant water status, hydraulic resistance, and capacitance. In: Pearcy, R W. et al. [eds] Plant Physiological Ecology: Field Methods and Instrumentation. Chapman & Hall, London, pp 161-183. .

Kraft, N.J.B., Valencia, R. & Ackerly, D.D. (2008) Functional traits and niche-based tree community assembly in an amazonian forest. *Science,* **322,** 580-582.

Kubiske, M.E. & Abrams, M.D. (1990) Pressure-Volume Relationships in Non-Rehydrated Tissue At Various Water Deficits. *Plant Cell and Environment,* **13,** 995-1000.

Kubiske, M.E. & Abrams, M.D. (1991a) Rehydration effects on pressure-volume relationships in four temperate woody species: variability with site, time of season and drought conditions. *Oecologia,* **85,** 537-542.

Kubiske, M.E. & Abrams, M.D. (1991b) Seasonal, diurnal and rehydration-induced variation of pressure-volume relationships in *Pseudotsuga menziesii*. *Physiologia Plantarum,* **83,** 107-116.

Lan, G., Zhu, H., Cao, M., Hu, Y., Wang, H., Deng, X., Zhou, S., Cui, J., Huang, J., He, Y., Liu, L., Xu, H. & Song, J. (2009) Spatial dispersion patterns of trees in a tropical rainforest in Xishuangbanna, southwest China. *Ecological Research,* **24,** 1117-1124.

Lenz, T.I., Wright, I.J. & Westoby, M. (2006) Interrelations among pressure-volume curve traits across species and water availability gradients. *Physiologia Plantarum,* **127,** 423-433.

Meinzer, F.C., Rundel, P.W., Sharifi, M.R. & Nilsen, E.T. (1986) Turgor and osmotic relations of the desert shrub *Larrea tridentata*. *Plant Cell and Environment,* **9,** 467-475.

Morgan, J.M. (1992) Adaptation to water deficits in 3 grain legume species. Mechanisms of turgor maintenance. *Field Crops Research,* **29,** 91-106.

Niinemets, U. (2001) Global-scale climatic controls of leaf dry mass per area, density, and thickness in trees and shrubs. *Ecology,* **82,** 453-469.

Nonami, H. & Schulze, E.D. (1989) Cell water potential, osmotic potential, and turgor in the epidermis and mesophyll of transpiring leaves - Combined measurements with the cell pressure probe and nanoliter osmometer. *Planta,* **177,** 35-46.

Poorter, L. & Markesteijn, L. (2008) Seedling traits determine drought tolerance of tropical tree species. *Biotropica,* **40,** 321-331.

Royer, D.L., Sack, L., Wilf, P., Lusk, C.H., Jordan, G.J., Niinemets, U., Wright, I.J., Westoby, M., Cariglino, B., Coley, P.D., Cutter, A.D., Johnson, K.R., Labandeira, C.C., Moles, A.T., Palmer, M.B. & Valladares, F. (2007) Fossil leaf economics quantified: calibration, Eocene case study, and implications. *Paleobiology,* **33,** 574-589.

Sack, L., Cowan, P.D., Jaikumar, N. & Holbrook, N.M. (2003) The 'hydrology' of leaves: co-ordination of structure and function in temperate woody species. *Plant Cell and Environment,* **26,** 1343-1356.

Sack, L., Pasquet-Kok, J. & Contributors, P.W. (2010) Leaf pressure-volume curve parameters http://www.publish.csiro.au/prometheuswiki/tiki-pagehistory.php?page=Leaf pressure-volume curve parameters&preview=10.

Scoffoni, C., McKown, A.D., Rawls, M. & Sack, L. (2012) Dynamics of leaf hydraulic conductance with water status: quantification and analysis of species differences under steady-state. *Journal of Experimental Botany,* **63,** 643-658.

Scoffoni, C., Pou, A., Aasamaa, K. & Sack, L. (2008) The rapid light response of leaf hydraulic conductance: new evidence from two experimental methods. *Plant Cell and Environment,* **31,** 1803-1812.

Scoffoni, C., Rawls, M., McKown, A., Cochard, H. & Sack, L. (2011) Decline of leaf hydraulic conductance with dehydration: relationship to leaf size and venation architecture. *Plant Physiology,* **156,** 832-843.

Shackel, K.A. (1987) Direct measurement of turgor and osmotic potential in individual epidermal cells. Independent confirmation of leaf water potential as determined by insitu psychrometry. *Plant Physiology,* **83,** 719-722.

Shepherd, W. (1975) Matric water potential of leaf tissue. Measurement and significance. *Journal of Experimental Botany,* **26,** 465-468.

Sokal, R.R. & Rohlf, F.J. (1995) *Biometry: the principles and practice of statistics in biological research. Third edition*. W.H. Freeman and Company, New York, New Yord, USA.

Turner, N.C. (1981) Techniques and experimental approaches for the measurement of plant water status. *Plant and Soil,* **58,** 339-366.

Turner, N.C. (1988) Measurement of plant water status by the pressure chamber technique. *Irrigation Science,* **9,** 289-308.

Tyree, M.T. & Hammel, H.T. (1972) Measurement of turgor pressure and water relations of plants by pressure bomb technique. *Journal of Experimental Botany,* **23,** 267-282.

Violle, C. & Jiang, L. (2009) Towards a trait-based quantification of species niche. *Journal of Plant Ecology-Uk,* **2,** 87-93.

Wardlaw, I.F. (2005) Consideration of apoplastic water in plant organs: a reminder. *Functional Plant Biology,* **32,** 561-569.

Warton, D.I., Wright, I.J., Falster, D.S. & Westoby, M. (2006) Bivariate line-fitting methods for allometry. *Biological Reviews,* **81,** 259-291.

Wenkert, W. (1980) Measurement of tissue osmotic pressure. *Plant Physiology,* **65,** 614-617.

CHAPTER 4

GLOBAL ANALYSIS OF PLASTICITY IN TURGOR LOSS POINT, A KEY DROUGHT TOLERANCE TRAIT

ABSTRACT

Many species face increasing drought under climate change. Plasticity has been predicted to strongly influence species' drought responses, but broad patterns in plasticity are poorly known for key drought tolerance traits. As soil dries, plants are well known to shift their turgor loss or "wilting" point (π_{tlp}) by accumulating solutes (i.e., "osmotic adjustment"). We conducted the first global analysis of this plasticity ($\Delta\pi_{tlp}$) for 283 wild and crop species in ecosystems worldwide. $\Delta\pi_{tlp}$ was widely prevalent but moderate (-0.44 MPa), accounting for 16% of post-drought π_{tlp}. Thus, pre-drought π_{tlp} was a considerably stronger predictor of post-drought π_{tlp} across species of wild plants. For cultivars of certain crops $\Delta\pi_{tlp}$ accounted for major differences in post-drought π_{tlp}. Climate was correlated with pre- and post-drought π_{tlp} but not $\Delta\pi_{tlp}$. Thus, despite the wide prevalence of plasticity, π_{tlp} from either season can reliably characterize species' constitutive drought tolerances and distributions relative to water supply.

Keywords: Osmotic adjustment, turgor loss point adjustment, turgor loss point, drought tolerance, ecosystem water availability, variance partitioning, plasticity

INTRODUCTION

Droughts are expected to become more frequent and severe worldwide due to climate change (Sheffield & Wood 2007). Quantifying the physiological traits that correlate with drought

survival and ecosystem water supply, such as the leaf water potentials associated with stomatal closure, wilting, and hydraulic dysfunction (Brodribb *et al.* 2003; Choat *et al.* 2007; Bartlett *et al.* 2012b) have potential to improve predictions of shifts in species' distributions and community composition, functional diversity, and ecosystem services (Higgins *et al.* 2012). However, most models of species responses to climate change have assumed fixed trait values and climate niches (Dormann 2007) even though plants express plasticity in many traits in response to resource availability (Choat *et al.* 2007; Valladares *et al.* 2007; Nicotra *et al.* 2010) that could widen the range of tolerable climatic conditions (Dormann 2007; Nicotra *et al.* 2010). Little is known about the magnitude of plasticity in drought tolerance traits across diverse species and ecosystems. We present the first global analysis of plasticity in a well-recognized drought tolerance trait, the turgor loss point, to elucidate its variation across ecosystems, especially relative to ecosystem water supply.

The turgor loss point (π_{tlp}; unit: MPa) is the negative water potential at which leaf cells lose turgor and the leaf wilts, closing stomata and ceasing gas exchange and growth (Cheung *et al.* 1975; Brodribb *et al.* 2003; Blackman *et al.* 2010). The π_{tlp} also represents the soil water potential below which the plant cannot take up sufficient water to recover from wilting. Plants with more negative π_{tlp} values maintain stomatal and hydraulic conductance, photosynthetic gas exchange, and growth under drier soil conditions and generally occur in drier ecosystems (Becker *et al.* 1988; Brodribb *et al.* 2003; Lenz *et al.* 2006; Blackman *et al.* 2010; Bartlett *et al.* 2012b). The π_{tlp} is one of the key leaf physiological traits estimated from the relationship between the leaf water potential and leaf water volume, known as the pressure-volume (p-v) curve. The π_{tlp} is mechanistically related to the other pressure-volume parameters: osmotic potential, or the water potential produced by the cell solute concentration at full hydration (π_o;

unit: MPa); elastic modulus of the cell wall, or cell wall stiffness (ε; unit: MPa); and apoplastic fraction, or the proportion of water found outside the cells (a_f) (Cheung *et al.* 1975; Bartlett *et al.* 2012b). Because the π_{tlp} represents both the leaf and soil dryness that induce wilting, it is considered to be the "higher-level" trait that most directly quantifies plant drought tolerance, and plants are expected to vary the other p-v parameters to achieve a sufficiently negative π_{tlp} value for their habitat water availability (Lenz *et al.* 2006; Bartlett *et al.* 2012b). A related pressure-volume parameter, the relative water content at turgor loss point (RWC_{tlp}; unit: %), or the leaf hydration at wilting, has also been considered an important measure of plant drought tolerance (Sinclair & Ludlow 1985). The relative importance of RWC_{tlp} and π_{tlp} to drought tolerance has long been debated in the literature (Sinclair & Ludlow 1985), and a recent meta-analysis suggested that π_{tlp} and not RWC_{tlp} drives species associations with habitat water supply (Bartlett *et al.* 2012b).

That same meta-analysis also showed that differences among species in π_{tlp} are primarily driven by differences in π_o rather than ε or a_f. Similarly, shifts in π_{tlp} for given species during drought are driven by shifts in π_o caused by changes in the symplastic solute concentration (i.e., "osmotic adjustment") rather than by shifts in ε or a_f, which have relatively negligible effects (Bartlett *et al.* 2012b). Plants of many species can decrease their π_{tlp} in response to seasonal or occasional soil droughts by accumulating solutes to decrease π_o in existing leaves, including ions (K^+, Ca^{2+}), sugars, polyols (glycerol, mannitol), amino acids (proline), amines (glycine betaine), and organic acids (Morgan 1984; Chen & Jiang 2010), or by developing new leaves with greater solute concentrations (Wright *et al.* 1992). Additionally, plants also show shifts in RWC_{tlp} in response to drought-induced changes in both π_o and ε (Bartlett *et al.* 2012b). Although plasticity in these traits has itself been considered a key drought tolerance trait for decades in comparisons

of coexisting species or crop cultivars (Zhang *et al.* 1999; Blum 2005), there has been no synthesis of the quantitative importance of plasticity in π_{tlp} and RWC_{tlp} across species and ecosystems. We compiled a novel global database to conduct a meta-analysis of seasonal changes in π_{tlp} and RWC_{tlp}, and in particular to address the following questions:

1) For droughted plants, is the primary determinant of π_{tlp} and RWC_{tlp} the pre-drought values, or the plastic shift during the drought? Significant plasticity in these traits could modify species' drought tolerance over the course of wet and dry seasons, and may influence community-level processes if shuffling of species' rankings in these traits influences trait-mediated interactions among co-occurring species (Valladares *et al.* 2007). However, if pre-drought π_{tlp} and RWC_{tlp} are the main determinants of post-drought π_{tlp} and RWC_{tlp}, then measurements taken at any season could be used to characterize species drought tolerances within or across communities, considerably simplifying sampling and modeling in diverse communities.

2) How does plasticity in π_{tlp} and RWC_{tlp} ($\Delta\pi_{tlp}$ and ΔRWC_{tlp}) vary across ecosystems, and is that variation explained by ecosystem differences in water supply? Plants generally exhibit greater plasticity in leaf morphology, and photosynthetic and biomass allocation traits in environments with greater seasonal or interannual variation in water supply (Matesanz *et al.* 2010), as do plants from generally resource-rich communities, associated with their more rapid growth and development (Grime & Mackey 2002). However, plasticity in traits that reflect cellular acclimation instead of new tissue growth, such as solute accumulation, may be largely independent of overall resource availability (Grime & Mackey 2002). If the magnitude of plasticity varies with average habitat water availability or seasonality in water availability, then it should exhibit considerable variation among ecosystems, and correlations of plasticity with

climate variables may then improve estimates of phenotypic plasticity for future species distribution models.

3) Do crop species exhibit greater plasticity in π_{tlp} and RWC_{tlp} than wild species (i.e., species growing in natural ecosystems)? Improving crop drought tolerance through selective breeding for increased osmotic adjustment has been a long-standing objective of agricultural research (Zhang *et al.* 1999; Chen & Jiang 2010). However, it is unknown whether selective breeding has made drought-induced plasticity more important in crops than wild species, and more important to differences in drought tolerance across crop cultivars within species than across species.

METHODS

We compiled a novel database from 88 previously published studies of turgor loss point (π_{tlp}), osmotic potential at full hydration (π_o), and total relative water content at turgor loss point (RWC_{tlp}) measured in well-watered soil and during drought. We did not find sufficient data for a comparable analysis of symplastic RWC_{tlp}, which only includes the water lost from inside cells. We compiled studies from the literature by searching for the keywords "osmotic adjustment", "turgor loss point", or "pressure volume curve" combined with "seasonal", "adjustment", "plasticity", "drought", "dry season", "water stress", "agriculture", or "crop" in the Web of Science and AGRICOLA databases and the Google Scholar search engine, and for the sources that cited or were cited by studies that met our criteria for inclusion. We applied six criteria to minimize variation in our π_{tlp} and plasticity data due to ontogenetic and methodological factors that are known to affect these measurements. Thus, we included studies that (1) sampled mature, fully-expanded leaves from (2) sapling or adult plants and not seedlings experiencing (3)

seasonal and not interannual changes in water availability in naturally-occurring ecosystems (4) for wild species, since we sought to characterize ecosystem differences in plasticity, and experimental drought treatments for crop species. We also only selected studies that (5) rehydrated samples for $\geq$ 6 hours prior to measurement, unless the study tested for and reported no effect of rehydration time on the p-v curve parameters, and measured these variables by (6) generating pressure-volume curves. We allowed an exception to criterion 6 to include new osmometer measurements for 13 species from the Xishuangbanna Tropical Botanical Garden forest plot in Yunnan, China, which we converted to pressure-volume curve values using a published calibration (Bartlett *et al.* 2012a), and we verified that the uncertainty of these π_{tlp} values was within the range of the p-v curve values (see Appendix sections Supplemental Methods 4.1 and 4.2). We checked if this calibration could be applied to other published osmometer data, but these measurements are highly sensitive to sampling technique (Brown & Shouse 1992), and the studies that collected osmometer data and met the other criteria either used different techniques or did not provide enough information to determine whether the sampling procedures were similar.

We collected species means for each variable, since all of the studies reported species summary statistics and not values for individual plants. This produced a dataset of 246 wild and 37 crop species for π_{tlp} plasticity, 207 wild and 33 crop species for π_o adjustment, and 90 wild and 30 crop species for RWC_{tlp} plasticity. For the studies that did not define wet and dry seasons but instead measured these variables throughout the year, we used their soil water potential or precipitation data to identify the wettest and driest sampling times at which leaves would be fully expanded.

Environmental data and categorization of biomes and functional types

Climate data were determined for each wild species in the database. Study site coordinates were used to extract local climate data at a 30 arc-second resolution for mean annual precipitation (MAP) from the WorldClim database, and annual potential evapotranspiration (PET) and aridity index (AI = MAP/PET) from the CGIAR-CSI database, which used the WorldClim data to calculate these variables (Hijmans *et al.* 2005; Trabucco & Zomer 2009) (Table S4.1, S4.2; Fig. S4.1). We used these variables to calculate a simple index of annual water balance (WB = MAP - PET). To determine whether plasticity was related to seasonality, we also calculated water balance for the months in which pre- and post-drought measurements were taken in each study, and calculated seasonal changes as post-drought – pre-drought values.

We classified species into biome categories based on the Global Plant Trait Network (GLOPNET) definitions, including temperate conifer (n = 15 species for $\Delta\pi_{tlp}$) and broadleaf forests (n = 37), tropical dry forest (n = 83) and tropical conifer (n = 2), Mediterranean/dry temperate (n = 55), semidesert (n = 27), grassland (n = 4), alpine/subalpine (n = 6), and coastal/wetland (n = 17) (Wright *et al.* 2004) (Table S4.2). Functional types within each biome were further categorized as herbaceous, deciduous, and evergreen for biomes with at least 5 species per category.

Statistical analyses

We calculated the plasticities of π_{tlp} ($\Delta\pi_{tlp}$), π_o ($\Delta\pi_o$), and RWC_{tlp} (ΔRWC_{tlp}) as post-drought minus pre-drought species means for each variable. Thus, a negative plasticity in $\Delta\pi_{tlp}$ and $\Delta\pi_o$ and a positive plasticity in ΔRWC_{tlp} signify an improvement in drought tolerance.

We first analyzed variation across species without accounting for variation within species for all 246 wild and 37 crop species; this is the principal analysis presented here, because it allowed us to draw conclusions from the widest possible range of species and ecosystem

diversity. We also performed a traditional meta-analysis, which analyzes effect sizes weighted by precision, and can achieve greater statistical power, but within-species variation was only reported for 85 wild and 18 crop species. We compared the findings of the principal analysis with the findings for mean $\Delta\pi_{tlp}$ values weighted by precision (i.e., standard errors for species values) for the subset of species with precision measures, and also, for all the species in the full dataset after assigning to species lacking precision measures the lowest precision reported in the subset of species with sufficient information (see Appendix section Supplemental Methods 4.3). Findings using precision-weighted effect sizes were in almost all cases the same as findings using unweighted effect sizes (see Appendix section Supplemental Results and Discussion 4.1).

Recent ecological meta-analyses have increased rigor by using multi-level mixed effects models to account for the non-independence of species nested within the same study (Qian *et al.* 2010; Nakagawa & Santos 2012). Because most studies in our compiled dataset contained multiple species, and each species was only represented in one study, we tested for significant mean plasticity across species with the model:

$$Y_{kj} = \mu + \alpha_j + \varepsilon_{kj} \qquad \text{Eqn 4.1}$$

where Y_k is the plasticity for the *k*th species in the *j*th study, α_j is the effect of study *j*, μ is the mean plasticity across species after accounting for study-level variation, and ε_{kj} is the residual error. We determined 95% confidence intervals for μ from 1000 nonparametric bootstraps, because $\Delta\pi_{tlp}$ was non-normal even with log or square-root transformations. The bootstraps sampled the study sites with replacement and the species within the selected sites without replacement (Ren *et al.* 2010). We analyzed the wild and crop species separately. Models were fit with the *lme4* package in R (version 3.1.0).

We used two methods to assess the relative importance of plasticity and pre-drought π_{tlp} and RWC_{tlp} to post-drought values. We focused these analyses on π_{tlp} and not $\pi_{o,}$ since π_{tlp} is the "higher-level" drought tolerance trait that plants shift using osmotic adjustment (Bartlett *et al*. 2012). First, we calculated the contribution of plasticity to post-drought values of π_{tlp} and RWC_{tlp} for each species as:

$$\pi_{tlp}\text{ plasticity contribution} = \frac{\Delta\pi_{tlp}}{post\text{-}drought\ \pi_{tlp}} \times 100 \qquad \text{Eqn 4.2}$$

$$RWC_{tlp}\text{ plasticity contribution} = \frac{\Delta RWC_{tlp}}{post\text{-}drought\ RWC_{tlp}} \times 100 \qquad \text{Eqn 4.3}$$

We calculated the mean and 95% confidence intervals for plasticity contribution across species as described above. If the mean plasticity contribution across species was < 50%, the magnitude of the pre-drought value was a more important determinant of the post-drought value than plasticity. To test for differences in plasticity contribution between wild and crop species, we fitted the following model with species type as a fixed effect and study as a random effect:

$$Y_k = \mu_\alpha + \alpha_j + \beta X_k + \varepsilon_k \qquad \text{Eqn 4.4}$$

Symbols follow Eqn 4.1, with β as the regression coefficients for the species types. We tested for significant differences with 1000 iterations of a permutation test, as plasticity contribution was also non-normal, even with standard transformations. Secondly, we compared the correlations of post-drought π_{tlp} and RWC_{tlp} with pre-drought and plasticity values using the model structure in Eqn 4.4, with study as a random effect and pre-drought or plasticity values as a fixed effect. We tested for significance with 1000 iterations of a permutation test and compared correlation strengths by determining 95% confidence intervals for the marginal r^2 for each correlation (Nakagawa *et al.* 2013), which represents the variance explained by the fixed effects. These correlations are not statistically independent, since one variable will be nearly equal to the residuals of the regression between the post-drought values and the other variable if the slope is

close to 1, as in these correlations. However, this does not predispose either pre-drought or plasticity values to be more strongly correlated with post-drought values than the other, so this test was able to determine which variable was most predictive of post-drought values.

To determine the variation in $\Delta\pi_o$ and $\Delta\pi_{tlp}$ across ecosystems, we tested for mean biome differences in $\Delta\pi_o$ and $\Delta\pi_{tlp}$ for all 9 biome and functional type categories with ≥ 5 species (Table S4.2). We modeled biome as a fixed effect and study as a random effect nested within biomes, following Eqn 4.4. There was insufficient replication to analyze RWC_{tlp}. We also used this model structure to test trait correlations with annual, pre-drought month, post-drought month, and seasonal differences in water balance, and annual aridity index for pre- and post-drought and plasticity in π_{tlp} and RWC_{tlp}. We tested significance with 1000 iterations of a permutation test.

We did not investigate phylogenetic patterning among species in our analyses for two technical reasons. Most importantly, published studies were not designed to resolve phylogenetic patterns, so data are not yet available for many closely-related species within lineages that have diversified across moisture gradients, which would provide the strongest insight into the evolutionary trajectory of these traits. Second, the data for $\Delta\pi_{tlp}$ and plasticity contribution was significantly non-normal (Fig. 4.1), and there do not yet exist nonparametric tests that can account for phylogeny, to our knowledge (see Appendix section Supplemental Methods 4.4). The importance of phylogenetic relatedness to variation in drought tolerance plasticity remains to be resolved, in particular in studies that would sample within genera or families that have radiated across moisture gradients.

RESULTS

Plasticity in drought tolerance in response to seasonal changes in water availability was pervasive among wild and crop plants. Wild species exhibited significant osmotic adjustment and plasticity in π_{tlp} (Fig. 4.1A, B), with a mean [95% confidence intervals] of -0.29 MPa [-0.25 to -0.36 MPa] for $\Delta\pi_o$ and -0.44 MPa [-0.37 to -0.53 MPa] for $\Delta\pi_{tlp}$. (Note, that by "mean", we refer to the intercept in the mixed model, i.e., the mean adjustment across species when accounting for the non-independence of species within the same study). Species varied widely in plasticity, with the Australian wetland species *Casuarina obesa,* Australian dry temperate species *Grevillea patentiloba*, and North American semidesert species *Prosopis glandulosa* achieving extremely high π_{tlp} plasticities of $\leq$ -2 MPa. For a minority of species, the mean $\Delta\pi_o$ and $\Delta\pi_{tlp}$ were $\geq$ 0, indicating that plants did not undergo osmotic adjustment or π_{tlp} plasticity to improve drought tolerance in the dry season; this was the case in 31 species for π_o (15% of the 207 species in our dataset) and for π_{tlp} (12.6% of 246 species total).

RWC_{tlp} also showed significant plasticity across species, with a mean adjustment of -0.74%, [95% CI = -3.63 to -0.72%], suggesting that acclimating to water stress causes wild plants to experience small but significant declines in their ability to maintain cell hydration at wilting point.

Pre-drought π_{tlp} is a stronger predictor of post-drought π_{tlp} than plasticity

Across wild species, the plasticity contribution accounted for 16.0% of the magnitude of post-drought π_{tlp} [95% CI = 14.0 to 18.9%]. Indeed, despite considerable variation across species, the plasticity contribution accounted for the majority (contribution > 50%) of post-drought π_{tlp} for only 2% of species, or 4 of 246 species (Fig. 4.1C). Thus, despite the prevalence of and considerable variation in π_o and π_{tlp} plasticity across species (Fig. 4.1A, B), pre-drought π_{tlp} is the main determinant of π_{tlp} during drought.

Across species, the post-drought π_{tlp} was also more strongly correlated with pre-drought π_{tlp} (marginal r^2 [95% CI] = 0.51 [0.29 to 0.64], $p < 0.0001$, n = 246 species) than with $\Delta\pi_{tlp}$ (marginal r^2 = 0.19 [0.10 to 0.27], $p < 0.0001$) (Fig. 4.2A, B). Pre-drought π_{tlp} was therefore a stronger determinant of π_{tlp} during drought than $\Delta\pi_{tlp}$ across species.

Conversely, the plasticity contribution of RWC_{tlp} accounted for -2.7% of post-drought RWC_{tlp} [-4.8 to -0.9], indicating that plants slightly decrease their RWC_{tlp} in response to water stress. Consistent with this small contribution of plasticity, pre-drought RWC_{tlp} (marginal r^2 [95% CI] = 0.42 [0.14 to 0.67], $p < 0.0001$, n = 90 species) was more strongly correlated with post-drought RWC_{tlp} than is plasticity (marginal r^2 = 0.13 [0.04 to 0.45], $p < 0.0001$).

The π_{tlp} but not plasticity is strongly associated with site-level environmental conditions

Given that overall the pre-drought π_{tlp} was a stronger predictor of post-drought π_{tlp} across wild species than $\Delta\pi_{tlp}$, we tested whether the relative importance of $\Delta\pi_{tlp}$ might still vary across ecosystems. For example, plasticity might be larger and more influential in biomes prone to seasonal drought. While previous work has demonstrated that π_{tlp} varies strongly across biomes (Bartlett *et al.* 2012b), we did not find significant differences among biome and functional type categories for $\Delta\pi_o$ and $\Delta\pi_{tlp}$ (Fig. 4.3) (both $p > 0.4$), when analyzing data for 240 species (all species in biome categories with $\geq$ 5 species) without accounting for within-species variability (i.e., without weighting by precision). For the smaller subset of 85 species for which within-species variability was available, weighting effect sizes by precision resulted in significant differences among biomes, but not according to biome water availability (see Appendix section Supplemental Results and Discussion 4.1).

Stronger correlations of π_{tlp} than of plasticity with climatic water supply

Site-level means for pre- and post-drought π_{tlp} were significantly correlated with site-level means for annual water balance (precipitation – potential evapotranspiration) (both $p < 0.001$, $n = 231$ species), water balance during the dry season (both $p < 0.04$), and annual aridity index (both $p < 0.01$), with more drought-tolerant species occurring in drier sites (Table S4.1). Pre- and post-drought π_{tlp} were not correlated with any other climate variables (all $p > 0.2$).

By contrast, there were no significant correlations between $\Delta\pi_{tlp}$ and $\Delta\pi_o$ values and any climate variables (all $p > 0.08$). There were also no significant correlations between climate and pre- and post-drought RWC_{tlp} or ΔRWC_{tlp} (all $p > 0.4$). Thus, π_{tlp} and not RWC_{tlp} or plasticity appears to drive species distributions relative to water supply.

Plasticity in π_{tlp} is strong for crop cultivars and an important determinant of cultivar differences in drought tolerance

Crop species subjected to experimental drought showed similar responses to drought as wild species undergoing seasonal drought (Fig. 4.2, S4.2). Thus, droughted crop plants exhibited a significant shift towards more negative π_{tlp} values (mean [95% CI] = -0.38 MPa [-0.10 to -0.42], $n = 37$ species), and also lower RWC_{tlp} values (-2.2% [-0.3 to -3.2], $n = 30$ species). ("Mean" refers to the mean adjustment across species when accounting for the non-independence of species within the same study; see Eqn 4.1). The mean plasticity contribution to post-drought π_{tlp} and RWC_{tlp} across crop species (crops = 18.3% for π_{tlp} and -2.8% for RWC_{tlp}) was not significantly different from that of the wild species (both $p > 0.06$).

Further, as in wild plant species, the post-drought π_{tlp} was more strongly correlated across all the crop species with pre-drought π_{tlp} (marginal r^2 [95% CI] = 0.84 [0.69 to 0.92], $p < 0.0001$, $n = 37$ species) than with $\Delta\pi_{tlp}$ (0.16 [0.01 to 0.43], $p = 0.01$) (Fig. 4.2C, D). However, post-drought π_{tlp} was significantly correlated with $\Delta\pi_{tlp}$ and not pre-drought π_{tlp} within two of the

species with sufficient cultivar replication for analysis ($n \geq 5$), *Coffea arabica* ($r^2 = 0.97$, $p = 0.001$ for $\Delta\pi_{tlp}$; $r^2 = 0.004$, $p = 0.92$ for pre-drought π_{tlp}, $n = 5$) and *Zea mays* ($r^2 = 0.53$, $p = 0.06$ for $\Delta\pi_{tlp}$; $r^2 = 0.01$, $p = 0.84$ for pre-drought $\pi_{tlp,}$ $n = 6$) (Fig. 4.2D), but post-drought π_{tlp} was not correlated with either $\Delta\pi_{tlp}$ or pre-drought π_{tlp} across cultivars of *Zoysia japonica* ($\Delta\pi_{tlp}$: $r^2 = 0.16$, $p = 0.18$; pre-drought π_{tlp}: $r^2 = 0.04$, $p = 0.60$, $n = 8$) or *Zoysia matrella* ($\Delta\pi_{tlp}$: $r^2 = 0.37$, $p = 0.12$; pre-drought π_{tlp}: $r^2 = 0.10$, $p = 0.54$, $n = 6$).

Across crop species subjected to experimental drought, post-drought RWC_{tlp} was significantly correlated with pre-drought RWC_{tlp} (marginal r^2 [95% CI] = 0.80 [0.49 to 0.86], $p < 0.0001$, $n = 30$ species) but not ΔRWC_{tlp} (0.003 [0.0001 to 0.12], $p = 0.75$). However, these relationships were inconsistent across cultivars, with post-drought RWC_{tlp} not correlated with either pre-drought RWC_{tlp} or ΔRWC_{tlp} across *Zea mays* ($r^2 = 0.09$, 0.13, $p > 0.25$; respectively) or *Zoysia matrella* ($r^2 = 0.009$, 0.005; $p > 0.5$) cultivars, while post-drought RWC_{tlp} was significantly correlated with pre-drought RWC_{tlp} but not ΔRWC_{tlp} across *Zoysia japonica* cultivars ($r^2 = 0.52$, 0.06, $p = 0.03$, 0.6) (Fig. S4.2).

Thus, while on average plasticity makes a similarly low contribution to overall drought π_{tlp} for wild and crop species, among different cultivars of given crop species, plasticity can be a major determinant of relative drought tolerance under experimental drought.

DISCUSSION

Our results showed a great prevalence across species of plasticity in π_{tlp} between the wet and the dry season ($\Delta\pi_{tlp}$), with post-drought π_{tlp} becoming significantly more negative across wild species, with a mean shift of –0.44 MPa, and 87% of the wild species in our dataset exhibiting a $\Delta\pi_{tlp} < 0$ MPa (Fig. 4.1). $\Delta\pi_{tlp}$ accounted for a relatively small proportion (16%) of post-drought

π_{tlp}, and was a weaker predictor of post-drought π_{tlp} than were pre-drought values (Fig. 4.1, 4.2). Wild plants exhibited a small but significant decline in RWC_{tlp}, with a mean shift of -0.74%, which highlights the fact that plants can use elastic adjustment to maintain constant RWC_{tlp} values, as π_{tlp} declines (Bartlett *et al.* 2012b).

Our analysis showed strong variation in π_{tlp} plasticity and the π_{tlp} plasticity contribution to post-drought π_{tlp} across species globally, as well as within sites and biomes (Fig. 4.2A, B). Co-occurring species may exhibit differences in π_{tlp} plasticity because of landscape-level heterogeneity in water availability, differences in drought tolerance among functional types, and/or differences in species' abilities to generate and accumulate solutes. Local topographic heterogeneity can produce differences in soil water availability and air temperature greater than mean annual differences among sites and biomes, and species that occur in drier microhabitats within a given site generally exhibit more negative turgor loss points than co-occurring specialists on wetter microhabitats (Becker *et al.* 1988; Austin & Van Niel 2011). Species with greater rooting depths also have access to greater water supply during the dry season and maintain higher leaf water potentials and photosynthetic rates (Wright *et al.* 1992; Cao 2000), although species with deeper roots have been found to have more (e.g. Wright *et al.* 1992) and less negative (e.g. Davis & Mooney 1986) turgor loss points in different ecosystems. Species in the same site may therefore experience highly different water stresses during drought (Becker *et al.* 1988). Plant functional type is another known contributor to species differences in π_{tlp}. On average, woody species are generally more drought tolerant than herbaceous species, and evergreens tend to be more tolerant than deciduous species (Calkin & Pearcy 1984). Our database did not contain enough replication of functional types within sites to test for the effects of functional type on variation in the plasticity of π_{tlp} among co-occurring species.

Species may also differ in their ability to generate or tolerate an increased symplastic solute concentration, given their variation in the solutes upregulated during osmotic adjustment, which can include sugars, amino acids (proline), ions (K^+, Ca^{2+}), amines (glycine betaine), organic acids, and polyols (glycerol, mannitol) (Morgan 1984; Zhang *et al.* 1999; Chen & Jiang 2010). Proline can also indirectly contribute to drought tolerance by removing reactive oxygen species to protect cell membranes, enzymes, proteins, and other cellular components from chemical damage (Chen & Jiang 2010). The metabolic cost may vary significantly among different solute types, resulting in species differences in their capacity to osmotically adjust. The species for which osmotic adjustment is more costly due to metabolic constraints may instead depend more strongly on plasticity in other anatomical and physiological traits to survive drought, such as root morphology, water use efficiency, or xylem cavitation vulnerability (Choat *et al.* 2007; Nicotra *et al.* 2010). Data are lacking on the degree to which species' solute preferences, metabolic pathways and costs of osmotic adjustment might be phylogenetically conserved. Further, for a given osmotic adjustment ($\Delta\pi_o$), the effect on $\Delta\pi_{tlp}$ can vary, according to other pressure-volume parameters; a lower elastic modulus allows a given $\Delta\pi_o$ to drive a larger $\Delta\pi_{tlp}$ (Bartlett *et al.* 2012b). Understanding species-level variation in plasticity and its underlying biochemistry will improve with characterization of ecological and phylogenetic patterns in osmolyte preference, their metabolic costs, and the underlying functional genetics (Zhang *et al.* 1999).

Improving crop resilience to drought through increased osmotic adjustment has been a long-standing goal in crop development, to ensure food and land-use sustainability under climate change (Blum 2005; Nicotra et al. 2010). However, our analysis has shown that the contribution of plasticity to post-drought π_{tlp} in crop species was not significantly greater than that of wild

species. Importantly, for cultivars within species, plasticity but not pre-drought π_{tlp} was significantly correlated with post-drought π_{tlp}. However, the differences between the findings for crop cultivars versus wild species may also be due to their experiencing experimental rather than seasonal drought. The experimental droughts may have been imposed more rapidly than the seasonal droughts, and in some cases the droughts were applied to plants without previous exposure to drought, known as drought hardening or conditioning (Hsiao *et al.* 1976). Plants experience their largest osmotic adjustment during their first drought exposure, and maintain a more negative π_{tlp} for longer periods of time during wet conditions when exposed to more cycles of drought stress, reducing their subsequent plasticity (Hsiao *et al.* 1976). Most of the crop species, including the *Coffea arabica, Zea mays,* and *Zoysia* cultivars, were well-watered prior to the drought experiments, which may exaggerate the contribution of plasticity to drought tolerance compared to wild species, which were likely to have undergone numerous cycles of seasonal drought. In sum, these findings point to the equal but potentially greater contribution of plasticity to drought tolerance differences across crop cultivars than across wild species, as well as the general benefits of $\Delta\pi_{tlp}$ as a trait for crop improvement.

For wild plants, the close correlation of pre- and post-drought π_{tlp}, and of climate with pre- and post-drought π_{tlp} but not $\Delta\pi_{tlp}$ (Table 4.1), showed that π_{tlp} measurements from either season can be used to reliably assess species' relative drought tolerances and relate physiological traits to ecology. This result, together with readily available high-resolution climate data and rapid methods for assessing π_{tlp} and π_o (Bartlett *et al.* 2012a), can facilitate the incorporation of drought tolerance data into species distribution modeling, and improve the prediction of species composition, functional diversity, and overall ecosystem function for diverse communities. Such a simplified approach treats species as having similar negligible values for plasticity in π_{tlp},

which will provide a useful baseline that will be accurate on average. However, we found that plasticity is considerable for a minority of species, and this can potentially shape their range of tolerable climatic conditions and ability to adapt to future conditions. Therefore, while annual measurements of π_{tlp} provide a reasonable simplification for characterizing drought tolerance for many species or communities, determining the underlying mechanistic constraints on π_{tlp} plasticity and its variation across species will further improve the accuracy of predictions of species responses to climate change.

ACKNOWLEDGEMENTS

This work was supported by National Science Foundation grants #IOS-0546784, #1108534, and #DEB-1046113 (to S.J. Davies), the Center for Tropical Forest Science – Forest Global Earth Observatory of the Smithsonian Institution, the Vavra Research Fellowship, and the UCLA department of Ecology and Evolutionary Biology. The Forestry Department of Yunnan Province provided the permission to access the field site in the Xishuangbanna Nature Reserve, and the XTBG staff provided considerable logistical support and field assistance. We also thank Jerome Chave and three anonymous reviewers for providing insightful suggestions to improve the manuscript.

Table 4.1. The proportion of variance of drought tolerance traits explained by climate. To account for variation among studies, we present marginal r^2 values, or the proportion of variance explained by fixed effects (Nakagawa *et al.* 2013), for mixed-effects models predicting drought tolerance traits with climate as a fixed effect and study as a random effect. Traits are pre- and post-drought turgor loss point ($\pi_{tlp,}$) and the plasticities of π_{tlp} and π_o. Climate variables are annual, wet season, and dry season water balance (WB = mean precipitation (MP) – mean potential evapotranspiration (PET)), seasonality (ΔWB = dry season- wet season WB), and annual aridity index (AI = MP/PET). Bold values are significant (permutation test; $p < 0.05$). 0 values indicate an $r^2 < 0.01$. Sites with lower annual water balance, water balance in the dry season, and AI contained species that were more drought-tolerant in both seasons. Plasticity was not correlated with climate.

	Pre-drought π_{tlp}	**Post-drought π_{tlp}**	**π_{tlp} plasticity**	**π_o plasticity**
Water Balance (WB)				
annual	**0.12**	**0.14**	0.02	0
wet	0	0.02	0.01	0
dry	**0.04**	**0.06**	0.02	0
ΔWB	0	0.01	0	0
Aridity index (AI)				
annual	**0.07**	**0.07**	0	0

FIGURE CAPTIONS

Figure 4.1. Histograms summarizing data in a global database for wild species for the plasticities between the wet and dry season of A) osmotic potential ($\Delta\pi_o$) (n = 207 species) and B) turgor loss point ($\Delta\pi_{tlp}$) (n = 246), and C) the percentage of post-drought π_{tlp} attributable to $\Delta\pi_{tlp}$, i.e., the "plasticity contribution" (n = 246). Most species improved their drought tolerance, with mean $\Delta\pi_o$ = -0.29 MPa and mean $\Delta\pi_{tlp}$ = -0.44 MPa. ("Mean" here refers to the intercept in the mixed model in Eqn 4.1, i.e., the mean adjustment across species when accounting for the non-independence of species within the same study). 31 species did not make π_{tlp} or π_o more negative ($\Delta\pi_{tlp}$ or $\Delta\pi_o \geq 0$ MPa) in response to drought, representing 12.6% and 15% of species, respectively. On average, $\Delta\pi_{tlp}$ accounted for 16.0% of post-drought π_{tlp}, suggesting that pre-drought π_{tlp} was the more important determinant of post-drought π_{tlp}.

Figure 4.2. Across 246 wild species (panels A,B) and 37 crops (C,D), post-drought turgor loss point (π_{tlp}) was more strongly correlated with pre-drought π_{tlp} (**A;** r^2=0.51, p<0.0001; **C;** r^2=0.84, p<0.0001) than with π_{tlp} plasticity ($\Delta\pi_{tlp}$) (**B;** r^2=0.19, p<0.0001; **D**; r^2=0.16, p=0.01). Post-drought π_{tlp} was correlated with $\Delta\pi_{tlp}$ but not pre-drought π_{tlp} across cultivars of *Coffea arabica* (dashed line) and *Zea mays* (dotted line) (**D**), and neither variable across cultivars of *Zoysia japonica* and *Zoysia matrella*. Biome symbols (A,B): alpine/subalpine (○), grassland (●), temperate conifer (▼), semidesert (▼), Mediterranean/dry temperate (▽), coastal (○), temperate broadleaf (▽), and dry tropical (●). Crop species symbols (C,D): *Helianthus annuus* (○), *Saccharum* (sugarcane) (●), *Zea mays* (○), *Phaseolus vulgaris* (●), *Zoysia japonica* (▼), *Zoysia matrella* (▽), *Festuca arundinacea* (◆), *Coffea arabica* (▼), *Capsicum chinense* (◆), *Olea*

europa (△), ,and.*Ceratonia siliqua* (▲). ▽=all species with <3 cultivars. Dark line= regression for species means, gray line= regression across cultivars.

Figure 4.3. Biome means for wild species for seasonal plasticity in turgor loss point ($\Delta\pi_{tlp}$) (n = 240 species), for biomes with at least 5 species. Functional types within each biome are categorized as herbaceous (H.), woody (W.), deciduous (D.) and evergreen (E.) for biomes with at least 5 species per category. Tropical conifer and grassland biomes are excluded due to small sample sizes, and experimental drought results in 37 crop species are graphed for comparison. Light blue bars indicate dry biomes, and dark blue bars are wet biomes. There were no significant differences in $\Delta\pi_{tlp}$ among biomes (permutation test, $p = 0.9$).

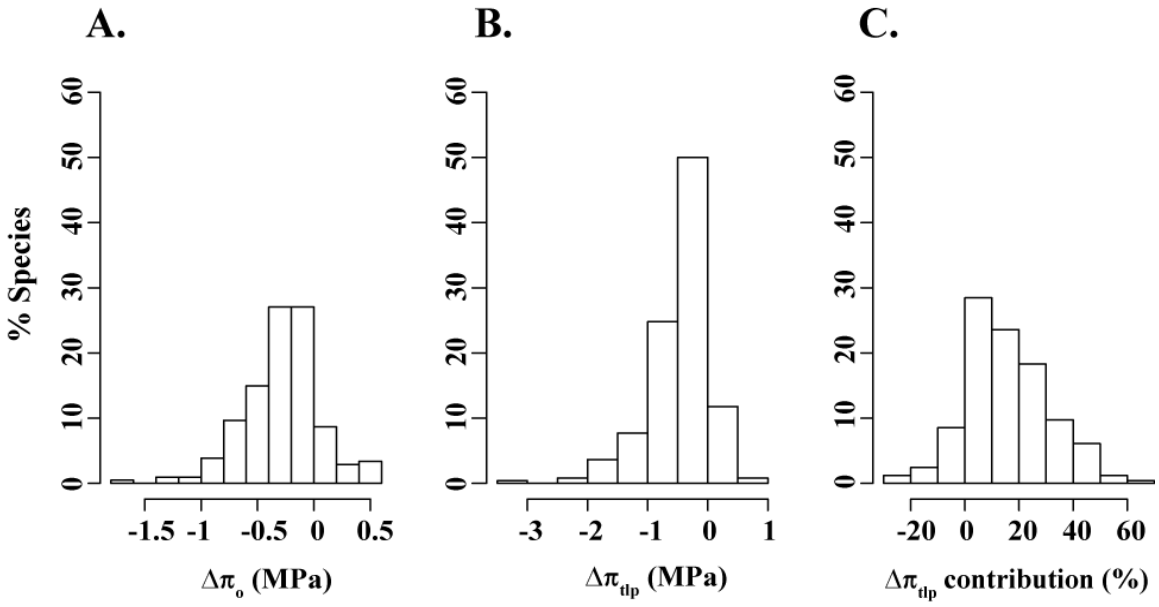
A.
B.
C.
% Species
0
10
20
30
40
50
60
-1.5
-1
-0.5
0
0.5
Δπo (MPa)
-3
-2
-1
0
1
Δπtlp (MPa)
-20
0
20
40
60
Δπtlp contribution (%)

Figure 4.1

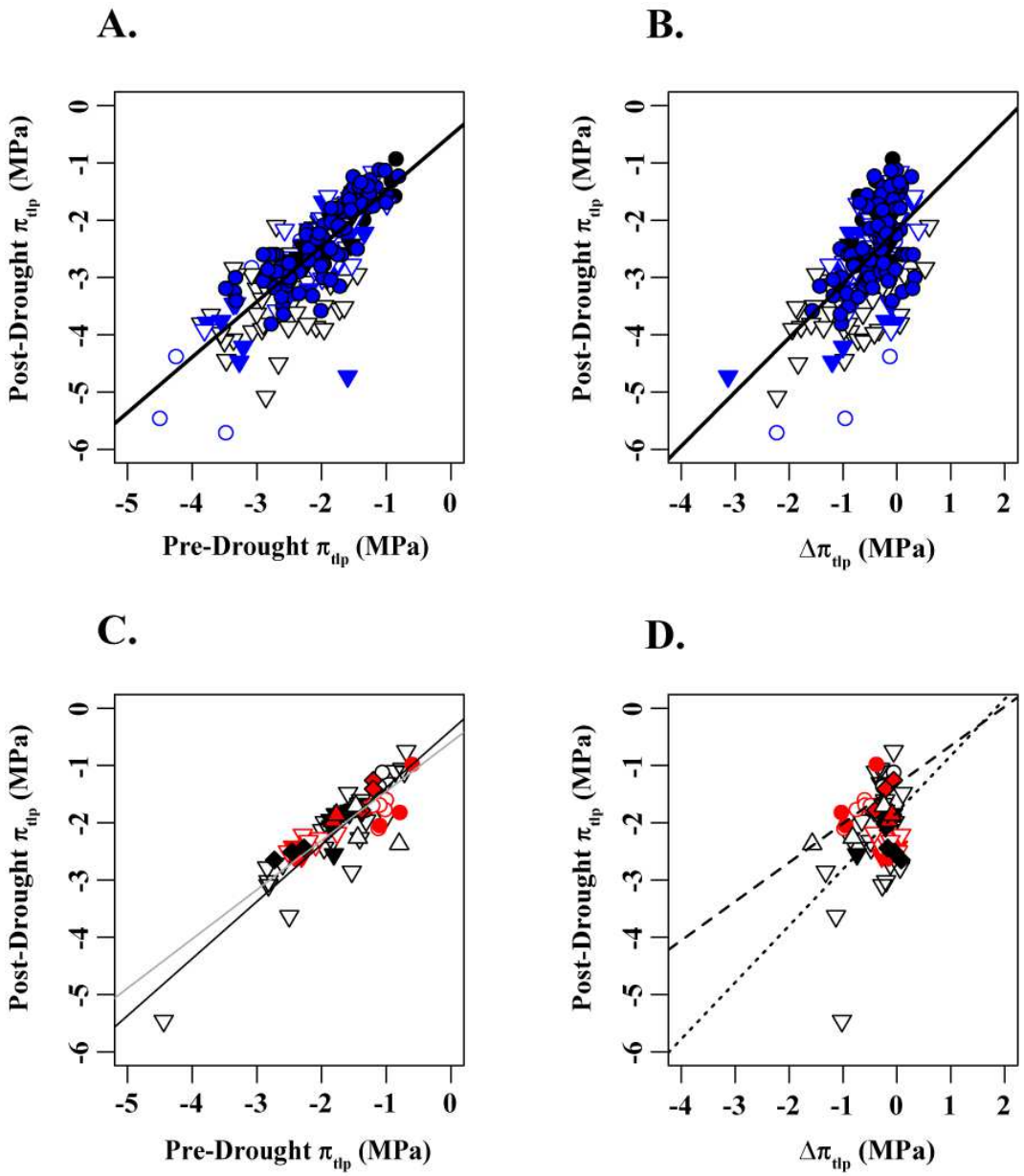
A.
B.
C.
D.
Post-Drought π_{tlp} (MPa)
Pre-Drought π_{tlp} (MPa)
$\Delta\pi_{tlp}$ (MPa)
0
-1
-2
-3
-4
-5
-6
1
2

Figure 4.2

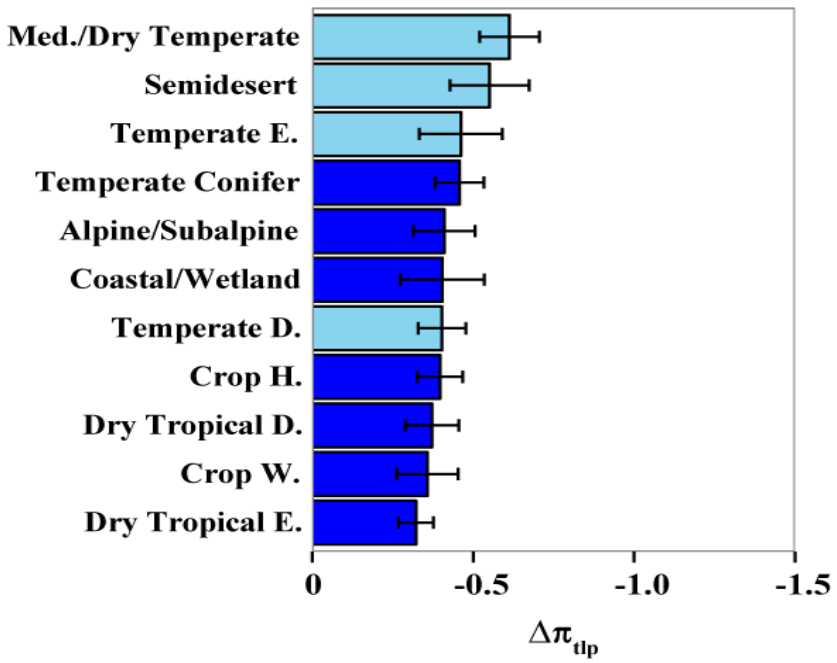
Med./Dry Temperate
Semidesert
Temperate E.
Temperate Conifer
Alpine/Subalpine
Coastal/Wetland
Temperate D.
Crop H.
Dry Tropical D.
Crop W.
Dry Tropical E.
0
-0.5
-1.0
-1.5
$\Delta\pi_{tlp}$

Figure 4.3

SUPPLEMENTAL MATERIAL

Table S4.1. Summary of a global database for 231 wild species (excluding 15 species for which data were averaged across multiple sites) of pre- and post-drought turgor loss point ($\pi_{tlp,}$), the plasticity of π_{tlp} ($\Delta\pi_{tlp}$), and the contribution of π_{tlp} plasticity to post-drought π_{tlp} (Contrib.), with climatic water availability mean annual precipitation (MAP), annual potential evapotranspiration (PET), annual aridity index (AI; = PET/MAP), water balance (WB; = MAP - PET) and seasonal differences in water balance (ΔWB = wet season WB – dry season WB) between the pre-drought and droughted months used in each study.

Table S4.2. Summary of means for a global database for 246 wild species of pre- and post-drought turgor loss point ($\pi_{tlp,}$), the plasticity of π_{tlp} ($\Delta\pi_{tlp}$), the contribution of π_{tlp} plasticity to post-drought π_{tlp}, and climatic water availability for biome categories and biome categories subdivided by functional type (i.e. temperate deciduous and temperate evergreen).

Table S4.3. Summary of data from a global database for cultivars of 37 crop species, for pre- and post-drought treatment turgor loss point (π_{tlp}), π_{tlp} plasticity ($\Delta\pi_{tlp}$), and percent contribution of plasticity in π_{tlp} to droughted π_{tlp} values.

Figure S4.1. A map of 60 site locations for all species analyzed in this study, color-coded by annual aridity index (mean annual precipitation/mean annual potential evapotranspiration); black locations have the lowest AI values and are wettest, whereas white areas have the highest AI values and are driest (Hijmans *et al.* 2005). This meta-analysis contains globally distributed study sites, with wide variation in local water supply.

Figure S4.2. Correlations in a global database for 30 crop species of pre- and post-drought values of leaf relative water content at turgor loss points (RWC_{tlp}), and its seasonal plasticity (ΔRWC_{tlp}). **A.** Pre- and post-drought RWC_{tlp} were significantly correlated across crop species (r^2= 0.74, $p < 0.0001$, n = 30 species), and across cultivars of *Zoysia japonica* ($r^2 = 0.52$, $p = 0.03$, ▼). Significant correlations are indicated with a line, with the black line showing correlations across species means, the gray line showing correlations across all cultivars, and the dotted line showing correlations across *Zoysia japonica* cultivars. **B.** Post-drought RWC_{tlp} was not correlated with ΔRWC_{tlp} across crop species ($r^2 = 0.02$, $p = 0.47$) or cultivars within species. Symbols follow Fig. 4.2.

Supplemental Methods 4.1. Osmometer measurements

Supplemental Methods 4.2. Uncertainty measurements

Supplemental Methods 4.3. Comparing the results of precision-weighted and unweighted effect sizes

Supplemental Methods 4.4. Phylogenetic relatedness

Supplemental Results and Discussion 4.1

Table S4.1. Summary of a global database for 231 wild species (excluding 15 species for which data were averaged across multiple sites) of pre- and post-drought turgor loss point ($\pi_{tlp,}$), the plasticity of π_{tlp} ($\Delta\pi_{tlp}$), and the contribution of π_{tlp} plasticity to post-drought π_{tlp} (Contrib.), with climatic water availability mean annual precipitation (MAP), annual potential evapotranspiration (PET), annual aridity index (AI; = PET/MAP), water balance (WB; = MAP - PET) and seasonal differences in water balance (ΔWB = wet season WB – dry season WB) between the pre-drought and droughted months used in each study. Drier sites have lower MAP, WB, and AI and higher PET values, and more seasonal sites have ΔWB values that are further from 0. Sites are expected to have negative ΔWB values, which indicate less precipitation and more potential evapotranspiration during the 'dry' months, but some sites exhibited less water stress, as the resolution of the climate data may not accurately characterize local seasonal trends, and/or the sites may lack a well-defined drought period.

Lat.	Lon.	$\pi_{tlp,\ pre\text{-}drought}$ (MPa)	$\pi_{tlp,\ drought}$ (MPa)	$\Delta\pi_{tlp}$ (MPa)	Contrib. (%)	N	MAP (mm)	PET (mm)	AI	WB (mm)	Wet Month	Dry Month	ΔWB (mm)	Reference
-46.52 N	-71.05 E	-2.6	-3.22	-0.62	19.2	7	188	848	0.19	-660	Feb	Nov	14	Scholz et al. 2012
-41.82 N	146.67 E	-2.17	-2.3	-0.13	5.3	2	1303	733	1.78	570	Apr	Dec	90	Sanger et al. 2011
-37.42 N	143.88 E	-2.55	-2.44	0.11	-3.4	3	734	1114	0.66	-380	Aug	Feb	143	Merchant et al. 2010
-33.75 N	117.45 E	-3.11	-3.5	-0.39	10.8	3	483	1303	0.36	-820	Jun	Mar	152	White et al. 2000
-32.71 N	116.06 E	-2.45	-2.2	0.25	-12.1	2	1215	1305	0.93	-90	Aug	Mar	235	Szota et al. 2011
-32.62 N	115.77 E	-3.54	-4.67	-1.13	21.2	3	879	1338	0.66	-459	Aug	Mar	173	Carter et al. 2006
-32.32 N	117.87 E	-2.78	-3.57	-0.79	20.9	20	375	1437	0.24	-1062	Sep	Mar	62	Mitchell et al. 2008
-22.25 N	-43.75 E	-2.46	-2.85	-0.39	14	26	1241	1440	1.02	-199	Jan	Jul	176	Wenhui 1998
-22.2 N	-41.42 E	-2.28	-2.47	-0.19	7.9	9	1200	1371	0.77	-171	Nov	Feb	57	Rosado & De Mattos 2010
-18.12 N	-68.95 E	-2.23	-2.25	-0.02	0.9	1	339	1055	0.32	-716	Feb	Sep	73	Garcia-Nunez et al. 2004
-12.57 N	131.08 E	-2	-2.09	-0.09	3.9	7	1509	1755	0.86	-246	Nov	Apr	14	Myers et al. 1997
4.97 N	117.77 E	-1.73	-2.04	-0.31	16	2	2329	1483	1.57	846	Jun	Apr	38	Gibbons & Newbery 2002
6.22 N	-5.03 E	-1.55	-1.9	-0.35	18.5	3	1200	1662	0.7	-462	Apr	Nov	54	Le Roux & Bariac 1998
8.62 N	-70.2 E	-1.4	-1.85	-0.45	24.3	1	850	1708	0.96	-858	Nov	Jan	109	Rada et al. 1985
8.87 N	-70.8 E	-1.69	-2.3	-0.61	26.5	1	822	981	0.85	-159	Feb	Jul	120	Rada et al. 2012
9.15 N	-79.85 E	-1.16	-1.34	-0.18	11.3	5	2600	1392	1.88	1208	Oct	Feb	234	Wright et al. 1992
10.83 N	-68.23 E	-3.16	-3.46	-0.3	9.4	3	1061	1525	0.7	-464	Oct	May	77	Rada et al. 1989
19.5 N	-105.05 E	-2.66	-3.08	-0.42	13.7	6	782	1824	0.42	-1042	Jul	Nov	62	Fanjul & Barradas 1987
21.15 N	100.83 E	-1.42	-1.4	0.02	-1.4	1	1666	1584	1.05	82	Jun	Apr	157	Liu et al. 2012
21.61 N	101.57 E	-1.59	-1.69	-0.1	5.2	13	1608	1425	0.89	183	Jul	Mar	283	Bartlett unpublished data

21.9 N	101.77 E	-1.27	-1.53	-0.26	16.4	5	1493	1394	1.04	99	Aug	Nov	178	Zhu & Cao 2009
21.9 N	101.77 E	-1.93	-2.24	-0.31	9.8	12	1709	1399	1.22	310	Jun	Apr	185	Fu et al. 2012
21.91 N	101.28 E	-2.59	-3.64	-1.05	28.8	1	1393	1589	0.88	-196	Jun	Apr	150	Wang et al. 2008
27.18 N	-81.35 E	-2.07	-2.07	0	0.4	3	1253	1637	0.77	-384	Sep	Feb	48	Abrams & Menges 1992
29.38 N	79.45 E	-1.77	-2.41	-0.64	26	10	1653	1000	1.77	653	Aug	Oct	182	Singh et al. 2006
30.81 N	34.9 E	-2.01	-2.16	-0.15	6.9	1	61	1478	0.13	-1418	Feb	Aug	138	Shrestha 2003
33.25 N	-116.38 E	-1.6	-4.73	-3.13	66.2	1	301	1805	0.11	-1504	Feb	Jul	193	Nilsen et al. 1983
33.43 N	-111.75 E	-2.94	-3.26	-0.32	9.9	5	230	1736	0.14	-1507	Feb	Jul	154	Monson & Smith 1982
33.59 N	-101.89 E	-2.51	-3.33	-0.82	24.6	1	450	1431	0.33	-981	Apr	May	-2	Wan et al. 1993
34.5 N	134.33 E	-1.55	-2.43	-0.89	36.4	1	1344	1023	1.32	321	May	Jul	-47	Miki et al. 2003
35.15 N	136.88 E	-2.26	-2.99	-0.73	24.7	3	1600	1072	1.58	528	Mar	Jan	22	Harayama et al. 2006
35.5 N	-83.4 E	-1.31	-1.59	-0.28	17.6	1	1487	1201	1.24	286	Jul	Aug	-6	Andersen & McLaughlin 1991
35.9 N	-79.3 E	-2.03	-2.42	-0.39	15.7	4	1157	1276	0.91	-119	Sep	Oct	-42.25	Roberts & Knoerr 1977
37.02 N	80.8 E	-1.56	-2.43	-0.87	35.7	3	33	1271	0.03	-1238	May	Jul	31	Thomas et al. 2008
37.4 N	-122.2 E	-3	-3.2	-0.2	7.5	2	626	1112	0.56	-486	May	Jul	31	Davis & Mooney 1986
38.18 N	15.55 E	-2.33	-2.75	-0.42	12.6	3	851	923	0.82	-72.1	May	Sep	-46	Lo Gullo & Salleo 1988
38.57 N	84.3 E	-1.3	-1.61	-0.31	19.3	1	19	1321	0.01	-1302	May	Jul	21	Liang et al. 2008
38.8 N	-92.2 E	-1.8	-2.48	-0.68	27.1	3	1009	1193	0.85	-184	May	Sep	59	Parker et al. 1982
39.08 N	-96.58 E	-1.35	-1.82	-0.47	25.2	3	872	1153	0.76	-281	Jun	Aug	56	Knapp 1984
39.1 N	-96.6 E	-1.86	-2.5	-0.63	24.3	3	863	1167	0.74	-304	Jun	Jul	55	Abrams & Knapp 1986
39.2 N	111.27 E	-1.79	-1.98	-0.18	7.9	7	455	1055	0.43	-600	May	Jun	-4	Chai et al. 2000
39.5 N	107.17 E	-2.55	-3.2	-0.65	20.3	1	208	994	0.21	-786	Jul	Sep	-50	Shi et al. 2008
41.12 N	-3.5 E	-1.47	-1.48	-0.01	-0.1	3	452	908	0.59	-456	Jun	Aug	-14	Kubiske & Abrams 1991b
41.89 N	-98.55 E	-1.35	-1.56	-0.21	13.5	1	620	1077	0.58	-457	Jun	Jul	32	Barnes 1985
43.43 N	10.7 E	-2.38	-2.92	-0.54	18.4	3	810	909	0.85	-99.4	May	Jul	68	Tognetti et al. 2000
43.44 N	-79.92 E	-2.58	-3.19	-0.62	19.3	1	845	867	0.98	-22	Aug	Sep	-38	Collier & Boyer 1989
44.58 N	-124.05 E	-1.74	-2.19	-0.45	19.6	2	1796	748	2.56	1048	Mar	Aug	227	Pavlik 1984
44.64 N	-123.19 E	-2.14	-2.58	-0.43	15.9	6	1085	1020	1.08	65	Jun	Aug	26	Davis 2005
44.71 N	-89.1 E	-1.5	-2.16	-0.66	29	3	814	903	0.9	-89	May	Aug	-5	Abrams 1988
46.17 N	-122.23 E	-1.15	-1.3	-0.15	10.9	2	2917	674	4.34	2243	Jul	Aug	-34	Chapin & Bliss 1988
46.2 N	-122.18 E	-0.9	-1.45	-0.55	37.4	2	3115	493	6.34	2622	Jun	Aug	46	Braatne & Bliss 1999
46.56 N	12.15 E	-2.03	-2.69	-0.66	24.5	1	1091	659	3.73	432	Jun	Aug	-23	Badalotti et al. 2000
46.8 N	-116.8 E	-2.38	-2.52	-0.13	5.4	4	698	932	0.75	-234	Jul	Aug	-27	Jackson & Spomer 1989
47.3 N	-121.6 E	-1.89	-2.54	-0.65	25.6	1	1316	607	2.15	709	May	Jul	113	Teskey et al. 1983
47.3 N	-71.2 E	-1.45	-1.7	-0.26	14.9	2	1902	614	3.06	1288	Jul	Aug	-7	Pothier & Margolis

														1990
47.81 N	-114.31 E	-1.89	-2.54	-0.65	25.1	3	604	921	0.66	-317	Jun	Jul	54	Aranda et al. 1996
47.81 N	-114.31 E	-1.61	-2.48	-0.87	35.1	1	461	925	0.49	-464	Jun	Aug	27	Foster 1992
47.9 N	-122.1 E	-1.56	-1.45	0.11	-6.3	2	1058	846	1.25	212	Jun	Sep	-49	Pezeshki & Hinckley 1988
48 N	7.85 E	-2.24	-2.77	-0.53	19.1	1	887	823	1.08	64	Sep	Mar	-31	Gross & Koch 1991
49.08 N	107.28 E	-1.52	-1.9	-0.38	20	1	289	756	0.38	-467	Jun	Jul	-32	Dulamsuren et al. 2009

Table S4.2. Summary of means for a global database for 246 wild species of pre- and post-drought turgor loss point ($\pi_{tlp,}$), the plasticity of π_{tlp} ($\Delta\pi_{tlp}$), the contribution of π_{tlp} plasticity to post-drought π_{tlp}, and climatic water availability for biome categories and biome categories subdivided by functional type (i.e. temperate deciduous and temperate evergreen). Biome categories are based on those from GLOPNET (Wright *et al.* 2004) Climatic water availability is characterized as mean annual precipitation (MAP), annual potential evapotranspiration (PET), annual water balance (WB = MAP – PET), seasonal difference in water balance (wet season – dry season WB), and aridity index (AI; = MAP/PET. Parentheses indicate the number of sites with $\geq$3 species, this is not indicated for functional type categories since a number of studies measured both evergreen and deciduous species.

Biomes & functional types	$\pi_{tlp,\ pre\text{-}drought}$ (MPa)	$\pi_{tlp,\ drought}$ (MPa)	$\Delta\pi_{tlp}$ (MPa)	% contribution	MAP (mm)	PET (mm)	WB (mm)	ΔWB (mm)	AI	N sites	N species
Alpine/Subalpine	-1.20	-1.61	-0.41	24.6	2289	837	1452	42	3.86	4 (0)	6
Coastal	-2.59	-3.00	-0.40	11.9	1189	1319	-130	101	0.95	4 (3)	17
Grassland	-1.35	-1.76	-0.40	22.3	809	1134	-325	50	0.71	2 (1)	4
Temperate	-1.95	-2.36	-0.41	15.9	999	1094	-95	24	0.97	14 (10)	37
Deciduous	-1.82	-2.22	-0.40	15.9	971	1084	-114	15	0.95	11	24
Evergreen	-2.61	-3.08	-0.46	15.8	1141	1140	1.5	66	1.09	3	6
Temperate Conifer	-2.03	-2.50	-0.46	18.3	947	855	91	-14	1.34	9 (0)	15
Med./ Dry Temperate	-2.51	-3.13	-0.61	17.0	744	1336	-592	63	0.58	10 (6)	55
Semidesert	-2.23	-2.78	-0.55	17.9	251	1216	-965	46	0.22	9 (4)	27
Dry Tropical	-1.98	-2.32	-0.34	13.5	1494	1410	85	181	1.12	17 (8)	83
Deciduous	-2.10	-2.48	-0.37	13.2	1331	1459	-128	154	1.03	5	24
Evergreen	-1.96	-2.28	-0.32	12.9	1555	1403	152	191	1.13	12	59
Tropical Conifer	-2.03	-2.49	-0.46	32.8	1653	1000	653	143	1.77	1 (0)	2

Table S4.3. Summary of data from a global database for cultivars of 37 crop species, for pre- and post-drought treatment turgor loss point (π_{tlp}), π_{tlp} plasticity ($\Delta\pi_{tlp}$), and percent contribution of plasticity in π_{tlp} to droughted π_{tlp} values.

Species and cultivars	$\pi_{tlp,\ pre\text{-}drought}$ (MPa)	$\pi_{tlp,\ drought}$ (MPa)	$\Delta\pi_{tlp}$ (MPa)	% contribution	References
					Jaimez *et al*.
Capsicum chinense	-1.26	-1.48	-0.22	14.0	1999
AMES1	-1.2	-1.26	-0.06	4.8	
ANMB1	-1.2	-1.41	-0.21	14.9	
ROOR1	-1.38	-1.78	-0.40	22.5	
					Wilson *et al.*
Cenchrus cilaris	-1.57	-1.79	-0.22	12.3	1980
					Correia *et al.*
Ceratonia siliqua	-1.80	-1.91	-0.11	5.7	2001
Espargal	-1.8	-1.89	-0.09	4.8	
Galhosa	-1.82	-1.97	-0.15	7.6	
Mulata	-1.77	-1.86	-0.09	4.8	
Chenopodium quinoa	-1.57	-1.83	-0.26	14.3	Jensen *et al.* 2000
					Ruiz-Sanchez *et*
Citrus limon	-2.60	-2.72	-0.12	4.4	*al.* 1997
Citrus reticulata	-1.99	-2.13	-0.14	6.6	Save *et al*. 1995
Citrus sinensis	-1.95	-1.99	-0.04	2.0	Save *et al.* 1995
	-1.82	-2.08	-0.26		Meinzer *et al.*
Coffea arabica				11.5	1990
Catuai	-1.86	-1.95	-0.09	4.6	
Guatemalan	-1.85	-2.06	-0.21	10.2	
Mokka	-1.81	-2.55	-0.74	29.0	
San Ramon	-1.78	-1.85	-0.07	3.8	
Yellow Caturra	-1.78	-1.98	-0.20	10.3	
Festuca arundinacea	-2.49	-2.53	-0.04	2.0	White *et al.* 1992
TF3	-2.73	-2.65	0.08	-3.0	
TF4	-2.27	-2.44	-0.17	7.0	
TF5	-2.46	-2.51	-0.05	2.0	
Fragaria annanasa	-1.89	-2.10	-0.21	10.0	Save *et al*. 1993
Helianthus annuus	-0.93	-1.09	-0.16	13.0	Maury *et al.* 2000
T57	-0.93	-1.12	-0.19	14.7	
Viki	-0.96	-1.12	-0.16	19.0	
T32	-0.90	-1.04	-0.14	5.4	
					Wilson *et al.*
Heteropogon contortus	-1.31	-1.96	-0.65	33.2	1980
					Jensen & Henson
Lupinus angustifolius	-0.72	-1.11	-0.39	35.1	1990
Lupinus cosentinii	-0.75	-1.06	-0.31	29.2	
					Torrecillas *et al.*
Lycopersicon esculentum	-0.86	-1.10	-0.24	21.8	1995
					Wilson *et al*.
Macroptilium atropurpureum	-1.01	-1.31	-0.3	22.9	1980
Medicago truncatula	-1.96	-2.44	-0.48	19.6	Nunes *et al.* 2008

	-1.24	-2.11	-0.88		Bacelar *et al.*
Olea europa				38.9	2006
Cobrancosa	-1.44	-2.26	-0.82	36.3	
Madural	-0.80	-2.37	-1.57	66.2	
Verdeal Transmontana	-1.47	-1.71	-0.24	14.0	
Oryza sativa	-1.41	-1.64	-0.23	14.3	Henson 1984
63-83	-1.42	-1.67	-0.25	14.9	
IR20	-1.39	-1.61	-0.22	13.7	
					Wilson *et al.*
Panicum maximum	-1.41	-2.27	-0.86	37.9	1980
Pennisetum glaucum	-1.59	-1.48	0.11	-7.4	Do et al. 1996
IC30	-1.59	-1.48	0.11	-7.4	
HKP	-1.59	-1.48	0.11	-7.4	
Phaseolus vulgaris	-0.83	-1.62	-0.79	47.2	Stoyanov 2005
Plovdiv 10	-0.79	-1.82	-1.03	56.6	
Dobrudjanski ran	-0.60	-0.98	-0.38	38.8	
Prelom	-1.10	-2.05	-0.95	46.3	
					Baslam *et al*.
Phoenix dactylifera	-1.53	-2.85	-1.32	46.3	2013
					Torrecillas *et al*.
Prunus armeniaca	-2.86	-3.02	-0.20	6.6	1998
					Mellisho *et al*.
Prunus persica	-2.84	-2.78	0.06	-2.2	2011
					Rodriguez *et al.*
Punica granatum	-2.50	-3.63	-1.13	31.1	2011
					Marsal & Girona
Pyrus communis	-2.82	-3.09	-0.27	8.7	1997
	-1.48	-1.79	-0.31		Saliendra &
Saccharum spp.				17.4	Meinzer 1991
H65-7052	-1.60	-1.79	-0.19	10.6	
H67-5630	-1.51	-1.79	-0.28	15.6	
H69-8235	-1.32	-1.78	-0.46	25.8	
	-0.69	-0.75	-0.06		Eamus &
Solanum melongena				8.0	Narayan 1990
	-1.00	-1.90	-0.90		Jones & Turner
Sorghum bicolor				47.3	1978
Shallu	-1.00	-1.90	-0.90	47.3	
RS 610	-1.00	-1.90	-0.90	47.3	
Triticum aestivum	-1.32	-1.75	-0.43	24.4	Quarrie 1983
Highbury	-1.37	-1.79	-0.42	23.5	
TW269/9	-1.27	-1.70	-0.43	25.3	
	-1.83	-2.32	-0.49		Patakas *et al.*
Vitis vinifera				21.1	2012
Zea mays	-1.13	-1.77	-0.64	35.7	Sobrado 1986
CENIAP-DMR	-1.12	-2.10	-0.98	46.6	
Criollo gallero	-1.33	-1.75	-0.42	24.0	
Intervarietal Falcon	-1.00	-1.60	-0.60	37.5	
Maize de Falcon	-1.02	-1.77	-0.75	42.3	
Minitia	-1.10	-1.69	-0.59	34.9	
Sintetico San Andres	-1.21	-1.70	-0.49	28.8	
Zizyphus jujuba	-4.44	-5.46	-1.02	18.7	Cruz *et al*. 2012

Zoysia japonica		-2.36	-2.52	-0.16	6.3	White *et al.* 2001
	DALZ8504	-2.28	-2.55	-0.27	10.6	
	DALZ8511	-2.36	-2.55	-0.19	7.5	
	DALZ8513	-2.21	-2.40	-0.19	7.9	
	El Toro	-2.31	-2.59	-0.28	10.8	
	K Common	-2.44	-2.42	0.02	-0.8	
	Meyer	-2.41	-2.57	-0.16	6.2	
	Palisades	-2.44	-2.52	-0.08	3.2	
	Crowne	-2.43	-2.56	-0.13	5.1	
Zoysia japonica x matrella						
	Emerald	-2.06	-2.30	-0.24	10.4	
Zoysia matrella		-2.15	-2.31	-0.3	12.6	
	Cavalier	-2.09	-2.39	-0.30	12.6	
	DALZ8501	-2.29	-2.21	0.08	-3.6	
	DALZ8506	-2.03	-2.27	-0.24	10.6	
	DALZ8510	-2.20	-2.32	-0.12	5.2	
	DALZ8515	-2.52	-2.50	0.02	-0.8	
	Diamond	-1.76	-2.18	-0.42	19.3	

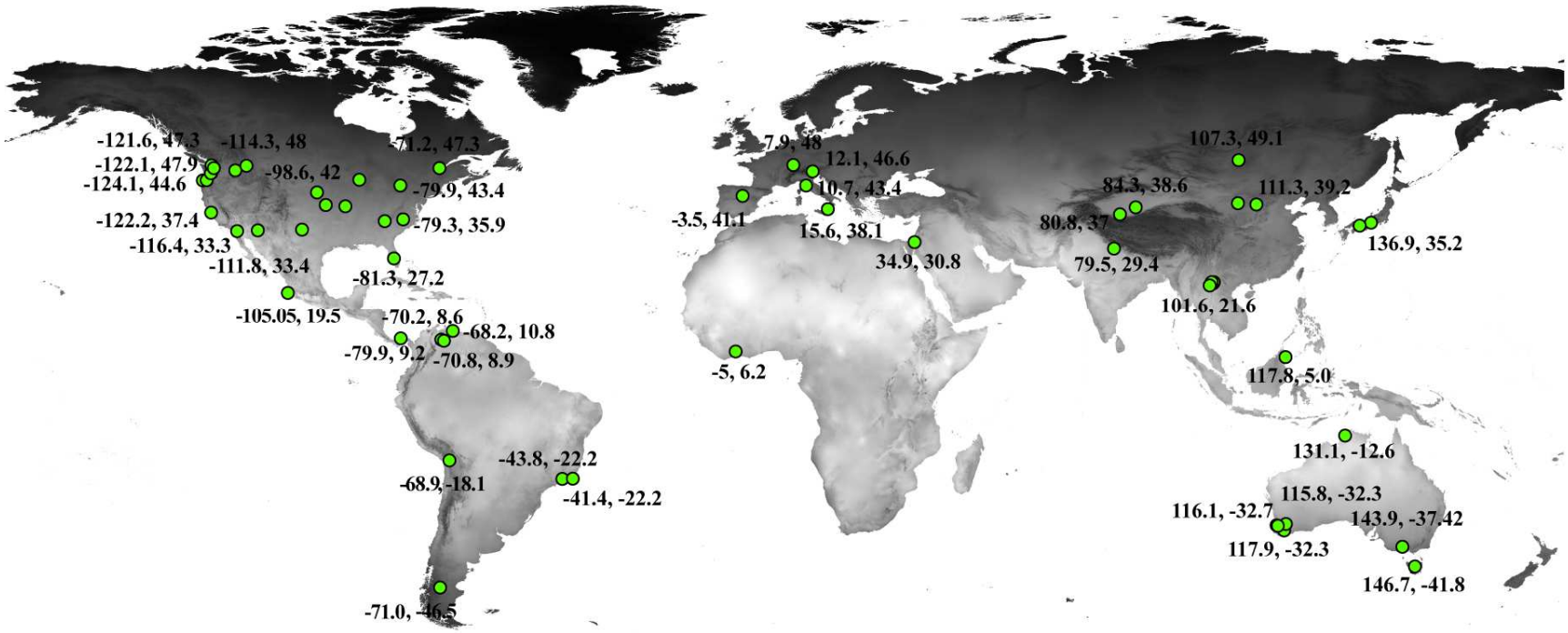
-121.6, 47.3
-114.3, 48
-71.2, 47.3
-122.1, 47.9
-124.1, 44.6
-98.6, 42
-79.9, 43.4
-122.2, 37.4
-79.3, 35.9
-116.4, 33.3
-111.8, 33.4
-81.3, 27.2
-105.05, 19.5
-70.2, 8.6
-68.2, 10.8
-79.9, 9.2
-70.8, 8.9
-43.8, -22.2
-68.9, -18.1
-41.4, -22.2
-71.0, -46.5
-7.9, 48
12.1, 46.6
10.7, 43.4
-3.5, 41.1
15.6, 38.1
34.9, 30.8
-5, 6.2
107.3, 49.1
84.3, 38.6
111.3, 39.2
80.8, 37
136.9, 35.2
79.5, 29.4
101.6, 21.6
117.8, 5.0
131.1, -12.6
115.8, -32.3
116.1, -32.7
143.9, -37.42
117.9, -32.3
146.7, -41.8

Figure S4.1

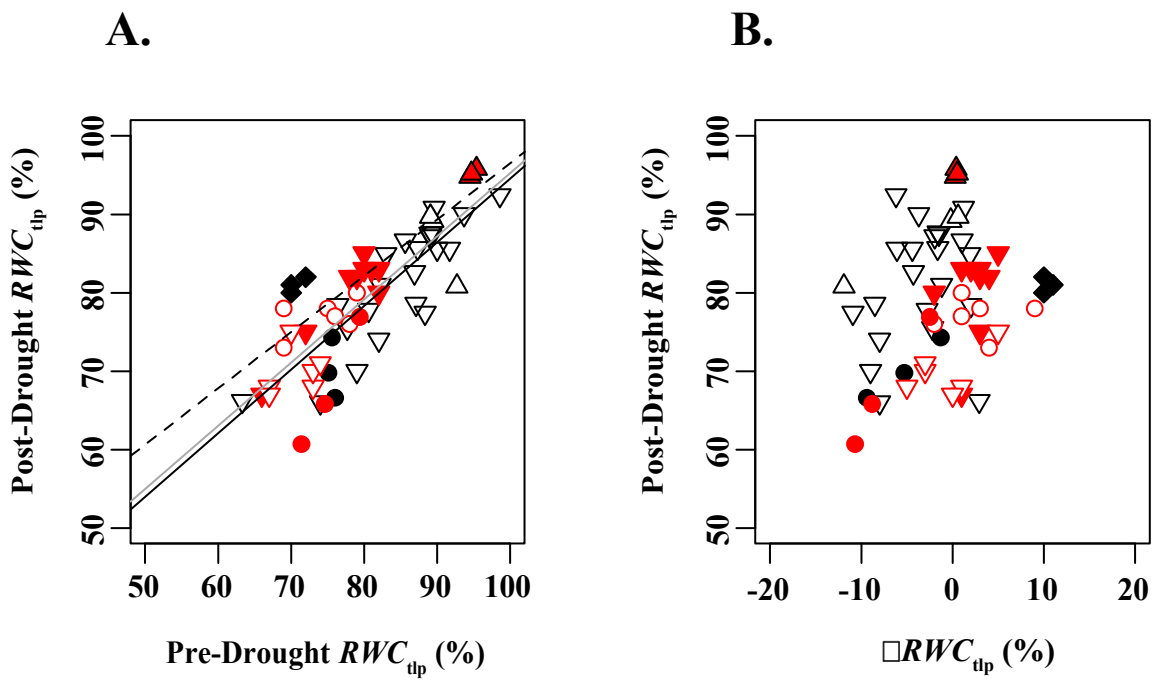
A.
B.
Post-Drought RWC_{tlp} (%)
Pre-Drought RWC_{tlp} (%)
□RWC_{tlp} (%)
50
60
70
80
90
100
-20
-10
0
10
20

Figure S4.2

REFERENCES

META-ANALYSIS DATA REFERENCES

Abrams M.D. (1988). Comparative water relations of three successional hardwood species in central Wisconsin. *Tree Physiol.*, 4, 263-273.

Abrams M.D. & Knapp A.K. (1986). Seasonal water relations of three gallery hardwood species in Northeast Kansas. *Forest Science*, 32, 687-696.

Abrams M.D. & Menges E.S. (1992). Leaf ageing and plateau effects on seasonal pressure-volume relationships in three sclerophyllous Quercus species in South-Eastern USA. *Funct. Ecol.*, 6, 353-360.

Andersen C.P. & McLaughlin S.B. (1991). Seasonal changes in shoot water relations of *Picea rubens* at two high elevation sites in the Smoky Mountains. *Tree Physiol.*, 8, 11-21.

Aranda I., Gil L. & Pardos J. (1996). Seasonal water relations of three broadleaved species (*Fagus sylvatica* L., *Quercus petraea* (Mattuschka) Liebl. and *Quercus pyrenaica* Willd.) in a mixed stand in the centre of the Iberian Peninsula. *Forest Ecol. Manag.*, 84, 219-229.

Bacelar E.A., Santos D.L., Moutinho-Pereira J.M., Gonçalves B.C., Ferreira H.F. & Correia C.M. (2006). Immediate responses and adaptative strategies of three olive cultivars under contrasting water availability regimes: Changes on structure and chemical composition of foliage and oxidative damage. *Plant Sci.*, 170, 596-605.

Badalotti A., Anfodillo T. & Grace J. (2000). Evidence of osmoregulation in *Larix decidua* at Alpine treeline and comparative responses to water availability of two co-occurring evergreen species. *Ann. For. Sci.*, 57, 623-633.

Barnes P.W. (1985). Adaptation to Water Stress in the Big Bluestem-Sand Bluestem Complex. *Ecology*, 66, 1908-1920.

Baslam M., Qaddoury A. & Goicoechea N. (2013). Role of native and exotic mycorrhizal symbiosis to develop morphological, physiological and biochemical responses coping with water drought of date palm, Phoenix dactylifera. *Trees*.

Braatne J.H. & Bliss L.C. (1999). Comparative physiological ecology of lupines colonizing early successional habitats on Mount St. Helens. *Ecology*, 80, 891-907.

Carter J.L., Veneklaas E.J., Colmer T.D., Eastham J. & Hatton T.J. (2006). Contrasting water relations of three coastal tree species with different exposure to salinity. *Physiol. Plantarum*, 127, 360-373.

Chai B.-f., Wang M.-b., Li H.-j. & Li C. (2000). Study on drought tolerance of local afforested trees in west of Shanxi province. *Journal of Soil and Water Conservation*, 14, 28-32.

Chapin D.M. & Bliss L.C. (1988). Soil-plant water relations of two subalpine herbs from Mount St. Helens. *Can. J. Bot.*, 66, 809-818.

Collier D.E. & Boyer M.G. (1989). The Water Relations of *Thuja occidentalis* L. from Two Sites of Contrasting Moisture Availability. *Bot. Gaz.*, 150, 445-448.

Correia M.J., Coelho D. & David M.M. (2001). Response to seasonal drought in three cultivars of *Ceratonia siliqua*: leaf growth and water relations. *Tree Physiol.*, 21, 645-653.

Cruz Z.N., Rodriguez P., Galindo A., Torrecillas E., Ondono S., Mellisho C.D., et al. (2012). Leaf mechanisms for drought resistance in Zizyphus jujuba trees. *Plant science : an international journal of experimental plant biology*, 197, 77-83.

Davis K.J. (2005). Comparison of the water relations characteristics of woody plants in western Oregon. In: *Botany and Plant Pathology*. Oregon State University.

Davis S.D. & Mooney H.A. (1986). Tissue water relations of four co-occurring chaparral shrubs. *Oecologia*, 70, 527-535.

Do F., Winkel T., Cournac L. & Louguet P. (1996). Impact of late-season drought on water relations in a sparse canopy of millet (Pennisetum glaucum (L.) R. Br.). *Field Crop Res.*, 48, 103-113.

Duhme F. & Hinckley T.M. (1992). Daily and seasonal variation in water relations of macchia shrubs and trees in France (Montpellier) and Turkey (Antalya). *Vegetatio*, 99-100, 185-198.

Dulamsuren C., Hauck M., Bader M., Osokhjargal D., Oyungerel S., Nyambayar S., et al. (2009). Water relations and photosynthetic performance in *Larix sibirica* growing in the forest-steppe ecotone of northern Mongolia. *Tree Physiol*, 29, 99-110.

Eamus D. & Narayan A. (1990). A pressure-volume analysis of *Solanum melongena* leaves. *J. Exp. Bot.*, 41, 661-668.

Fanjul L. & Barradas V.L. (1987). Diurnal and Seasonal Variation in the Water Relations of Some Deciduous and Evergreen Trees of a Deciduous Dry Forest of the Western Coast of Mexico. *Journal of Applied Ecology*, 24, 289-303.

Foster J.R. (1992). Photosynthesisand water relations of the floodplain tree, boxelder (*Acer negundo* L.). *Tree Physiol.*, 11, 133-149.

Fu P.L., Jiang Y.J., Wang A.Y., Brodribb T.J., Zhang J.L., Zhu S.D., et al. (2012). Stem hydraulic traits and leaf water-stress tolerance are co-ordinated with the leaf phenology of angiosperm trees in an Asian tropical dry karst forest. *Ann Bot*, 110, 189-99.

Garcia-Nunez C., Rada F., Boero C., Gonzalez J., Gallardo M., Azocar A., et al. (2004). Leaf gas exchange and water relations in *Polylepis tarapacana* at extreme altitudes in the Bolivian Andes. *Photosynthetica*, 42, 133-138.

Gibbons J.M. & Newberry D.M. (2002). Drought avoidance and the effect of local topography on trees in the understorey of Bornean lowland rain forest. *Plant Ecol.*, 164, 1-18.

Gross K. & Koch W. (1991). Water relations of *Picea abies*. I. Comparison of water relations parameters of spruce shoots examined at the end of the vegetation period and in winter. *Physiol. Plantarum*, 83, 290-295.

Harayama H., Ikeda T., Ishida A. & Yamamoto S.I. (2006). Seasonal variations in water relations in current-year leaves of evergreen trees with delayed greening. *Tree Physiol.*, 26, 1025-1033.

Henson I.E. (1984). Effects of atmospheric humidity on abscisic acid accumulation and water status in leaves of rice (*Oryza sativa* L.). *Annals of Botany*, 54, 569-582.

Hijmans R.J., Cameron S.E., Parra J.L., Jones P.G. & Jarvis A. (2005). Very high resolution interpolated climate surfaces for global land areas. *Int. J. Climatol.*, 25, 1965-1978.

Jackson P.A. & Spomer G.G. (1979). Biophysical adaptations of four western conifers to habitat water conditions. *Bot. Gaz.*, 140, 428-432.

Jaimez R.E., Rada F. & Garcia-Nunez C. (1999). The effect of irrigation frequency on water and carbon relations in three cultivars of sweet pepper (Capsicum chinense Jacq), in a tropical semiarid region. *Scientia Horticulturae*, 81, 301-308.

Jensen C.R., Jacobsen S.E., Andersen M.N., Núñez N., Andersen S.D., Rasmussen L., et al. (2000). Leaf gas exchange and water relation characteristics of field quinoa (*Chenopodium quinoa* Willd.) during soil drying. *Eur. J. Agron.*, 13, 11-25.

Jones M.M. & Turner N.C. (1978). Osmotic adjustment in leaves of sorghum in response to water deficits. *Plant Physiol.*, 61, 122-126.

Knapp A.K. (1984). Water relations and growth of three grasses during wet and drought years in a tallgrass prairie. *Oecologia*, 65, 35-43.

Kubiske M.E. & Abrams M.D. (1991). Rehydration effects on pressure-volume relationships in four temperate woody species: variability with site, time of season and drought conditions. *Oecologia*, 85, 537-542.

Le Roux X. & Bariac T. (1998). Seasonal variations in soil, grass and shrub water status in a West African humid savanna. *Oecologia*, 113, 456-466.

Li Q. & Xu H. (1992). The changes of main water parameters in Pinus tablaeformis with season and provenance. *Acta Phytoecologica et Geobotanica Sinica*, 16, 326-335.

Liang S.M., Yan H.L., Zhang X.M., Xie T.T., Zhu J.T. & Zhang Z.W. (2008). Physiological response of natural C. taklimakanensis B.R.Pan et. G.M.Shen to unconfined groundwater in the hinterland of the Taklimakan Desert. *Chinese Science Bulletin*, 53, 112-118.

Liu J.-Y., Fu P.L., Wang Y.-J. & Cao K.-F. (2012). Different drought-adaptation strategies as characterized by hydraulic and water-relations traits of evergreen and deciduous figs in a tropical karst forest. *Plant Science Journal*, 30, 484-493.

Lo Gullo M.A., Salleo S. & Rosso R. (1986). Drought avoidance strategy in *Ceratonia siliqua* L, a mesomorphic-leaved tree in the xeric Mediterranean area. *Annals of Botany*, 58.

Marsal J. & Girona J. (1997). Effects of water stress cycles on turgor maintenance processes in pear leaves (*Pyrus communis*). *Tree Physiol.*, 17, 327-333.

Maury P., Berger M., Mojayad F. & Planchon C. (2000). Leaf water characteristics and drought acclimation in sunflower genotypes. *Plant Soil*, 223, 153-160.

Meinzer F.C., Grantz D.A., Goldstein G. & Saliendra N.Z. (1990). Leaf water relations and maintenance of gas exchange in coffee cultivars grown in drying soil. *Plant Physiol.*, 94, 1781-1787.

Mellisho C.D., Cruz Z.N., Conejero W., OrtuÑO M.F. & RodrÍGuez P. (2011). Mechanisms for drought resistance in early maturing cvar Flordastar peach trees. *J. Ag. Sci.*, 149, 609-616.

Miki N., Otsuki K., Sakamoto K., Nishimoto T. & Yoshikawa K. (2003). Leaf water relations in Pinus densiflora Sieb. et Zucc. on different soil moisture conditions. *J. For. Res.-Jpn.*, 8, 153-161.

Mitchell P.J., Veneklaas E.J., Lambers H. & Burgess S.S.O. (2008). Leaf water relations during summer water deficit: differential responses in turgor maintenance and variation in leaf structure among different plant communities in south-western Australia. *Plant Cell Environ.*, 31, 1791-1802.

Monson R.K. & Smith S.D. (1982). Seasonal water potential components of Sonoran Desert plants. *Ecology*, 63, 113-113.

Myers B.A., Duff G.A., Eamus D., Fordyce I.R., O'Grady A. & Williams R.J. (1997). Seasonal variation in water relations of trees of differing leaf phenology in a wet-dry tropical savanna near Darwin, Northern Australia. *Australian Journal of Botany*, 45, 225-240.

Nilsen E.T., Sharifi M.R., Rundel P.W., Jarrell W.M. & Virginia R.A. (1983). Diurnal and Seasonal Water Relations of the Desert Phreatophyte Prosopis Glandulosa (Honey Mesquite) in the Sonoran Desert of California. *Ecology*, 64, 1381-1381.

Nunes C., de Sousa Araújo S., da Silva J.M., Fevereiro M.P.S. & da Silva A.B. (2008). Physiological responses of the legume model *Medicago truncatula* cv. Jemalong to water deficit. *Environ. Exp. Bot.*, 63, 289-296.

Parker W.C., Pallardy S.G., Hinckley T.M. & Teskey R.O. (1982). Seasonal Changes in Tissue Water Relations of Three Woody Species of the Quercus-Carya Forest Type. *Ecology*, 63, 1259-1267.

Patakas A., Nikolaou N., Zioziou E., Radoglou K. & Noitsakis B. (2002). The role of organic solute and ion accumulation in osmotic adjustment in drought-stressed grapevines. *Plant Sci.*, 163, 361-367.

Pavlik B.M. (1984). Seasonal changes of osmotic pressure, symplasmic water content and tissue elasticity in the blades of dune grasses growing in situ along the coast of Oregon. *Plant Cell Environ.*, 7, 531-539.

Pezeshki S.R. & Hinckley T.M. (1998). Water relations characteristics of *Alnus rubra* and *Populus trichocarpa*: responses to field drought *Can. J. For. Res.*, 18, 1159-1166.

Pothier D. & Margolis H.A. (1990). Changes in the water relations of balsam fir and white birch saplings after thinning. *Tree Physiol.*, 6, 371-380.

Quarrie S.A. (1983). Characterization of spring wheat genotypes differing in drought-induced abscisic acid accumulation II. Leaf water relations. *J. Exp. Bot.*, 34, 1528-1540.

Rada F., Azócar A. & Rojas-Altuve A. (2012). Water relations and gas exchange in Coespeletia moritziana (Sch. Bip) Cuatrec., a giant rosette species of the high tropical Andes. *Photosynthetica*, 50, 429-436.

Rada F., Goldstein G., Azocar A. & Meinzer F. (1985). Daily and seasonal osmotic changes in a tropical treeline species. *J. Exp. Bot.*, 36, 989-1000.

Rada F., Goldstein G., Orozco A., Montilla M., Zabala O. & Azocar A. (1989). Osmotic and turgor relations of three mangrove ecosystem species. *Aust. J. Plant. Physiol.*, 16, 477-486.

Roberts S.W. & Knoerr K.R. (1977). Components of Water Potential Estimated from Xylem Pressure Measurements in Five Tree Species. *Oecologia*, 28, 191-202.

Rodríguez P., Mellisho C.D., Conejero W., Cruz Z.N., Ortuño M.F., Galindo A., et al. (2012). Plant water relations of leaves of pomegranate trees under different irrigation conditions. *Environ. Exp. Bot.*, 77, 19-24.

Rosado B.H.P. & de Mattos E.A. (2010). Interspecific variation of functional traits in a CAM-tree dominated sandy coastal plain. *J. Veg. Sci.*, 21, 43-54.

Ruiz-Sanchez M.C., Domingo R., Savé R., Biel C. & Torrecillas A. (1997). Effects of water stress and rewatering on leaf water relations of lemon plants. *Biol. Plantarum*, 39, 623-631.

Saliendra N.Z. & Meinzer F.C. (1991). Symplast volume, turgor, stomatal conductance and growth in relation to osmotic and elastic adjustment in droughted sugarcane *J. Exp. Bot.*, 42, 1251-1259.

Sanger J.C., Davidson N.J., O'Grady A. & Close D.C. (2001). Are the patterns of regeneration in the endangered *Eucalyptus gunnii* ssp. divaricata shifting in response to climate? *Austral Ecology*, 36.

Savé R., Biel C., Domingo R., Ruiz-Sánchez M.C. & Torrecillas A. (1995). Some physiological and morphological characteristics of citrus plants for drought resistance. *Plant Sci.*, 110, 167-172.

Savé R., Peñuelas J., Marfà O. & Serrano L. (1993). Changes in leaf osmotic and elastic properties and canopy structure of strawberries under mild water stress. *Hortscience*, 28, 925-927.

Scholz F.G., Bucci S.J., Arias N., Meinzer F.C. & Goldstein G. (2012). Osmotic and elastic adjustments in cold desert shrubs differing in rooting depth: coping with drought and subzero temperatures. *Oecologia*.

Shi S.-l., Wang Y.-C. & Zhou J.-H. (2008). The change of water parameters in *Tetraena mongolica* with season and habitat. *Acta Ecologica Sinica*, 28, 6079- 6089.

Shrestha M.K., Stock W.D., Ward D. & Golan-Goldhirsh A. (2003). Water status of isolated Negev desert populations of *Acacia raddiana* with different mortality levels. *Plant Ecol.*, 168, 297-307.

Singh S.P., Zobel D.B., Garkoti S.C., Tewari A. & Negi C.M.S. (2006). Patterns in water relations of central Himalayan trees. *Tropical Ecology*, 47, 159-182.

Sobrado M.A. (1986). Tissue water relations and leaf growth of tropical corn cultivars under water deficits. *Plant Cell Environ.*, 9, 451-457.

Stoyanov Z.Z. (2005). Effects of water stress on leaf water relations of young bean plants. *Journal of Central European Agriculture*, 1.

Teskey R.O., Grier C.C. & Hinckley T.M. (1983). Change in photosynthesis and water relations with age and season in A*bies amabilis*. *Can. J. For. Res.*, 14, 77-84.

Thomas F.M., Foetzki A., Gries D., Bruelheide H., Li X., Zeng F., et al. (2008). Regulation of the water status in three co-occurring phreatophytes at the southern fringe of the Taklamakan Desert. *Journal of Plant Ecology*, 5, 227-235.

Tognetti R., Raschi A. & Jones M.B. (2000). Seasonal patterns of tissue water relations in three Mediterranean shrubs co-occurring at a natural CO_2 spring. *Plant Cell Environ.*, 23, 1341-1351.

Torrecillas A., Galego R., PéRez-Pastor A. & Ruiz-SáNchez M.C. (1999). Gas exchange and water relations of young apricot plants under drought conditions. *J. Ag. Sci.*, 132, 445-452.

Torrecillas A., Guillaume C., Alarcón J.J. & Ruiz-Sánchez M.C. (1995). Water relations of two tomato species under water stress and recovery. *Plant Sci.*, 105, 169-176.

Trabucco A. & Zomer R.J. (2009). Global Aridity Index (Global-Aridity) and Global Potential Evapo-Transpiration (Global-PET) Geospatial Database. . In: (ed. Information CCfS). CGIAR-CSI GeoPortal http://www.csi.cgiar.org/.

Wan C., Sosebee R.E. & McMichael B.L. (1993). Drought-induced changes in water relations in broom snakeweed (*Gutierrezia sarothrae*) under greenhouse- and field-grown conditions. *Environ. Exp. Bot.*, 33, 323-330.

Wang A.Y., Jiang Y.-J., Hao G.-Y. & Cao K.-F. (2008). The Effect of Seasonal Drought to Plant Hydraulics and Photosynthesis of Three Dominant Evergreen Tree Species in Seasonal Tropical Rainforest of Xishuangbanna Limestone Area. *Acta Botanica Yunnanica*, 30, 325-332.

Wenhui Z. (1998). Water relations balance parameters of 30 woody species from Cerrado vegetation in the wet and dry season. *J. Fore. Res-Jpn.*, 9, 233-239.

White D.A., Turner N.C. & Galbraith J.H. (2000). Leaf water relations and stomatal behavior of four allopatric *Eucalyptus* species planted in Mediterranean southwestern Australia. *Tree Physiol.*, 20, 1157-1165.

White R.H., Engelke M.C., Anderson S.J., Ruemmele B.A., Marcum K.B. & Taylor G.R. (2001). Zoysiagrass water relations. *Crop Science* 41, 133-138.

Wilson J.R., Ludlow M.M., Fisher M.J. & Schulze E. (1980). Adaptation to Water Stress of the Leaf Water Relations of Four Tropical Forage Species. *Aust. J. Plant. Physiol.*, 7, 207-220.

Wright I.J., Reich P.B., Westoby M., Ackerly D.D., Baruch Z., Bongers F., et al. (2004). The worldwide leaf economics spectrum. *Nature*, 428, 821-827.

Wright S.J., Machado J.L., Mulkey S.S. & Smith A.P. (1992). Drought acclimation among tropical forest shrubs (*Psychotria*, Rubiaceae). *Oecologia*, 89, 457-463.

Zeng F., Zhang X., Foetzki A., Li X., Li X. & Runge M. (2002). Water relation characteristics of *Alhagi sparsifolia* and consequences for a sustainable management. *Sci. China Ser. D.*, 45, 125-131.

Zhu S.-D. & Cao K.-F. (2009). Hydraulic properties and photosynthetic rates in co-occurring lianas and trees in a seasonal tropical rainforest in southwestern China. *Plant Ecol.*, 204, 295-304.

TEXT REFERENCES

Austin M.P. & Van Niel K.P. (2011). Improving species distribution models for climate change studies: variable selection and scale. *J. Biogeogr.*, 38, 1-8.

Bartlett M.K., Scoffoni C., Ardy R., Zhang Y., Sun S., Cao K., et al. (2012a). Rapid determination of comparative drought tolerance traits: using an osmometer to predict turgor loss point. *Methods Eco. Evol.*, 3, 880-888.

Bartlett M.K., Scoffoni C. & Sack L. (2012b). The determinants of leaf turgor loss point and prediction of drought tolerance of species and biomes: a global meta-analysis. *Ecol. Lett.*, 15, 393-405.

Becker P., Rabenold P.E., Idol J.R. & Smith A.P. (1988). Water potential gradients for gaps and slopes in a Panamanian tropical moist forest's dry season. *J. Trop. Ecol.*, 4, 173-184.

Blackman C.J., Brodribb T.J. & Jordan G.J. (2010). Leaf hydraulic vulnerability is related to conduit dimensions and drought resistance across a diverse range of woody angiosperms. *New Phytol.*, 188, 1113-1123.

Blum A. (2005). Drought resistance, water-use efficiency, and yield potential—are they compatible, dissonant, or mutually exclusive? *Aust. J. Agr. Res.*, 56, 1159.

Brodribb T., Holbrook N.M., Edwards E.J. & Gutierrez M.V. (2003). Relations between stomatal closure, leaf turgor and xylem vulnerability in eight tropical dry forest trees. *Plant Cell Environ.*, 26, 443-450.

Brown R.W. & Shouse P.J. (1992). Measuring Plant and Soil Water Potentials with Thermocouple Psychrometers: Some Concerns. *Agronomy Journal*, 84, 78-86.

Calkin H.W. & Pearcy R.W. (1984). Seasonal progressions of tissue and cell water relations parameters in evergreen and deciduous perennials. *Plant Cell Environ.*, 7, 347-352.

Cao K.-F. (2000). Water relations and gas exchange of tropical saplings during a prolonged drought in a Bornean heath forest, with reference to root architecture. *J. Trop. Ecol.*, 16, 101-116.

Chen H. & Jiang J.-G. (2010). Osmotic adjustment and plant adaptation to environmental changes related to drought and salinity. *Environ. Rev.*, 18, 309-319.

Cheung Y.N.S., Tyree M.T. & Dainty J. (1975). Water relations parameters on single leaves obtained in a pressure bomb and some ecological interpretations. *Can. J. Bot.*, 53, 1342-1346.

Choat B., Sack L. & Holbrook N.M. (2007). Diversity of hydraulic traits in nine *Cordia* species growing in tropical forests with contrasting precipitation. *New Phytol.*, 175, 686-698.

Dormann C.F. (2007). Promising the future? Global change projections of species distributions. *Basic and Applied Ecology*, 8, 387-397.

Grime J.P. & Mackey J.M.L. (2002). The role of plasticity in resource capture by plants. *Evol. Ecol.*, 16, 299-307.

Higgins S.I., O'Hara R.B., Bykova O., Cramer M.D., Chuine I., Gerstner E.-M., et al. (2012). A physiological analogy of the niche for projecting the potential distribution of plants. *J. Biogeogr.*, 39, 2132-2145.

Hsiao T.C., Acevedo E., Fereres E. & Henderson D.W. (1976). Water Stress, growth, and osmotic adjustment. *Philos. T. R. Soc. B*, 273, 479-500.

Lenz T.I., Wright I.J. & Westoby M. (2006). Interrelations among pressure-volume curve traits across species and water availability gradients. *Physiol. Plantarum*, 127, 423-433.

Matesanz S., Gianoli E. & Valladares F. (2010). Global change and the evolution of phenotypic plasticity in plants. *Annals of the New York Academy of Sciences*, 1206, 35-55.

Messier J., McGill B.J. & Lechowicz M.J. (2010). How do traits vary across ecological scales? A case for trait-based ecology. *Ecol. Lett.*, 13, 838-848.

Morgan J.M. (1984). Osmoregulation and water stress in higher plants. *Ann. Rev. Plant Physio.*, 35, 299-319.

Nakagawa S. & Santos E.S.A. (2012). Methodological issues and advances in biological meta-analysis. *Evol. Ecol.*, 26, 1253-1274.

Nakagawa S., Schielzeth H. & O'Hara R.B. (2013). A general and simple method for obtaining R2 from generalized linear mixed-effects models. *Methods Eco. Evol.*, 4, 133-142.

Nicotra A.B., Atkin O.K., Bonser S.P., Davidson A.M., Finnegan E.J., Mathesius U., et al. (2010). Plant phenotypic plasticity in a changing climate. *Trends Plant. Sci.*, 15, 684-692.

Qian S.S., Cuffney T.F., Alameddine I., McMahon G. & Reckhow K.H. (2010). On the application of multilevel modeling in environmental and ecological studies. *Ecology*, 91, 355-361.

Ren S., Lai H., Tong W., Aminzadeh M., Hou X. & Lai S. (2010). Nonparametric bootstrapping for hierarchical data. *J. Appl. Stat.*, 37, 1487-1498.

Sheffield J. & Wood E.F. (2007). Characteristics of global and regional drought, 1950–2000: Analysis of soil moisture data from off-line simulation of the terrestrial hydrologic cycle. *J. Geophys. Res.*, 112.

Sinclair T.R. & Ludlow M.M. (1985). Who taught plants thermodynamics? The unfulfilled potential of plant water potential. *Functional Plant Biology*, 12, 213-217.

Valladares F., Gianoli E. & Gómez J.M. (2007). Ecological limits to plant phenotypic plasticity. *New Phytol.*, 176, 749-763.

Zhang J., Nguyen H.T. & Blum A. (1999). Genetic analysis of osmotic adjustment in crop plants. *J. Exp. Bot.*, 50, 291-302.

CHAPTER 5

DROUGHT TOLERANCE AS A DRIVER OF TROPICAL FOREST ASSEMBLY: RESOLVING SPATIAL SIGNATURES FOR MULTIPLE PROCESSES

ABSTRACT

Spatial patterns in trait variation reflect underlying community assembly processes, allowing us to test hypotheses about their trait and environmental drivers by identifying the strongest correlates of characteristic spatial patterns. For 43 evergreen tree species (> 1cm dbh) in a 20 ha seasonal tropical rainforest plot in Xishuangbanna, China, we compared the ability of drought tolerance traits, other physiological traits and commonly measured functional traits to predict the spatial patterns expected from the assembly processes of habitat associations, niche overlap-based competition, and hierarchical competition. We distinguished the neighborhood-scale (0-20m) patterns expected from competition from larger-scale habitat associations with a wavelet method. Species' drought tolerance and habitat variables related to soil water supply were strong drivers of habitat associations, and drought tolerance showed a significant spatial signal for influencing competition. Overall, the traits most strongly associated with habitat, as quantified using multivariate models, were leaf density, leaf turgor loss point (π_{tlp}; also known as the leaf wilting point), and stem hydraulic conductivity (r^2 range for the best fit models = 0.27-0.36). At neighborhood scales, species spatial associations were positively correlated with similarity in π_{tlp}, consistent with predictions for hierarchical competition. Although the correlation between π_{tlp} and interspecific spatial associations was weak ($r^2 < 0.01$), this showed a persistent influence of drought tolerance on neighborhood interactions and community assembly. Quantifying the full impact of traits on competitive interactions in forests may require incorporating plasticity among

individuals within species, especially among specific life stages, and moving beyond individual traits to integrate the impact of multiple traits on whole-plant performance and resource demand.

Keywords: Spatial associations, drought tolerance, turgor loss point, functional traits, environmental filtering, habitat associations, competition, community assembly, tropical forest

INTRODUCTION

Species spatial distribution patterns are shaped by underlying community assembly processes (McIntire and Fajardo 2009). Non-neutral processes influence plant species distributions through their interactions with species traits (Adler et al. 2013), enabling spatial patterns in trait variation to provide powerful evidence of the drivers of community assembly. Tropical forests exhibit spatial signatures of multiple processes, including trait associations with microhabitats, and, at the neighborhood scale (< 20m), trait patterns that are consistent with the effects of competitive interactions (Kraft et al. 2008, Paine et al. 2012). However, inferring processes from patterns has been hampered by the inability of earlier statistical methods to disentangle multiple patterns, and, hence, the underlying processes, occurring at overlapping spatial scales (Wiegand et al. 2009, Detto and Muller-Landau 2013). Identifying the traits and environmental characteristics that most strongly impact assembly has also been limited by the use of traits that capture an important but narrow range of plant function (Wright et al. 2004, Kraft et al. 2008, Bartlett et al. 2012).

Plant vegetative traits impact several ecological processes simultaneously: (a) habitat association, wherein species with similar traits co-occur in microhabitats due to similar resource requirements; (b) niche-based competition, wherein species trait differences enhance coexistence by reducing niche overlap, so competitive exclusion is strongest among similar species; and (c)

hierarchical competition, wherein species trait differences reduce coexistence by increasing fitness differences, so the strongest competitors have similar trait values and exclude species with different, less competitive trait values (Chesson 2000, Kraft et al. 2008, Mayfield and Levine 2010, Kunstler et al. 2012). These processes can be identified by spatial signatures in trait variation (Fig. 5.1A-C). Habitat association is predicted to result in the aggregation of functionally similar species in similar environments, at the scale of edaphic and topographic environmental variation. Competition, which is expected to act at the scale of neighborhood interactions (< 20m), is predicted to cause neighboring species to differ in traits that influence niche differences (sensu Chesson 2000). Alternatively, for traits that influence fitness in general, hierarchical competition may result in the aggregation of similar species at the neighborhood scale, excluding species that differ strongly from the competitively superior. These patterns will also emerge for closely related species if traits are phylogenetically conserved (Mayfield and Levine 2010).

Evidence for traits influencing community structure through habitat association is strong, but still coarse. Previous studies have found a spatial signature for habitat associations through strong relationships between traits and habitat categories within communities (i.e., ridges and valleys or soil types) (Becker et al. 1988, Comita and Engelbrecht 2009, Katabuchi et al. 2012), and smaller ranges in trait variation within subsamples of a community than would be expected if trait values were distributed randomly throughout (Kraft et al. 2008, Swenson and Enquist 2009). These studies laid the groundwork for a higher resolution of the drivers of habitat associations. One important advance is the use of quantitative rather than categorical habitat variables, an approach that identified a significant relationship between topography and functional traits at the Xishuangbanna long-term forest dynamics plot (XSBN), a seasonal

tropical rainforest in Yunnan, China (Liu et al. 2014). Species with trait values often associated with fast growth, including lower seed mass and wood density, occurred in valleys rather than on ridges (Liu et al. 2014). Further, while previous studies have often focused on leaf and stem economic spectrum traits, such as leaf mass per area and wood density (Kraft et al. 2008, Liu et al. 2014), which capture important trade-offs between rapid growth and the mechanical strength and longevity of leaf and wood tissue (Wright et al. 2004), species differences in water use or drought tolerance are increasingly recognized as important drivers of species distributions within and across communities (Baltzer et al. 2008, Comita and Engelbrecht 2009, Bartlett et al. 2012). Species that experience hydraulic dysfunction, wilting and leaf death at greater leaf water deficits occur in drier ecosystems and drier habitat categories within ecosystems (Becker et al. 1988, Choat et al. 2007, Baltzer et al. 2008, Comita and Engelbrecht 2009, Bartlett et al. 2012). Thus, we sampled traits that characterize drought tolerance and water use as well as quantitative environmental variation to test hypotheses about the trait and environmental drivers of habitat associations in a tropical community (detailed in Tables 5.1 and 5.2). We sampled the turgor loss point (π_{tlp}), a key drought tolerance trait that represents leaf vulnerability to wilting, and sapwood area- and leaf area-specific stem conductivity (K_S and K_L), physiological traits contributing to the capacity to transport water to sustain transpiration and photosynthetic carbon gain (Choat et al. 2007, Bartlett et al. 2012). Species with more negative π_{tlp} values typically maintain photosynthesis under drier conditions, while higher conductivity is often associated with lower drought tolerance due to anatomical trade-offs (Brodribb et al. 2003, Choat et al. 2007). To broadly characterize plant function, we also sampled the commonly-measured leaf structural and economic spectrum traits leaf dry mass per area (*LMA*), leaf density (ρ), leaf dry matter content (*LDMC*), and nitrogen concentration per unit mass (N_{mass}) (Wright et al. 2004). To quantify

habitat, we not only used topographic variables, but also variables that characterize solar radiation and vegetation structure, which can drive landscape variation in water supply more strongly than topography under dry conditions (Grayson et al. 1997).

Previous studies have also found spatial signatures for competition. For example, studies have reported lower trait similarity among co-occurring species than expected from dispersal, consistent with trait differences reducing niche overlap between species (Kraft et al. 2008, Swenson and Enquist 2009). However, these studies did not test for a spatial signature for hierarchical competition, which may be even more important as a process influencing assembly if traits contribute to fitness differences across species (Chesson 2000, Mayfield and Levine 2010). Indeed, previous studies of neighborhood interactions have found increased growth and survival in trees with functionally similar interspecific neighbors, consistent with both habitat association (Uriarte et al. 2010, Paine et al. 2012) and hierarchical competition (Kunstler et al. 2012), but a previous study at the XSBN plot found that trait similarity was lower in valley than ridge habitats, suggesting stronger competition among fast-growing species (Liu et al. 2014). We distinguished for the first time between a signature of trait influence on habitat associations and competition (niche-based and hierarchical) using statistical methods that separate neighborhood from larger-scale spatial patterns (Fig. 5.1A-C), by implementing a wavelet transform of tree coordinates to produce analytically tractable functions for the correlation between two species' points at given distances (e.g., 2 and 5m from focal trees), that are independent of correlations at other distances (Detto and Muller-Landau 2013). Further, competition can be strongly influenced by size (Canham et al. 2004, Uriarte et al. 2010), and we developed a novel analysis to account for tree size in determining species associations across spatial scales. These approaches allowed us to rigorously test hypotheses about the impact of drought tolerance, physiology and functional

traits on community assembly in a diverse tropical system (Table 5.1).

METHODS

Trait measurements

Physiological and functional traits were measured for 3-6 saplings (dbh ranged from 1 to 10 cm) of 43 evergreen species (see Appendix section Supplemental Methods 5.1 for methods). We focused on saplings to minimize variation due to life stage and canopy position. The study species account for 71% of the total stem density at the 20-ha (400m by 500m) Xishuangbanna (XSBN) forest dynamics plot in Yunnan, China (101°34'26"-47"E and 21°36'42"-58"N) (Lan et al. 2011b). All trees $\geq$ 1 cm in diameter have been censused and the topography mapped at 10m intervals according to standard Center for Tropical Forest Science protocols (Condit 1998). The plot is a seasonal tropical rain forest with a mean annual temperature of 21.0°C and precipitation of 1532mm, with 80% of rainfall occurring during the May-October wet season (Lan et al. 2011b). For the traits that are expected to exhibit seasonal plasticity, we measured π_{tlp}, *LMA*, *LDMC* and ρ during the dry season and N_{mass} during the wet season (see Appendix section Supplemental Methods 5.1). We assessed K_S and K_L in both seasons.

Testing for habitat associations

Species' habitats were characterized with variables previously shown to be associated with landscape variation in water and energy fluxes in other forests: (1) elevation; (2) slope; (3) the ratio of the upslope area to the local slope, or topographic wetness index *(TWI*); (4) convexity; the linearly transformed aspect variables (5) eastness and (6) northness; and average daily (7) direct and (8) diffuse light in the wet season and (9 and 10) dry season (Tables S5.1- S5.3; Figs S5.1- S5.6). Previous studies have established that sites with higher daily light exposure or a more southern or western aspect are drier due to greater evaporation (Grayson et al. 1997,

Bennie et al. 2008), sites with a lower topographic wetness index (*TWI*) are drier due to greater water drainage away from the area (Sorensen et al. 2006), and sites with higher elevation (Becker et al. 1988) or convexity (more ridge- than valley-shaped) are drier due to both greater evaporation and greater water drainage away (Daws et al. 2002, Leij et al. 2004) (Table 5.2). Sites with a higher slope may be drier due to greater drainage (Leij et al. 2004) or wetter due to lower light interception (Galicia et al. 1999). Diffuse and direct light were considered separately because long-term carbon balance is more strongly associated with diffuse light, but direct light may induce greater evaporation and soil dryness (Mercado et al. 2009). These variables were calculated from the plot elevation map for each 10m × 10m quadrat with ArcGIS 9.3 (ESRI, Redlands, CA, USA), and species means for each variable were calculated from the number of individuals in each quadrat. We compared the predictive ability of species means for environmental variables (e.g., *Elevation*) and of species means weighted by species abundance relative to the total density in each quadrat, to quantify the habitats where a species is over-represented in the community (e.g., $Elevation_{WA}$, see Appendix section Supplemental Methods 5.2). We also characterized habitat with vegetation structure variables for "neighborhood crowding" in 20m radius circular neighborhoods. We determined (1) average neighbor basal area, (2) overall neighborhood basal area, (3) tree density (i.e., number of stems per ground area), and (4) neighborhood basal area scaled by focal tree size, or the ratio of total neighborhood basal area to focal tree area (Table S5.2, Fig. S5.4), using all trees in the neighborhood. We expected crowding to increase competition for water, although crowding can also reduce evaporation through greater shading (Coomes and Grubb 2000, Canham et al. 2004).

We first tested univariate correlations between species trait means and habitat variables (Table S5.4, S5.5), and then multivariate correlations, since many of the habitat variables were

significantly correlated. We predicted trait means from multivariate habitat models (Table S5.6) and determined the best-fit models using the Aikake Information Criterion corrected for small sample sizes (AICc), then assessed which best-fit models were robust to spatial autocorrelation using torus translation tests (Harms et al. 2001). Best-fit models were defined as those with an AICc $\leq$ 2 units from the minimum AICc identified for each trait variable and for which a more parsimonious model with a subset of the same predictor variables was not also identified as a best-fit model (Burnham and Anderson 2010). If the model with the minimum AICc value was rejected for a more parsimonious model, it was used to define the threshold AICc value for the best-fit models, but it was not considered to be supported enough to be discussed further.

Testing for spatial signals of interspecific competition using wavelet analyses

To identify spatial patterns for competition, we used a wavelet method to calculate the pairwise interspecific spatial association for each combination of species pairs at 32 scales between 0-20m (Detto and Muller-Landau 2013) (n = 820 pairs). The wavelet method separates the correlation between two spatial processes into independent values at each scale, so the correlations at local scales are independent from larger-scale patterns. Values are > 0 for clustered species, 0 for randomly associated species, and < 0 for segregated species. We used 20m as the largest scale because neighborhood effects on performance dissipate beyond that distance in tropical forests (Hubbell et al. 2001, Uriarte et al. 2004). Previous spatial analyses at XSBN, which did not distinguish between processes with wavelet decomposition, found largely random associations beyond that distance (Lan et al. 2012). We excluded the gap-distributed species *Mallotus garrettii* and *Microcos chungii* from these analyses, as we expected associations between gap and understory species to reflect gap locations more strongly than competitive outcomes.

Because larger trees exhibit greater resource uptake, and, thus, a stronger exclusionary

influence on neighbors than smaller trees (Canham et al. 2004), we tested the hypothesis that large trees would show the strongest characteristic spatial patterns for competition (Table 5.1). Spatial analyses that do not account for tree size weight co-occurrence with small and large trees equally, despite the greater exclusionary pressure of the large trees. We implemented a novel analysis that weighted each tree according to its basal area, so that the spatial patterns of large trees were more influential to the overall spatial association (see Fig. S5.7 and Appendix section Supplemental Methods 5.3 for detailed methods). This weighting makes species pairs with clustered large trees positively associated and pairs with segregated large trees negatively associated.

Testing for hierarchical competition

To test for a signature of hierarchical competition, we classified species means for each trait as high (species mean > 50^{th} percentile of species means) or low (species mean $\leq 50^{th}$ percentile of species means) and categorized each species pair as "both high," "both low," or "contrasting" for each trait. We then calculated the mean spatial association and 95% confidence intervals from 1000 bootstraps for each category. We considered the trait categories to exhibit significantly different spatial associations at scales for which their 95% confidence intervals did not overlap.

Testing for niche overlap-based competition

To test for niche overlap-based competition, we tested the Pearson and rank correlations of the absolute values of differences in species means for each trait with the spatial association between each species pair at each of the 32 scales. Correlations were considered significant if the p-value for both the rank and Pearson correlations was $p \leq p_{critical} = 0.0083$, which is a significance level of 0.05 corrected for 224 multiple tests (32 scales for 7 traits) (Benjamini and Yekutieli 2001).

Testing for an influence of phylogeny on habitat association and competition

We generated a phylogeny for the 42 species with available sequence data (Yang et al. 2014a), excluding *Walsura robusta*. We calculated Pagel's λ statistic for each trait and habitat variable, applied phylogenetic least-squared regression to the univariate and best-fit multivariate models relating traits to habitat, and tested for an effect of relatedness on competition by correlating spatial associations with the branch lengths separating the species in each pair.

RESULTS

Tests of habitat association: leaf drought tolerance is a strong trait driver of habitat preference

Five of the six measured traits were significantly correlated with habitat, as expected from hypothesis 1, with r^2 for the best-fit models ranging from 0.04 - 0.36 (Table 5.3, Fig. 5.2). We report only the best-fit models that were more predictive than spatial autocorrelation (Table S5.7).

Supporting hypothesis 2, which predicted the drought tolerance and physiology traits would correlate with habitat (Tables 5.1, 5.3), leaf density (ρ) was strongly correlated with habitat (r^2 for best-fit models = 0.34 - 0.36), as was the drought tolerance trait π_{tlp} (r^2 for best-fit models = 0.18 - 0.32) and the physiology traits K_L and K_S (r^2 for best-fit models = 0.24 - 0.27 and 0.22, respectively). These traits were more strongly correlated with habitat than the economics spectrum traits *LDMC* and N_{mass} (r^2 for best-fit models = 0.10 - 0.11 and 0.04, respectively), and *LMA* was the only trait for which none of the best-fit models were significant (Table S5.7).

In the best-fit models for ρ, species with denser leaves were associated with more crowded neighborhoods and sites with a greater topographic wetness index (*TWI*) (Table 5.3; Fig. 5.2). The correlation between ρ and neighborhood density supports hypothesis 2, which

predicts that species with lower leaf investment will occur in less shaded habitats. Four of the 5 best-fit models for π_{tlp} supported hypothesis 2, with drought tolerant species associated with drier values for 4 of the 5 habitat variables identified as predictors. In those 4 models, more drought tolerant species were associated with sites with a higher convexity, more western aspect, greater scaled neighborhood basal area, and larger neighboring trees. In the remaining model, drought tolerance was associated with a more western aspect, as predicted, but with less dense neighborhoods, contrary to expectation (Table 5.2). By contrast, none of the best-fit models for K_L and K_S fully supported hypothesis 2. Species with a greater K_L occurred in sites with a higher elevation, slope, and neighborhood basal area, contrary to prediction (Tables 5.2, 5.3), although a greater K_L was also associated with lower light exposure, as expected if shaded sites are wetter. Species with a higher K_S were associated with higher convexity and neighborhood basal area, contrary to hypothesis 3.

The functional traits *LDMC* and N_{mass} were weakly correlated with habitat (r^2 range = 0.04 - 0.11) (Table 5.3). Species with a greater *LDMC* were found in more western sites and those with higher N_{mass} were found in more crowded neighborhoods, contrary to our prediction that species with greater leaf nutrient investment and lower structural investment would be associated with greater light exposure and not with indicators of habitat water supply (Table 5.1, 5.2). However, the low r^2 values indicate that these traits are not strongly linked with habitat.

Tests of hierarchical competition: large trees of drought tolerant species are spatially clustered

Large trees were significantly more clustered for species pairs with more negative mean π_{tlp} values, or greater drought tolerance, than species pairs with contrasting π_{tlp} values at scales from 8-11m, supporting hypotheses 5, 6 and 10 (Fig. 5.1D). The mean spatial association (i.e., the correlation between the spatial patterns of the species in each pair) for each of these two

categories and the difference in mean spatial association between them were small in magnitude; the mean spatial association at 8-11m was 0.006 to 0.007 for the "high drought tolerance" category, where both species have a more negative π_{tlp} than the 50th percentile of species means, and -0.004 to -0.003 for the category of contrasting species pairs. The large trees of more drought tolerant species were thus more significantly clustered than random, while those of species with contrasting drought tolerances were significantly segregated. The less drought tolerant species did not exhibit significantly different associations from the other categories. No other traits showed significant differences in spatial association among categories (Fig. S5.8, S5.9).

Tests of niche overlap-based competition: spatial associations were unrelated to trait differences

Pairwise spatial associations were not significantly correlated with species differences in any trait, either for associations unweighted (maximum r^2 for each trait = 0.004-0.008, minimum p = 0.02-0.07, p_{rank} = 0.03-0.07, n = 820 pairs) or weighted by tree size (max. r^2 for each trait = 0.004-0.008, min. p = 0.02-0.07, p_{rank} = 0.03-0.07), contrary to hypotheses 5 and 8 (Fig. S5.10). (The p-value threshold for significance is 0.0083; i.e., 0.05 corrected for multiple correlations).

Tests of phylogenetic effects: relatedness does not influence spatial patterning for these species

None of the trait or habitat variables exhibited Pagel's λ values significantly greater than 0 (Table S5.8, Fig. S5.11, S5.12). A significant phylogenetic signal was found for univariate correlations between ρ and *LMA*, and ρ, *LDMC,* and habitat (Table S5.9 - S5.10), but not the best-fit habitat models for any trait (Table S5.11). Relatedness was not correlated with pairwise spatial associations, either unweighted (max. r^2 across scales = 0.006; min. p = 0.03; p_{rank} = 0.006) or weighted by size (max. r^2 across scales = 0.004; min. p = 0.05; p_{rank} = 0.02) (Fig. S5.10H).

DISCUSSION

Trait variation at the Xishuangbanna plot exhibited spatial signatures for habitat associations and competition. The drought tolerance trait π_{tlp} produced the only signal for both competition and habitat association, providing the first demonstration that leaf drought tolerance plays a critical role in multiple assembly processes in tropical communities.

We expected trait and habitat correlations to be strong, since many species here show significant associations with topography and soil type (Lan et al. 2011a, Hu et al. 2012), and these species' functional traits have been found to correlate with topography (Liu et al. 2014). Indeed, 5 of the 6 traits, with the exception of *LMA*, were more strongly correlated with habitat than expected from spatial autocorrelation (Tables 5.3 and S5.7; hypothesis 1 in Table 5.1). While *LMA* is known to vary across habitats in tropical forests (Kraft et al. 2008), this pattern may reflect a correlation between *LMA* and traits that more directly drive habitat associations, as supported by the significant correlation and coevolution between *LMA* and leaf density (r^2 = 0.09, p = 0.04, λ =1) (Tables S5.4, S5.5, S5.9, S5.10). Leaf density (ρ) was the strongest trait correlate with habitat (maximum r^2 for best-fit models = 0.36). Species with higher ρ occurred in sites with denser neighborhoods and a higher topographic wetness index (*TWI*) (Table 5.3, Fig. 5.2). These results are consistent with predictions from the leaf economics spectrum that species with greater structural investment will occur in more shaded, and hence more crowded neighborhoods (Wright et al. 2004); indeed, increased crowding during succession in a tropical forest favors species with greater leaf structural investment, with a stronger trend found for ρ than *LMA* or *LDMC* (Lohbeck et al. 2013). These results are also consistent with the correlation between topography and leaf area index (*LAI*) found in other tropical forests, suggesting that

sites with a higher *TWI* exhibit a higher *LAI* and thus more shade from neighboring trees (Moser et al. 2007).

This is the first study to quantify an impact of variation in drought tolerance on species differences in habitat preference within a forest (Fig. 5.2). Our findings importantly extend previous studies that contrasted π_{tlp} between one species each from different habitat categories within a forest, which found that the more drought tolerant species occurred in the drier ridge habitats, thus suggesting an important role for π_{tlp} in driving habitat preferences within forests (Becker et al. 1988, Gibbons and Newberry 2002). The π_{tlp} was the trait with the second strongest correlation with environment (max. $r^2 = 0.32$), demonstrating for the first time across habitats within a forest the stronger alignment of species distributions with π_{tlp} than with K_S, K_L, and *LMA* as has been observed across forests and biomes globally (Choat et al. 2007, Bartlett et al. 2012). Species with a more negative π_{tlp} were generally found in drier sites, showing expected correlations (Table 5.2, 5.3) for 4 of the 5 best-fit habitat predictors, including a more western aspect and a higher scaled basal area, average neighbor size, and convexity. A western aspect was especially important, present in every best-fit model for π_{tlp}, and consistent with strong effects of aspect on performance in tropical seedlings (Inman-Narahari et al. 2014). Contrary to prediction, more drought tolerant species also occurred in less dense neighborhoods, suggesting that decreased shading impacted water supply more than reduced competition, as observed in some other tropical forests (Lebrija-Trejos et al. 2010). The stem conductivity traits K_L and K_S were more weakly correlated with habitat (max. $r^2 = 0.27, 0.22$; respectively), and more conductive species did not occur in wetter sites, contrary to expectation from the trade-offs between conductivity and drought tolerance (Choat et al. 2007). Thus, while K_S and K_L are important drivers of growth rate (Fan et al. 2012), these traits weakly impact distributions within

the forest. A more negative π_{tlp} was also associated with denser leaves ($r^2 = 0.19$, $p = 0.003$; Table S5.4, S5.5); however, these traits were most strongly related to different habitat variables (Table 5.3). Thus, the correlation of π_{tlp} with habitat was not driven by ρ; rather, habitat associations reflect the impact of environmental variation on integrated plant function, such as this coordinated investment in leaf structure and drought tolerance (Fig. 5.2).

Vegetation structure was an especially important environmental driver, with crowding variables identified as predictors in 11 of the 14 best-fit models (Table 5.3). The predictors for the strongest best-fit models ($r^2 > 0.3$) included convexity, aspect, and crowding, as expected, since these variables drive landscape-level patterns in water supply during drought (hypothesis 3) (Grayson et al. 1997), but not canopy-level solar radiation, suggesting vegetation structure has a stronger impact on light availability. Further, only 6 of the best-fit models included predictors corrected for quadrat density, suggesting that mean variable values are representative of habitat.

We found novel evidence for a significant impact of leaf drought tolerance on neighborhood interactions, although the spatial signature for competition was weak. As hypothesized for hierarchical competition, species pairs where both species have more negative π_{tlp} values had significantly more aggregated large trees than pairs with contrasting π_{tlp} values at scales from 8-11m (hypothesis 9) (Fig. 5.1D), while pairwise differences were not correlated with interspecific clustering for any trait (hypothesis 10) (Fig. S5.10). This pattern is consistent with species that have greater drought tolerance being superior competitors. Indeed, ecohydrology models show that species with more negative π_{tlp} values exhibit greater transpiration and depletion of soil water (Laio et al. 2001). We found no significant signal for niche overlap-based competition (hypotheses 7, 8). These results concur with previous studies showing that position in a trait hierarchy predicts competitive impacts on growth and survival

more strongly than trait differences (Kunstler et al. 2012, Kraft et al. 2014), while demonstrating a novel role for leaf drought tolerance in determining species fitness differences. A previous study found greater trait differences among valley-associated species at the XSBN plot and interpreted this result as evidence for stronger competition among species with traits that produce rapid growth and mortality (i.e., lower wood density) (Liu et al. 2014). However, our results did not support such a relationship, which would have reduced clustering among drought sensitive species and among species with low K_S, as those trait values are associated with valley sites (Table 5.3). The signal in π_{tlp} alone suggests drought tolerance more directly impacts resource depletion than leaf economics traits (hypothesis 5) (Laio et al. 2001). The presence of a signal for competition in associations weighted by tree size and not unweighted associations is consistent with large trees more strongly impacting competitive interactions (hypothesis 4). This analysis does not identify which life stage drives exclusion; this pattern is consistent with drought tolerant species excluding drought sensitive trees slowly over time, as the trees become larger, or with drought tolerant adults preventing less tolerant juveniles from establishing. Overall, these results provide novel support for the further development of size-weighting methods for spatial point patterns.

The spatial signature for competition was statistically significant but extremely weak ($r^2 < 0.01$), which is expected for several reasons. First, we quantified traits for saplings to represent differences among all trees larger than 1cm in diameter. This is a common study design (e.g. Kraft et al. 2008, Katabuchi et al. 2012), as traits are generally correlated across life stages, and variation within species is typically smaller within than across species (Thomas and Winner 2002, Markesteijn et al. 2007). However, shifts in traits across life stages and plasticity among individuals may widen the range of tolerable habitats or alter competitive outcomes, weakening

the spatial signatures of trait means measured for saplings. Second, this weak relationship is also consistent with the difficulty of scaling up individual traits to the whole-plant performance and resource demand that determine competitive impacts (Hérault et al. 2011). Strongly predicting the effect of traits on competition is likely to require a mechanistic approach for predicting whole-plant performance and resource use from many traits. These results may also be consistent with interspecific competition having a relatively small impact on assembly compared to pest/pathogen interactions or conspecific competition. Indeed, conspecific neighbors impact growth and survival more strongly than heterospecifics (Uriarte et al. 2010, Terborgh 2012).

We did not find a phylogenetic pattern in any trait, an impact of phylogeny on the best-fit habitat models, or a correlation between relatedness and spatial association (Table S5.8 - S5.11, Fig. S5.10, S5.12). Previous studies in this plot found significant lability in *LDMC* and *SLA* and co-evolution between *SLA* and topography (Yang et al. 2014a, Yang et al. 2014b), suggesting that sampling such a large number of species (> 200) enabled the resolution of these phylogenetic patterns. Greater sampling within clades may be especially important, as long branch lengths can obscure phylogenetic signal (Townsend et al. 2010), and our species span 38 genera and 25 families.

Spatial patterns in trait variation can provide powerful insights into the drivers of community assembly, as well as an analytical framework that can be applied to other forests to identify global patterns in the impact of different traits and habitat variables on assembly. Applying these analyses to other forests will raise several important considerations. Here we assessed evergreen species, which potentially exhibit greater resource demand and, thus, competition than deciduous species during the dry season so that analyzing both functional types could obscure the effects of trait differences on competitive interactions. Deciduous species

account for 2% of stem density at XSBN, allowing patterns in evergreens to capture important processes at this site, but accounting for differences in competitive interactions between functional types will be crucial in forests with more deciduous trees. Disturbance history can also strongly impact spatial patterns in trait variation. Over 80% of the XSBN forest has been unlogged for at least 200 years, while part of the ridge was logged 40 years ago (Lan et al. 2011a). This management history is consistent with the association between drought tolerant species and ridge sites, as disturbed sites favor drought tolerant species (Lebrija-Trejos et al. 2010), and with the greater spatial aggregation found among drought tolerant adults than adults with contrasting trait values, if drought tolerant species colonized logged areas and excluded sensitive species. While the continuous variation in drought tolerance observed across this landscape (Fig. 5.2E) suggests that localized disturbance is not sufficient to explain these patterns, future studies should consider these effects in more disturbed forests. Overall, these findings suggest that leaf drought tolerance and structural investment are promising avenues for further research. In addition, the low predictive power for interspecific associations indicates the need to progress from correlative trait signatures to a mechanistic framework to quantitatively infer ecological processes from traits to further resolve the drivers of assembly across communities.

ACKNOWLEDGMENTS

We thank Matteo Detto, Charles Canham, and Robert Freckleton for their invaluable guidance with the analyses, and Nathan Kraft, Isabelle Maréchaux, and Faith Inman-Narahari for helpful and insightful comments and discussion. This study was financially supported by the National Key Basic Research Program of China (#2014CB954100), the National Science Foundation

#IOS-0546784, #1108534, and #DEB-1046113 (to S.J. Davies), the Center for Tropical Forest Science -Forest Global Earth Observatory of the Smithsonian Institution, and the Vavra and Pauley Fellowships. Y. Z., S-w. S., and K-F. C. were supported by the National Natural Science Foundation of China (#31170399). XSBN staff provided logistical help, especially Chen Yajun.

Table 5.1. Hypothesized relationships between key ecological processes and spatial patterns in trait variation.

Process	Pattern	Hypotheses
Habitat association	Functionally similar species will co-occur at the spatial scale of environmental variation	(1) Trait values will correlate with habitat variables across species (2) Drought tolerance and physiology traits will be strong drivers of habitat association and strong correlates with habitat, as established for economic spectrum traits. More drought tolerant species will occur in drier habitats, while species with greater conductivities will occur in wetter sites. Species with higher nutrient and lower structural investment will occur in less shaded habitats, and these traits will relate weakly to water supply. (Habitat and trait variables described in Table 5.2 and Fig. 5.2) (3) Traits will strongly correlate with habitat variables that determine water supply in dry conditions, including neighborhood crowding, solar radiation, and topographic aspect and convexity (Table 5.2)
Competition	Species will show significant spatial associations at the neighborhood scale when accounting for larger-scale habitat patterns	(4) Spatial associations weighted by tree size will show a stronger spatial signal for competition, as larger trees are typically stronger competitors (5) Drought tolerance and physiology traits will show strong spatial patterns, as they directly impact ability to deprive neighbors of resources (6) Pairwise differences in phylogenetic relatedness will show the same correlations with spatial associations as phylogenetically conserved traits
Niche overlap-based competition	Functionally distinct species will be more clustered at the neighborhood scale	(7) Species pairs with distinct trait values will be more clustered than pairs where both species have high or low trait values (8) The absolute value of pairwise trait differences will significantly correlate with pairwise spatial associations
Hierarchical competition	Functionally similar species will be more clustered at the neighborhood scale	(9) Species pairs where both members have high or low mean trait values will be significantly more aggregated than pairs with contrasting means (10) The absolute value of pairwise trait differences will not correlate with pairwise spatial associations

Table 5.2. The habitat variables have known relationships to light and water supply, allowing us to predict their correlations with traits. A + predicts that higher values are associated with greater leaf structural investment (LI; higher *LMA*, *LDMC*, and ρ; lower N_{mass}), higher conductivity (C; higher K_s and K_L), or lower drought tolerance (π_{tlp}), as $\pi_{tlp} < 0$. Values are the min, **mean**, and max.

Habitat variable	π_{tlp}	C	LI	Values	Functional significance
Elevation (m)	-	-	+	731, **760**, 805	Higher elevation sites receive less water drainage and shading from upslope areas (Becker et al. 1988).
Convexity (m m^{-1})	-	-	+	-3.4, **-0.08**, 1.5	Elevation relative to surroundings. Convex, drier sites receive more light and less drainage (Daws et al. 2002).
Slope (°)	-	-	0	18.4, **25.3**, 29.8	More sloping sites may receive less drainage (making them drier) or less light (wetter) (Galicia et al. 1999).
Topographic wetness index (TWI)	+	+	0	4.4, **5.5,** 7.7	Ratio of upslope area to local slope. Wetter sites, with a higher TWI, receive more drainage from upslope areas than they lose due to local slope (Sorensen et al. 2006).
East/west aspect	+	+	-	-0.55, **-0.21**, 0.70	Western, drier sites (-) have more light at the hottest time of day, increasing evaporation (Bennie et al. 2008).
North/south aspect	+	+	-	-0.63**, -0.21**, 0.28	Southern, drier sites (-) have more light, and thus evaporation, in the northern hemisphere (Leij et al. 2004).
Solar radiation (W m^{-2})	-	-	+	3778, **3955**, 4091 1077**, 1122**, 1186 2291**, 2739**, 3145 853**, 888**, 939	Values are for mean direct light during the wet season, diffuse light during the wet season, direct light during the dry season, and diffuse light during the dry season, respectively. Sites with greater light exposure have more evaporation (Galicia et al. 1999). Direct light should induce more evaporation than diffuse, and dry season radiation should influence water supply more than the wet season (Grayson et al. 1997).
Crowding	-	-	0	4.16, **5.48,** 6.58 7838, **20249**, 47712 507, **610**, 725 22.9, **25.5**, 28.3	Values are for crowding measured as the mean total neighborhood basal area (BA; m^2), mean neighborhood basal area normalized by focal tree area (Scaled BA), mean total neighborhood tree density (Density), and mean neighbor size (cm^2), respectively. Drought tolerant species should occur in crowded neighborhoods, which will deplete water faster; however, greater density could also increase shading (Canham et al. 2004).

Table 5.3. The best-fit models predicting traits from habitat that were more predictive than autocorrelation (Table S5.7), their r^2 values, number of parameters fit (K), and difference in AICc from the model with the lowest AICc (ΔAICc). An * indicates the model with the lowest AICc was rejected for a more parsimonious model. Leaf density (ρ) was the strongest correlate with habitat, followed by π_{tlp}, and these correlations largely matched our hypotheses (Table 5.2).

Predictors	**R^2**	**K**	**ΔAIC_c**
Predicted variable: ρ			
+Neighborhood Density, +TWI_{WA}	0.36	4	0
+Neighborhood Density, +TWI	0.34	4	1.1
Predicted variable: π_{tlp}			
-Average Neighbor BA, +Eastness	0.24	4	0.9*
-Neighborhood Scaled BA, -Convexity, +Eastness, +Neighborhood Scaled BA*Convexity	0.32	6	1.2
+$Eastness_{WA}$	0.18	3	1.5
+Neighborhood Density, +Eastness	0.22	4	1.8
-Average Neighbor BA, -Convexity, +Eastness, +Average Neighbor BA*Convexity	0.31	6	1.8
Predicted variable: K_L			
+$Elevation_{WA}$, +Neighborhood BA, +$Slope_{WA}$, -$Elevation_{WA}$*Neighborhood BA	0.27	6	0
+$Elevation_{WA}$, +Neighborhood BA, -Direct Light Wet $Season_{WA}$,	0.25	6	1.8
+Elevation, +Neighborhood BA, +Slope, -Elevation*Neighborhood BA	0.24	6	1.8
Predicted variable: K_S			
+$Convexity_{WA}$, +Neighborhood BA, -$Convexity_{WA}$*Neighborhood BA	0.22	5	0
Predicted variable: *LDMC*			
-$Eastness_{WA}$	0.11	3	0
-Eastness	0.10	3	0.1
Predicted variable: N_{mass}			
+Average Neighbor BA	0.04	3	0

FIGURE CAPTIONS

Figure 5.1. Simulations showing characteristic spatial patterns in trait variation and results of the wavelet analysis for each assembly process (**A**-**C**), and the observed signature of hierarchical competition for the drought tolerance trait turgor loss point (π_{tlp}) (**D**). Niche competition spatially clusters neighbors with different trait values (**A**, indicated by the colors in the neighborhood in the red circle), while hierarchical competition and habitat association aggregate similar trees (**B**, **C**). Habitat association also correlates trait values with habitat (**C**). Wavelet analyses separate neighborhood patterns from larger-scale habitat associations and show that species with similar trait values (red = high, blue = low) are more clustered than species with contrasting trait values (gray) for hierarchical competition (**B**), with no differences under habitat association (**C**). π_{tlp} was the only trait with a signal for competition (**D**) (Fig. S5.8). The larger trees of drought tolerant species pairs (red; n = 190 pairs) were more aggregated than those with contrasting π_{tlp} values (gray, n = 420) at scales from 8-11m, consistent with hierarchical competition. Bands show 95% confidence intervals. There were no differences for analyses unweighted by tree size (Fig. S5.9).

Figure 5.2. The predictive power of habitat variables for the traits characterizing leaf structural investment, drought tolerance, and plant growth rate. The strongest correlates in each category are leaf density (ρ, $r^2 = 0.36$; **A**), turgor loss point (π_{tlp}, $r^2 = 0.32$; **B**), and leaf-area specific conductivity (K_L, $r^2 = 0.27$; **C**). Greater leaf structural investment is also quantified by higher *LMA* (range = 36 - 134, mean = 62 g m^{-2}) and *LDMC* (0.22 - 0.62, 0.35 g g^{-1}), and faster growth is also associated with higher K_S (0.14 - 2.19, 0.91 kg m^{-1} MPa^{-1} s^{-1}) and N_{mass} (1.2 - 3.1, 2.1%) (Wright et al. 2004, Fan et al. 2012). (See Fig. S5.1 for trait variation across species). Mean ρ

(D), π_{tlp} (**E**), and K_L (**F**) in each 10×10m quadrat vary strongly across the landscape in accordance with habitat heterogeneity (see Fig. S5.5, S5.6 for maps of variation in the habitat predictors).

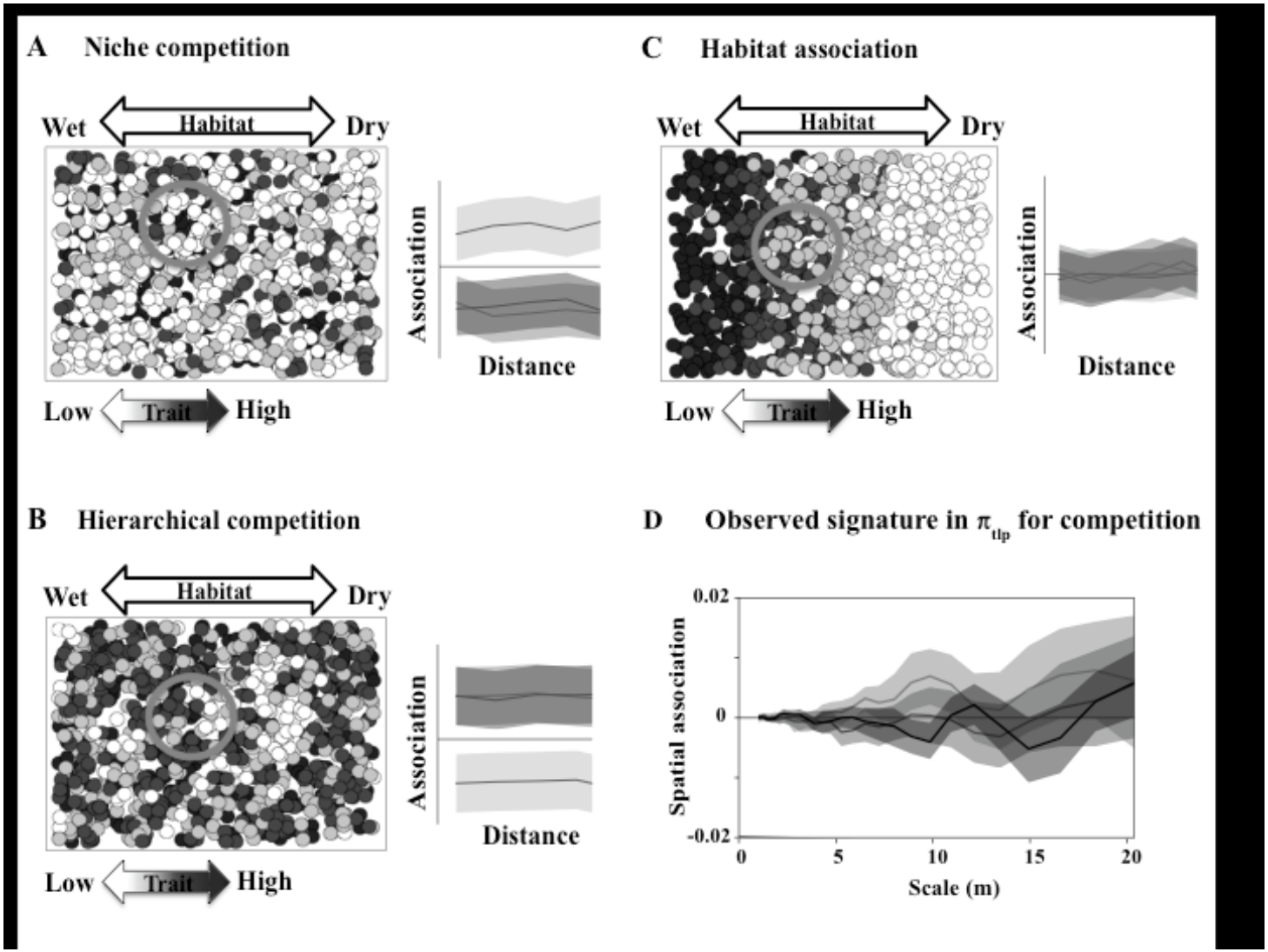
A Niche competition
Wet
Habitat
Dry
Low
Trait
High
Association
Distance
C Habitat association
Wet
Habitat
Dry
Low
Trait
High
Association
Distance
B Hierarchical competition
Wet
Habitat
Dry
Low
Trait
High
Association
Distance
D Observed signature in π_{tlp} for competition
Spatial association
0.02
0
-0.02
0
5
10
15
20
Scale (m)

Figure 5.1

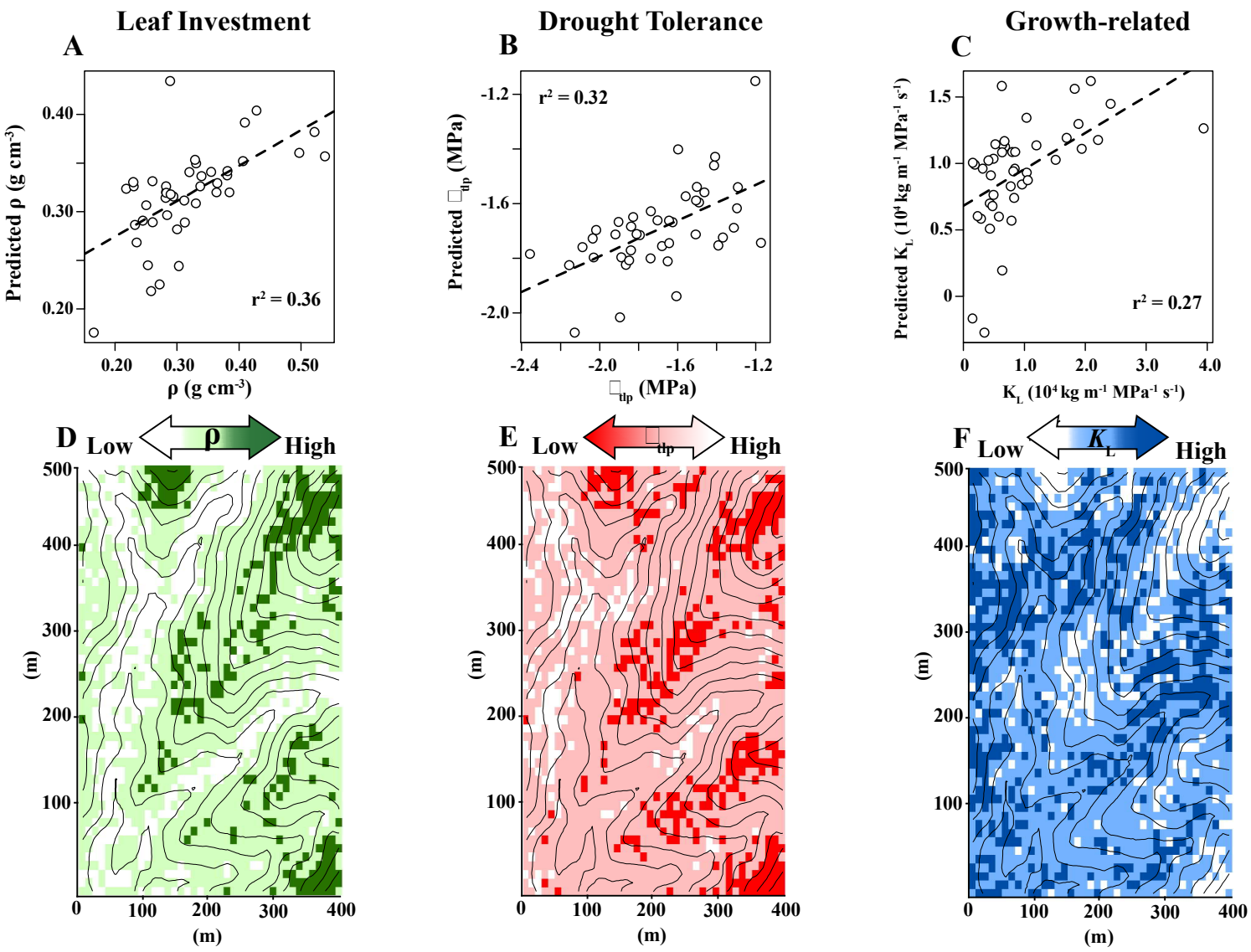
Leaf Investment
A
Predicted ρ (g cm-3)
ρ (g cm-3)
r2 = 0.36
Drought Tolerance
B
Predicted Ψtlp (MPa)
Ψtlp (MPa)
r2 = 0.32
Growth-related
C
Predicted KL (10-4 kg m-1 MPa-1 s-1)
KL (10-4 kg m-1 MPa-1 s-1)
r2 = 0.27
D Low ρ High
E Low Ψtlp High
F Low KL High
(m)
(m)
(m)

Figure 5.2

SUPPLEMENTAL MATERIALS

Table S5.1. Mean trait values and percent relative abundances for each of the 43 study species.

Table S5.2. Mean habitat variables for the topographic variables elevation, convexity, slope, topographic wetness index (*TWI*) and the linearly transformed aspect variables eastness and northness, the light variables daily mean diffuse and direct light during the wet and dry seasons, and the neighborhood crowding variables average total neighborhood basal area, total basal area scaled by the area of the focal tree, neighborhood density, and average neighbor basal area.

Table S5.3. Species means for habitat variables corrected for local quadrat density, which represents the habitats where a species is disproportionately overrepresented in the local tree density.

Table S5.4. Pearson correlation coefficients for univariate correlations among species means for trait and habitat variables uncorrected for differences in quadrat density, which represent the habitats species occur in rather than where they are overrepresented relative to local tree density.

Table S5.5. Pearson correlation coefficients values for univariate correlations among species means for traits and habitat variables, where habitat means are corrected for quadrat density and represent the habitats where species are disproportionately overrepresented.

Table S5.6. The model structures used to predict species habitat associations from mean trait values.

Table S5.7. The observed r values for the best-fit habitat models compared to the 95% confidence interval of the r values obtained from 1000 torus translations.

Table S5.8. Pagel's λ values for each trait and habitat variable.

Table S5.9. Pagel's λ values for each univariate correlation among the trait and habitat variables, which measures the phylogenetic signal in the phylogenetic least-squares regression.

Table S5.10. Pagel's λ values for each univariate correlation among the trait and habitat variables, using habitat variables that are corrected by variation in tree density to represent the habitats where species are overrepresented relative to local tree density.

Table S5.11. Pagel's λ values estimated for the best-fit multivariate models between traits and habitat variables (Table S5.3).

Figure S5.1. Histograms of species means for the traits turgor loss point (π_{tlp}, **A**), nitrogen concentration (N_{mass}, **B**), leaf mass per unit area (*LMA,* **C**), leaf density (ρ, **D**), leaf dry matter content (*LDMC,* **E**), stem hydraulic conductivity normalized by sapwood area (K_S, **F**), and stem hydraulic conductivity normalized by leaf area (K_L, **G**).

Figure S5.2. Histograms of species means for the topographic habitat variables elevation, convexity, topographic wetness index (*TWI*), slope, and the linearly-transformed aspect variables

eastness and northness (panels **A- F**), and for species means corrected for variation in quadrat density to weight habitats where species are overrepresented relative to local tree density (**G- L**).

Figure S5.3. Histograms showing species means for average daily diffuse and direct beam solar radiation in the wet (May – October) and dry (November – April) seasons (panels **A**-**D**), and species means corrected for variation in quadrat density (panels **E**-**H**).

Figure S5.4. Histograms of species means for the neighborhood crowding variables, assessed for 20m radius neighborhoods around each individual tree.

Figure S5.5. Plot maps color-coded by convexity (**A**), slope (**B**), topographic wetness index (*TWI*; **C**), eastness (**D**), and northness (**E**). Dark colors represent lower convexity (valleys), greater wetness, and a more western and a more southern aspect. Elevation is shown in contour lines (red). All habitat characteristics are highly variable across the landscape, allowing for species differences in resource requirements to produce strong habitat associations, but also correlated (Tables S5.4, S5.5), producing complex trait-habitat associations.

Figure S5.6. Daily direct (**A, C**) and diffuse (**B, D**) solar radiation averaged for the wet (May-October) and dry (November-April) seasons (W m^{-2}). Blue indicates wet season (**A, B**) and red indicates dry season radiation (**C, D**). Darker colors indicate deeper shade. Radiation is higher in the wet season, and intensity across the landscape varies with the season and type of radiation.

Figure S5.7. The spatial associations (**A**) and map of tree locations, with points scaled by tree size (**B-D**), for three simulations demonstrating how spatial patterns in tree size impact the size-weighted spatial association analysis (see Appendix section Supplemental Methods 5.3 for methods). Weighting trees by size makes spatial patterns for large adult trees more influential to the overall spatial association, since large trees are expected to exclude neighbors more strongly than small trees. We first calculated spatial associations from unweighted tree density (**A**, black line) (dotted lines are 95% confidence intervals for a random association). We then simulated tree DBHs as a function of nearest interspecific neighbor distance, first assuming that tree size scaled positively with nearest interspecific neighbor distance (**A**, blue line; B) so that more distantly spaced trees were larger, and then that size scaled negatively with distance (**A**, red line; C), so that more closely spaced trees were larger. In the third simulation, tree size varied randomly with proximity to interspecific neighbors (**A**, gray band represents bootstrapped 95% confidence intervals; D). Unweighted tree density shows that the two species are randomly associated. When the larger trees are more distantly spaced, the size-weighted spatial association shows significant *segregation* at scales around 50m (**A**, blue line), and when the larger trees are more closely spaced, the size-weighted association shows significant *aggregation* at scales < 60m (**A**, red line). When tree size varies randomly with proximity, weighting by size does not produce significantly different spatial association measures from density alone (**A**, gray band). The first simulation shows that the large adult trees of the two species do not persist together over time, which is consistent with strong competition, while the second simulation would indicate that large adult trees are able to persist in the same neighborhoods over long periods of time, which is consistent with negligible or weak competition. Thus, conducting both size-

weighted and unweighted analyses provides additional insights into the ecological processes underlying species spatial distributions.

Figure S5.8. The average and 95% confidence intervals for pairwise spatial associations weighted by tree size, calculated across 32 scales between 0 - 20m for species pairs with low trait values (trait mean $\leq 50^{th}$ percentile of species means, n = 210 species pairs, indicated in blue), high trait values (trait mean > 50^{th} percentile of species means, n = 190 species pairs, indicated in red), or contrasting trait values (one species mean is high and the other low, n = 420 species pairs, indicated in black). Traits are nitrogen concentration per unit mass (N_{mass}, panel **A**), turgor loss point (π_{tlp}, **B**), leaf mass per unit area (*LMA*, **C**), leaf density (ρ, **D**), leaf dry matter content (*LDMC*, **E**), stem hydraulic conductivity per sapwood area (K_S, **F**), and stem conductivity per leaf area (K_L, **G**). Correlations are for density-based (black points) and biomass (blue points) spatial associations (n = 820 species pairs). More drought tolerant species pairs, with more negative π_{tlp} values (**B**; shown in red), are significantly more clustered than species pairs with contrasting π_{tlp} values at scales from 8-11m (mean association = 0.006 – 0.007 for more drought tolerant pairs and -0.004 – -0.003 for contrasting pairs), as consistent with hierarchical competition (hypothesis 9, Table 5.1), although these spatial associations are extremely weak, with covariance between species accounting for less than 1% of the variation in their spatial distributions. No other traits showed significant differences in spatial association among these trait categories.

Figure S5.9. The average and 95% confidence intervals for density-based pairwise spatial associations across 32 scales between 0 - 20m for the following trait categories: both species

have low trait values (mean $\leq 50^{th}$ percentile of species means, n = 210 species pairs; blue), high trait values (mean > 50^{th} percentile of species means, n = 190 species pairs; red), or contrasting trait values (one species mean is high and the other low, n = 420 species pairs; black). The panels follow Figure S5.8. The confidence intervals are derived from the 95th percentiles of 1000 bootstraps. Species associations are scaled between -1 and 1 to be analogous to r^2 values. Scale is the distance at which spatial associations are evaluated. There were no significant differences in spatial association among trait categories for any of the traits for density-based spatial associations.

Figure S5.10. The r^2 values for the correlations between the absolute value of pairwise trait differences and interspecific spatial associations at 32 scales between 0-20m. Panels A – G follow Fig. S5.8, and H is phylogenetic relatedness. Correlations are for density (black points) and size-weighted (blue points) spatial associations (n = 820 species pairs). Correlations with relatedness were conducted on a subset of 42 species, excluding *Walsura robusta* due to a lack of phylogenetic information. A p-value threshold of ≤ 0.0083 for both pearson (p) and rank (p_{rank}) correlations was used to define significance. Trait differences were not significantly correlated with density-based or size-weighted spatial associations at any scale, contrary to expectations from niche overlap-based competition (hypothesis 8, Table 5.1).

Figure S5.11. We constructed a molecular phylogeny for the 42 study species with existing sequence data, excluding *Walsura robusta* due to a lack of phylogenetic information (see Yang et al. 2014 for methods).

Figure S5.12. There was no significant phylogenetic signal in interspecific variation of any of the trait or habitat variables, according to Pagel's λ (see Table S5.8). The trait variables are turgor loss point (π_{tlp}), nitrogen concentration per unit mass (N_{mass}), leaf mass per unit area (LMA), leaf density (ρ), leaf dry matter content (*LDMC*), stem hydraulic conductivity per unit sapwood area (K_S), and G) stem hydraulic conductivity per unit leaf area (K_L). The abbreviated habitat variables are diffuse and direct canopy solar radiation during the wet and dry seasons, average total neighborhood basal area, total neighborhood basal area scaled by the size of the focal tree, total neighborhood density, and the average neighboring tree basal area. The size of the circles indicates the trait values at each tip, with larger circles representing larger trait values, as well as greater drought tolerance, which is a more negative turgor loss point. Tip labels are the same as in Figure S5.11.

Supplemental Methods 5.1. Trait measurements.

Supplemental Methods 5.2. Habitat variables and computational methods.

Supplemental Methods 5.3. Simulations demonstrating the size-weighting method for the wavelet analyses.

Table S5.1. Mean trait values and percent relative abundances for each of the 43 study species. Traits are leaf nitrogen concentration (N_{mass}), turgor loss point, or the leaf water potential at wilting (π_{tlp}), leaf mass per unit area (*LMA*), leaf density (ρ), leaf dry matter content (*LDMC*), stem hydraulic conductivity normalized by sapwood area (K_S), and stem hydraulic conductivity normalized by leaf area (K_L).

Species	**Code**	**Abundance (%)**	N_{mass} **(%)**	π_{tlp} **(MPa)**	***LMA*** **(g m^{-2})**	**ρ (g cm^{-3})**	***LDMC*** **(g g^{-1})**	K_S **(kg m^{-1} MPa^{-1} s^{-1})**	K_L **(kg m^{-1} MPa^{-1} s^{-1})**
Aglaia abbreviata	AGLAAB	0.08	2.16	-2.13	47.8	0.32	0.31	1.88	2.21×10^{-4}
Aglaia perviridis	AGLAPE	0.17	1.94	-1.90	53.9	0.35	0.35	1.17	6.84×10^{-5}
Antidesma montanum	ANTIMO	0.48	1.86	-1.17	57.6	0.33	0.30	1.87	3.94×10^{-4}
Baccaurea ramiflora	BACCRA	3.36	1.96	-1.31	78.9	0.28	0.30	0.37	8.01×10^{-5}
Barringtonia pendula	BARRPE	0.60	2.43	-1.29	69.4	0.28	0.25	1.67	1.04×10^{-4}
Beilschmiedia robusta	BEILRB	0.13	2.35	-1.63	68.7	0.28	0.29	0.24	4.93×10^{-5}
Chisocheton siamensis	CHISSI	0.82	3.13	-1.49	46.6	0.25	0.27	0.54	3.16×10^{-5}
Cinnamomum bejolghota	CINNBE	1.40	1.66	-1.70	93.4	0.36	0.39	1.44	9.62×10^{-5}
Cleidion brevipetiolatum	CLEIBR	1.02	2.66	-2.03	64.0	0.38	0.35	0.44	4.34×10^{-5}
Cylindrokelupha yunnanensis	CYLIYU	0.08	2.19	-1.50	54.0	0.30	0.39	1.66	1.89×10^{-4}
Dichapetalum gelonioides	DICHGE	1.28	2.92	-1.90	56.8	0.38	0.35	0.74	6.39×10^{-5}
Diospyros nigrocortex	DIOSNI	0.40	2.03	-2.09	86.1	0.38	0.38	0.79	5.83×10^{-5}
Drypetes hoaensis	DRYPHO	0.59	1.75	-1.61	49.9	0.34	0.39	1.33	1.04×10^{-4}
Elaeocarpus glabripetalus alatus	ELAEGL	0.18	1.65	-1.68	47.8	0.33	0.33	0.48	6.37×10^{-5}
Eurya austroyunnanensis	EURYAU	0.83	1.51	-1.41	58.9	0.31	0.33	0.82	8.49×10^{-5}
Ficus fistulosa	FICUFI	0.82	1.76	-1.30	55.7	0.24	0.25	0.40	5.24×10^{-5}
Ficus langkokensis	FICULA	1.40	2.19	-1.60	39.0	0.27	0.34	1.22	2.09×10^{-4}
Garcinia cowa	GARCCO	4.54	1.55	-1.84	84.3	0.31	0.30	0.97	7.76×10^{-5}
Garcinia lancilimba	GARCLA	0.65	1.80	-1.65	69.9	0.36	0.62	0.90	8.32×10^{-5}
Knema furfuracea	KNEMFU	3.31	1.84	-1.89	102.1	0.50	0.46	0.36	2.88×10^{-5}
Knema globularia	KNEMGL	0.64	2.09	-1.64	60.9	0.41	0.32	0.70	8.43×10^{-5}
Lasianthus verticillatus	LASIVE	0.28	2.07	-1.83	68.9	0.22	0.33	1.55	1.51×10^{-4}
Leea compactiflora	LEEACO	1.10	2.03	-1.51	65.3	0.30	0.35	0.14	1.49×10^{-5}

Macropanax dispermus	MACRDI	0.43	2.37	-1.74	61.0	0.26	0.27	0.64	4.34×10^{-5}
Mallotus garrettii	MALLGA	0.72	1.88	-1.64	36.7	0.24	0.35	0.42	7.89×10^{-5}
Mezzettiopsis creaghii	MEZZCR	3.46	2.51	-1.74	49.1	0.23	0.32	0.78	6.73×10^{-5}
Microcos chungii	MICRCH	0.38	2.03	-1.87	45.0	0.29	0.31	0.78	3.45×10^{-5}
Myristica yunnanensis	MYRIYU	0.16	1.94	-1.51	72.4	0.28	0.29	0.60	6.29×10^{-5}
Nephelium chryseum	NEPHCH	1.15	1.87	-1.79	60.7	0.52	0.42	0.62	4.93×10^{-5}
Phoebe lanceolata	PHOELA	2.52	1.91	-1.92	65.5	0.43	0.46	0.77	6.35×10^{-5}
Pittosporopsis kerrii	PITTKE	21.9	1.90	-1.84	74.5	0.26	0.32	1.49	1.69×10^{-4}
Pometia tomentosa	POMETO	0.50	2.41	-2.04	46.8	0.54	0.44	0.52	1.87×10^{-5}
Pseuduvaria indochinensis	PSEUIN	0.94	2.54	-2.02	54.8	0.33	0.34	1.35	1.06×10^{-4}
Pterospermum menglunense	PTERME	0.15	2.31	-1.85	63.7	0.28	0.43	2.19	2.41×10^{-4}
Saprosma ternata	SAPRTE	2.83	1.86	-1.41	49.6	0.25	0.27	0.21	2.32×10^{-5}
Parashorea chinensis	PARACH	8.29	2.65	-1.81	43.1	0.29	0.40	1.82	1.20×10^{-4}
Sloanea tomentosa	SLOATO	0.53	1.41	-1.56	60.4	0.29	0.38	0.72	4.50×10^{-5}
Sumbaviopsis albicans	SUMBAL	0.48	2.72	-2.36	63.7	0.26	0.38	0.23	1.53×10^{-5}
Syzygium latilimbum	SYZYLA	0.83	1.20	-1.37	133.9	0.34	0.40	1.30	1.94×10^{-4}
Tabernaemontana corymbosa	TABECO	0.23	2.80	-1.46	41.9	0.23	0.22	0.81	8.20×10^{-5}
Trigonostemon thyrsoideum	TRIGTH	0.85	2.06	-1.39	56.0	0.23	0.23	0.63	4.78×10^{-5}
Urophyllum chinense	UROPCH	0.29	2.35	-1.20	37.1	0.17	0.22	0.94	1.83×10^{-4}
Walsura robusta	WALSRO	0.17	2.37	-2.16	68.4	0.41	0.38	0.65	4.12×10^{-5}

Table S5.2. Mean habitat variables for the topographic variables elevation, convexity, slope, topographic wetness index (*TWI*) and the linearly transformed aspect variables eastness and northness, the light variables daily mean diffuse and direct light during the wet and dry seasons, and the neighborhood crowding variables average total neighborhood basal area, total basal area scaled by the area of the focal tree, neighborhood density, and average neighbor basal area. Crowding variables are calculated for 20m radius circular neighborhoods. These habitat means are uncorrected for differences in quadrat density, and represent habitats where the species occurs, instead of where the species is overrepresented relative to local density. Negative convexity values indicate concave valley sites, while positive values indicate convex ridge sites. Eastness and northness values close to 1 indicate more east- and north-facing sites, respectively, while values closer to -1 have a more western and southern exposure.

Species	Elevation (m)	Convexity	Slope (°)	Northness	Eastness	TWI	Diff. Wet (W m^{-2})	Dir. Wet (W m^2)	Diff. Dry (W m^2)	Dir. Dry (W m^2)	Neigh. BA (m^2)	Scaled Neigh. BA.	Neigh. Density	Av. Neigh. Size (cm^2)
Aglaia abbreviata	744	-0.56	23.2	-0.30	-0.17	6.35	1110	3983	878	2769	6.20	41392	570	27.9
Aglaia perviridis	769	-0.73	29.1	-0.05	-0.34	6.06	1094	3811	866	2547	6.38	30821	614	28.3
Antidesma montanum	761	-0.06	27.2	-0.08	-0.32	5.25	1110	3880	878	2610	5.98	18856	648	25.3
Baccaurea ramiflora	764	0.68	25.8	-0.17	-0.33	5.10	1145	3961	906	2738	4.96	10200	641	24.4
Barringtonia pendula	766	-0.64	26.7	-0.20	-0.04	5.94	1108	3905	877	2706	5.55	13556	588	26.5
Beilschmiedia robusta	766	0.33	27.0	-0.40	-0.13	5.26	1109	3933	878	2841	6.02	27506	633	26.4
Chisocheton siamensis	759	0.54	25.8	-0.24	-0.13	5.28	1123	3947	889	2759	5.43	14696	613	25.6
Cinnamomum bejolghota	767	0.74	24.9	-0.20	-0.26	5.06	1144	3985	905	2756	5.15	18759	643	24.0
Cleidion brevipetiolatum	737	-2.02	21.5	-0.25	-0.17	7.05	1097	4008	868	2755	5.77	19333	510	28.0
Cylindrokelupha yunnanensis	775	1.47	24.8	-0.63	-0.09	4.37	1168	4085	925	3145	4.50	17544	646	24.5
Dichapetalum gelonioides	764	1.24	26.6	-0.14	-0.33	4.76	1142	3928	904	2692	5.49	19527	667	24.4
Diospyros nigrocortex	733	-1.57	19.6	-0.22	-0.28	6.68	1118	4069	885	2786	5.81	16911	553	26.1
Drypetes hoaensis	736	-0.07	21.5	-0.18	-0.43	5.55	1122	4028	888	2737	6.23	31700	611	25.0
Elaeocarpus glabripetalus alatus	731	-2.86	20.0	-0.34	-0.06	7.69	1110	4060	878	2838	5.37	18374	507	27.3
Eurya austroyunnanensis	759	1.17	26.0	-0.17	0.17	4.68	1140	3953	902	2736	4.47	7838	636	23.7
Ficus fistulosa	760	0.40	26.0	-0.20	-0.09	5.18	1134	3949	898	2755	4.61	23486	618	23.5
Ficus langkokensis	769	1.40	26.3	-0.34	0.30	4.62	1148	3983	909	2896	4.16	9038	600	24.7

Garcinia cowa	775	0.74	24.3	-0.32	-0.31	5.00	1158	4038	917	2881	4.86	13891	636	24.6
Garcinia lancilimba	771	0.27	25.7	-0.23	-0.38	5.18	1139	3967	902	2777	5.61	27535	631	25.9
Knema furfuracea	781	0.55	27.7	-0.06	-0.47	5.06	1134	3889	898	2602	5.91	22487	665	25.4
Knema globularia	746	-0.53	23.1	-0.26	-0.19	5.98	1112	3994	880	2765	6.03	21326	601	26.2
Lasianthus verticillatus	770	1.11	27.6	0.01	-0.47	4.87	1131	3870	895	2560	5.93	47712	655	25.5
Leea compactiflora	745	-1.21	21.8	-0.33	0.37	6.45	1115	4041	883	2834	4.16	24449	516	23.4
Macropanax dispermus	747	-0.75	23.4	-0.19	-0.36	5.81	1117	3991	884	2736	4.97	18565	576	24.8
Mallotus garrettii	754	-1.95	23.5	-0.12	-0.14	6.16	1081	3946	855	2634	5.61	15901	537	25.5
Mezzettiopsis creaghii	744	-1.14	23.7	-0.26	-0.21	6.20	1098	3975	869	2769	6.06	13558	544	28.1
Microcos chungii	794	0.74	29.8	0.28	-0.55	4.93	1129	3778	894	2291	6.45	28710	725	25.3
Myristica yunnanensis	756	0	28.0	-0.20	-0.24	5.48	1092	3863	865	2690	6.27	20519	612	27.6
Nephelium chryseum	777	0.30	26.5	-0.15	-0.32	5.33	1135	3930	899	2679	5.50	18163	670	24.1
Parashorea chinensis	756	0.73	25.6	-0.22	-0.34	5.06	1132	3961	896	2766	5.37	23491	696	22.9
Phoebe lanceolata	776	1.40	24.2	-0.27	-0.42	4.76	1173	4043	929	2854	4.49	9954	663	23.5
Pittosporopsis kerrii	773	1.17	26.0	-0.16	-0.4	4.78	1152	3963	912	2724	5.19	15566	678	24.1
Pometia tomentosa	751	-1.03	24.6	-0.24	-0.24	5.79	1105	3959	875	2747	5.55	15943	584	25.5
Pseuduvaria indochinensis	758	-0.56	27.9	-0.15	-0.31	5.79	1087	3859	861	2650	6.28	21283	586	28.1
Pterospermum menglunense	755	-1.46	23.8	-0.28	0.03	6.09	1096	3990	867	2785	4.73	10929	544	23.3
Saprosma ternata	756	0.33	25.9	-0.16	-0.20	5.20	1123	3935	889	2700	5.54	28037	629	24.9
Sloanea tomentosa	749	-0.61	24.0	-0.22	-0.20	6.03	1111	3966	879	2726	5.86	10701	578	26.8
Sumbaviopsis albicans	768	-1.55	26.9	-0.36	-0.09	6.00	1077	3916	853	2807	5.67	21283	512	28.3
Syzygium latilimbum	759	0.02	26.2	-0.12	-0.35	5.40	1128	3924	893	2657	5.89	15809	629	25.7
Tabernaemontana corymbosa	805	1.51	24.2	-0.42	-0.42	4.60	1186	4091	939	2998	4.86	35845	663	24.8
Trigonostemon thyrsoideum	752	-1.86	23.4	-0.24	-0.28	6.54	1097	3989	868	2767	5.60	16409	567	26.0
Urophyllum chinense	751	1.06	28.7	-0.31	0.70	4.74	1109	3881	878	2804	4.42	15521	556	24.5
Walsura robusta	766	-0.08	28.1	0.01	-0.50	5.67	1114	3843	882	2519	6.58	17601	659	25.9

Table S5.3. Species means for habitat variables corrected for local quadrat density, which represents the habitats where a species is disproportionately overrepresented in the local tree density. Symbols are the same as Table S5.2.

Species	$Elevation_{WA}$ (m)	$Convexity_{WA}$	$Slope_{WA}$ (°)	$Northness_{WA}$	$Eastness_{WA}$	TWI_{WA}	Diff. Wet_{CWA} (W m^{-2})	Dir. Wet_{WA} (W m^{-2})	Diff. Dry_{WA} (W m^{-2})	Dir. Dry_{WA} (W m^{-2})
Aglaia abbreviata	742	-1.36	21.6	-0.37	-0.12	7.19	1107	4021	876	2817
Aglaia perviridis	766	-1.16	28.1	-0.13	-0.30	6.30	1086	3847	859	2622
Antidesma montanum	758	-0.57	26.4	-0.15	-0.23	5.63	1104	3911	874	2677
Baccaurea ramiflora	763	0.40	25.3	-0.21	-0.26	5.28	1144	3978	906	2773
Barringtonia pendula	762	-1.32	25.1	-0.25	0.04	6.43	1104	3944	874	2749
Beilschmiedia robusta	764	-0.23	26.6	-0.40	-0.07	5.58	1104	3937	874	2844
Chisocheton siamensis	758	-0.07	24.7	-0.27	-0.05	5.74	1120	3971	887	2784
Cinnamomum bejolghota	764	0.37	24.4	-0.22	-0.17	5.38	1141	3997	903	2775
Cleidion brevipetiolatum	738	-3.04	20.1	-0.28	-0.14	7.92	1093	4032	865	2769
Cylindrokelupha yunnanensis	777	1.10	24.5	-0.67	-0.04	4.45	1170	4101	926	3177
Dichapetalum gelonioides	763	1.02	26.3	-0.19	-0.25	4.88	1143	3946	905	2733
Diospyros nigrocortex	732	-2.48	18.4	-0.27	-0.23	7.52	1116	4094	883	2810
Drypetes hoaensis	736	-0.85	20.8	-0.20	-0.36	6.29	1118	4043	885	2762
Elaeocarpus glabripetalus alatus	732	-3.44	18.8	-0.36	-0.06	8.42	1110	4082	878	2844
Eurya austroyunnanensis	759	0.90	25.2	-0.20	0.23	4.85	1141	3978	903	2769
Ficus fistulosa	759	0.19	25.5	-0.22	0	5.34	1134	3966	898	2775
Ficus langkokensis	769	1.27	25.9	-0.37	0.36	4.69	1151	3999	911	2918
Garcinia cowa	773	0.41	23.7	-0.35	-0.25	5.26	1157	4052	916	2906
Garcinia lancilimba	768	-0.15	25.1	-0.28	-0.32	5.54	1135	3984	899	2814
Knema furfuracea	777	0.13	26.9	-0.11	-0.41	5.37	1130	3911	895	2648

Knema globularia	744	-1.55	21.7	-0.30	-0.13	6.78	1107	4020	876	2790
Lasianthus verticillatus	769	0.90	27.5	-0.05	-0.43	4.97	1128	3883	893	2609
Leea compactiflora	746	-1.69	21.2	-0.33	0.39	6.76	1113	4050	881	2827
Macropanax dispermus	746	-1.27	22.5	-0.20	-0.33	6.27	1115	4009	882	2743
Mallotus garrettii	753	-2.74	22.2	-0.14	-0.15	6.72	1079	3980	854	2665
Mezzettiopsis creaghii	743	-1.94	22.4	-0.31	-0.16	6.87	1094	4006	865	2801
Microcos chungii	790	0.31	29.0	0.24	-0.51	5.09	1125	3802	891	2335
Myristica yunnanensis	755	-0.62	27.1	-0.26	-0.16	5.98	1089	3889	862	2738
Nephelium chryseum	774	-0.08	25.7	-0.21	-0.25	5.65	1135	3958	898	2728
Phoebe lanceolata	755	0.25	25.1	-0.27	-0.29	5.36	1128	3978	893	2802
Parashorea chinensis	754	-0.12	25.2	-0.21	-0.13	5.51	1121	3957	887	2738
Pittosporopsis kerrii	777	1.26	23.9	-0.33	-0.37	4.88	1175	4061	931	2901
Pometia tomentosa	772	0.95	25.6	-0.21	-0.35	4.93	1153	3983	912	2774
Pseuduvaria indochinensis	749	-1.77	23.2	-0.28	-0.18	6.42	1101	3989	871	2781
Pterospermum menglunense	757	-1.13	26.9	-0.22	-0.24	6.18	1082	3892	857	2717
Saprosma ternata	754	-1.89	23.1	-0.30	0.12	6.25	1093	4005	865	2798
Sloanea tomentosa	747	-1.41	22.5	-0.24	-0.16	6.69	1107	3999	876	2755
Sumbaviopsis albicans	766	-2.12	26.2	-0.38	-0.05	6.47	1064	3920	843	2811
Syzygium latilimbum	757	-0.42	25.4	-0.17	-0.28	5.69	1127	3948	892	2702
Tabernaemontana corymbosa	803	1.32	23.7	-0.46	-0.38	4.79	1187	4106	940	3029
Trigonostemon thyrsoideum	750	-2.47	22.4	-0.28	-0.24	7.09	1092	4011	864	2791
Urophyllum chinense	751	0.65	28.3	-0.33	0.72	4.96	1109	3892	878	2820
Walsura robusta	763	-0.59	27.1	-0.02	-0.47	6.14	1111	3870	879	2558

Table S5.4. Pearson correlation coefficients for univariate correlations among species means for trait and habitat variables uncorrected for differences in quadrat density, which represent the habitats species occur in rather than where they are overrepresented relative to local tree density. Light variables are abbreviated from daily averages of overall, direct, and diffuse radiation for the wet and dry seasons. Neighborhood crowding variables are abbreviated from neighborhood basal area, neighborhood basal area scaled by the area of the focal tree, density, and average neighbor basal area for 20m radius circular neighborhoods. Colored squares are significant correlations (yellow = between traits, red = between traits and habitat variables, blue = between habitat variables). Significant trait correlations follow observed trends in the literature. K_S and K_L are coordinated to optimize photosynthetic water supply, *LDMC* and leaf density both measure leaf structural investment, which is also associated with $\pi_{tlp,}$ and *LMA* and N_{mass} are inversely correlated due to the trade-off between leaf structural and nutrient investment (Brodribb and Feild 2000, Niinemets 2001, Wright et al. 2004, Bartlett et al. 2012). More drought tolerant species and species with greater leaf density, which indicates greater leaf structural investment, are associated with more crowded and more western-facing sites, although average neighborhood basal area is the neighborhood crowding variable correlated with π_{tlp} and leaf density is correlated with neighborhood density. Species with a greater *LDMC*, another measure of leaf investment, are also found in more western-facing sites. The highly significant correlations among many habitat variables make it difficult to determine the drivers of trait/habitat associations; identifying habitat associations thus requires multivariate models.

	N_{mass}	K_S	K_L	ρ	LDMC	LMA	Neig. BA	Neig. Sc BA	Neig. D	Neig. Ave	Elevation	Slope	Convexity	Eastness	Northness	TWI	O Dry	Direct Dry	Dif. Dry	Ov Wet	Direct Wet	Dif. Wet
π_{tlp}	-0.28	0.01	0.28	**-0.44**	**-0.43**	-0.04	**-0.39**	-0.26	-0.01	-0.33	0	0.06	0.16	**0.40**	-0.16	-0.20	0.20	0.20	0.12	0.09	0.07	0.12
N_{mass}		-0.03	-0.13	-0.14	-0.22	**-0.45**	0.04	0.13	-0.09	0.20	0.08	0.11	0.03	0.05	-0.16	-0.04	0.10	0.12	-0.09	-0.06	-0.05	-0.09
K_S			**0.79**	-0.11	0.10	0.02	0.15	0.23	0.21	0.11	0.06	0.17	0.26	-0.14	0.06	-0.23	0	-0.02	0.14	-0.05	-0.11	0.14
K_L				-0.20	-0.04	0.01	0	0.07	0.11	0.04	0.01	0.18	0.24	0.09	-0.05	-0.24	0.07	0.07	0.09	-0.05	-0.09	0.09
ρ					**0.62**	**0.30**	0.25	-0.01	**0.37**	-0.10	0.07	-0.01	0.07	**-0.39**	0.13	-0.01	-0.16	-0.20	0.18	0.03	-0.03	0.18
LDMC						0.31	0.22	0.10	0.22	0.02	0.06	0.04	0.07	**-0.32**	0.14	-0.08	-0.09	-0.12	0.10	-0.01	-0.04	0.10
LMA							0.15	-0.10	0.18	-0.01	0.07	0.04	0.06	-0.32	0.13	-0.04	-0.08	-0.10	0.14	0.01	-0.03	0.14
Neigh. BA								**0.40**	0.08	**0.68**	-0.11	0.20	**-0.33**	**-0.59**	**0.53**	**0.33**	**-0.67**	**-0.64**	**-0.51**	**-0.60**	**-0.53**	**-0.51**
Scaled BA									0.18	0.21	0.15	0.11	0.08	**-0.32**	0.18	-0.02	-0.19	-0.20	0	-0.14	-0.17	0
Density										**-0.46**	**0.71**	**0.56**	**0.81**	**-0.54**	**0.40**	**-0.78**	-0.17	-0.27	**0.66**	-0.06	-0.30	0.66
Av. Size											-0.28	0.01	**-0.54**	-0.13	0.03	**0.57**	-0.26	-0.19	**-0.63**	**-0.41**	-0.27	**-0.63**
Elevation												**0.62**	**0.66**	**-0.33**	0.17	**-0.71**	0	-0.09	**0.58**	-0.05	-0.26	**0.58**
Slope													**0.53**	-0.09	**0.45**	**-0.59**	**-0.46**	**-0.49**	0.02	**-0.71**	**-0.85**	0.01
Convexity														-0.09	0.04	**-0.96**	0.20	0.09	**0.78**	0.13	-0.11	**0.78**
Eastness															**-0.48**	0.08	**0.36**	**0.41**	-0.20	0.07	0.15	-0.20
Northness																-0.06	**-0.94**	**-0.97**	-0.17	**-0.67**	**-0.74**	-0.17
TWI																	-0.16	-0.07	**-0.70**	-0.06	0.17	**-0.69**
Over. Dry																		**0.99**	**0.48**	**0.84**	**0.83**	**0.49**
Direct Dry																			0.37	**0.80**	**0.82**	**0.37**
Dif. Dry																				**0.63**	**0.40**	**1.00**
Over. Wet																					**0.96**	**0.63**
Direct Wet																						**0.40**

Table S5.5. Pearson correlation coefficients values for univariate correlations among species means for traits and habitat variables, where habitat means are corrected for quadrat density and represent the habitats where species are disproportionately overrepresented. Abbreviations follow conventions for Table S5.4. Neighborhood crowding variables are excluded to avoid spurious correlations between crowding and habitat means incorporating quadrat density, which is a component of the 20m radius circular neighborhoods. Colored squares are significant correlations (yellow = between traits, red = between traits and habitat variables, blue = between habitat variables). Light blue and light red squares are correlations that are only significant for uncorrected means (see Table S5.4). Somewhat fewer correlations are significant between density-corrected habitat means, while the same correlations are observed among traits and between trait and habitat variables; i.e. an association between greater leaf density and drought tolerance and more crowded and western-facing habitats, and between greater *LDMC* and a more western aspect.

	N_{mass}	K_S	K_L	ρ	LDMC	LMA	$Elevation_{wa}$	$Slope_{wa}$	$Convexity_{wa}$	$Eastness_{wa}$	$Northness_{wa}$	TWI_{wa}	$Overall\ Dry_{wa}$	$Direct\ Dry_{wa}$	$Dif.\ Dry_{wa}$	$Overall\ Wet_{wa}$	$Direct\ Wet_{wa}$	$Dif.\ Wet_{wa}$
π_{tlp}	-0.28	0.01	0.28	**-0.44**	**-0.43**	-0.04	0.01	0.07	0.17	**0.43**	-0.14	-0.23	0.20	0.19	0.14	0.10	0.07	0.14
N_{mass}		-0.03	-0.13	-0.14	-0.22	**-0.45**	0.09	0.09	0.01	0.05	-0.17	-0.02	0.09	0.11	-0.09	-0.07	-0.05	-0.09
K_S			**0.79**	-0.11	0.10	0.02	0.06	0.15	0.23	-0.11	-0.03	-0.19	0.07	0.06	0.13	-0.01	-0.06	0.13
K_L				-0.20	-0.04	0.01	0.01	0.18	0.22	0.11	-0.12	-0.22	0.14	0.13	0.09	-0.02	-0.06	0.09
ρ					**0.62**	**0.30**	0.05	-0.02	0.05	**-0.38**	0.19	0.02	-0.13	-0.17	0.17	0.04	-0.01	0.17
LDMC						0.31	0.05	0.05	0.06	-0.32	0.11	-0.06	-0.07	-0.09	0.08	-0.01	-0.04	0.08
LMA							0.05	0.06	0.06	-0.30	0.12	-0.04	-0.07	-0.10	0.12	0	-0.04	0.12
$Elevation_{wa}$								**0.64**	**0.72**	-0.29	0.10	**-0.76**	0.10	0.01	**0.59**	-0.02	-0.25	**0.59**
$Slope_{wa}$									**0.62**	-0.05	**0.38**	**-0.70**	**-0.34**	**-0.38**	0.09	**-0.66**	**-0.83**	0.08
$Convexity_{wa}$										-0.05	0.02	**-0.96**	0.26	0.14	**0.79**	0.12	-0.16	**0.79**
$Eastness_{wa}$											**-0.43**	0.01	**0.31**	**0.36**	-0.15	0.05	0.12	-0.15
$Northness_{wa}$												-0.05	**-0.92**	**-0.96**	-0.19	**-0.64**	**-0.70**	-0.19
TWI_{wa}													-0.21	-0.11	**-0.69**	-0.02	0.24	**-0.69**
$Over.\ Dry_{wa}$														**0.99**	**0.54**	**0.82**	**0.78**	**0.58**
$Direct\ Dry_{wa}$															0.41	**0.78**	**0.78**	0.41
$Dif.\ Dry_{wa}$																**0.64**	0.38	**1.00**
$Over.\ Wet_{wa}$																	**0.96**	**0.64**
$Direct\ Wet_{wa}$																		0.39

Table S5.6. Species habitat associations were used to predict mean trait values according to these model structures, which outline possible relationships between means for light (LIGHT: daily diffuse and direct radiation averaged for six month wet and dry seasons; W m^{-2}), crowding (NEIGHBORHOOD: basal area; m^2, scaled basal area; m^2 m^{-2}, average tree size; m^2, and tree density for 20m radius circular neighborhoods), topographic variables (TOPO: slope; elevation; convexity, eastness, northness, and topographic wetness index), and their interactions. Parameter numbers include fitted coefficients, the intercept, and the error term. Model comparisons were made with AIC values corrected for small sample size (AICc; n = 43 species).

Model structures
3 parameter:
TOPO
LIGHT
NEIGHBORHOOD
4 parameter:
TOPO1 + TOPO2
TOPO + LIGHT
NEIGHBORHOOD + TOPO
NEIGHBORHOOD + LIGHT
5 parameter:
TOPO1*TOPO2 + TOPO1 + TOPO2
TOPO*LIGHT + TOPO + LIGHT
NEIGHBORHOOD*TOPO + NEIGHBORHOOD + TOPO
NEIGHBORHOOD*LIGHT + NEIGHBORHOOD + LIGHT
NEIGHBORHOOD + TOPO + LIGHT
NEIGHBORHOOD + TOPO1 + TOPO2
LIGHT + TOPO1 + TOPO2
6 parameter:
NEIGHBORHOOD*TOPO + NEIGHBORHOOD + TOPO + LIGHT
TOPO*LIGHT + TOPO + LIGHT + NEIGHBORHOOD
TOPO1*LIGHT + TOPO1 + LIGHT + TOPO2
TOPO1*TOPO2 + TOPO1 + TOPO2 + LIGHT
TOPO1*TOPO2 + TOPO1 + TOPO2 + NEIGHBORHOOD
NEIGHBORHOOD*LIGHT + NEIGHBORHOOD + LIGHT + TOPO
NEIGHBORHOOD*TOPO1 + NEIGHBORHOOD + TOPO1 + TOPO2

Table S5.7. The observed r values for the best-fit habitat models were compared to the 95% confidence interval of the r values obtained from 1000 torus translations. Models with r values greater than the 95% confidence intervals from the torus translations (indicated with an *) were significantly more strongly correlated than predicted by the null hypothesis of chance similarities between species' spatial distribution patterns and habitat variation. We conducted torus translation tests by generating 1000 x-y distances between 0 and 400m for x and 0 and 500m for y, then recalculating the mean habitat variables and best-fit trait-habitat correlations for all trees moved by these distances.

Predictors	**95% CI**	**R**	
Predicted variable: π_{tlp}			
-Average Neighbor BA, +Eastness	[0.16 - 0.40]	0.49	*
-Neighborhood Scaled BA, -Convexity, +Eastness, +Neighborhood Scaled BA*Convexity	[0.23 - 0.50]	0.57	*
$+Eastness_{WA}$	[0.01 - 0.35]	0.43	*
+Neighborhood Density, +Eastness	[0.01 - 0.35]	0.47	*
-Average Neighbor BA, -Convexity, +Eastness, +Average Neighbor BA*Convexity	[0.18 - 0.51]	0.56	*
Predicted variable: LMA			
+Convexity, +Diffuse Light Dry Season, -Eastness, -Convexity*Diffuse Light Dry Season	[0.16 - 0.47]	0.46	
+Convexity, +Diffuse Light Wet Season, -Eastness, -Convexity*Diffuse Light Wet Season	[0.16 - 0.47]	0.46	
Predicted variable: ρ			
$+NeighborhoodDensity, +TWI_{WA}$	[0.37 - 0.53]	0.60	*
+Neighborhood Density, +TWI	[0.37 - 0.52]	0.58	*
Predicted variable: N_{mass}			
+Average Neighbor BA	[0.02 - 0.04]	0.20	*
$-Northness_{WA}$	[0.01 - 0.27]	0.17	
-Northness	[0.01 - 0.32]	0.16	
+Neighborhood Scaled BA	[0.16 - 0.24]	0.13	
+Direct Light Dry Season	[0 - 0.31]	0.12	
$+DirectLightDrySeason_{WA}$	[0.01 - 0.26]	0.11	
+Slope	[0 - 0.22]	0.11	
-Neighborhood Density	[0.09 - 0.10]	0.09	
$+Slope_{WA}$	[0 - 0.29]	0.09	
$-DiffuseLightWetSeason_{WA}$	[0 - 0.26]	0.09	
$-DiffuseLightDrySeason_{WA}$	[0 - 0.26]	0.09	
$+Elevation_{WA}$	[0 - 0.27]	0.09	
-Diffuse Light Wet Season	[0 - 0.27]	0.09	
-Diffuse Light Dry Season	[0 - 0.27]	0.09	
+Elevation	[0 - 0.21]	0.08	
$-DirectLightWetSeason_{WA}$	[0 - 0.28]	0.05	
$+Eastness_{WA}$	[0 - 0.26]	0.05	
+Eastness	[0 - 0.18]	0.04	
+Neighborhood BA	[0.03 - 0.06]	0.04	
-Direct Light Wet Season	[0 - 0.25]	0.04	
-TWI	[0 - 0.27]	0.04	
+Convexity	[0 - 0.29]	0.03	

+Convexity$_{WA}$	[0 - 0.26]	0.03	
-TWI$_{WA}$	[0 - 0.27]	0.02	
Predicted variable: K_S			
+Convexity$_{WA}$, +Neighborhood BA, -Convexity$_{WA}$*Neighborhood BA	[0.15 - 0.44]	0.45	*
+Convexity, +Average Neighbor BA	[0.29 - 0.44]	0.39	
-TWI$_{WA}$, -Neighborhood BA, +TWI$_{WA}$*Neighborhood BA	[0.15 - 0.49]	0.45	
+Elevation$_{WA}$, +Neighborhood BA, -TWI$_{WA}$, -Elevation$_{WA}$*Neighborhood BA	[0.18 - 0.51]	0.50	
+Elevation$_{WA}$, +Neighborhood BA, +Slope$_{WA}$, -Elevation$_{WA}$*Neighborhood BA	[0.17 - 0.50]	0.50	
+Elevation$_{WA}$, +Neighborhood BA, +Convexity$_{WA}$, -Elevation$_{WA}$*Neighborhood BA	[0.18 - 0.50]	0.49	
+Convexity$_{WA}$, +Average Neighbor BA	[0.29 - 0.45]	0.38	
-TWI, +Average Neighbor BA	[0.29 - 0.44]	0.38	
+Convexity, +Neighborhood BA	[0.14 - 0.38]	0.36	
+Elevation, +Neighborhood BA, +Slope, -Elevation*Neighborhood BA	[0.17 - 0.49]	0.48	
-Elevation$_{WA}$, -TWI$_{WA}$, +Average Neighbor BA	[0.30 - 0.48]	0.42	
Predicted variable: K_L			
+Elevation$_{WA}$, +Neighborhood BA, +Slope$_{WA}$, -Elevation$_{WA}$*Neighborhood BA	[0.09 - 0.46]	0.52	*
+Elevation$_{WA}$, +Neighborhood BA, -Direct Light Wet Season$_{WA}$, +Elevation$_{WA}$*Neighborhood BA	[0.09 - 0.45]	0.50	*
-Elevation$_{WA}$, -TWI$_{WA}$, +Average Neighbor BA	[0.37 - 0.53]	0.44	
+Elevation, +Neighborhood BA, +Slope, -Elevation*Neighborhood BA	[0.08 - 0.45]	0.49	*
Predicted variable: LDMC			
-Eastness$_{WA}$	[0 - 0.29]	0.32	*
-Eastness	[0.01 - 0.27]	0.32	*

Table S5.8. Pagel's λ values for each trait and habitat variable estimated using maximum likelihood, and the log likelihoods (ln L) for the fitted λ value, a λ value = 0, which indicates no phylogenetic signal, and a λ value = 1, which indicates that the trait correlations between species correspond with those expected from Brownian evolution. Trait correlations are calculated from a molecular phylogeny of 42 species (Fig. S5.11), excluding *Walsura robusta* due to a lack of sequence information. The estimated λ values are not significantly different from 0 for any of the trait or habitat variables according to likelihood ratio tests, and for many traits the fitted λ value produces a significantly better model fit than λ =1 (indicated with an *). The absence of a significant signal in these variables may reflect the fairly distant relationships between most of the species sampled in this study, since long branch lengths can obscure phylogenetic signal (Townsend et al. 2010), and the 42 study species span 38 genera and 26 families.

Trait	**Fitted λ**	**ln L λ**	**ln L λ = 0**	**ln L λ = 1**
π_{tlp}	0	-4.3	-4.3	-8.3*
N_{mass}	0	-22.5	-22.5	-24.8*
K_S	0	-32.4	-32.4	-36.6*
K_L	0	339.4	339.4	332.6*
LDMC	0	49.3	49.3	39.0*
LMA	2.3	-181	-181.8	-182.2
ρ	0	47.3	47.3	40.8*
Neighborhood Basal Area	0.01	-38.4	-40.2	-38.4
Neighborhood Scaled BA	0	-439.0	-439.0	-443.9*
Neighborhood Density	0	-226.2	-226.2	-227.9
Neighborhood Average Size	0	313.1	311.2	312.7
Elevation	0	-173.7	-173.7	-180.1*
Slope	0	-94.4	-94.4	-101.7*
Convexity	0.02	-62.5	-63.9	-62.5
Eastness	0	1.1	1.1	-2.8*
Northness	0	24.5	24.5	19.4*
TWI	0.01	-44.8	-46.0	-44.8
Direct Light Dry Season	0	-263.1	-263.1	-267.2*
Diffuse Light Dry Season	3.14	-183.7	-184.3	-184.7
Direct Light Wet Season	0	-237.1	-237.1	-243.6*
Diffuse Light Wet Season	4.97	-193.3	-193.8	-194.2
$Elevation_{WA}$	0	-172.3	-172.3	-178.3*
$Slope_{WA}$	0	-97.4	-97.4	-104.9*
$Convexity_{WA}$	0.02	-68.5	-70.1	-68.7
$Eastness_{WA}$	0	1.5	1.5	-2.5*
$Northness_{WA}$	0	26.2	26.2	21.0*
TWI_{WA}	0.01	-54.9	-55.9	-55.3
Direct Light Dry $Season_{WA}$	0	-260.6	-260.6	-264.2*
Diffuse Light Dry $Season_{WA}$	3.75	-187	-187.7	-187.9
Direct Light Wet $Season_{WA}$	0	-236.0	-236.0	-243.0*
Diffuse Light Wet $Season_{WA}$	5.93	-196.6	-197.2	-197.5

Table S5.9. Pagel's λ values for each univariate correlation among the trait and habitat variables, which measures the phylogenetic signal in the phylogenetic least-squares regression. Habitat variables are uncorrected by quadrat density. Colored squares are correlations for which the estimated λ value produces a significantly better model fit than a λ value of 0, which would indicate no phylogenetic signal. The model fit for the two λ values was compared with likelihood ratio tests. Yellow boxes indicate a significant phylogenetic signal in the correlation between traits, and red boxes between traits and habitat variables. There is a significant phylogenetic signal in the correlations between leaf density (ρ) and leaf mass per unit area (*LMA*), and between habitat and leaf density and leaf dry matter content (*LDMC*), indicating co-evolution between habitat and leaf structural investment. The only trait/habitat correlation tested here that has been evaluated before at XTBG is between *LMA* and northness (Yang et al. 2014), which showed a significant relationship for a larger species set (n = 229), but not in this study, suggesting that greater sampling of species, especially within clades, may be required to detect a significant effect of phylogeny.

	N_{mass}	K_S	K_L	ρ	LDMC	LMA	Neig. BA	Neig. Sc BA	Neig. D.	Neig. Size	Elevation	Slope	Convexity	Eastness	Northness	TWI	Overall Dry	Direct Dry	Dif. Dry	Overall Wet	Direct Wet	Dif. Wet
π_{tlp}	0.22	0	0	0	0	0	0.10	0	0	0.19	0	0	0	0	0	0	0	0	0	0	0	0
N_{mass}		0	0	0	0	0	0	0	0	0	0	0	0	0	0	0	0	0	0	0	0	0
K_S			0	0	0	0	0	0	0	0	0	0	0	0	0	0	0	0	0	0	0	0
K_L				0	0	0	0	0	0	0	0	0	0	0	0	0	0	0	0	0	0	0
ρ					0	**1**	**1**	**1**	1	**1**	**1**	**1**	**1**	1	**1**	**1**	**1**	**1**	**1**	**1**	**1**	**1**
LDMC						0.92	**1**	**1**	**1**	**1**	**1**	**1**	**1**	0.94	**1**	**1**	**1**	**1**	**1**	**1**	**1**	**1**
LMA							0	0	0	0	0	0	0	0	0	0	0	0	0	0	0	0
Neigh. BA								0.22	0	0	0.17	0	0	0	0	0	0	0	0	0	0	0
Scaled BA									0	0	0	0	0	0.43	0	0	0	0	0	0	0	0
Density										0	0	0	0	0	0	0.40	0	0	0.31	0	0	0.31
Av. Size											0.36	0	0	0	0	0.05	0	0	0	0	0	0
Elevation												0	0	0	0	0	0	0	0.25	0	0	0.24
Slope													0.49	0.22	0.08	0.56	0	0	0.27	0	0	0.27
Convexity														0	0	0.33	0	0	0	0	0	0
Eastness															0	0	0	0	0	0	0	0
Northness																0	0	0.02	0	0	0	0
TWI																	0	0	0	0	0	0
Over. Dry																		0	0	0	0	0
Direct Dry																			0	0	0	0
Dif. Dry																				0	0	0.24
Over. Wet																					0	0
Direct Wet																						0

Table S5.10. Pagel's λ values for each univariate correlation among the trait and habitat variables, using habitat variables that are corrected by variation in tree density to represent the habitats where species are overrepresented relative to local tree density. Colored squares indicate correlations for which the estimated λ value produces a significantly better model fit than a model with no phylogenetic signal (λ = 0). The model fit was compared with likelihood ratio tests. As in Table S5.9, yellow indicates significant phylogenetic signal in the correlation between traits, and red between traits and habitat variables. The results are the same as for the habitat variables uncorrected by quadrat density (Table S5.9), with a significant phylogenetic signal in the correlations between leaf density (ρ) and leaf mass per unit area (*LMA*), and between habitat and leaf density and leaf dry matter content (*LDMC*). The quadrat density-corrected habitat variables also support co-evolution between leaf structural investment and habitat.

	N_{mass}	K_S	K_L	ρ	LDMC	LMA	Elevation$_{wa}$	Slope$_{wa}$	Convexity$_{wa}$	Eastness$_{wa}$	Northness$_{wa}$	TWI$_{wa}$	Overall Dry$_{wa}$	Direct Dry$_{wa}$	Dif. Dry$_{wa}$	Overall Wet$_{wa}$	Direct Wet$_{wa}$	Dif. Wet$_{wa}$
π_{tlp}	0.22	0	0	0	0	0	0	0	0	0	0	0	0	0	0	0	0	0
N_{mass}		0	0	0	0	0	0	0	0	0	0	0	0	0	0	0	0	0
K_S			0	0	0	0	0	0	0	0	0	0	0	0	0	0	0	0
K_L				0	0	0	0	0	0.70	0	0	0.65	0	0	0.45	0	0	0.46
ρ					0	**1**	**1**	**1**	**1**	1	**1**	**1**	**1**	**1**	**1**	**1**	**1**	**1**
LDMC						0.92	**1**	**1**	**1**	0.95	**1**	**1**	**1**	**1**	**1**	**1**	**1**	**1**
LMA							0	0	0	0	0	0	0	0	0	0	0	0
Elevation$_{wa}$								0	0	0	0	0	0	0	0.18	0	0	0.17
Slope$_{wa}$									0.44	0	0	0.52	0	0	0.11	0	0	0.10
Convexity$_{wa}$										0	0	0.21	0	0	0	0	0	0
Eastness$_{wa}$											0	0	0	0	0	0	0	0
Northness$_{wa}$												0	0	0	0	0	0	0
TWI$_{wa}$													0	0	0	0	0	0
Over. Dry$_{wa}$														0	0	0	0	0
Direct Dry$_{wa}$															0	0	0	0
Dif. Dry$_{wa}$																0	0	0.18
Over. Wet$_{wa}$																	0	0
Direct Wet$_{wa}$																		0

Table S5.11. Pagel's λ values estimated for the best-fit multivariate models between traits and habitat variables (Table 5.3 in the main text), and the p-values for the likelihood ratio tests comparing the models with the fitted λ values and models with λ = 0 (indicating no phylogenetic signal) and λ = 1 (indicating a phylogenetic correlation consistent with Brownian evolution). Phylogenetic information is only available for 42 of the 43 species, so these tests exclude the species *Walsura robusta*. We checked that the direction of the correlation between each habitat predictor and trait variable occurred in the same direction in the phylogenetically corrected model for 42 species as the uncorrected model for all 43 species, and that the r^2 values for the phylogenetically corrected model were comparable to the r^2 values for the full species set (the r^2 Best fit column). Significant differences in model fit between the fitted λ values and λ = 0 and λ =1 are indicated with an *. Only the best-fit models that are significantly more predictive than random spatial autocorrelation are included (Appendix section Supplemental Methods 5.2, Table S5.7). None of the estimated λ values produced a significantly better model fit than λ = 0, while λ = 1 produced a significantly worse fit than the estimated λ values for most of the models. Thus, despite the significant phylogenetic signal for univariate correlations between leaf structural investment and habitat (Tables S5.9, S5.10), phylogeny did not significantly impact the multivariate correlations between traits and habitat. There does not appear to have been significant co-evolution between traits and the habitat variables that are most strongly predictive of habitat associations.

Predictors	Fitted λ	p λ = 0	p λ = 1	r^2 Best fit	r^2 fitted λ
Predicted variable: ρ					
+Neighborhood Density, +TWI_{WA}	0.80	0.20	0.76	0.36	0.28
+Neighborhood Density, +TWI	1.0	0.13	0.99	0.34	0.22
Predicted variable: π_{tlp}					
-Average Neighbor BA, +Eastness	0.11	0.75	0.01*	0.24	0.23
-Neighborhood Scaled BA, -Convexity, +Eastness, +Neighborhood Scaled BA*Convexity	0	0.99	0.02*	0.32	0.22
+$Eastness_{WA}$	0	0.99	0.003*	0.18	0.16
+Neighborhood Density, +Eastness	0	0.99	0.003*	0.22	0.21
-Average Neighbor BA, -Convexity, +Eastness, +Average Neighbor BA*Convexity	0.27	0.43	0.02*	0.31	0.28
Predicted variable: K_L					
+$Elevation_{WA}$, +Neighborhood BA, +$Slope_{WA}$, -$Elevation_{WA}$*Neighborhood BA	0	0.99	0.03*	0.27	0.28
+$Elevation_{WA}$, +Neighborhood BA, -Direct Light Wet $Season_{WA}$, +$Elevation_{WA}$*Neighborhood BA	0	0.99	0.04*	0.25	0.26
+Elevation, +Neighborhood BA, +Slope, -Elevation*Neighborhood BA	0	0.99	0.05	0.24	0.25
Predicted variable: K_S					
+$Convexity_{WA}$, +Neighborhood BA, -$Convexity_{WA}$*Neighborhood BA	0	0.99	<0.001*	0.22	0.23
Predicted variable: LDMC					
-$Eastness_{WA}$	0.94	0.08	0.79	0.11	0.04
-Eastness	0.94	0.08	0.79	0.10	0.04
Predicted variable: N_{mass}					
+Average Neighbor BA	0	0.99	<0.001*	0.04	0.04

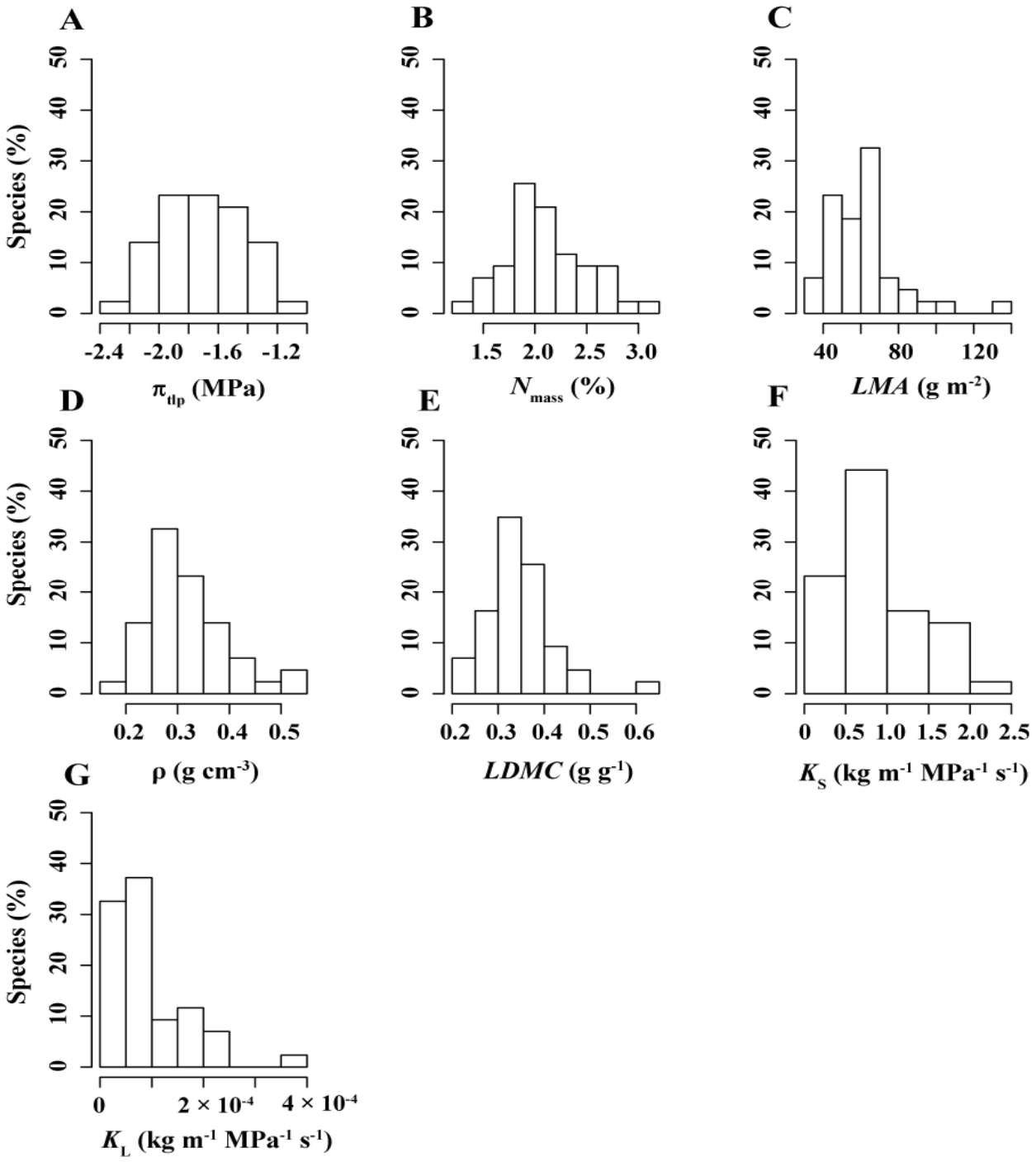
A
B
C
D
E
F
G
Species (%)
0
10
20
30
40
50
-2.4
-2.0
-1.6
-1.2
π_{tlp} (MPa)
1.5
2.0
2.5
3.0
N_{mass} (%)
40
80
120
LMA (g m^{-2})
0.2
0.3
0.4
0.5
ρ (g cm^{-3})
0.2
0.3
0.4
0.5
0.6
LDMC (g g^{-1})
0
0.5
1.0
1.5
2.0
2.5
K_S (kg m^{-1} MPa^{-1} s^{-1})
0
2×10^{-4}
4×10^{-4}
K_L (kg m^{-1} MPa^{-1} s^{-1})

Figure S5.1

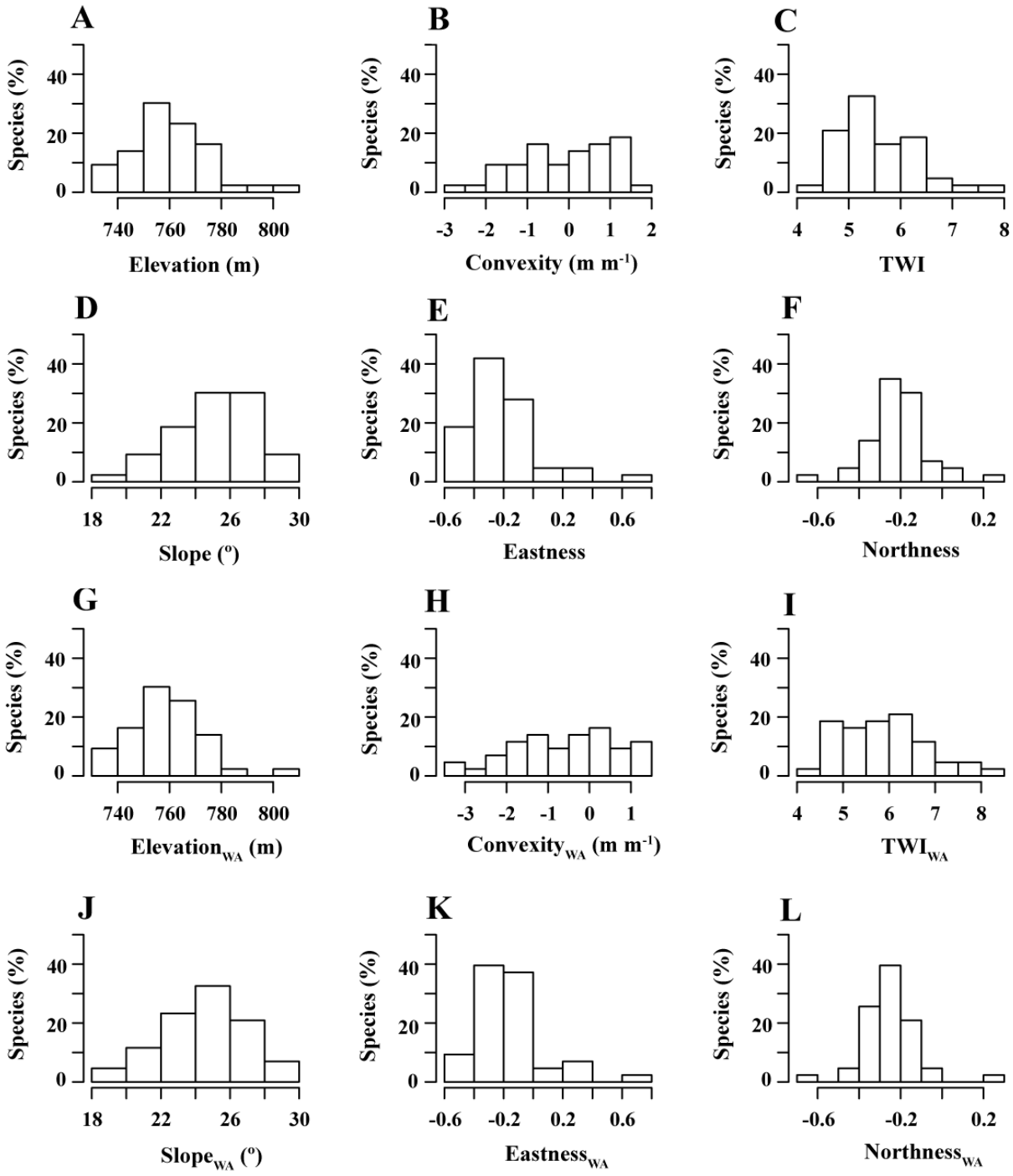
A
Species (%)
0
20
40
740
760
780
800
Elevation (m)
B
Species (%)
0
20
40
-3
-2
-1
0
1
2
Convexity (m m-1)
C
Species (%)
0
20
40
4
5
6
7
8
TWI
D
Species (%)
0
20
40
18
22
26
30
Slope (°)
E
Species (%)
0
20
40
-0.6
-0.2
0.2
0.6
Eastness
F
Species (%)
0
20
40
-0.6
-0.2
0.2
Northness
G
Species (%)
0
20
40
740
760
780
800
Elevation WA (m)
H
Species (%)
0
20
40
-3
-2
-1
0
1
Convexity WA (m m-1)
I
Species (%)
0
20
40
4
5
6
7
8
TWI WA
J
Species (%)
0
20
40
18
22
26
30
Slope WA (°)
K
Species (%)
0
20
40
-0.6
-0.2
0.2
0.6
Eastness WA
L
Species (%)
0
20
40
-0.6
-0.2
0.2
Northness WA

Figure S5.2

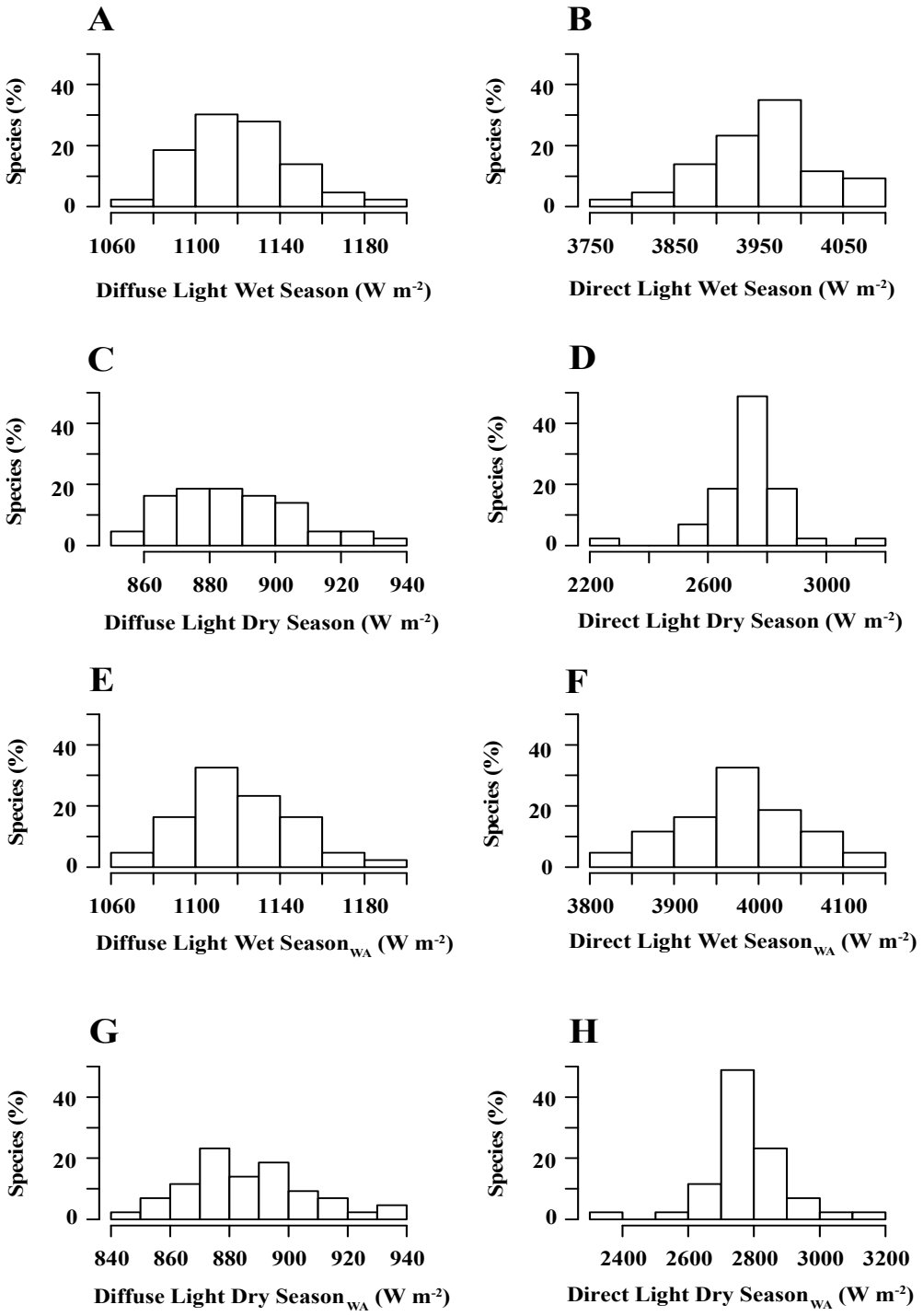
A
Species (%)
0
20
40
1060
1100
1140
1180
Diffuse Light Wet Season (W m-2)
B
Species (%)
0
20
40
3750
3850
3950
4050
Direct Light Wet Season (W m-2)
C
Species (%)
0
20
40
860
880
900
920
940
Diffuse Light Dry Season (W m-2)
D
Species (%)
0
20
40
2200
2600
3000
Direct Light Dry Season (W m-2)
E
Species (%)
0
20
40
1060
1100
1140
1180
Diffuse Light Wet SeasonWA (W m-2)
F
Species (%)
0
20
40
3800
3900
4000
4100
Direct Light Wet SeasonWA (W m-2)
G
Species (%)
0
20
40
840
860
880
900
920
940
Diffuse Light Dry SeasonWA (W m-2)
H
Species (%)
0
20
40
2400
2600
2800
3000
3200
Direct Light Dry SeasonWA (W m-2)

Figure S5.3

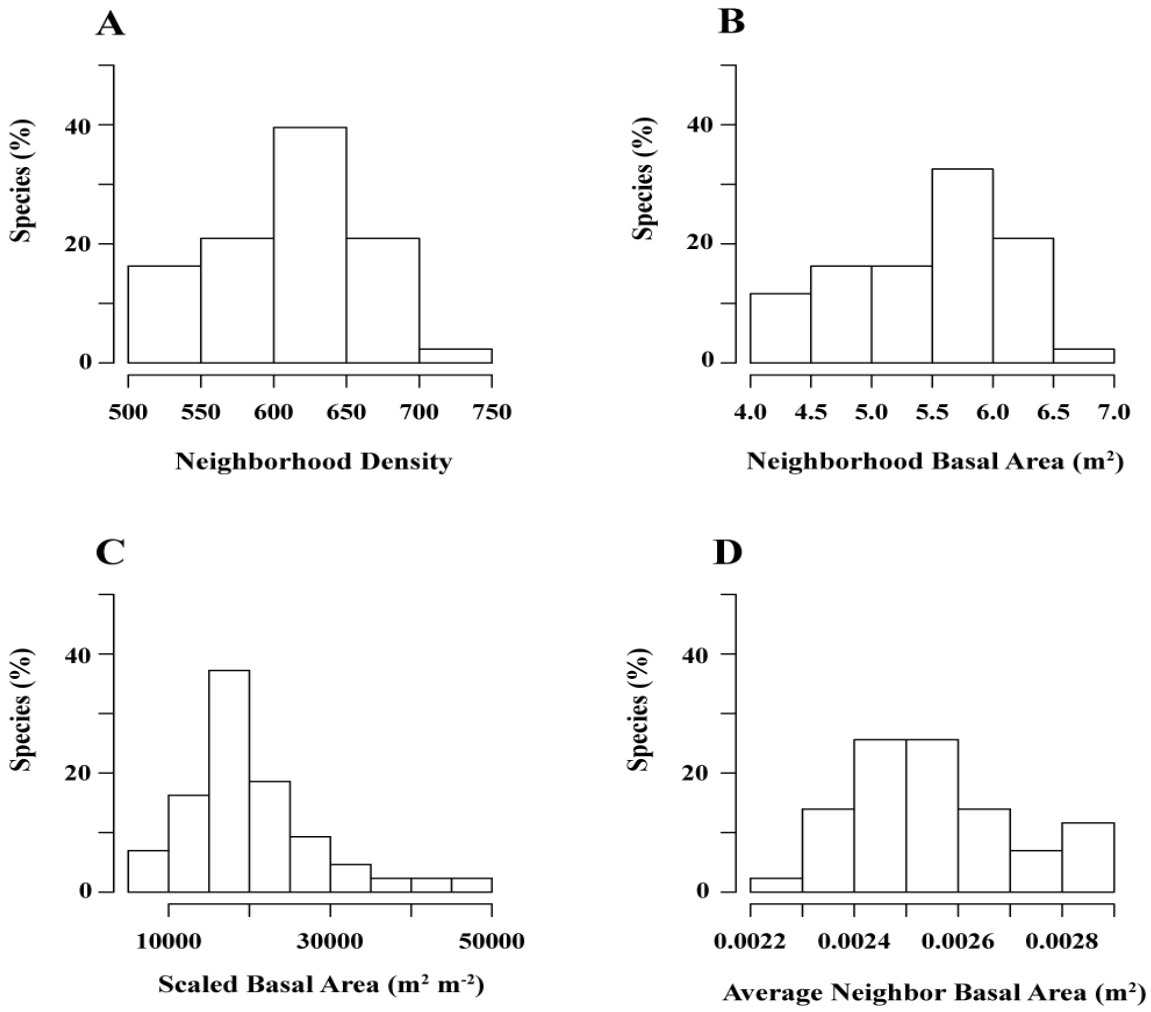
A
Species (%)
0
20
40
500
550
600
650
700
750
Neighborhood Density
B
Species (%)
0
20
40
4.0
4.5
5.0
5.5
6.0
6.5
7.0
Neighborhood Basal Area (m²)
C
Species (%)
0
20
40
10000
30000
50000
Scaled Basal Area (m² m⁻²)
D
Species (%)
0
20
40
0.0022
0.0024
0.0026
0.0028
Average Neighbor Basal Area (m²)

Figure S5.4

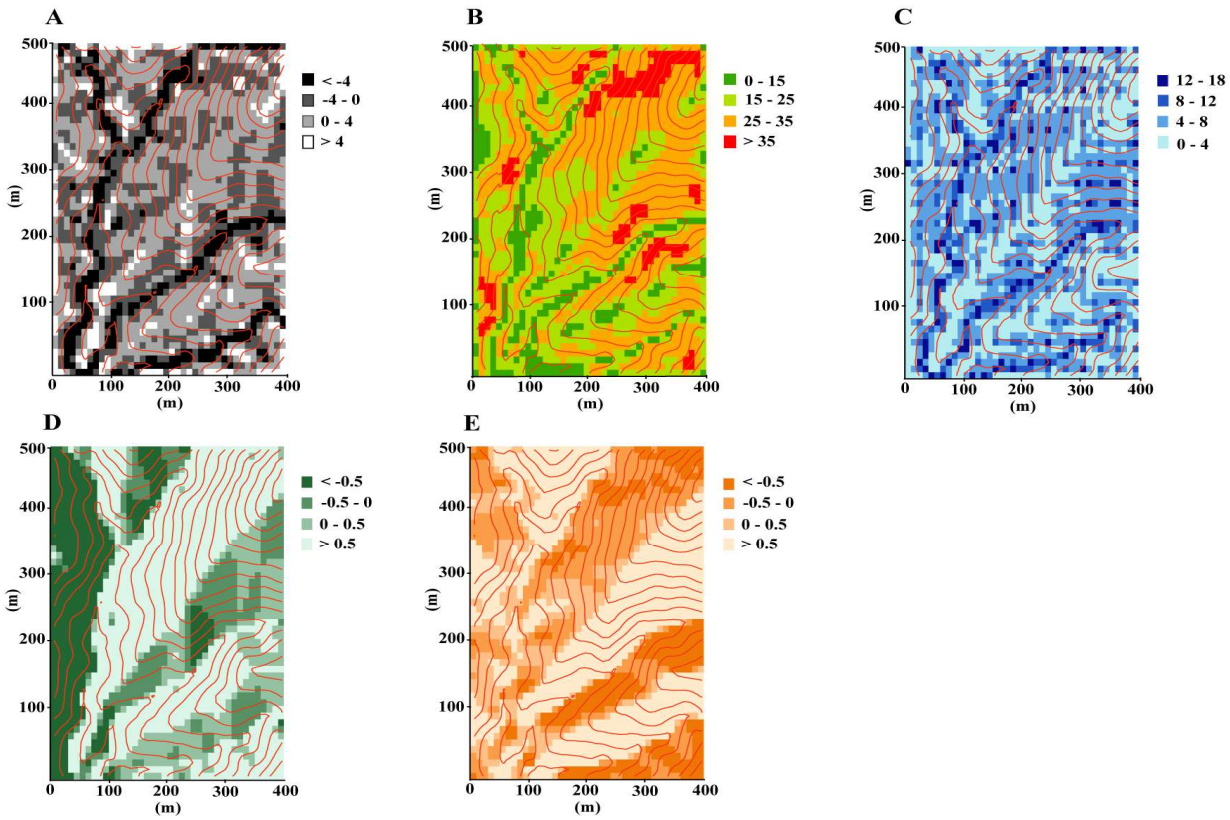
A
< -4
-4 - 0
0 - 4
> 4
B
0 - 15
15 - 25
25 - 35
> 35
C
12 - 18
8 - 12
4 - 8
0 - 4
D
< -0.5
-0.5 - 0
0 - 0.5
> 0.5
E
< -0.5
-0.5 - 0
0 - 0.5
> 0.5
(m)
0
100
200
300
400
500

Figure S5.5

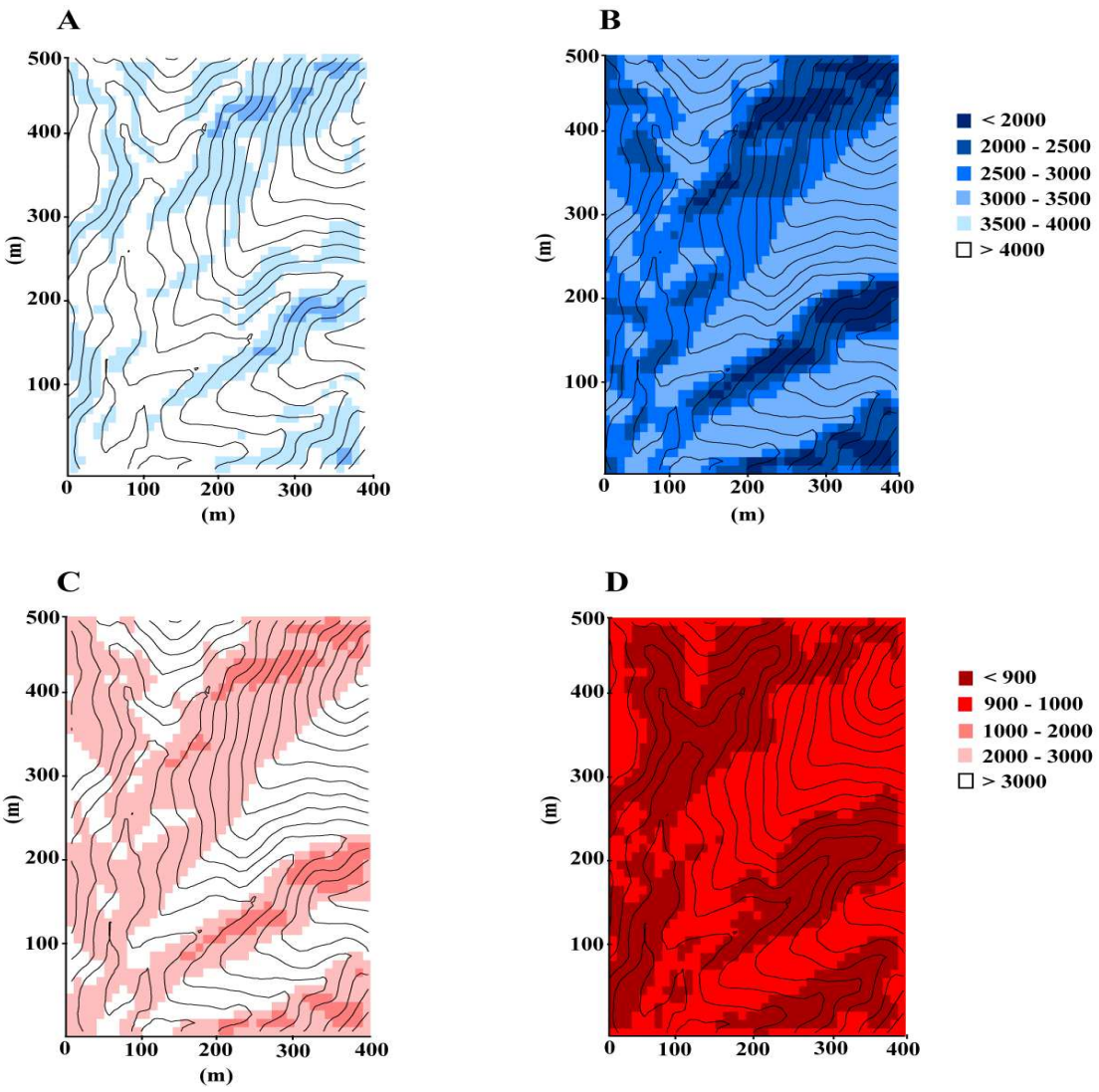
A
B
C
D
500
400
300
200
100
0
100
200
300
400
(m)
< 2000
2000 - 2500
2500 - 3000
3000 - 3500
3500 - 4000
> 4000
< 900
900 - 1000
1000 - 2000
2000 - 3000
> 3000

Figure S5.6

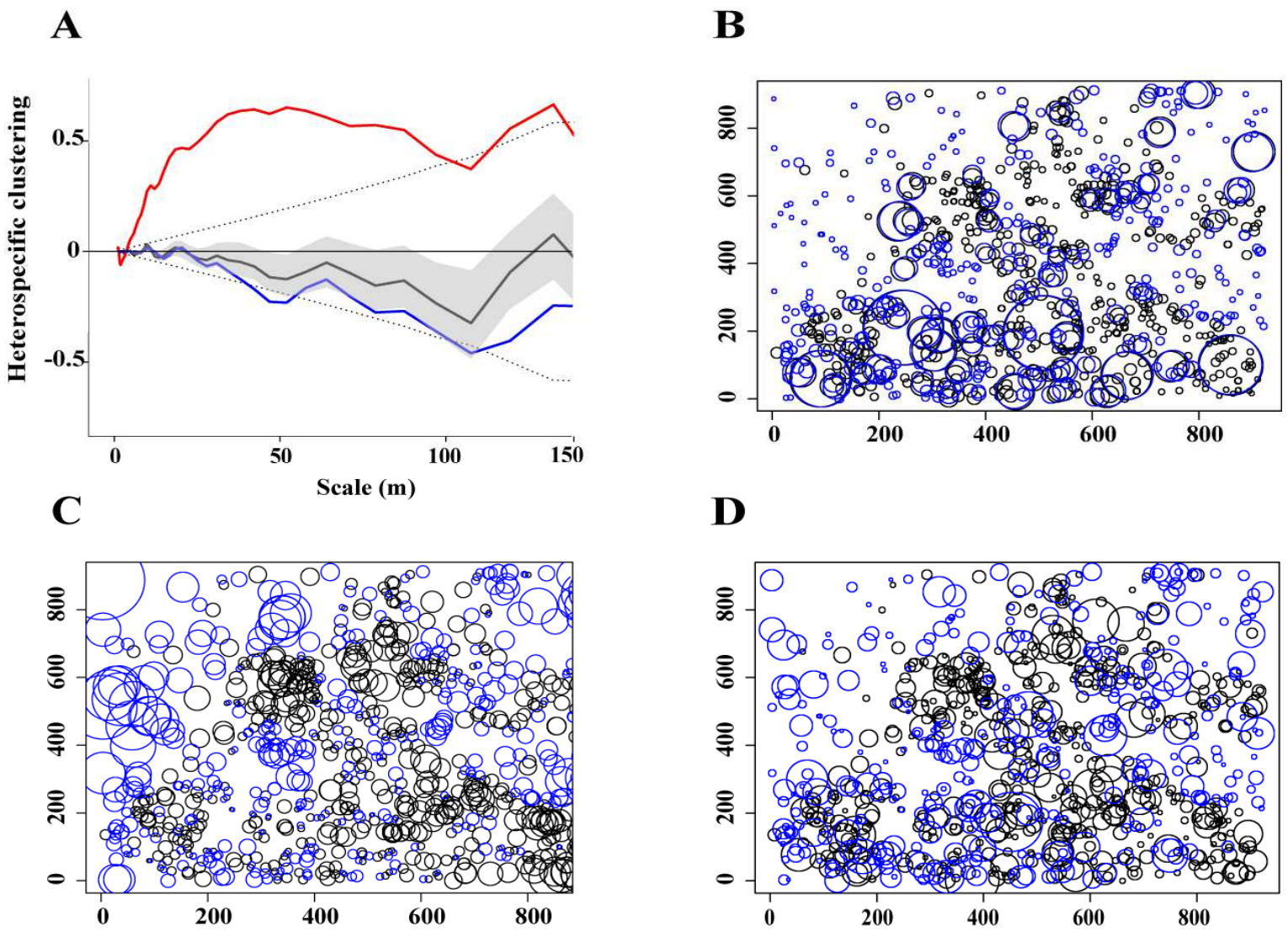
A
B
C
D
Heterospecific clustering
0.5
0
-0.5
0
50
100
150
Scale (m)
0
200
400
600
800

Figure S5.7

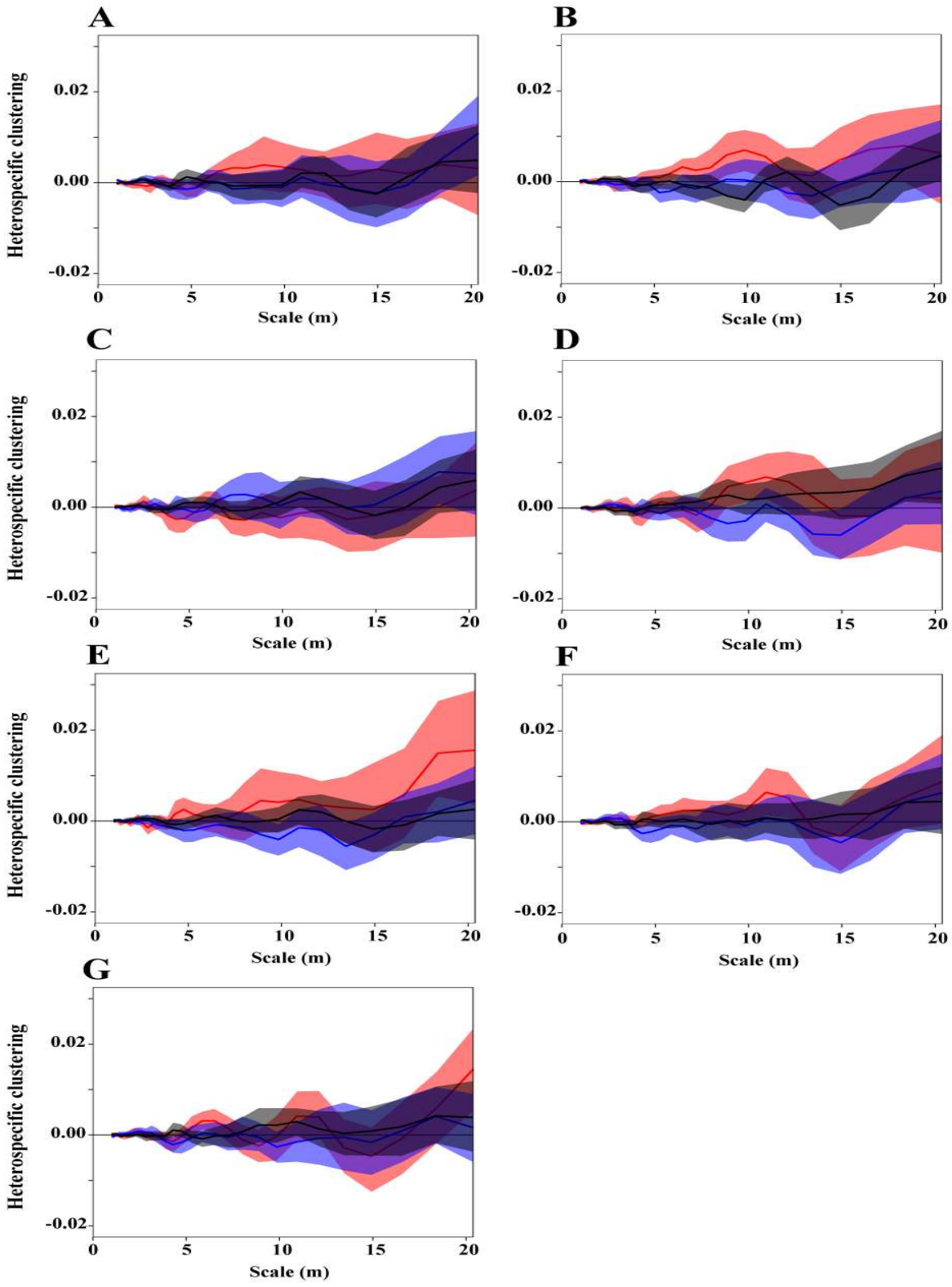
A
B
C
D
E
F
G
Heterospecific clustering
0.02
0.00
-0.02
0
5
10
15
20
Scale (m)

Figure S5.8

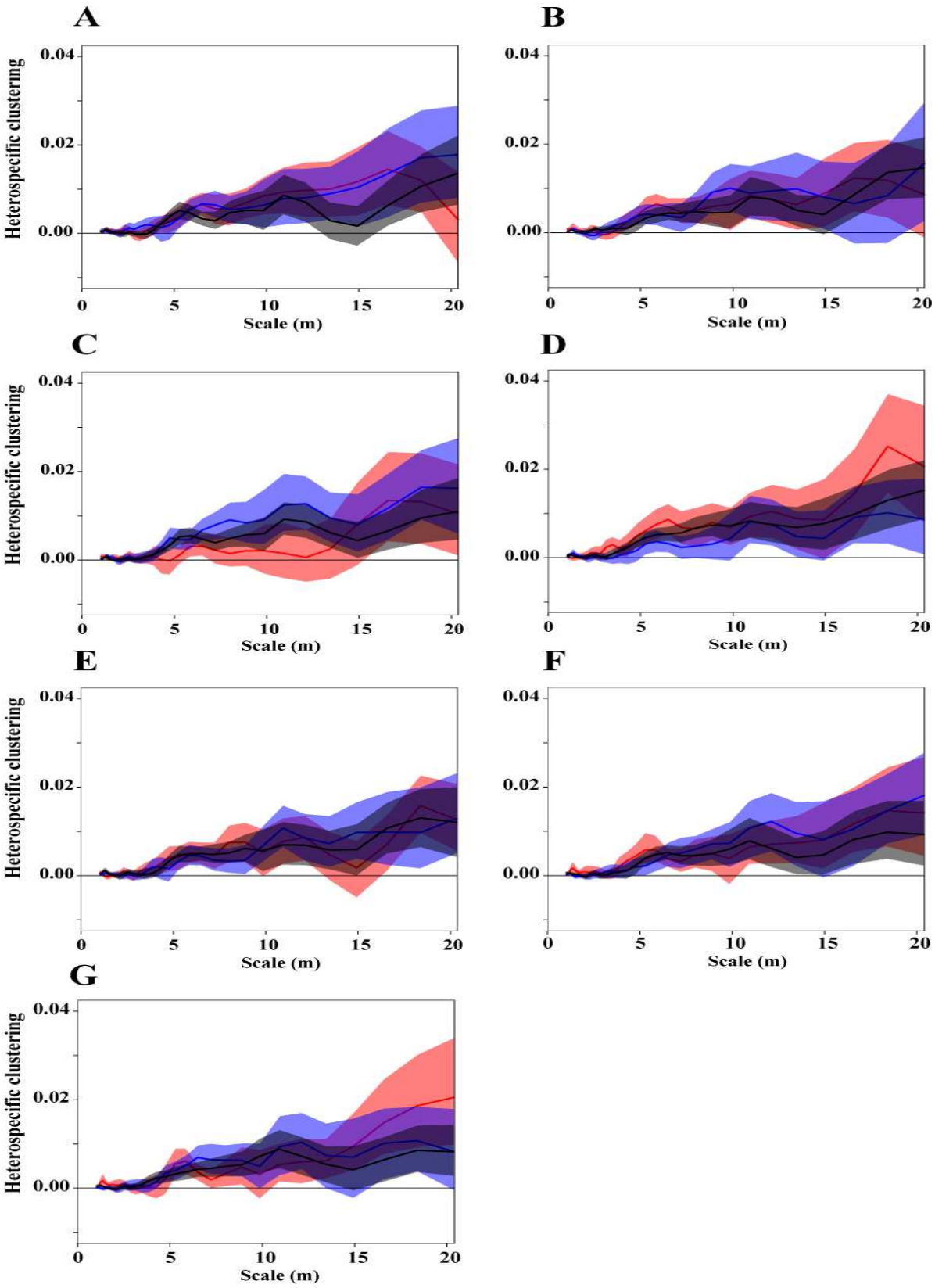
A
B
C
D
E
F
G
Heterospecific clustering
0.04
0.02
0.00
0
5
10
15
20
Scale (m)

Figure S5.9

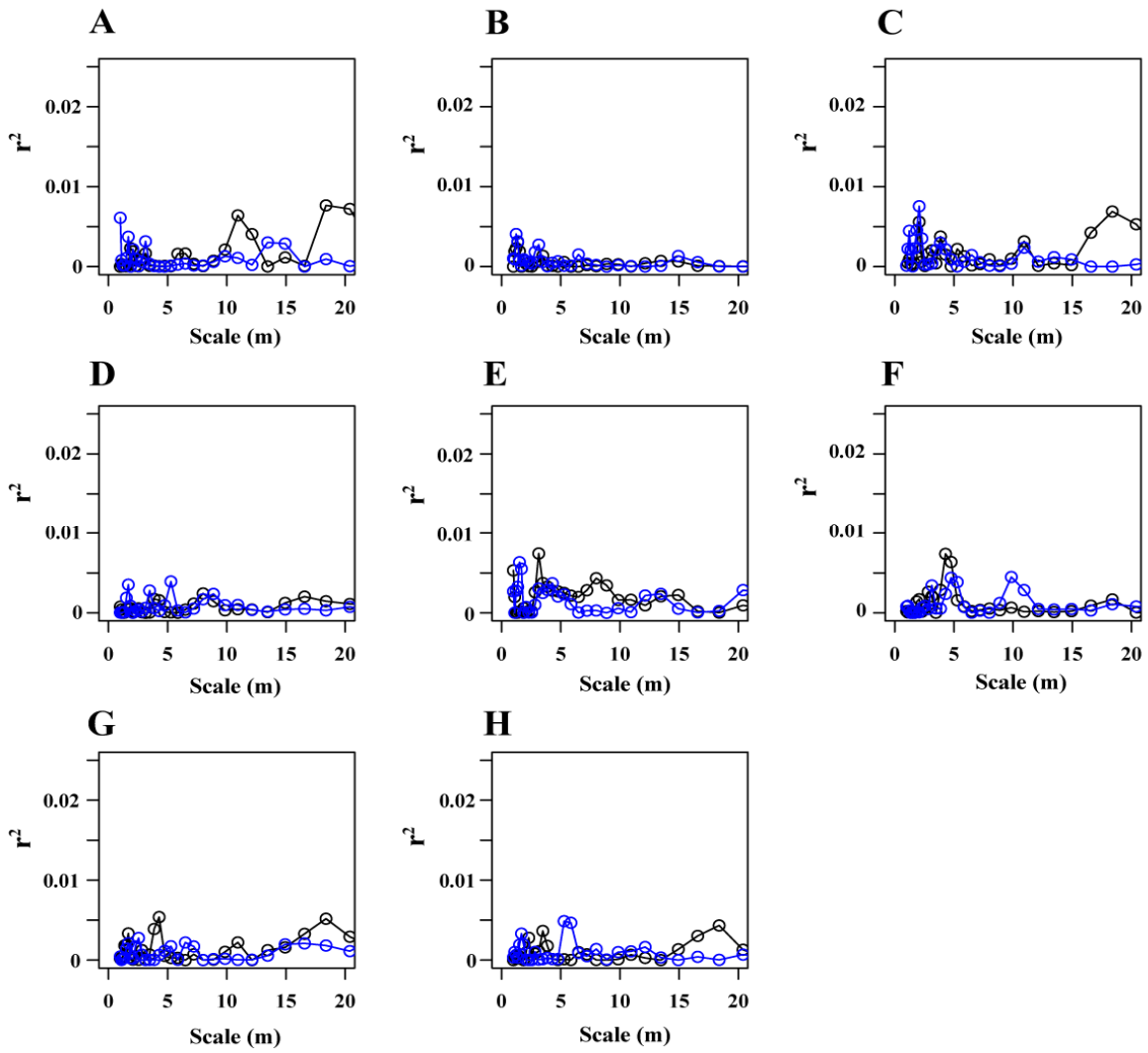

Figure S5.10


Macropanax dispermus
Pittosporopsis kerrii
Tabernaemontana corymbosa
Urophyllum chinense
Lasianthus verticillatus
Saprosma ternata
Diospyros nigrocortex
Eurya austroyunnanensis
Barringtonia pendula
Leea compactiflora
Syzygium latilimbum
Parashorea chinensis
Microcos chungii
Pterospermum menglunense
Nephelium chryseum
Pometia tomentosa
Chisocheton siamensis
Aglaia perviridis
Aglaia abbreviata
Ficus langkokensis
Ficus fistulosa
Cylindrokelupha yunnanensis
Elaeocarpus glabripetalus
Sloanea tomentosa
Dichapetalum gelonioides
Drypetes hoaensis
Baccaurea ramiflora
Antidesma montanum
Mallotus garrettii
Trigonostemon thyrsoideum
Cleidion brevipetiolatum
Sumbaviopsis albicans
Garcinia cowa
Garcinia lancilimba
Mezzettiopsis creaghii
Pseuduvaria indochinensis
Myristica yunnanensis
Knema furfuracea
Knema globularia
Beilschmiedia robusta
Phoebe lanceolata
Cinnamomum bejolghota

Figure S5.11

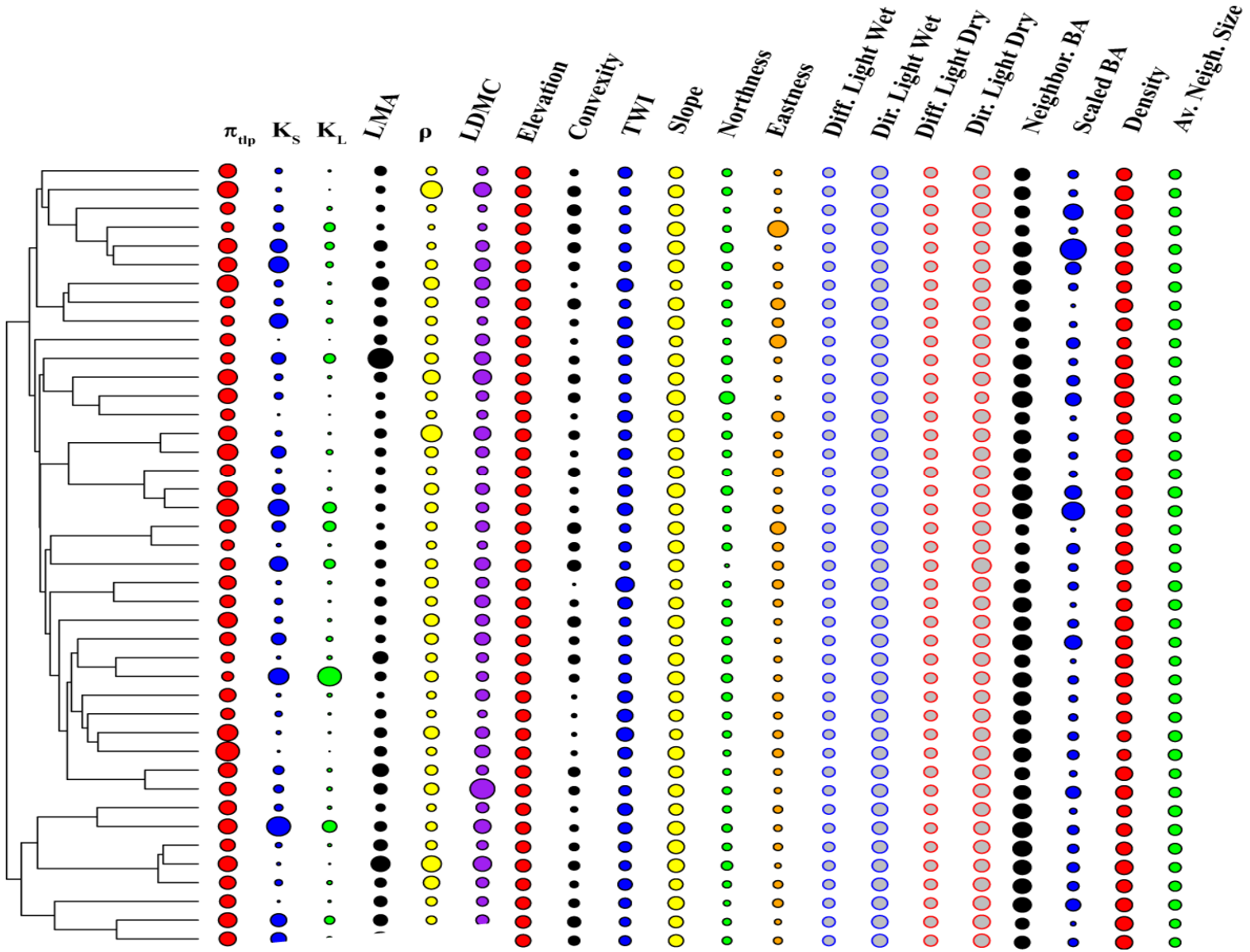
π_{tlp}
K_S
K_L
LMA
ρ
LDMC
Elevation
Convexity
TWI
Slope
Northness
Eastness
Diff. Light Wet
Dir. Light Wet
Diff. Light Dry
Dir. Light Dry
Neighbor. BA
Scaled BA
Density
Av. Neigh. Size

Figure S5.12

REFERENCES

Adler, P. B., A. Fajardo, A. R. Kleinhesselink, and N. J. B. Kraft. 2013. Trait-based tests of coexistence mechanisms. Ecology Letters **16**:1294-1306.

Baltzer, J. L., S. J. Davies, S. Bunyavejchewin, and N. S. M. Noor. 2008. The role of desiccation tolerance in determining tree species distributions along the Malay–Thai Peninsula. Functional Ecology **22**:221-231.

Bartlett, M. K., C. Scoffoni, and L. Sack. 2012. The determinants of leaf turgor loss point and prediction of drought tolerance of species and biomes: a global meta-analysis. Ecology Letters **15**:393-405.

Becker, P., P. E. Rabenold, J. R. Idol, and A. P. Smith. 1988. Water potential gradients for gaps and slopes in a Panamanian tropical moist forest's dry season. Journal of Tropical Ecology **4**:173-184.

Benjamini, Y. and D. Yekutieli. 2001. The control of the false discovery rate in multiple testing under dependency. The Annals of Statistics **29**:1165-1188.

Bennie, J., B. Huntley, A. Wiltshire, M. O. Hill, and R. Baxter. 2008. Slope, aspect and climate: Spatially explicit and implicit models of topographic microclimate in chalk grassland. Ecological Modelling **216**:47-59.

Brodribb, T., N. M. Holbrook, E. J. Edwards, and M. V. Gutierrez. 2003. Relations between stomatal closure, leaf turgor and xylem vulnerability in eight tropical dry forest trees. Plant, Cell & Environment **26**:443-450.

Burnham, K. P. and D. R. Anderson. 2010. Model selection and multi-model inference: a practical information-theoretic approach. 2nd edition. Springer.

Canham, C. D., P. T. LePage, and K. D. Coates. 2004. A neighborhood analysis of canopy tree

competition: effects of shading versus crowding. Canadian Journal of Forest Research **34**:778-787.

Chesson, P. 2000. Mechanisms of maintenance of species diversity. Annual Review of Ecology and Systematics **31**:343-358.

Choat, B., L. Sack, and N. M. Holbrook. 2007. Diversity of hydraulic traits in nine *Cordia* species growing in tropical forests with contrasting precipitation. New Phytologist **175**:686-698.

Comita, L. S. and B. M. J. Engelbrecht. 2009. Seasonal and spatial variation in water availability drive habitat associations in a tropical forest. Ecology **90**:2755-2765.

Condit, R. 1998. Tropical Forest Census Plots. Springer, Georgetown, Texas.

Coomes, D. A. and P. J. Grubb. 2000. Impacts of root competition in forests and woodlands: a theoretical framework and review of experiments. Ecological Monographs **70**:171-207.

Daws, M. I., C. E. Mullins, D. F. R. P. Burslem, S. R. Paton, and J. W. Daling. 2002. Topographic position affects the water regime in a semideciduous tropical forest in Panama. Plant and Soil **238**:79-90.

Detto, M. and H. C. Muller-Landau. 2013. Fitting ecological process models to spatial patterns using scalewise variances and moment equations. The American Naturalist **181**:E68-82.

Fan, Z.-X., S.-B. Zhang, G.-Y. Hao, J. W. Ferry Slik, and K.-F. Cao. 2012. Hydraulic conductivity traits predict growth rates and adult stature of 40 Asian tropical tree species better than wood density. Journal of Ecology **100**:732-741.

Galicia, L., J. Lopez-Blanco, A. E. Zarco-Arista, V. Filips, and F. Garcia-Oliva. 1999. The relationship between solar radiation interception and soil water content in a tropical deciduous forest in Mexico. Catena **36**:153-164.

Gibbons, J. M. and D. M. Newberry. 2002. Drought avoidance and the effect of local topography on trees in the understorey of Bornean lowland rain forest. Plant Ecology **164**:1-18.

Grayson, R. B., A. W. Western, F. H. S. Chiew, and G. Blöschl. 1997. Preferred states in spatial soil moisture patterns: Local and nonlocal controls. Water Resources Research **33**:2897-2908.

Harms, K. E., R. Condit, S. P. Hubbell, and R. B. Foster. 2001. Habitat associations of trees and shrubs in a 50-ha neotropical forest plot. Journal of Ecology **89**:947-959.

Hérault, B., et al. 2011. Functional traits shape ontogenetic growth trajectories of rain forest tree species. Journal of Ecology **99**:1431-1440.

Hu, Y.-H., et al. 2012. Dominant species and dispersal limitation regulate tree species distributions in a 20-ha plot in Xishuangbanna, southwest China. Oikos **121**:952-960.

Hubbell, S. P., J. A. Ahumada, R. Condit, and R. B. Foster. 2001. Local neighborhood effects on long-term survival of individual trees in a neotropical forest. Ecological Res **16**:859-875.

Inman-Narahari, F., R. Ostertag, G. P. Asner, S. Cordell, S. P. Hubbell, and L. Sack. 2014. Trade-offs in seedling growth and survival within and across tropical forest microhabitats. Ecology and Evolution:1-13.

Katabuchi, M., H. Kurokawa, S. J. Davies, S. Tan, and T. Nakashizuka. 2012. Soil resource availability shapes community trait structure in a species-rich dipterocarp forest. Journal of Ecology **100**:643-651.

Kraft, N. J. B., G. M. Crutsinger, E. J. Forrestel, and N. C. Emery. 2014. Functional trait differences and the outcome of community assembly: an experimental test with vernal pool annual plants. Oikos **123**:1391-1399.

Kraft, N. J. B., R. Valencia, and D. D. Ackerly. 2008. Functional traits and niche-based tree

community assembly in an Amazonian forest. Science **322**:580-582.

Kunstler, G., et al. 2012. Competitive interactions between forest trees are driven by species' trait hierarchy, not phylogenetic or functional similarity: implications for forest community assembly. Ecology Letters **15**:831-840.

Laio, F., A. Porporato, L. Ridolfi, and I. Rodriguez-Iturbe. 2001. Plants in water-controlled ecosystems: active role in hydrologic processes and response to water stress. II. Probabilistic soil moisture dynamics. Advances in Water Resources **24**:707-723.

Lan, G., et al. 2012. Spatial distribution and interspecific associations of tree species in a tropical seasonal rain forest of China. PLoS One **7**:e46074.

Lan, G., Y. Hu, M. Cao, and H. Zhu. 2011a. Topography related spatial distribution of dominant tree species in a tropical seasonal rain forest in China. Forest Ecology and Management **262**:1507-1513.

Lan, G., H. Zhu, and M. Cao. 2011b. Tree species diversity of a 20-ha plot in a tropical seasonal rainforest in Xishuangbanna, southwest China. Journal of Forest Research **17**:432-439.

Lebrija-Trejos, E., E. A. Perez-Garcia, J. A. Meave, F. Bongers, and L. Poorter. 2010. Functional traits and environmental filtering drive community assembly in a species-rich tropical system. Ecology **91**:386-398.

Leij, F. J., N. Romano, M. Palladino, M. G. Schaap, and A. Coppola. 2004. Topographical attributes to predict soil hydraulic properties along a hillslope transect. Water Resources Research **40**:1-15.

Liu, J., T. Yunhong, and J. W. F. Slik. 2014. Topography related habitat associations of tree species traits, composition and diversity in a Chinese tropical forest. Forest Ecology and Management **330**:75-81.

Lohbeck, M., et al. 2013. Successional changes in functional composition contrast for dry and wet tropical forest. Ecology **94**:1211-1216.

Markesteijn, L., L. Poorter, and F. Bongers. 2007. Light-dependent leaf trait variation in 43 tropical dry forest tree species. American Journal of Botany **94**:515-525.

Mayfield, M. M. and J. M. Levine. 2010. Opposing effects of competitive exclusion on the phylogenetic structure of communities. Ecology Letters **13**:1085-1093.

McIntire, E. J. B. and A. Fajardo. 2009. Beyond description: the active and effective way to infer processes from spatial patterns. Ecology **90**:46-56.

Mercado, L. M., et al. 2009. Impact of changes in diffuse radiation on the global land carbon sink. Nature **458**:1014-1017.

Moser, G., D. Hertel, and C. Leuschner. 2007. Altitudinal Change in LAI and Stand Leaf Biomass in Tropical Montane Forests: a Transect Study in Ecuador and a Pan-Tropical Meta-Analysis. Ecosystems **10**:924-935.

Paine, C. E., et al. 2012. Phylogenetic density dependence and environmental filtering predict seedling mortality in a tropical forest. Ecology Letters **15**:34-41.

Sorensen, R., U. Zinko, and J. Seibert. 2006. On the calculation of the topographic wetness index: evaluation of different methods based on field observations. Hydrology and Earth System Sciences **10**:101-112.

Swenson, N. G. and B. J. Enquist. 2009. Opposing assembly mechanisms in a Neotropical dry forest: implications for phylogenetic and functional community ecology. Ecology **90**:2161-2170.

Terborgh, J. 2012. Enemies maintain hyperdiverse tropical forests. The American Naturalist **179**:303-314.

Thomas, S. C. and W. E. Winner. 2002. Photosynthetic differences between saplings and adult trees: an integration of field results by meta-analysis. Tree physiology **22**:117-127.

Townsend, J. P., Z. Su, and Y. I. Tekle. 2010. Phylogenetic signal and noise: Predicting the power of a data set to resolve phylogeny. Systematic Biology **61**:835-849.

Uriarte, M., R. Condit, C. D. Canham, and S. P. Hubbell. 2004. A spatially explicit model of sapling growth in a tropical forest: does the identity of neighbours matter? Journal of Ecology **92**:348-360.

Uriarte, M., et al. 2010. Trait similarity, shared ancestry and the structure of neighbourhood interactions in a subtropical wet forest: implications for community assembly. Ecology Letters **13**:1503-1514.

Wiegand, T., I. Martinez, and A. Huth. 2009. Recruitment in tropical tree species: revealing complex spatial patterns. The American Naturalist **174**:E106-140.

Wright, I. J., et al. 2004. The worldwide leaf economics spectrum. Nature **428**:821-827.

Yang, J., et al. 2014a. Functional traits of tree species with phylogenetic signal co-vary with environmental niches in two large forest dynamics plots. Journal of Plant Ecology **7**:115-125.

Yang, J., et al. 2014b. Functional and phylogenetic assembly in a Chinese tropical community across size classes, spatial scales and habitats. Functional Ecology **28**:520-529.

CHAPTER 6

RESOLVING THE TEMPORAL SEQUENCE AND CORRELATIONS OF PLANT DROUGHT RESPONSES: COORDINATION AMONG STOMATAL, HYDRAULIC, AND WILTING TRAITS

ABSTRACT

Climate change is expected to exacerbate drought for many plants, making drought tolerance a key driver of species and ecosystem responses. Plant drought tolerance is determined by multiple traits, but the relationships among traits, either within individual plants or across species, have not been evaluated for general patterns across plant diversity. We meta-analyzed the available data for stomatal closure, wilting, declines in hydraulic conductivity in the leaves, stems, and roots, and plant mortality for 300 woody angiosperm and 49 gymnosperm species. These analyses resolved the general temporal sequence of drought responses within plants under increasing water stress, and the drivers of correlations among traits across species. The sequence addresses several key debates in the literature, showing that, for the angiosperms, 95% stomatal closure generally occurs after wilting and at similar water potentials to 50% loss of stem hydraulic conductivity. The root and stem hydraulic vulnerability traits occur at more drought tolerant positions along the gymnosperm sequence. Across species, the analyses show functional coordination among the hydraulic traits and the wilting point, or turgor loss point, beyond that expected from shared ancestry and co-selection with environmental water stress. These correlations provide a framework for hypothesizing plant responses to a wide range of water stress from one or two sampled traits, increasing the ability to rapidly characterize drought tolerance across diverse species. This resolution of the relationships among the drought tolerance

traits also provides crucial, empirically-supported insight into representing variation in multiple traits in models of plant and ecosystem responses to drought.

Keywords: Drought tolerance, stem hydraulics, leaf hydraulics, stomatal closure, turgor loss point, meta-analysis

INTRODUCTION

Plants worldwide are expected to face more frequent and severe droughts under climate change (Sheffield and Wood 2007). Characterizing drought tolerance for diverse species is key to improved predictions of ecosystem responses to global change (McDowell et al. 2013), and ecological and phylogenetic patterns have been established across many species for individual drought tolerance traits (Maherali et al. 2004, Bartlett et al. 2012b, Blackman et al. 2012, Choat et al. 2012, Klein 2014). However, plant drought tolerance is determined by multiple traits. The relationships among traits within individual plants and across species have not been evaluated for general patterns across global plant diversity. We applied meta-analyses to the available data for diverse species worldwide to comprehensively elucidate global patterns in the relationships among stomatal, hydraulic, and mesophyll drought tolerance traits. We focused on clarifying relationships among traits within plants of given species, i.e., to determine the temporal sequence in which traits become important under increasing water stress. Additionally, we evaluated whether correlations across species are driven by functional coordination, covariance with water stress, and/or phylogenetic relatedness.

Classical drought tolerance traits quantify the water potentials that induce declines in key physiological processes, such as stomatal conductance, hydraulic conductivity, and cell turgor

pressure. Thus, the order of the declines within individual plants characterizes the relative sensitivity of each trait to water stress. Previous studies have compared values for some drought tolerance traits (e.g. (Brodribb et al. 2003, Bucci et al. 2012, Guyot et al. 2012)), but have not included enough traits or species to test for a general sequence in drought tolerance traits that applies broadly across species. Applying meta-analyses to identify a general sequence can rigorously address questions in the physiology literature that previous studies have either been unable to test or to conclusively resolve, including the hypothesis that plants undergo stomatal closure at sufficiently high water potentials to prevent wilting (Klein 2014) and/or substantial declines in leaf and stem hydraulic conductivity (Johnson et al. 2009, Cochard and Delzon 2013). Further, placing the maximum water stress that a plant reaches under natural conditions, measured here as the most negative stem water potential experienced during the growing season (Ψ_{min}), along this sequence provides insight into the drought responses plants actually experience. When the stomata are closed, Ψ_{min} reflects the water potential of the soil, but this variable more broadly captures the integrated effects of both plant traits (i.e., rooting depth, leaf phenology) and the environment (i.e., soil type, climate) on plant water status (Bhaskar and Ackerly 2006). We compiled hypotheses from the literature to develop and test a framework for the overall sequence of these traits (Fig. 6.1A).

Previous studies have shown that across species, the water potential thresholds for stomatal closure, wilting, and hydraulic dysfunction in the leaves, stems, and roots are intercorrelated (Brodribb et al. 2003, Brodribb and Holbrook 2003, Maherali et al. 2006, Baltzer et al. 2008, Bucci et al. 2012). Meta-analyzing these correlations can provide additional insights into their drivers. Drought tolerance traits can be correlated across species due to (a) functional coordination, such as mechanistic and developmental linkages; (b) concerted convergence

(Patterson and Givnish 2002), i.e., co-selection by the environment, wherein traits are directionally selected by water supply to optimize overall plant function, even when the traits are not otherwise linked; and/or (c) shared ancestry. We compiled hypotheses from the literature for the drivers of each trait correlation (Fig. 6.2A), and evaluated these hypotheses by testing for greater coordination among traits than explained by water stress (measured as Ψ_{min}) and relatedness. We also synthesized these correlations into a framework for extrapolating plant responses to a wide range of water stress from one or two traits, to expedite characterizing drought tolerance across many species.

We compiled species means from the published literature for 300 woody angiosperm and 49 gymnosperm species from 174 studies for the water potential thresholds for wilting, declines in stomatal conductance (g_s) and hydraulic conductivity (K) of leaves, stems and roots, and whole-plant death to evaluate hypotheses from the literature for the temporal sequence of these traits and the drivers of their correlations across species (trait symbols and definitions in Table 6.1, references in Table S6.1, and ranges in Fig. S6.1). Several controversies have recently arisen regarding measurements of stem and root hydraulic traits (Sperry et al. 2012), in particular about whether non-sigmoidal hydraulic vulnerability relationships (i.e., of K vs. Ψ) are caused by methodological artefacts that overestimate vulnerability. Thus we included all available data in our compilation to provide a state of the art synthesis, but confirmed our conclusions for the smaller dataset derived from sigmoidal relationships (n = 283), and present these results in the main text and the results from all curve shapes in the supplement. We compiled and synthesized hypotheses for the temporal sequence in Fig. 6.1A, and for the drivers of correlations across species in Fig. 6.2A.

METHODS

To compile the drought tolerance trait dataset, we drew upon references from several recent meta-analyses of variation in individual drought tolerance traits (Bartlett et al. 2012b, Choat et al. 2012, Klein 2014, Nardini and Luglio 2014), and conducted Web of Science and Google Scholar searches using the keywords "turgor loss point", "wilting point", "stomatal closure", "stomatal conductance", "lethal leaf water potential", and "hydraulic vulnerability" or "cavitation" paired with "leaf", "stem", or "root". These studies measured traits with standard methods (detailed in Appendix section Supplemental Methods 6.1). To minimize ontogenetic and methodological variation, we included only studies that met the following criteria. For all traits, we included only studies that sampled 1) mature leaves, stems, or roots from 2) sapling or adult plants, and not seedlings, growing in 3) naturally occurring ecosystems or urban conditions for wild species, or typical agricultural conditions for crop species. For the π_{tlp} values, we selected only studies that measured 4) leaves that were rehydrated $\geq$ 6 h prior to measurement, unless the study reported no significant effect of a shorter rehydration time. We included g_S Ψ_{50} and Ψ_{95} values only from studies that 5) measured Ψ_L and g_S for leaves collected at the same time and 6) included Ψ_L values that were less negative than -1.5 MPa, to capture early declines in g_S.

We established the temporal sequence by conducting paired t-tests for all pairwise combinations of traits assessed for at least 5 species, and analyzed the angiosperms and gymnosperms separately. We evaluated the correlations among traits across all species with standard major axis regressions using the *smatr* package for R software (v. 3.2.1) (Warton et al. 2012). We identified the drivers of these correlations by fitting regression models predicting each trait as a function of 1) Ψ_{min}, to characterize water stress, and 2) Ψ_{min} and one trait variable. To account for

relatedness in these models we constructed a phylogeny with Phylocom (Webb et al. 2008), applied principal coordinates analysis to decompose the branch lengths into eigenvectors, and used the *spdep* package to identify the most parsimonious set of eigenvectors that removed phylogenetic autocorrelation in the residuals to include as predictors (Bivand and Piras 2015). We used Aikake Information Criteria corrected for small sample sizes (AICc) to evaluate support for the model including the trait predictor. For the models with a supported trait predictor (AICc of nested model – AICc of full model $\geq$ 2), we used hierarchical partitioning to calculate the independent effect of the predictors, using the *hier.part* package (Walsh and Mac Nally 2013). The independent effect measures the percent variance in the response variable explained by all predictors that is attributable to each predictor, and is analogous to a partial correlation, but robust to correlations among predictors (Murray and Conner 2009).

RESULTS AND DISCUSSION

Temporal sequence of drought response traits

The water potential thresholds for the drought responses generally followed our hypothesized sequence, with differences between angiosperms and gymnosperms (Fig. 6.1).

In the angiosperms, 50% declines in stomatal conductance (g_S Ψ_{50}) occurred at the least negative water potentials, followed sequentially by 50% declines in leaf hydraulic conductivity (K_{leaf} Ψ_{50}), wilting (π_{tlp}), and 50% and 88% declines in stem hydraulic conductivity (K_{stem} Ψ_{50} and Ψ_{88}) (Fig. 6.1A, B). The position of these traits in the sequence was clearly resolved by paired t-tests, which showed significant differences between all of these traits ($p < 0.03$; Table S6.2). Also as predicted, K_{stem} Ψ_{12}, K_{leaf} Ψ_{50}, and K_{root} Ψ_{50} occurred at similar water potentials. However, the position of these traits in the sequence could not be clearly resolved, as K_{stem} Ψ_{12}

was not significantly different from g_S Ψ_{50} or g_S Ψ_{95} ($p > 0.15$), and K_{root} Ψ_{50} was not significantly different from π_{tlp} ($p = 0.42$). Conversely, stomatal closure, the Ψ_{leaf} corresponding to 95% decline in stomatal conductance (g_S Ψ_{95}), occurred at a different point in the temporal sequence than predicted. We expected plants to close stomata to prevent leaf wilting and stem hydraulic dysfunction, but stomatal closure tended to occur significantly after wilting ($p < 0.0001$) and on average at a similar water potential as K_{stem} Ψ_{50} ($p = 0.14$) and K_{leaf} Ψ_{50} ($p = 0.07$) (Table S6.2). Placing Ψ_{min} in this sequence indicated the drought responses that plants experience under seasonal water stress in natural conditions. Ψ_{min} occurred in the later stages of water stress, at similar water potentials as K_{leaf} Ψ_{50}, wilting, and stomatal closure ($p > 0.2$), yet significantly before K_{stem} Ψ_{50} ($p < 0.0001$). The water potential at plant death was the most negative trait (plant Ψ_{lethal}). This sequence was robust to leaf phenology (Table S6.3) and to stem vulnerability curve shape, while K_{root} Ψ_{50} was significantly less negative than π_{tlp} ($p < 0.001$) when including all vulnerability curve shapes (Table S6.4; Fig. S6.2).

The gymnosperms showed the same general sequence, but with the root and stem hydraulic traits shifted towards more drought tolerant positions (Fig. 6.1C; Table S6.2). K_{leaf} Ψ_{50}, π_{tlp}, and Ψ_{min} occurred earliest in water stress, at similar water potentials ($p > 0.2$), followed sequentially by K_{stem} Ψ_{12}, K_{root} Ψ_{50}, and K_{stem} Ψ_{50} and Ψ_{88}, which were all significantly different from all other traits ($p < 0.03$). There were insufficient data to test stomatal traits.

The sequence addresses several key debates in the literature about the role of these traits in plant responses to drought. The position of Ψ_{min} shows that, on average, both angiosperm and gymnosperm species are adapted to recover from wilting and leaf hydraulic dysfunction during the most stressful conditions typical for their habitat (Johnson et al. 2009, Johnson et al. 2012), while diverging in their likelihood of experiencing substantial (i.e. 50%) stem xylem embolism

in natural conditions. The "high embolism resistance" paradigm predicts stomatal closure to occur near K_{stem} Ψ_{12}, with plants reaching stem water potentials near K_{stem} Ψ_{50} only under decennial levels of drought, while the "high embolism repair" paradigm expects plants to approach K_{stem} Ψ_{50} daily, and maintain function through frequent embolism repair (Cochard and Delzon 2013, Delzon and Cochard 2014, Klein et al. 2014). We found Ψ_{min} to occur before K_{stem} Ψ_{12} in the gymnosperms, and before and generally close to K_{stem} Ψ_{50} in the angiosperms, as also shown by a previous meta-analysis of stem hydraulic dysfunction that included the K_{stem} Ψ_{50} data in this study (Choat et al. 2012). Because the Ψ_{min} values in this study are determined from monthly measurements during a year with typical climate, our sequence suggests that angiosperms generally reach K_{stem} Ψ_{50} annually, or less frequently, while the gymnosperms reach K_{stem} Ψ_{50} considerably more rarely. Indeed, angiosperms generally exhibit greater recovery from declines in K_{stem}, through higher stem water storage and/or a capacity to refill embolisms and grow new xylem in branching patterns that circumvent embolized conduits (Johnson et al. 2012, Choat et al. 2015, Morris et al. 2016).

In the angiosperms, the sequence also contradicts long-standing hypotheses that predicted stomatal closure to occur at sufficiently high water potentials to protect plants from wilting (Cochard et al. 2002) and moderate stem hydraulic dysfunction (Salleo et al. 2000). However, it is important to note that, during transpiration, the leaf experiences more negative water potentials than the stem, given the high resistance of the leaf hydraulic pathway (Sack and Holbrook 2006). This water potential difference protects the stem and, especially, the roots from extreme tension that would drive embolism during dehydration; thus, for a plant experiencing a Ψ_{leaf} equal to g_S Ψ_{95}, the actual Ψ_{stem} should be less negative, i.e., closer to soil water potential. This point is also important for interpreting K_{root} Ψ_{50}. Under strong drought, the water potential drops across

organs are expected to be highly variable, depending on organ hydraulic conductivity, influx from water storage compartments, and, for roots, the hydraulic conductivity at the root-soil interface. Either *in situ* psychrometer measurements or a modeling approach is needed to determine the actual stem and root water potentials and conductivities a plant would experience at a given soil water potential and transpiration rate. Despite this caveat, the angiosperm sequence supports the hypotheses that belowground processes are crucial drivers of plant drought responses, and that root vulnerability limits water uptake in many ecosystems (Jackson et al. 2000).

Correlations across species in drought tolerance traits

We found significant correlations among most of the drought tolerance traits, with r values ranging from 0.38 to 0.90 (Fig. 6.3; Table S6.5; n = 9 - 151). The non-significant correlations were between K_{stem} Ψ_{12} and g_S Ψ_{50} (p = 0.4, n = 17), K_{leaf} Ψ_{50} and g_S Ψ_{95} (p = 0.1, n = 12), and K_{leaf} Ψ_{50} and K_{stem} Ψ_{88} (p = 0.2, n = 50). The stomatal and leaf hydraulic trait correlations represent particularly small species sets, indicating a need for more measurements of these traits. All traits were significantly correlated with Ψ_{min}, with r values ranging from 0.29 to 0.87 (Fig. S6.3; Table S6.5). These correlations were robust to vulnerability curve shape, except that K_{leaf} Ψ_{50} and K_{stem} Ψ_{88} were correlated when including data for all curves (p = 0.03, n = 58; Table S6.6).

Disentangling the basis for trait correlations

We found support for hypotheses from the literature (Fig. 6.2A) that attributed drought tolerance trait correlations to functional coordination, co-selection by environmental water stress, or phylogenetic relatedness. Of the 38 trait correlations with sufficient data to test ($n \geq 10$), 11 correlations were improved beyond the correlation of traits with Ψ_{min} alone by accounting for a

trait predictor (29%), 4 by accounting for phylogeny (11%), and 6 by accounting for both (16%) (Table S6.7). Thus, for 55% of trait correlations we could resolve functional or phylogenetic linkages beyond simply a correlation potentially arising from co-selection by water supply. These correlations validated one hypothesis and contradicted others (Fig. 6.2). Incorporating π_{tlp} improved prediction of K_{leaf} Ψ_{50}, as expected; indeed, π_{tlp} accounted for 76% of the variation in K_{leaf} Ψ_{50} explained by all predictors. However, contrary to prediction, accounting for K_{root} Ψ_{50} improved prediction of the stem hydraulic traits and vice versa, with the trait predictors explaining 72 – 96% of the variation in the response variables. K_{stem} Ψ_{12} and Ψ_{50} were also coordinated with K_{leaf} Ψ_{50}, with trait predictors explaining 55 – 78% of variation, and with π_{tlp}, with trait predictors accounting for 29 – 37% of variation. The drivers of the correlations between π_{tlp} and K_{root} Ψ_{50} and K_{stem} Ψ_{88} could not be resolved, since either trait or phylogenetic variables were identified as the best-fit predictors, depending on the response variable. There were insufficient data to test the hypotheses that K_{leaf} Ψ_{50} mechanistically drives the stomatal traits and threshold for leaf death (leaf Ψ_{lethal}), or that the stem and root hydraulic traits drive lethal plant water potential.

Functional coordination as a driver of trait correlations

The π_{tlp} and the hydraulic traits show strong functional coordination. The coordination between K_{leaf} Ψ_{50} and π_{tlp} supports the hypothesized mechanistic effect of turgor loss in the mesophyll on declines in K_{leaf} via the extraxylary pathway (Scoffoni et al. 2014). As a leaf dries, and the mesophyll cells lose turgor, the cells shrink and become spatially separated (Scoffoni et al. 2014), which disrupts water transport (Buckley 2015). The extraxylary pathway accounts for a significant proportion of overall leaf conductivity (~25 – 70%) (Sack and Holbrook 2006), and the vulnerability of this pathway strongly impacts K_{leaf} Ψ_{50} (Scoffoni et al. 2014). Indeed, species

with more negative π_{tlp} values undergo less cell shrinkage under dehydration and have slower declines in K_{leaf} with leaf water potential (Scoffoni et al. 2014). Conversely, the coordination between K_{stem} Ψ_{12} and Ψ_{50} and π_{tlp} appears to be driven by the linkages of these traits with K_{leaf} Ψ_{50}. Including the stem hydraulic traits did not improve prediction of π_{tlp} from K_{leaf} Ψ_{50}, or vice versa, and K_{leaf} Ψ_{50} is a stronger predictor of π_{tlp} than K_{stem} Ψ_{50}, and vice versa (Table S6.7). The basis for the linkage of K_{root} and K_{leaf} Ψ_{50} to the stem hydraulic traits might arise because hydraulic function in these organs is directly related. At a given transpiration rate, stem and root conductivity influence Ψ_{leaf}, and K_{leaf} impacts the gradient between Ψ_{leaf}, Ψ_{stem}, and Ψ_{root} (Tyree and Ewers 1991, Sack and Holbrook 2006). Thus, selection for optimal plant performance during drought would produce greater coordination among these traits than predicted from concerted convergence, wherein water stress selects for each trait independently. Further, this coordination is also expected if vulnerability depends on traits that are developmentally constrained across organs, e.g., xylem conduit pit membrane properties. Including stem and root hydraulic trait values from non-sigmoidal vulnerability curves removed the coordination between the stem hydraulic traits and π_{tlp} and K_{leaf} Ψ_{50}, and between K_{stem} Ψ_{50} and K_{root} Ψ_{50}, further justifying our consideration of methodology in resolving the coordination among these traits (Table S6.8).

Concerted convergence as a driver of trait correlations

Concerted convergence appears to contribute to the correlations of stomatal traits with other drought tolerance traits. The absence of a functional coordination between π_{tlp} and the stomatal traits is consistent with previous findings that the guard cells that control stomatal aperture (Buckley and Mott 2002), are largely hydraulically isolated from bulk leaf turgor (Buckley 2005). While the drivers of stomatal closure are not fully resolved, the hydromechanical model of stomatal regulation predicts that guard cells regulate their aperture in response to the water

status at the stomatal evaporation site; this water status, in turn, is influenced by the hydraulic conductivity of the stems, leaves, and roots (Salleo et al. 2000, Brodribb and Holbrook 2003, Buckley 2005). Thus, linkages with K_{leaf} Ψ_{50} could produce the observed correlation between π_{tlp} and the stomatal traits.

The hydromechanical model further predicts that declines in stomatal conductance, especially earlier declines under mild to moderate water stress, respond directly to K_{leaf} rather than K_{stem} (Lo Gullo et al. 2003, Brodribb and Holbrook 2004), and to earlier rather than later declines in hydraulic conductivity (Brodribb et al. 2003). Contrary to these predictions, g_S Ψ_{95} was significantly correlated with stem but not leaf vulnerability, and g_S Ψ_{50} was significantly correlated with later (Ψ_{50} and Ψ_{88}) and not earlier (Ψ_{12}) declines in K_{stem}. Instead, the statistical independence of g_S Ψ_{95} and K_{leaf} Ψ_{50} is consistent with previous studies of diverse species showing wide interspecific variation in the safety margins between stomatal closure and leaf hydraulic dysfunction (Johnson et al. 2009), wherein species vary between an "isohydric" behavior that maintains high Ψ_{leaf} and K_{leaf} values via early stomatal closure, and an "anisohydric" behavior that maintains gas exchange to low Ψ_{leaf} values at the expense of hydraulic function. The correlation between stomatal traits and K_{stem} Ψ_{50} and Ψ_{88} corroborates a previous meta-analysis of species from ecosystems worldwide (Klein 2014), but contradicts two studies within ecosystems (Brodribb et al. 2003, Skelton et al. 2015). Our findings that the stomatal traits were not functionally coordinated with the stem hydraulic traits reconciled these apparent discrepancies, showing that the correlation between these traits is secondary, being largely driven by their respective associations with water stress, and would thus be weaker for species within ecosystems.

The significant correlation of each trait with Ψ_{min} supports the selective pressure of water stress on all of the drought tolerance traits, as well as the use of any of these traits to predict species distributions relative to water supply. Notably, the strong correlation with the stomatal traits ($r = 0.87$) suggests g_S Ψ_{50} and Ψ_{95} may be especially important influences on species distributions. Testing that hypothesis requires measuring more traits for the same species, and focusing on closely related species within clades that have diversified across habitats with a wide range of water availabilities.

Application of framework for drought tolerance traits

This meta-analysis provides systematic resolution of the general sequence of drought responses within plants under increasing water stress, and further, clarifies the roles of trait coordination, concerted convergence with the environment, and shared ancestry in driving the correlations of stomatal, hydraulic, and mesophyll drought tolerance traits.

This meta-analytic perspective also points to key developments that are needed to improve the predictive capacity of trait-based approaches for plant drought tolerance. Namely, many additional physiological processes contribute to growth and survival during drought. Capacitance, or ability to use stored water to buffer water loss, embolism refilling, and metabolic synthesis of ABA, non-structural carbohydrates, and osmoprotectant compounds are all predicted to influence drought survival, but roles of these traits and their interactions with the classical hydraulic and water-relations drought tolerance traits are not well understood (Delzon and Cochard 2014, Klein et al. 2014, Skelton et al. 2015). Even the role of these classical traits in driving the threshold for plant mortality (plant Ψ_{lethal}) is not well understood. For one, measurements of plant Ψ_{lethal} are sparse in the literature, and most studies use different definitions for plant death (Baltzer et al. 2008, Li et al. 2015). Measures of plant Ψ_{lethal} correlate

with π_{tlp} (Baltzer et al. 2008), as shown here, and with leaf and stem hydraulic traits across small species sets ($n \leq 5$) (Blackman et al. 2009, Urli et al. 2013, Li et al. 2015), consistent with the prediction that irreversible stem embolism causes plant death (Urli et al. 2013). However, further studies are needed to determine whether these traits relate to plant Ψ_{lethal} independently of concerted convergence, and how multiple traits interact to drive plant mortality.

Despite these current unknowns, the strong sequence of drought responses and correlations among traits provide a framework representative of many species for extrapolating plant responses to a wide range of water stress from a small number of traits. For example, extrapolating from the correlations with the stem hydraulic traits, which have been measured for many species (Choat et al. 2012), or π_{tlp}, which can be easily assessed with a rapid method (Bartlett et al. 2012a), provides a reasonable estimate for less commonly measured traits, until such data become available in the literature for more species (see Supplementary spreadsheet tool for estimating traits from these correlations, "SupplementalSpreadsheetTool6.1.xlsx"). The functional coordination among these traits supports predicting K_{root} Ψ_{50} from K_{stem} Ψ_{50} (r^2 = 0.77) and K_{leaf} Ψ_{50} from π_{tlp} ($r^2 = 0.43$). The stomatal traits were more strongly correlated with π_{tlp} ($r^2 = 0.38 – 0.53$) than with K_{stem} Ψ_{50}, but the role of concerted convergence in these correlations supports further validating these relationships within communities. These "first pass" estimates lend expediency to characterizing drought tolerance for many species and ecosystems, and enable more detailed modeling of drought responses, since most species have currently only been assessed for a few traits.

ACKNOWLEDGEMENTS

We thank Sylvain Delzon for insightful and helpful discussion, and Sylvain Delzon, Tim Brodribb, Chris Blackman, and Hervé Cochard for contributing valuable stem hydraulic data. This work was funded by the NSF GRFP (#1108534), the UCLA EEB Department, the UCLA Dissertation Year Fellowship, and the Charles E. & Sue K. Young Graduate Fellowship.

Table 6.1. The symbol, definition, and functional significance of the drought tolerance traits and the environmental water supply and general plant water status variables. N is the number of species compiled for each trait. All units are MPa.

Symbol	Definition	N	Significance
Ψ_W	Water potential		Potential energy of water; a thermodynamically explicit and scalable index of water status
Ψ_{leaf}, Ψ_{stem},Ψ_{root}	Ψ_W of the leaf, stem, and root		Index of hydration and the demand for water of each organ
π_{tlp}	Bulk leaf turgor loss point, the Ψ_L where turgor potential = 0	285	Point at which, on average, leaf cells lose turgor and the leaf wilts (Bartlett et al. 2012b)
g_S Ψ_{50}	Ψ_L at 50% loss of stomatal conductance	49	Ψ_W at 50% loss is a standard and thus comparable measure of drought tolerance across physiological processes (Klein 2014)
g_S Ψ_{95}	Ψ_L at 95% loss of stomatal conductance	49	Approximates the maximum leaf water stress a plant can tolerate while maintaining gas exchange & C uptake
K_{leaf} Ψ_{50}	Ψ_L at 50% loss of leaf conductivity	117	Hydraulic traits measure drought impacts on the water supply for transpiration, which limits gas exchange & C uptake (Cochard et al. 2002). Leaf water supply is hypothesized to be the most direct hydraulic constraint on transpiration (Brodribb and Holbrook 2003)
K_{stem} Ψ_{12}	Ψ_{stem} at 12% loss of stem conductivity	208	Early declines in stem water supply are expected to impact gas exchange & C uptake more directly than later declines (Brodribb et al. 2003)
K_{stem} Ψ_{50}	Ψ_{stem} at 50% loss of stem conductivity	286	Hypothesized to correspond closely to the maximum water stress plants tolerate in natural conditions (Choat et al. 2012)
K_{stem} Ψ_{88}	Ψ_{stem} at 88% loss of stem conductivity	204	Hypothesized to be the point of irreversible xylem damage (Urli et al. 2013)
K_{root} Ψ_{50}	Ψ_{root} at 50% loss of root conductivity	44	Roots are hypothesized to be the 'weakest link' (least tolerant organ), limiting tolerance of the entire hydraulic system (Jackson et al. 2000)
Plant Ψ_{lethal}	Ψ_L at plant death; here, the Ψ_L at which all leaves show tissue damage	15	Integrates physiological and metabolic drought responses and recovery and directly links drought to performance (Baltzer et al. 2008)
Ψ_{min}	Seasonal minimum water potential, the most negative Ψ_{stem} at midday in the growing season	174	The strongest environmental water stress at which plants of a given species maintain their leaves in a typical year, a function of climate, habitat, topography, and plant traits such as rooting depth, leaf habitat and water storage (Bhaskar and Ackerly 2006)

FIGURE CAPTIONS

Fig 6.1. The hypothesized (**A**) and observed temporal sequence of drought tolerance traits within individual plants for the angiosperms (**B**) and gymnosperms (**C**). Panel **A** shows the relationship between organ water potential (Ψ_W) and the percent decline in several key physiological variables, including stomatal conductance (g_S, blue), hydraulic conductivity in the leaves, roots and stems (K_{leaf} and K_{root}, purple; K_{stem}, red), and turgor pressure ($\Psi_{P,}$ yellow). The circles show the order in which given declines in each function are predicted to occur. For a plant undergoing increasing drought (defined as dry soil and high evaporative demand), 50% declines in stomatal conductance (g_S Ψ_{50}) are expected to occur first, slowing transpirational water loss (Blackman et al. 2009), followed by moderate (50%) declines in leaf and root hydraulic conductivity (K_{leaf} Ψ_{50} and K_{root} Ψ_{50}) and minor (12%) declines in stem conductivity (K_{stem} Ψ_{12}), suggesting that leaf decline protects the more costly stem xylem from considerable embolism (Tyree and Ewers 1991). (These are labeled #2-4 but shown in the same position, as their order is not hypothesized). Stomatal closure, measured as a 95% decline in g_S (g_S Ψ_{95}), is hypothesized to occur after these declines (#5), so that carbon uptake can be maintained (Johnson et al. 2009), but before thresholds for potentially major damage, including loss of turgor pressure in the bulk of leaf cells, or wilting (π_{tlp}, #6), and 50% declines in stem conductivity (K_{stem} Ψ_{50}, #7) (Brodribb et al. 2003, Klein 2014). K_{stem} Ψ_{50} is hypothesized to limit the environmental water stress that plants tolerate, and thus, we expected plants to reach the most negative Ψ_{stem} values that they experience under natural growing conditions (Ψ_{min}, #8) near K_{stem} Ψ_{50} (Choat et al. 2012). 88% declines in stem conductivity (K_{stem} Ψ_{88}) have been hypothesized to induce irreversible xylem damage, and thus to occur somewhat before plant death (plant Ψ_{lethal}) (Urli et al. 2013), which we estimated as the leaf water potential at which all leaves showed tissue damage (Baltzer et al.

2008). We tested these hypotheses with paired t-tests. For clarity, panels **B** and **C** show the mean of each trait from all pairwise trait comparisons, and the tested pairwise means and statistical differences are reported in Table S6.2. The traits generally followed our hypothesized sequence, with the exception of K_{root} Ψ_{50}, K_{stem} Ψ_{12}, and g_S Ψ_{95} (indicated by arrows). In the angiosperms (**B**), g_S Ψ_{95} occurred after π_{tlp} and was not significantly different from K_{stem} Ψ_{50}. The gymnosperms generally followed this sequence (**C**), but with K_{stem} Ψ_{12} and K_{root} Ψ_{50} shifted to more drought tolerant positions. There were insufficient data to test their stomatal traits.

Fig 6.2. The hypothesized drivers of the correlations among the drought tolerance traits across species (**A**) and the observed coordination between traits for the correlations that were significant after accounting for species' water supply limit (Ψ_{min}) and phylogenetic relatedness (**B**). Most of the trait correlations are predicted to be driven by the selective pressure of Ψ_{min} acting on every trait, as the 'weakest link' hypothesis predicts overall plant function during drought is determined by the most sensitive trait (Tyree and Ewers 1991, Brodribb et al. 2003, Buckley 2005) (**A,** dashed lines). However, π_{tlp} was hypothesized to mechanistically influence K_{leaf} Ψ_{50} (Scoffoni et al. 2014) (**A**, solid lines). K_{leaf} Ψ_{50}, in turn, would drive g_S Ψ_{50} and Ψ_{95} and the threshold Ψ_{leaf} for leaf death (leaf Ψ_{lethal}) (Lo Gullo et al. 2003, Brodribb and Holbrook 2004), and the stem and root hydraulic traits would influence the Ψ_{leaf} threshold for plant death (Urli et al. 2013). As predicted, π_{tlp} was significantly more correlated with K_{leaf} Ψ_{50} than expected from concerted convergence alone (**A**, blue lines; Table S6.7), and π_{tlp} accounted for 76% of the explained variation in K_{leaf} Ψ_{50} (**B**). Contrary to prediction, the stem hydraulic traits were also more strongly correlated with K_{root} Ψ_{50}, K_{leaf} Ψ_{50}, and π_{tlp} than expected from concerted

convergence, with the trait predictor accounting for 29 – 96% of explained variation. The other hypotheses had insufficient data to test (**A**, gray lines).

Fig. 6.3. Correlations among the drought tolerance traits across species. Blue points represent angiosperms, and black points represent gymnosperms. Solid black lines are significant standard major axis (SMA) regressions. All significant correlations remained significant after correcting for multiple tests (Benjamini and Hochberg 1995). The r values are shown on each panel, and p-values and sample sizes are in Table S6.5. We did not meta-analyze variation in plant Ψ_{lethal} (**F**), since most published studies use different definitions for plant death, but instead show this correlation from the largest study of these traits (Baltzer et al. 2008) for comparison with the correlations between π_{tlp} and the other traits. All of these traits were significantly correlated, except for K_{leaf} Ψ_{50} and g_S Ψ_{95} (**I**). For graphical clarity, correlations with K_{stem} Ψ_{12} and Ψ_{88} are not shown. All of the stem hydraulic traits showed the same correlations, except that K_{stem} Ψ_{12} was not significantly correlated with g_S Ψ_{50} and K_{leaf} Ψ_{50} was not significantly correlated with K_{stem} Ψ_{88} (Table S6.5).

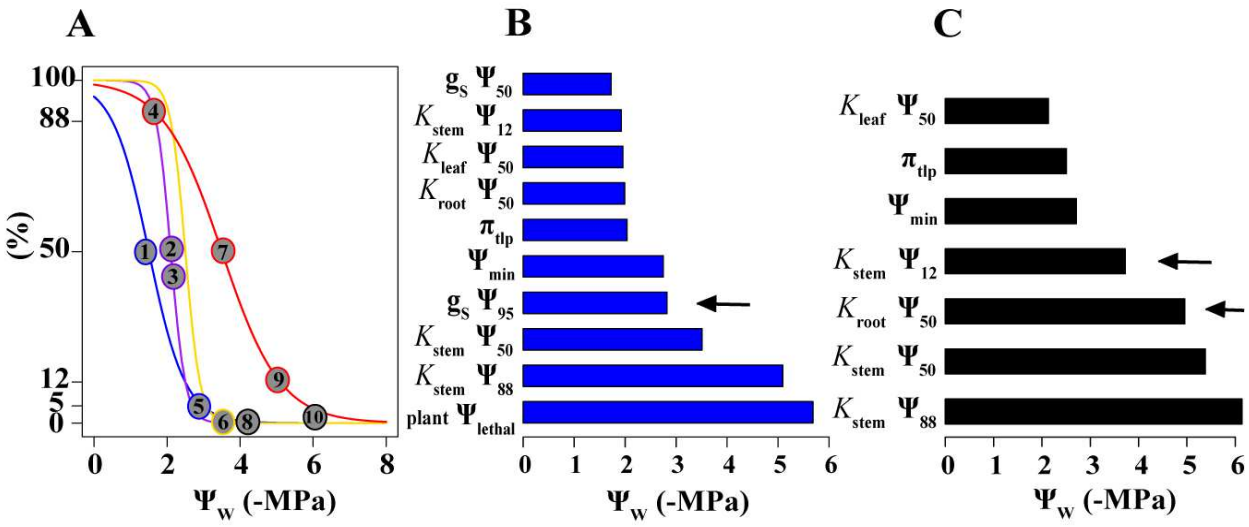
A
B
C
100
88
50
12
5
0
(%)
0
2
4
6
8
Ψw (-MPa)
gs Ψ50
Kstem Ψ12
Kleaf Ψ50
Kroot Ψ50
πtlp
Ψmin
gs Ψ95
Kstem Ψ50
Kstem Ψ88
plant Ψlethal
0
1
2
3
4
5
6
Ψw (-MPa)
Kleaf Ψ50
πtlp
Ψmin
Kstem Ψ12
Kroot Ψ50
Kstem Ψ50
Kstem Ψ88
0
1
2
3
4
5
6
Ψw (-MPa)

Figure 6.1

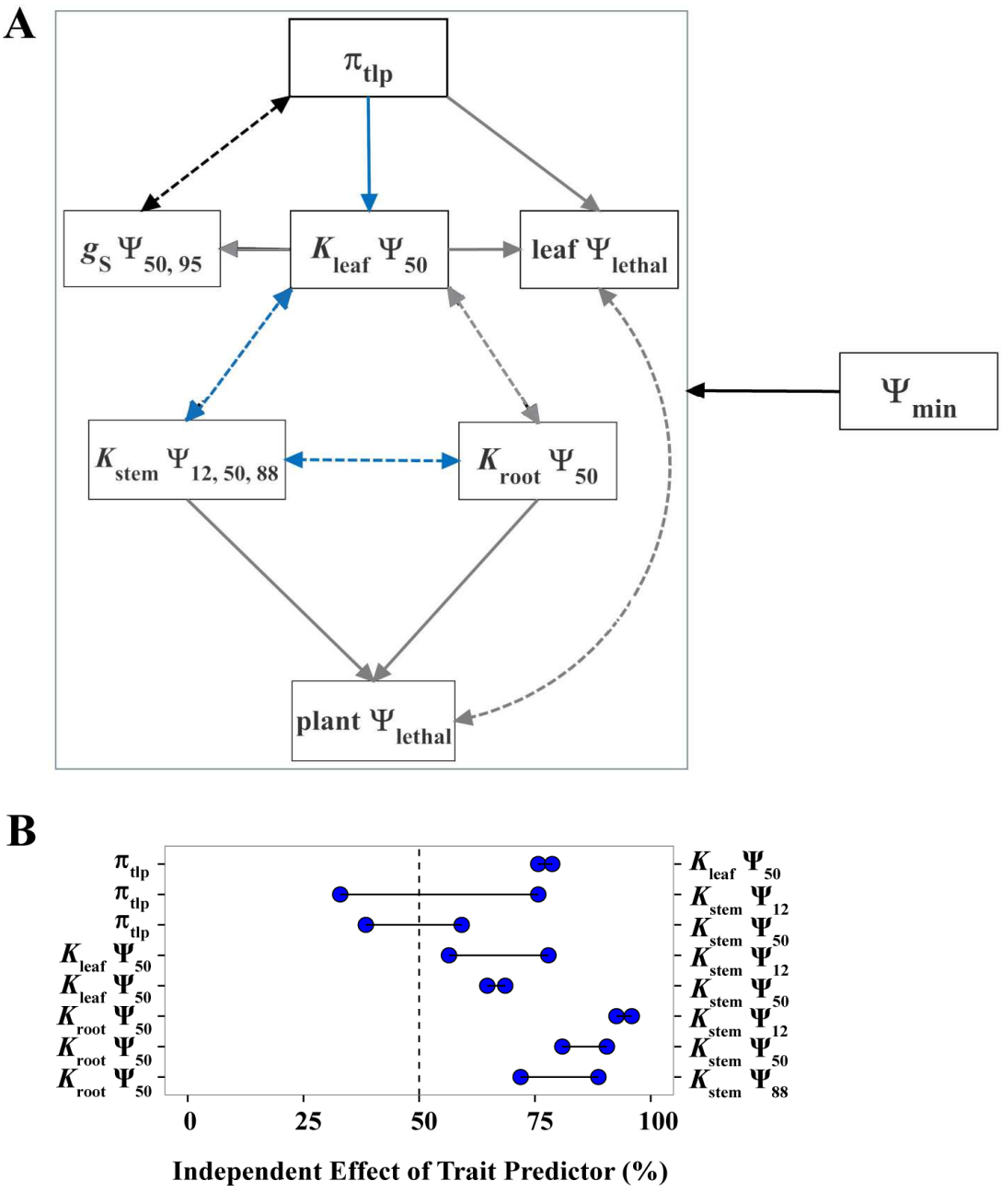
A
π_{tlp}
g_S $\Psi_{50, 95}$
K_{leaf} Ψ_{50}
leaf Ψ_{lethal}
Ψ_{min}
K_{stem} $\Psi_{12, 50, 88}$
K_{root} Ψ_{50}
plant Ψ_{lethal}
B
π_{tlp}
π_{tlp}
π_{tlp}
K_{leaf} Ψ_{50}
K_{leaf} Ψ_{50}
K_{root} Ψ_{50}
K_{root} Ψ_{50}
K_{root} Ψ_{50}
K_{leaf} Ψ_{50}
K_{stem} Ψ_{12}
K_{stem} Ψ_{50}
K_{stem} Ψ_{12}
K_{stem} Ψ_{50}
K_{stem} Ψ_{12}
K_{stem} Ψ_{50}
K_{stem} Ψ_{88}
0
25
50
75
100
Independent Effect of Trait Predictor (%)

Figure 6.2

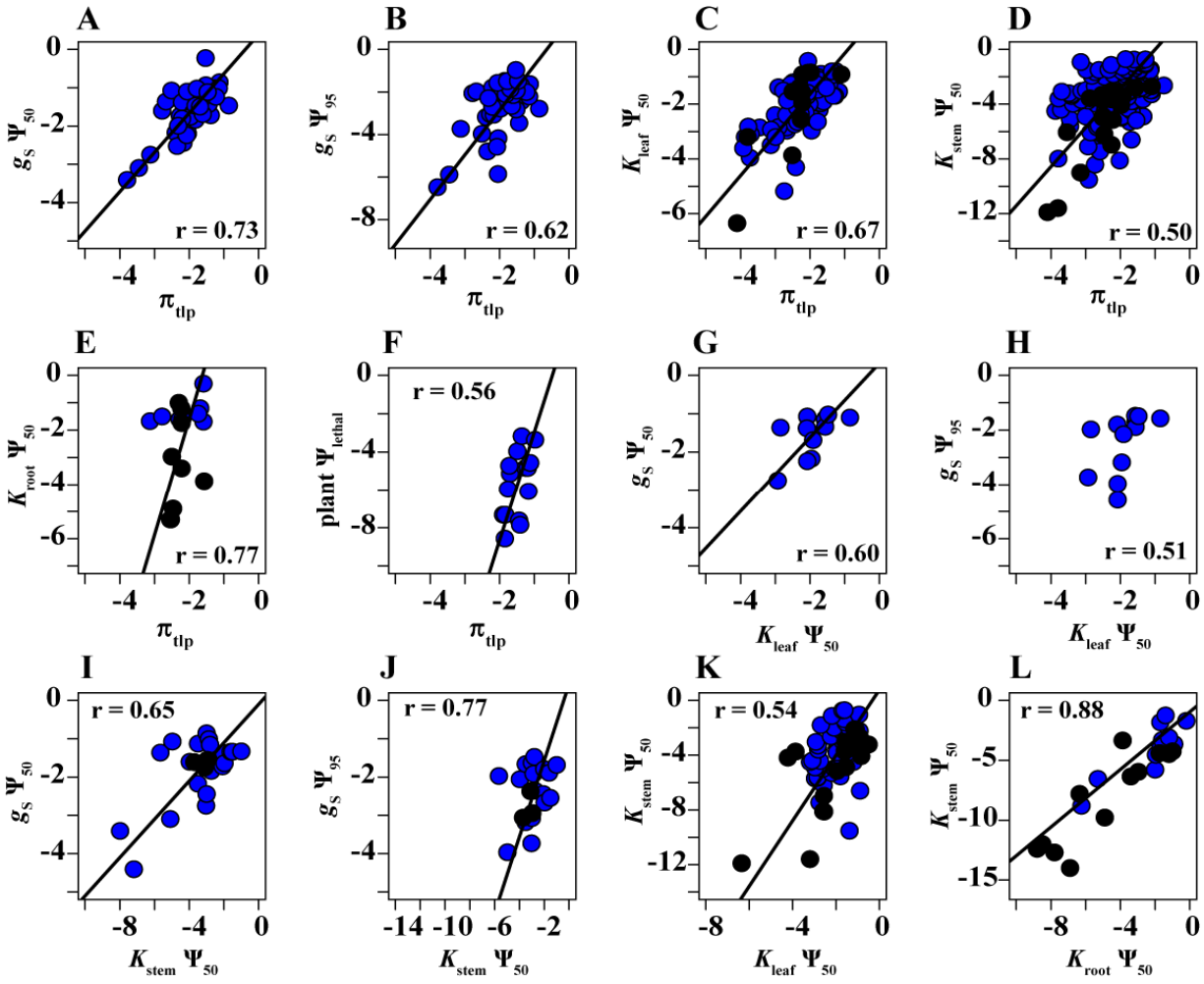
A
B
C
D
E
F
G
H
I
J
K
L
r = 0.73
r = 0.62
r = 0.67
r = 0.50
r = 0.77
r = 0.56
r = 0.60
r = 0.51
r = 0.65
r = 0.77
r = 0.54
r = 0.88
$g_S\ \Psi_{50}$
$g_S\ \Psi_{95}$
$K_{leaf}\ \Psi_{50}$
$K_{stem}\ \Psi_{50}$
$K_{root}\ \Psi_{50}$
plant Ψ_{lethal}
π_{tlp}
$K_{leaf}\ \Psi_{50}$
$K_{stem}\ \Psi_{50}$
$K_{root}\ \Psi_{50}$

Figure 6.3

SUPPLEMENTAL MATERIALS

Table S6.1. Values for the water potential at 50% and 95% stomatal closure (g_s Ψ_{50} and g_s Ψ_{95}, respectively), 50% declines in leaf, stem, and root hydraulic conductivity (K_{leaf}, K_{stem}, and K_{root} Ψ_{50}, respectively), 12% and 88% declines in K_{stem} (K_{stem} Ψ_{12} and Ψ_{88}), the turgor loss point (π_{tlp}), and plant death (plant Ψ_{lethal}) collected from the literature for 300 woody angiosperm and 49 gymnosperm species assessed for at least two traits.

Table S6.2. The paired t-tests comparing each trait combination with data for $\geq$ 5 species.

Table S6.3. The paired t-tests showing that the angiosperm temporal sequence (Fig. 6.1B) is largely robust to leaf phenology.

Table S6.4. Paired t-tests showing that the angiosperm temporal sequence (Fig. 6.1B) is robust to differences in the shape of the stem vulnerability curves, but potentially influenced by the shape of the root vulnerability curves in this compiled dataset.

Table S6.5. Univariate standardized major axis (SMA) correlations between each pair of traits measured for at least 5 species.

Table S6.6. The univariate standardized major axis (SMA) correlations between each pair of traits measured for at least 5 species, including the stem and root hydraulic trait values interpolated from non-sigmoidally shaped vulnerability curves.

Table S6.7. The r^2, Aikake Information Criterion corrected for small sample size (AICc) values, and sample size (N) for models predicting each trait as a function of 1) one other trait, Ψ_{min} (minimum seasonal water potential, a measure of maximum environmental water stress), and where relevant, phylogeny, and 2) a nested model excluding the trait predictor variable.

Table S6.8. The analyses for the drivers of the trait correlations from Table S6.7, repeated for the dataset including stem and root hydraulic trait values interpolated from non-sigmoidally shaped vulnerability curves.

Fig. S6.1. Trait distributions for the leaf water potential (Ψ_L) at 50% stomatal closure (g_s Ψ_{50}, panel **A**), 50% declines in leaf hydraulic conductivity (K_{leaf} Ψ_{50}, **B**), the turgor loss point (π_{tlp}, **C**), and 95% stomatal closure (g_s Ψ_{95}, **D**), the stem water potential at 12% declines in stem hydraulic conductivity (K_{stem} Ψ_{12}, **E**), 50% declines in stem conductivity (K_{stem} Ψ_{50}, **F**), and 88% declines in stem conductivity (K_{stem} Ψ_{88}, **G**), and root water potential at 50% declines in root hydraulic conductivity (K_{root} Ψ_{50}, **H**), the leaf water potential at plant death (plant Ψ_{lethal}, **I**), and the minimum seasonal stem water potential at midday, an index of environmental water supply (Ψ_{min}, **K**). Blue dashed lines indicate trait means. The gray bars in **E-H** show trait values calculated from sigmoidally shaped stem and root hydraulic vulnerability curves, while the white bars show trait values calculated from the other vulnerability curve shapes.

Fig. S6.2. The temporal sequence of the drought tolerance traits, tested for the larger dataset (n = 300 species) that includes stem and root hydraulic trait values interpolated from non-sigmoidally shaped vulnerability curves. The pairwise trait comparisons used to establish this sequence are in

Tables S6.2 and S6.4. Panels A and C are replotted from Fig. 6.1. The angiosperm temporal sequence is robust to differences in stem vulnerability curve shape, but K_{root} Ψ_{50} is shifted to a less drought tolerant position in the sequence for this larger dataset (indicated with an arrow), as K_{root} Ψ_{50} is now significantly less negative than π_{tlp} ($p < 0.01$, Table S6.4), consistent with a potential confounding effect of vulnerability curve shape on root hydraulic trait values.

Fig. S6.3. Standardized major axis (SMA) correlations across species between the drought tolerance traits and the minimum seasonal water potential at midday (Ψ_{min}), an index of environmental water supply. Blue points represent angiosperms, and black points are gymnosperms. The r values are shown in each panel. Lines indicate significant correlations, and all correlations remained significant after correcting for multiple comparisons. P-values and sample sizes are in Table S6.5. All of the traits were significantly correlated with Ψ_{min}, indicating that all of these traits can predict species distributions relative to water supply, and that no trait emerges as a primary driver of ecological drought tolerance.

Supplemental Methods 6.1.

Table S6.1. Values for the water potential at 50% and 95% stomatal closure (g_s Ψ_{50} and g_s Ψ_{95}, respectively), 50% declines in leaf, stem, and root hydraulic conductivity (K_{leaf}, K_{stem}, and K_{root} Ψ_{50}, respectively), 12% and 88% declines in K_{stem} (K_{stem} Ψ_{12} and Ψ_{88}), and the turgor loss point (π_{tlp}), collected from the literature for 300 woody angiosperm and 49 gymnosperm species assessed for at least two traits. 201 species (162 angiosperms and 39 gymnosperms) completely supported our hypothesized temporal sequence of 50% stomatal closure occurring at the least negative water potential, followed by K_{leaf} Ψ_{50}, 95% stomatal closure, π_{tlp}, K_{stem} Ψ_{50}, K_{stem} Ψ_{88}, and then plant Ψ_{lethal} occurring at the most negative water potential. (The justification for these hypotheses is explained in Fig. 6.1.) We also tested the hypothesis that K_{root} Ψ_{50} would be less negative than K_{stem} Ψ_{50}, but there was not sufficient information in the literature to strongly indicate the relative sequence of K_{root} $\Psi_{50,}$ K_{leaf} Ψ_{50}, and K_{stem} Ψ_{12}, so we did not evaluate the order of those traits for these species. The species that completely supported the hypothesized sequence are indicated with a Y in the "Support" column. 46 species (43 angiosperms and 3 gymnosperms) did not support any of our hypothesized sequences (indicated as N), and 102 species (95 angiosperms and 7 gymnosperms) supported some of our hypotheses but not others (P). The references for these data are shown below. Minimum seasonal water potential values (Ψ_{min}) and, for the stem and root hydraulic traits, the shape of the hydraulic vulnerability curves, are included in the supplementary data spreadsheet, "SupplementaryData6.1.csv".

Species	Biome	g_s Ψ_{50}	g_s Ψ_{95}	K_{leaf} Ψ_{50}	π_{tlp}	K_{stem} Ψ_{50}	K_{stem} Ψ_{88}	K_{root} Ψ_{50}	Supports Hypothe-ses?	g_s $\Psi_{50,95}$ Ref	K_{leaf} Ψ_{50} Ref	π_{tlp} Ref	K_{stem} $\Psi_{12,50,88}$ Ref	K_{root} Ψ_{50} Ref
Angiosperms														
Acacia greggii	Semidesert				-4.25	-0.88	-4.06		N			(8)	(9)	
Acer campestre	Temperate			-1.32	-1.9	-3.87	-4.60		Y		(10)	(10)	Cochard (unpub.), (11)	
Acer grandidentatum	Temperate				-2.45	-3.66	-7.14	-0.86	Y			(12)	(12)	
Acer monspessulanum	Med./ Dry Temperate			-1.89	-2.2	-3.31	-4.61	-1.6	Y		(10)	(10)	(13)	(13)
Acer negundo	Temperate				-1.59	-1.34	-2.74	-0.3	P			(14)	(15)	(16)
Acer pseudoplatanus	Temperate			-1.19	-1.4	-2.37	-2.71		Y		(10)	(10)	Cochard (unpub.), (11)	
Acer rubrum	Temperate				-1.59	-3.9	-6.00	-1.69	Y			(17)	(17)	(18)
Acer saccharum	Temperate	-1.6	-2.02		-2.78	-3.97	-3.97	-1.5	P	(19)		(19)	(20, 21)	(22), (23)
Acmena acuminatissima	Tropical Dry				-1.47	-1.94	-3.85		Y			(24)	(24)	
Acronychia pedunculata	Tropical Dry				-1.73	-1.86	-4.12		Y			(24)	(24)	
Adansonia rubrostipa	Tropical Dry				-1.12	-1.1	-2.82		P			(25)	(25)	
Adansonia za	Tropical Dry				-1.26	-1.7	-3.49		Y			(25)	(25)	
Adenostoma fasciculatum	Med./ Dry Temperate				-3.79	-7.98	-12.0		Y			(26)	(27)	
Adesmia boronioides	Semidesert			-2.74	-2.44	-4.42	-7.58		P		(28)	(29)	(28)	
Aegiphila lhotskiana	Tropical Dry			-0.8	-1.25				Y		(30)	(30)		
Aegiphila sellowiana	Tropical Dry			-1.7	-1.33				N		(30)	(30)		
Aidia canthioides	Tropical Dry				-1.31	-1.95	-4.55		Y			(24)	(24)	
Alberta magna	Med./ Dry Temperate	-1.76	-2.56		-1.97				Y	(31)		(31)		
Alchornea	Tropical Dry				-1.32	-0.9	-1.96		P			(24)	(24)	

trewioides														
Aleurites moluccana	Tropical Dry			-1.11	-1.97	-2.17	-3.74		Y		(32)	(33)	(32)	
Allocasuarina campestris	Med./ Dry Temperate				-2.99	-2.96	-8.50		P			(34)	(34)	
Alnus glutinosa	Temperate					-1.91	-2.77	-2.25	P				Cochard (unpub.), (35)	(35)
Alnus incana	Temperate					-1.7	-2.15	-0.2	Y				(36)	(16)
Alphonsea mollis	Tropical Dry				-2.2	-1.82	-3.31		P			(37)	(37)	
Amborella trichopoda	Tropical Moist				-1.1	-3	-4.07		Y			(38)	(39)	
Anacardium excelsum	Tropical Dry				-1.13	-1.45	-2.50	-0.76	Y			(40)	(40)	(40)
Aporosa dioica	Tropical Dry				-0.97	-1.43	-2.52		Y			(24)	(24)	
Aporosa globifera	Tropical Dry				-1.49				Y			(7)		
Aporosa microstachya	Tropical Dry				-1.7				Y			(7)		
Aporosa symplocoides	Tropical Dry				-1.25				Y			(7)		
Arbutus menziesii	Med./ Dry Temperate			-5.18	-2.74				N		(41)			
Arbutus unedo	Med./ Dry Temperate				-1.68	-3.09	-4.84	-1.2	Y			(42)	(13)	(13)
Arctostaphylos glandulosa	Med./ Dry Temperate		-3.09	-5.88	-3.45	-5.09			P	(43)		(44)	(43)	
Ardisia quinquegona	Tropical Dry				-1.93	-2.88	-6.54		Y			(24)	(24)	
Ascarina rubricaulis	Tropical Moist				-1.4	-2.8	-3.39		Y			(38)	(45)	
Ascarina solmsiana	Tropical Moist				-0.75	-2.63	-3.63		Y			(38)	(45)	
Atherosperma moschatum	Temperate	-1.01	-1.36	-1.48	-1.78				Y	(46)	(47)	(47)		
Atriplex confertifolia	Semidesert					-4.25	-7.10	-1.53	Y				(48)	(48, 49)
Austrobaileya scandens	Tropical Moist				-1.3	-0.5	-1.97		P			(38)	(45)	
Baccaurea	Tropical Dry				-1.28	-2	-4.11		Y			(50)	(50)	

ramiflora														
Balfourodendron riedelianum	Tropical Moist			-2.19	-2.27	-1.13	-2.57		P		(51)	(51, 52)	(51, 52)	
Banksia attenuata	Med./ Dry Temperate				-2.73	-2.69	-6.00		P			(53)	(54)	
Banksia sphaerocarpa	Med./ Dry Temperate				-3.12	-3.7	-5.30		Y			(34)	(34)	
Bauhinia variegata	Tropical Dry				-1.15	-1.55	-5.98		Y			(50)	(50)	
Berberis microphylla	Med./ Dry Temperate			-3.2	-3.87	-4.5	-6.91		Y		(28)	(29)	(28)	
Betula occidentalis	Temperate				-2.27	-1.6	-2.01	-0.69	P			(1)	(55)	(16, 55, 56)
Betula papyrifera	Temperate				-1.65	-2.34	-3.12		Y			(57)	(36)	
Bischofia javanica	Tropical Dry			-0.81		-1.27	-2.40		Y		(32)		(32, 58)	
Blastus cochinchinensis	Tropical Dry				-1.25	-4.26	-6.40		Y			(24)	(24)	
Blepharocalyx salicifolius	Tropical Dry				-2.52	-1.72	-4.08	-1.4	P			(59)	(59)	(60)
Bursaria spinosa	Tropical Dry			-3.2	-2.99				N		(47)	(47)		
Bursera simaruba	Tropical Dry	-1.33	-1.68		-1.39	-0.95	-1.80		P	(4)		(4)	(4)	
Calycophyllum candidissimum	Tropical Dry	-1.55	-1.96		-1.3	-2.87	-4.30		P	(4)		(4)	(4)	
Camelia sasanqua	Temperate			-1.78	-2.12				Y		(31)	(31)		
Canella winterana	Tropical Dry				-3	-0.23	-1.01		N			(61)	(45)	
Caryocar brasiliense	Tropical Dry				-1.45	-1.48	-4.02		Y			(59)	(59)	
Castanopsis chinensis	Tropical Dry				-2.33	-3.04	-9.27		Y			(24)	(24)	
Castanopsis chrysophylla	Temperate			-2.4	-2.68				Y		(41)	(41)		
Castanopsis fissa	Tropical Dry				-2.35	-1.37	-3.14		P			(24)	(24)	
Casuarina obesa	Wetland/Mangrove				-4.59	-1.39			N			(53)	(62)	
Ceanothus crassifolius	Med./ Dry Temperate					-8.8	-11.8	-6.24	Y				(63, 64) (65)	(64, 66, 67)
Ceanothus cuneatus	Med./ Dry Temperate	-4.41	-8.37			-7.19			P	(43)			(43)	

Ceanothus leucodermis	Med./ Dry Temperate			-3.56	-7.86	-2.79	Y			(64, 65)	(64, 66)
Cedrela fissilis	Tropical Moist	-1.7	-1.28	-0.73			N	(51)	(51, 52)	(51, 52)	
Celtis philippensis	Tropical Dry		-2.98	-1.5	-2.90		N		(37)	(37)	
Ceratonia siliqua	Med./ Dry Temperate	-2.55	-2.02	-8.12	-9.05		P	(68)	(68)	(69)	
Cercis canadensis	Temperate			-2.52	-6.50	-0.9	Y			(18)	(18)
Cercis siliquastrum	Temperate	-2.7		-1.8	-3.20		P	(70)		(70)	
Cercocarpus betuloides	Med./ Dry Temperate	-2.76	-2.59	-7.46			P	(31)	(31)	(71)	
Chrysothamnus nauseosus	Semidesert			-2.9	-3.90	-1.2	Y			(48)	(48, 49)
Chrysothamnus viscidiflorus	Semidesert			-4.25	-6.70	-1.31	Y			(48)	(49); (48)
Cipadessa baccifera	Tropical Dry		-1.78	-2.45	-4.70		Y		(37)	(37)	
Cistus albidus	Med./ Dry Temperate			-5.78	-8.86	-2	Y			(13)	(13)
Cistus laurifolius	Med./ Dry Temperate			-3.65	-6.36	-0.9	Y			(13)	(13)
Cleistanthus sumatranus	Tropical Dry		-1.72	-3.19			Y		(37)	(37)	
Clerodendrum fortunatum	Tropical Dry		-1.54	-1.89	-3.99		Y		(24)	(24)	
Codiaeum variegatum	Tropical Dry	-0.92		-2.23	-3.27		Y	(32)		(32, 58)	
Colliguaja integerrima	Semidesert	-3.1	-3.71	-4.4	-5.98		Y	(28)	(29)	(28)	
Comarostaphylis diversifolia	Med./ Dry Temperate	-2.85	-3.45	-5.61			Y	(31)	(31)	(71)	
Combretum latifolium	Tropical Dry		-1.29	-1.12	-3.76		P		(50)	(50)	
Cordia alliodora	Tropical Moist		-1.97	-3.27	-5.59		Y		(72)	(72)	
Cordia americana	Tropical Dry	-1.63	-1.58	-1.37			N	(51)	(51, 52)	(51, 52)	
Cordia cymosa	Tropical Moist		-1.5	-1.2	-2.55		P		(72)	(72)	

Cordia dentata	Tropical Moist				-2.14	-3.6	-6.25		Y			(72)	(72)	
Cordia lasiocalyx	Tropical Moist				-1.63	-2.57	-4.27		Y			(72)	(72)	
Cordia lucidula	Tropical Moist				-1.4	-1.58	-2.97		Y			(72)	(72)	
Cordia panamensis	Tropical Moist				-2	-2.33	-3.61		Y			(72)	(72)	
Cornus florida	Temperate				-2.28	-3.9	-7.10	-1.6	Y			(73)	(74)	(18, 74)
Corylus cornuta	Temperate			-2.51	-1.93				N		(75)	(75)		
Corymbia callophylla	Med./ Dry Temperate				-2.62	-1.5			N			(76)	(76)	
Croton yanhuii	Tropical Dry				-1.82	-1.48	-2.60		P			(37)	(37)	
Cryptocarya chinensis	Tropical Dry				-1.52	-3.78	-6.75		Y			(24)	(24)	
Cryptocarya concinna	Tropical Dry				-1.77	-1.74	-4.44		P			(24)	(24)	
Curatella americana	Tropical Dry			-1.17	-1.91	-1.48	-2.17		P		(77)	(77)	(78)	
Cyathodes straminea	Temperate			-2	-2.02				Y		(47)	(47)		
Diospyros morrisiana	Tropical Dry				-1.79	-0.89	-1.22		N			(24)	(24)	
Diplospora dubia	Tropical Dry				-1.93	-2.21	-4.75		Y			(24)	(24)	
Dryandra sessilis	Med./ Dry Temperate				-2.82	-1.93	-3.40		P			(34)	(34)	
Dryandra vestita	Med./ Dry Temperate				-2.97	-3.19	-7.05		Y			(34)	(34)	
Drypetes indica	Tropical Dry			-1.68		-2.32	-4.00		Y		(32)		(32, 58)	
Dysoxylum papuanum	Tropical Moist			-2.24	-2.12	-2.63	-4.24		P			(79)	(79)	
Elaeocarpus grandis	Tropical Moist			-1.66	-2.16	-3.06			Y			(79)	(79)	
Encelia californica	Med./ Dry Temperate	-2.27	-4.32			-0.82			N	(43)			(43)	
Encelia farinosa	Semidesert				-2.63	-6.13			Y			(8)	(9)	
Enterolobium cyclocarpum	Tropical Dry	-1.84	-2.36		-1.82	-2.73	-3.50		P	(4)		(4)	(4)	

Ericameria nauseosus	Semidesert					-2.90	-3.90	-1.20	Y					(48)	(49)
Eriogonum cinereum	Med./ Dry Temperate	-2.26	-4.29			-1.97			N	(43)				(43)	
Eucalyptus accedens	Med./ Dry Temperate				-3.48	-3.2			N				(76)	(76)	
Eucalyptus albida	Med./ Dry Temperate				-3.14	-0.92	-2.80		N				(34)	(34)	
Eucalyptus capillosa	Med./ Dry Temperate				-3.69	-3.08	-5.70		P				(34)	(34)	
Eucalyptus coccifera	Med./ Dry Temperate			-2.65	-2.36				N		(47)		(47)		
Eucalyptus globoidea	Med./ Dry Temperate				-1.22	-1.20			N				(80)	(80)	
Eucalyptus marginata	Med./ Dry Temperate				-2.48	-2.39	-5.00		P				(76)	(76)	
Eucalyptus pauciflora	Med./ Dry Temperate	-1.34	-1.82	-1.56	-1.6	-1.61	-2.90		Y	(81)	(81)		(81)	(81)	
Eucalyptus pulchella	Med./ Dry Temperate			-4.31	-2.41				N		(47)		(47)		
Eucalyptus piperita	Med./ Dry Temperate				-1.27	-0.99			N				(80)	(80)	
Eucalyptus sclerophylla	Med./ Dry Temperate			-1.50	-1.15				N				(80)	(80)	
Eucalyptus sieberi	Med./ Dry Temperate			-1.51	-1.02				N				(80)	(80)	
Eucalyptus tetrodonta	Med./ Dry Temperate	-2.3		-2.13					N		(82)		(82)		
Eucalyptus wandoo	Med./ Dry Temperate				-3.41	-3.41			Y				(76)	(76)	
Fagus sylvatica	Temperate				-2.04	-3.08	-3.90	-0.4	Y				(83)	(84-86)	(87)
Ficus pisocarpa	Tropical Dry				-1.38	-0.81	-1.37		N				(37)	(37)	
Ficus auriculata	Tropical Dry	-0.73	-3.14		-0.86				P	(88)			(88)		
Ficus benjamina	Tropical Dry	-1.2	-2.40		-1.65				P	(88)			(88)		
Ficus concinna	Tropical Dry	-1.99	-2.27		-2.32				Y	(88)			(88)		
Ficus curtipes	Tropical Dry	-1.11	-1.44		-1.47				Y	(88)			(88)		
Ficus esquiroliana	Tropical Dry	-0.91	-1.93		-1.15				P	(88)			(88)		
Ficus hispida	Tropical Dry	-1.23	-1.85		-1.23				P	(88)			(88)		
Ficus racemosa	Tropical Dry	-1.17	-3.02		-1.44				P	(88)			(88)		

Ficus religosa	Tropical Dry	-1.49	-1.80		-1.69				P	(88)		(88)			
Ficus semicordata	Tropical Dry	-0.5	-2.15		-1.52				P	(88)		(88)			
Ficus tinctoria	Tropical Dry	-1.37	-2.16		-1.82				P	(88)		(88)			
Fraxinus americana	Temperate				-2.14	-1.92			N			(14)	(89)		
Fraxinus ornus	Temperate				-2.84	-2.2	-4.20		P			(70)	(90)		
Gaultheria hispida	Temperate			-1.32	-2.08				Y		(47)	(47)			
Genipa americana	Tropical Dry			-1.27	-2.55				Y		(91)	(91)			
Gironniera subaequalis	Tropical Dry				-1.07	-2.98	-3.65		Y			(24)	(24)		
Glyricidia sepium	Tropical Dry	-1.69	-2.15	-1.91	-1.61				P	(91)	(91)	(91)			
Grayia spinosa	Semidesert					-5.25	-9.00	-2.24	Y				(48)		(48, 49)
Hakea lissosperma	Temperate	-1.35	-1.92	-2.85	-2.67	-5.66	-6.41		P	(46)	(47)	(47)	Cochard, Brodribb, Blackman (unpub.)		
Hakea microcarpa	Med./ Dry Temperate			-3.96	-3.73				N		(47)	(47)			
Hazardia squarrosa	Med./ Dry Temperate	-1.74	-3.30		-1.42				N	(43)			(43)		
Hedera canariensis	Temperate	-1.10	-1.57	-0.85	-2.06				P	(6)	(6)	(6)			
Heteromeles arbutifolia	Med./ Dry Temperate			-2.57	-2.53	-6.2	-8.12		P		(31)	(31)	(92)		
Hevea brasiliensis	Tropical Dry			-1.06		-1.27	-2.38		Y		(32)		(32, 58)		
Hybanthus prunifolius	Tropical Dry				-1.74	-2.6	-6.00		Y			(93)	(94)		
Hymenaea courbaril	Tropical Dry	-2.44	-3.07		-2.17	-3	-3.90		P	(4)		(4)	(4)		
Hymenaea martiana	Tropical Dry			-1.4	-2.32	-2.8	-0.66		Y		(30)	(30)	(30)		
Hymenaea stignocarpa	Tropical Dry			-1.6	-2.64	-3.17			Y		(30)	(30)	(30)		
Ilex aquifolium	Temperate			-0.89	-1.68	-6.6	-9.70		Y		(95)	(95)	(13)		(13)
Illicium anisatum	Temperate				-1.35	-3.66	-4.70		Y			(38)	(45)		
Illicium floridanum	Temperate				-1.1	-3.28	-4.25		Y			(38)	(45)		
Irvingia malayana	Tropical Dry				-1.85				Y			(7)			
Isopogon gardneri	Med./ Dry Temperate				-2.93	-3.75	-7.00		Y			(34)	(34)		
Juglans regia nigra	Temperate	-0.23	-0.96		-1.53				Y	(96)		(96)			

Khaya senegalensis	Med./ Dry Temperate			-1.5	-2.77				Y		(82)	(82)		
Kielmeyera coriacea	Tropical Dry					-1.91		-0.8	Y				(97)	(60)
Lagerstroemia tomentosa	Tropical Dry				-1.94	-1.29	-2.80		P			(37)	(37)	
Lantana camara	Tropical Dry			-0.8	-1.37				Y		(31)	(31)		
Lasiococca comberi	Tropical Dry				-2.73	-1.66	-3.43		P			(37)	(37)	
Liquidambar styraciflua	Temperate				-2.34	-3.12	-5.30	-0.78	Y			(98)	(18)	(18, 74)
Liriodendron tulipifera	Temperate				-1.13	-3			Y			(17)	(17)	
Lomatia polymorpha	Med./ Dry Temperate			-1.57	-2.47				Y		(47)	(47)		
Lomatia tinctoria	Med./ Dry Temperate	-0.74	-3.17	-2.08	-2.51	-4.97	-5.57		Y	(46)	(47)	(47)	(69), Cochard, Brodribb, Blackman (unpub.)	
Lycium chilense	Semidesert			-2.97	-1.96	-4.9			P		(28)	(29)	(28)	
Macaranga denticulata	Tropical Dry			-1.27		-1.14	-1.86		N		(32)		(32, 58)	
Machilus chinensis	Tropical Dry				-1.98	-2.52	-5.78		Y			(24)	(24)	
Maclura tinctoria	Tropical Moist			-1.61	-1.85	-0.71	-2.25		P		(51)	(51, 52)	(51, 52)	
Magnolia grandiflora	Temperate			-0.42	-2.06	-2.02			P		(31)	(31)	(62)	
Malacothamnus fasciculatus	Med./ Dry Temperate	-2.21	-4.20			-0.94			N	(43)			(43)	
Mallotus paniculatus	Tropical Dry				-1.48	-1.32	-2.80		P			(24)	(24)	
Mallotus penangensis	Tropical Dry				-1.19				Y			(7)		
Mallotus wrayi	Tropical Moist				-2.19	-0.53			N			(99)	(100)	
Malosma laurina	Med./ Dry Temperate	-1.74	-3.04		-2.27	-0.68			P	(43)		(43)	(43)	
Melastoma sanguineum	Tropical Dry				-1.4	-1.2	-2.67		P			(24)	(24)	

Melicope pteleifolia	Tropical Dry		-1.65	-2.7	-5.02		Y		(24)	(24)	
Memecylon ligustrifolium	Tropical Dry		-1.13	-1.03	-2.11		P		(24)	(24)	
Miconia cuspidata	Tropical Dry		-2.66	-3.4			Y		(30)	(30)	
Miconia pohliana	Tropical Dry		-1.75	-3.1			Y		(30)	(30)	
Microdesmis casearifolia	Tropical Dry		-1.96	-2.6	-6.06		Y		(24)	(24)	
Milletia atropurpurea	Tropical Dry		-1.17				Y		(7)		
Millettia cubittii	Tropical Dry		-1.6	-0.74	-1.38		N		(37)	(37)	
Millettia pachycarpa	Tropical Dry		-1.52	-1.32	-2.65		P		(50)	(50)	
Mischocarpus pentapetalus	Tropical Dry		-1.54	-1.79	-2.98		Y		(24)	(24)	
Mulinum spinosum	Semidesert	-2.97	-2.66	-5.7	-11.0		P	(28)	(29)	(28)	
Myrsine ferruginea	Tropical Dry	-1	-1.79	-3.08			Y	(30)	(30)	(30)	
Myrsine guianensis	Tropical Dry	-1.1	-1.76	-2.12			Y	(30)	(30)	(30)	
Neoscortechenia kingii	Tropical Dry		-1.72				Y		(7)		
Nothofagus alessandri	Temperate	-1.7	-1.79	-4.3	-6.56		Y	(101)	(101)	(101)	
Nothofagus antarctica	Temperate	-2.21	-1.73	-5.3	-6.79		P	(101)	(101)	(101)	
Nothofagus cunninghamii	Temperate	-1.7	-2.09	-2.31	-2.70		Y	(47)	(47)	Cochard, Brodribb, Blackman (unpub.)	
Nothofagus dombeyi	Temperate	-1.47	-1.63	-3.8	-7.25		Y	(101)	(101)	(101)	
Nothofagus glauca	Temperate	-0.94	-1.95	-3.2	-7.89		Y	(101)	(101)	(101)	
Nothofagus gunnii	Temperate	-1.53	-1.82				Y	(47)	(47)	(101)	
Nothofagus obliqua	Temperate	-1.2	-1.68	-4.5			Y	(101)	(101)	(101)	
Nothofagus pumilio	Temperate	-1.97	-1.68	-3.8	-6.70		P	(101)	(101)	(101)	
Nyssa sylvatica	Temperate			-1.82	-2.20	-1.7	Y			(18)	(18)
Ochroma pyramidale	Tropical Dry		-1.6	-1	-1.40		N		(102)	(102)	
Olea europaea	Med./ Dry		-2.93	-7.1			Y		(103)	(104)	

Olearia hookeri	Temperate Med./ Dry Temperate			-2.36	-2.27				N		(47)	(47)		
Olearia pinifolia	Temperate			-1.71	-2.09				Y		(47)	(47)		
Orites diversifolia	Temperate			-1.25	-1.84				Y		(47)	(47)		
Ouratea hexasperma	Tropical Dry				-2.34	-1.48	-4.60		P			(59)	(59)	
Ouratea lucens	Tropical Dry				-1.87	-1.8	-4.50		P			(93)	(94)	
Oxydendrum arboreum	Med./ Dry Temperate					-4.54	-5.70	-1.95	Y			(51)	(18)	(18)
Palaquim sumatrana	Tropical Dry				-1.9				Y			(7)		
Parashorea densiflora	Tropical Dry				-1.84				Y			(7)		
Peltophorum dubium	Tropical Moist			-0.94	-1.36	-1.03	-2.03		P		(51)	(51, 52)	(51, 52)	
Phillyrea angustifolia	Med./ Dry Temperate			-1.38	-2.91	-9.53	-10.4		Y		(95)	(95)	(69)	
Phillyrea latifolia	Med./ Dry Temperate				-2.55	-6.55	-10.0	-5.3	Y			(105)	(13)	(13)
Pieris japonica	Temperate			-2.12	-2.37				Y		(41)	(41)		
Pistacia terebinthus	Med./ Dry Temperate				-2.73	-8.42	-10.4		Y			(103)	(69)	
Pistacia weinmannifolia	Tropical Dry				-3.37	-3.98	-7.33		Y			(37)	(37)	
Pittosporum bicolor	Temperate			-1.87	-2.66				Y		(47)	(47)		
Plachonia careya	Med./ Dry Temperate			-2.64	-1.78				N		(106)	(47)		
Platanus racemosa	Temperate				-2.03	-1.56			N			(31)	(62)	
Populus balsamifera	Temperate				-2.33	-1.72	-2.61	-1.07	P			(1)	(35)	(35)
Populus euphratica	Med./ Dry Temperate	-2.52	-4.80		-2.35				N	(107)		(108)		
Populus trichocarpa	Temperate				-1.74	-1.25	-1.49	-1.4	N			(109)	(110)	(111)
Prionostemma aspera	Tropical Dry				-2.07	-1.14	-6.00		P			(40)	(40)	(40)
Prosopis velutina	Med./ Dry Temperate					-1.98	-7.14	-5.45	P				(9, 112)	(112)

Protium panamense	Tropical Moist			-2.33	-2.57	-1.7			P		(41)	(41)	(113)	
Prunus armeniaca	Crop				-2.86	-6.07			Y			(114)	(115)	
Prunus mahaleb	Temperate			-1.8	-2.62	-5.55	-6.71		Y		(95)	(95)	(115)	
Prunus virginiana	Temperate				-2.54	-3.8			Y			(1)	(22)	
Prunus serotina	Temperate				-1.94	-4.27			Y			(14)		
Pseudobombax septenatum	Tropical Dry				-1.28	-1	-1.40		P			(102)	(102)	
Psychotria horizontalis	Tropical Dry				-1.34	-4.9	-6.20		Y			(116)	(94)	
Pygeum topengii	Tropical Dry				-1.28	-1.2	-2.99		P			(24)	(24)	
Pyrus amygdaliformis	Temperate				-3.41	-3.29	-5.15		P			(103)	(117)	
Qualea parviflora	Tropical Dry				-2.22	-1.65	-5.10	-1	P			(59)	(59)	(60)
Quercus agrifolia	Med./ Dry Temperate			-2.4	-3.01	-1.97			P		(31)	(31)	(71)	
Quercus alba	Temperate				-2.52	-1.37	-2.60	-1.16	P			(118)	(18)	(18)
Quercus berberidifolia	Med./ Dry Temperate	-1.34	-2.54			-1.51			P	(43)			(43)	
Quercus falcata	Temperate					-0.92	-1.80	-0.81	Y				(18)	(18)
Quercus fusiformis	Med./ Dry Temperate					-0.5	-0.97	-0.5	P				(119)	(119)
Quercus garryana	Temperate			-3.61	-3.92				Y		(75)	(41)		
Quercus ilex	Med./ Dry Temperate			-3.5	-3.13	-3.3	-5.50	-1.67	P		(10)	(120)	(121)	(13, 122)
Quercus nigra	Temperate					-1.31	-2.70	-0.86	Y				(18)	(18)
Quercus oleoides	Tropical Dry	-2.75	-3.73	-2.93	-3.12	-3.03	-3.90		P	(4)	(91)	(91)	(4)	
Quercus petraea	Med./ Dry Temperate	-2.16	-3.04	-1.96	-2.39	-3.5	-4.25	-0.53	P	(123)	(10)	(10)	(124)	(87)
Quercus phellos	Temperate					-1.42	-2.30	-1.24	Y				(18)	(18)
Quercus pubescens	Med./ Dry Temperate	-3.37	-4.10	-2.84	-2.91	-3.3	-5.50		P	(68)	(10)	(10)	(121)	
Quercus robur	Temperate				-2.32	-2.8	-3.46		Y			(125)	(124)	
Quercus rubra	Temperate			-1.98	-2.92	-2.06	-3.32	-1.15	P		(75)	(75)	(18, 126)	(18)
Quercus semiserrata	Tropical Moist				-1.44				Y			(7)		
Quercus wislizeni	Med./ Dry Temperate					-2.49		-0.83	Y				(71)	(127)
Quisqualis indica	Tropical Dry				-1.37	-1.43	-3.69		Y			(50)	(50)	

Raphiolepis indica	Temperate	-2.24	-4.06	-2.08	-2.07				N	(31)	(6)	(31)			
Rhamnus californica	Med./ Dry Temperate				-2.52	-2.51	-4.09	-0.74	P			(26)	(64, 65)	(64, 66)	
Rhamnus crocea	Med./ Dry Temperate					-5.17	-8.66	-2.03	Y				(64, 65)	(64, 66)	
Rhamnus ilicifolia	Med./ Dry Temperate					-5.92	-9.83	-2.55	Y				(64, 65)	(64, 66)	
Rhedera trinervis	Tropical Dry	-1.16	-1.47	-1.57	-1.85	-2.8	-4.70		Y	(4)	(91)	(4)	(4)		
Rhododendron macrophylum	Temperate			-1.95		-2.96	-5.00		Y		(75)		(128)		
Rhodomyrtus tomentosa	Tropical Dry				-1.29	-1.1	-3.16		N			(24)	(24)		
Rhus ovata	Med./ Dry Temperate	-2.19	-4.17		-2.04	-0.56			N	(43)		(129)	(43)		
Richea scoparia	Temperate			-1.41	-1.53				Y		(47)	(47).			
Rinorea anguifera	Tropical Dry				-1.76				Y			(7)			
Sapium sebiferum	Tropical Dry				-2.05	-1.01	-1.56		N			(24)	(24)		
Sarcosperma laurinum	Tropical Dry				-1.75	-3.14	-7.86		Y			(24)	(24)		
Schefflera heptaphylla	Tropical Dry				-1.56	-2.59	-4.53		Y			(24)	(24)		
Schefflera macrocarpa	Tropical Dry				-1.67	-1.72	-3.95		Y			(59)	(59)		
Schima superba	Tropical Dry				-1.54	-5.19	-8.99		Y			(24)	(24)		
Schinus johnstonii	Semidesert			-2.82	-3.78	-3.6			P		(28)	(29)	(28)		
Schinus terebinthifolius	Tropical Dry				-2.5	-1.68	-5.33		P			(130)	(15)		
Schisandra glabra	Temperate				-0.85	-1.06	-1.97		Y			(38)	(45)		
Senecio filaginoides	Semidesert			-2.6	-1.98	-5	-7.33		P		(28)	(29)	(28)		
Shorea guiso	Tropical Dry				-1.41				Y			(7)			
Shorea lepidota	Tropical Dry				-1.36				Y			(7)			
Shorea macroptera	Tropical Dry				-0.98				Y			(7)			
Shorea parvifolia	Tropical Dry				-1.12				Y			(7)			
Sideroxylon lanuginosum	Med./ Dry Temperate					-2.6		-0.42	Y				(119)		
Simarouba glauca	Tropical Dry	-1.38	-1.79	-2.09	-2.21	-2	-2.70		P	(4)	(91)	(4)	(4)	(119)	
Sorbus torminalis	Med./ Dry Temperate					-3.18	-4.86	-0.9	Y				(13)	(13)	
Styrax ferrugineus	Tropical Dry			-1.2	-2.49	-3.35			Y		(30)	(30)	(30)		

Styrax pohlii	Tropical Dry			-1.4	-2.46	-2			P		(30)	(30)	(30)	
Sweitenia macrophylla	Tropical Dry	-1.79	-2.60		-2.21				Y	(4)		(4)		
Symplocos lanceolata	Tropical Dry			-1.3	-1.45	-1.5			Y		(30)	(30)	(30)	
Symplocos mosenii	Tropical Dry			-1.3	-1.95	-1.6			P		(30)	(30)	(30)	
Syzygium cumini	Tropical Dry			-2.03	-1.69	-0.97			N		(131)	(131)	(131)	
Syzygium latilimbum	Tropical Dry			-1.54	-1.17	-2.08			P		(131)	(131)	(131)	
Syzygium levinei	Tropical Dry				-1.75	-1.37			N			(24)	(24)	
Syzygium rehderianum	Tropical Dry				-1.85	-1.71			N			(24)	(24)	
Syzygium sayeri	Tropical Dry			-1.72	-1.86	-2.1			Y		(79)	(79)	(79)	
Syzygium szemaoense	Tropical Dry				-1.52	-1.95			Y			(50)	(50)	
Tachigalia versicolor	Tropical Moist			-1.41	-2.39	-1.6			P		(41)	(41)	(113)	
Tamarix ramosissima	Semidesert				-2.05	-0.65	-1.42	-2.99	N			(108)	(15)	(132)
Tasmannia lanceolata	Temperate	-1.13	-1.56	-1.56	-1.79	-3.49	-3.99		Y	(46)	(47)	(47)	Cochard, Brodribb, Blackman (unpub.)	
Telopea truncata	Temperate			-1.58	-2.07				Y		(47)	(47)		
Tetradymia glabrata	Semidesert					-5.5	-11.0	-2.56	Y				(48)	(22, 48, 49)
Toxicodendron succedaneum	Tropical Moist				-1.59	-1.51	-3.07		P			(24)	(24)	
Trichostigma octandrum	Tropical Dry				-1.49	-2.9	-6.50		Y			(40)	(40)	(40)
Trimenia neocaledonica	Tropical Moist				-1.15	-1.25	-3.68		Y			(38)	(45)	
Turpinia pomifera	Tropical Dry				-1.4	-2.05	-3.62		Y			(37)	(37)	
Ulmus alata	Temperate					-0.4	-2.50	-0.13	Y				(74)	(74)
Vaccinium myrtillus	Temperate	-1.72	-2.44		-1.38	-2.08			P	(133)		(133)	(133)	
Vaccinium vitis-idaea	Temperate	-1.64	-2.67		-1.88	-1.97			P	(133)		(133)	(133)	

Viburnum tinus	Med./ Dry Temperate			-1.3	-2				Y		(134)	(95)	(135)		
Vitis vinifera	Crop		-1.89	-1.13	-1.51				Y	(136)		(136)			
Vochysia ferruginea	Tropical Dry			-2.03	-2.25	-1			P		(41)	(41)	(113)		
Xanthophyllum hainanense	Tropical Dry				-1.73	-1.5	-3.76		P			(24)	(24)		
Gymnosperms															
Abies alba	Temperate	-1.61	-3.06			-3.71	-3.31		Y	(137)			(138)		
Abies balsamea	Temperate				-1.57	-2.79	-3.34	-3.87	P			(57)	(139)	(139)	
Abies concolor	Temperate			-1.95	-2.22	-5.15	-6.36	-3.4	Y		(140)	(141)	(142)	(22)	
Abies grandis	Temperate				-2.27	-3.65	-4.07		Y			(141)	(143)		
Abies lasiocarpa	Temperate					-3.3		-3.3	N			(144)	(144)	(145)	
Austrocedrus chilensis	Temperate			-0.91	-1.1	-2.7	-4.4		Y		(146)	(146)	(146)		
Ginkgo biloba	Temperate				-2.22	-3.1			Y			(1)	(144)		
Juniperus arizonica	Temperate					-13.8		-9.5	Y				(147)	(147)	
Juniperus ashei	Temperate					-13.1		-9.4	Y				(147)	(147)	
Juniperus barbadensis	Temperate					-12.8		-7.2	Y				(147)	(147)	
Juniperus communis	Temperate				-3.54	-6.05	-8.12		Y			(148)	(138, 143, 149, 150)		
Juniperus deppeana	Temperate					-8.9	-12.4	-8.8	Y				(147)	(147)	
Juniperus flaccida	Temperate					-7.8	-12.7	-7.8	N				(147)	(147)	
Juniperus lucayana	Temperate					-8.3		-6.3	Y				(147)	(147)	
Juniperus maritima	Temperate					-7.58	-7.81	-6.35	Y				(151)	(151)	
Juniperus monosperma	Temperate			-3.2	-3.8	-11.6		-9.3	Y		(152)	(153)	(147)	(147)	
Juniperus occidentalis	Temperate				-3.15	-9	-12	-8.5	Y			(136, 154)	(147)	(147)	
Juniperus osteosperma	Temperate			-6.35	-4.1	-11.9		-10.4	P		(140)	(155)	(147)	(147)	
Juniperus pinchotii	Temperate					-14.1		-7.7	Y				(147)	(147)	
Juniperus scopulorum	Temperate					-7.7	-14	-6.9	Y				(147)	(147)	

Juniperus sillcicola	Temperate					-6.6		-4.7	Y				(147)	(147)
Juniperus virginiana	Temperate				-2.47	-6.2	-9.79	-4.9	Y			(118)	(147)	(147)
Larix decidua	Temperate				-2.26	-3.53	-4.44		P			(156)	(150)	
Picea abies	Temperate			-3.87	-2.51	-3.74	-4.33		P		(140)	(157)	(85, 138, 143, 158-161)	
Picea engelmannii	Temperate			-4.22		-4.18	-5		P		(140)		(138)	
Picea glauca	Temperate					-2.73		-4.3	N				(139)	(139)
Picea mariana	Temperate				-2.53	-3.31		-5.3	P			(162)	(139)	(139)
Picea rubens	Temperate				-1.94	-3.48			Y			(163)	(164)	
Pinus cembra	Temperate				-2.34	-3.39	-3.85		Y			(156)	(138, 150, 160)	
Pinus echinata	Temperate					-3.21		-1.47	Y				(18)	(18)
Pinus edulis	Temperate			-1.54	-2.5	-4.88	-5.96	-2.97	Y		(152)	(153)	(165)	(165)
Pinus elliotii	Temperate					-1.52		-1.33	Y				(166)	(166)
Pinus flexilis	Temperate			-1.6		-3.71	-4.21		Y		(140)		(143)	
Pinus halepensis	Temperate	-1.75	-2.37			-3.11		-0.88	Y	(137)			(167)	(167)
Pinus nigra	Temperate			-1.52	-2.28	-3.2	-4.79		Y		(168)	(168)	(13)	
Pinus palustris	Temperate					-1.81		-1.31	Y				(166)	(166)
Pinus pinaster	Temperate			-0.5		-3.22	-4.79		Y		(169)		(169)	
Pinus pinea	Temperate					-3.65		-1.01	Y				(167)	(167)
Pinus ponderosa	Temperate			-1.57	-2.23	-3.01	-4.48	-1.2	Y		(41)	(41)	(110, 138, 143, 145, 170, 171)	(172)
Pinus sylvestris	Temperate	-1.55	-2.94			-2.96	-4.34		Y	(137)			(173)	
Pinus taeda	Temperate			-0.91	-2.22	-3.33	-4.4	-1.74	Y		(174)	(174)	(18, 48, 74)	(18)
Pinus virginiana	Temperate			-0.84	-1.98	-4.07	-5.32		Y		(17)	(17)	(17)	
Pseudotsuga menziesii	Temperate			-1.39	-2.3	-3.41	-4.25	-1	Y		(41)	(41)	(142, 143, 145, 175-177)	(172)
Sequoia sempervirens	Temperate				-1.97	-3.4			Y			(178)		
Sequoiadendron giganteum	Temperate			-2.59		-8.1			Y		(140)		(144, 179)	
Taxodium distichum	Temperate			-1.15		-2.1			Y		(140)			
Taxus baccata	Temperate			-2.56	-2.26	-6.97	-9.05		P		(180)	(180)	(138, 144)	
Tetraclinis	Temperate					-8.55		-2.65	Y				(167)	(167)

articulata							
Thuja occidentalis	Temperate	-2.88	-3.57	-4.71	Y	(181)	(21)

Table S6.2. The paired t-tests comparing each trait combination with data for ≥ 5 species. These tests establish the temporal sequences in Fig. 6.1. Mean columns show the mean ± the standard error. N is the number of species. In the P column, * shows $p < 0.05$, ** is $p < 0.01$, and *** is $p < 0.001$. All of the significantly different comparisons remained so after correcting for multiple tests (Benjamini & Hochberg 1995). All of the stem and root hydraulic trait values are interpolated from sigmoidally shaped hydraulic vulnerability curves.

Mean		Mean		P	N	Mean		Mean		P	N
Angiosperms						**Gymnosperms**					
g_S Ψ_{50}	-1.68± 0.19	K_{stem} Ψ_{12}	-2.23 ± 0.36	0.15	15	K_{leaf} Ψ_{50}	-2.22 ± 0.46	π_{tlp}	-2.46 ± 0.23	0.45	12
	-1.53± 0.16	K_{leaf} Ψ_{50}	-1.91 ± 0.17	*	12		-2.06 ± 0.53	Ψ_{min}	-2.50 ± 0.37	0.26	11
	-1.60± 0.10	π_{tlp}	-1.95 ± 0.10	**	40		-2.42 ± 0.44	K_{stem} Ψ_{12}	-3.62 ± 0.55	*	14
	-1.96± 0.16	Ψ_{min}	-3.12 ± 0.36	***	25		-2.42 ± 0.71	K_{root} Ψ_{50}	-4.29 ± 1.48	0.08	7
	-1.85± 0.21	K_{stem} Ψ_{50}	-3.47 ± 0.42	***	20		-2.16 ± 0.37	K_{stem} Ψ_{50}	-5.02 ± 0.71	***	17
	-1.72± 0.18	K_{stem} Ψ_{88}	-4.42 ± 0.62	***	15		-1.80 ± 0.31	K_{stem} Ψ_{88}	-5.18 ± 0.37	***	13
K_{stem} Ψ_{12}	-2.19± 0.30	K_{leaf} Ψ_{50}	-2.02 ± 0.11	0.58	41	π_{tlp}	-2.61 ± 0.21	Ψ_{min}	-2.69 ± 0.31	0.61	12
	-1.80± 0.29	K_{root} Ψ_{50}	-1.78 ± 0.38	0.95	11		-2.54 ± 0.14	K_{stem} Ψ_{12}	-3.41 ± 0.39	**	20
	-1.62± 0.16	π_{tlp}	-2.09 ± 0.07	***	99		-2.64 ± 0.23	K_{root} Ψ_{50}	-4.78 ± 0.99	*	11
	-2.24± 0.35	g_S Ψ_{95}	-2.67 ± 0.34	0.22	15		-2.44 ± 0.14	K_{stem} Ψ_{50}	-4.81 ± 0.53	***	24
	-1.46± 0.13	Ψ_{min}	-2.70 ± 0.18	***	82		-2.34 ± 0.13	K_{stem} Ψ_{88}	-5.76 ± 0.57	***	18
K_{leaf} Ψ_{50}	-1.96± 0.09	π_{tlp}	-2.21 ± 0.06	**	93	Ψ_{min}	-2.84 ± 0.28	K_{stem} Ψ_{12}	-3.60 ± 0.46	*	16
	-1.91± 0.17	g_S Ψ_{95}	-2.45 ± 0.32	0.07	12		-2.98 ± 0.41	K_{root} Ψ_{50}	-4.27 ± 1.06	0.17	11
	-2.00± 0.11	Ψ_{min}	-1.89 ± 0.15	0.46	60		-2.77 ± 0.27	K_{stem} Ψ_{50}	-5.04 ± 0.62	***	21
	-1.91± 0.09	K_{stem} Ψ_{50}	-3.59 ± 0.26	***	53		-2.48 ± 0.23	K_{stem} Ψ_{88}	-5.50 ± 0.60	***	16
	-1.99± 0.11	K_{stem} Ψ_{88}	-5.40 ± 0.40	***	37						
						K_{stem} Ψ_{12}	-4.25 ± 0.51	K_{root} Ψ_{50}	-5.99 ± 0.71	**	18
K_{root} Ψ_{50}	-1.80 ± 0.46	π_{tlp}	-2.17 ± 0.19	0.42	9		-3.71 ± 0.32	K_{stem} Ψ_{50}	-6.18 ± 0.61	***	32
	-2.13 ± 0.47	Ψ_{min}	-3.56 ± 0.66	*	13		-3.33 ± 0.28	K_{stem} Ψ_{88}	-6.52 ± 0.65	***	25
	-2.10 ± 0.47	K_{stem} Ψ_{50}	-4.02 ± 0.58	***	13						
	-2.15 ± 0.51	K_{stem} Ψ_{88}	-5.93 ± 0.92	***	12	K_{root} Ψ_{50}	-4.95 ± 0.58	K_{stem} Ψ_{50}	-6.66 ± 0.73	***	29
							-4.79 ± 0.82	K_{stem} Ψ_{88}	-8.12 ± 1.12	***	12
π_{tlp}	-1.95± 0.10	g_S Ψ_{95}	-2.74 ± 0.21	***	40						
	-2.25± 0.06	Ψ_{min}	-2.14 ± 0.12	0.31	126	K_{stem} Ψ_{50}	-4.76 ± 0.38	K_{stem} Ψ_{88}	-6.38 ± 0.61	***	27
	-2.15± 0.06	K_{stem} Ψ_{50}	-3.17 ± 0.16	***	127						

	-2.09± 0.07	K_{stem} Ψ_{88}	-4.89 ± 0.24	***	100
	-1.48± 0.08	plant Ψ_{lethal}	-5.69 ± 0.44	***	15
Ψ_{min}	-3.12± 0.35	g_S Ψ_{95}	-3.34 ± 0.35	0.20	25
	-2.69± 0.17	K_{stem} Ψ_{50}	-3.33 ± 0.16	***	107
	-2.76± 0.19	K_{stem} Ψ_{88}	-5.49 ± 0.28	***	82
	-2.68± 0.34	K_{stem} Ψ_{12}	-2.23 ± 0.36	0.22	15
g_S Ψ_{95}	-3.04 ± 0.41	K_{stem} Ψ_{50}	-3.47± 0.42	0.14	20
	-2.68 ± 0.34	K_{stem} Ψ_{88}	-4.43 ± 0.62	**	15
K_{stem} Ψ_{50}	-3.22 ± 0.17	K_{stem} Ψ_{88}	-5.13 ± 0.23	***	117

Table S6.3. The paired t-tests showing that the angiosperm temporal sequence (Fig. 6.1B) is largely robust to leaf phenology. The mean columns show the mean ± the standard error. N is the number of species. In the P column, * shows $p < 0.05$, ** shows $p < 0.01$, and *** shows $p < 0.001$. Deciduous angiosperms are generally found to have less drought tolerant leaves but similarly tolerant stems as evergreens (Maherali et al. 2004, Bartlett et al. 2012b), but analyzing the evergreen and deciduous angiosperms separately and combined produced the same sequence, with a few exceptions (shown in bold). In the evergreen species (n = 158), K_{stem} Ψ_{12} was not significantly different from π_{tlp}. In the deciduous species (n = 76), the π_{tlp} was not significantly different from K_{leaf} Ψ_{50}, K_{root} Ψ_{50}, or g_S Ψ_{95}, and K_{root} Ψ_{50} was not significantly different from Ψ_{min}. However, of the 56 pairwise trait comparisons with sufficient data to test for the two functional types, 51 (91%) showed the same pattern as for all of the angiosperm species combined (Table S6.1). The exceptions reduced the resolution between adjacent traits in the sequence but did not directionally shift traits to more drought tolerant or drought sensitive positions along the sequence for either functional type. This suggests the exceptions represent reductions in statistical power from smaller sample sizes, rather than functional differences in the temporal sequences of drought responses for evergreen and deciduous species. We did not test for phenology differences in the gymnosperms, as all species but three (*Larix decidua, Gingko biloba,* and *Taxodium distichum*) were evergreen.

Mean			Mean	P	N	Mean			Mean	P	N
Evergreen (n = 158)						**Deciduous (n = 76)**					
g_S Ψ_{50}	-1.76± 0.26	K_{stem} Ψ_{12}	-2.88 ± 0.53	0.12	8	g_S Ψ_{50}	-1.54± 0.23	K_{stem} Ψ_{12}	-1.50 ± 0.30	0.88	7
	-1.49± 0.20	K_{leaf} Ψ_{50}	-1.94 ± 0.22	*	9		-	K_{leaf} Ψ_{50}	-	-	3
	-1.64± 0.12	π_{tlp}	-2.00 ± 0.13	**	27		-1.54± 0.18	π_{tlp}	-1.84 ± 0.14	*	13
	-2.20± 0.23	Ψ_{min}	-3.69 ± 0.52	***	15		-1.61± 0.16	Ψ_{min}	-2.27 ± 0.26	***	10
	-2.05± 0.31	K_{stem} Ψ_{50}	-3.88 ± 0.64	*	12		-1.55± 0.20	K_{stem} Ψ_{50}	-2.85 ± 0.31	**	8
	-1.76± 0.26	K_{stem} Ψ_{88}	-4.88 ± 0.98	**	9		-1.72± 0.18	K_{stem} Ψ_{88}	-4.43 ± 0.62	**	15
K_{stem} Ψ_{12}	-2.77± 0.49	K_{leaf} Ψ_{50}	-2.15 ± 0.15	0.24	22	K_{stem} Ψ_{12}	-1.53± 0.25	K_{leaf} Ψ_{50}	-1.87 ± 0.15	0.26	19
	-2.27± 0.47	K_{root} Ψ_{50}	-2.27 ± 0.77	0.99	5		-1.41± 0.31	K_{root} Ψ_{50}	-1.36 ± 0.24	0.92	6
	-1.82± 0.25	**π_{tlp}**	**-2.27 ± 0.11**	**0.09**	**52**		-1.39± 0.18	π_{tlp}	-1.89 ± 0.08	***	47
	-2.88± 0.53	g_S Ψ_{95}	-3.09 ± 0.57	0.74	8		-1.50± 0.30	g_S Ψ_{95}	-2.19 ± 0.31	0.06	7
	-1.62± 0.21	Ψ_{min}	-2.99 ± 0.25	***	43		-1.29± 0.12	Ψ_{min}	-2.38 ± 0.21	***	39
K_{leaf} Ψ_{50}	-1.97± 0.11	π_{tlp}	-2.71 ± 0.07	***	68	K_{leaf} Ψ_{50}	**-1.94± 0.14**	**π_{tlp}**	**-2.09 ± 0.12**	**0.22**	**25**
	-1.94± 0.22	g_S Ψ_{95}	-2.52 ± 0.40	0.14	9		-	g_S Ψ_{95}	-	-	3
	-2.00± 0.13	Ψ_{min}	-1.70 ± 0.16	0.07	46		-2.03± 0.17	Ψ_{min}	-2.50 ± 0.35	0.16	14
	-1.93± 0.12	K_{stem} Ψ_{50}	-3.80 ± 0.36	***	33		-1.88± 0.14	K_{stem} Ψ_{50}	-3.23 ± 0.35	**	20
	-2.09± 0.16	K_{stem} Ψ_{88}	-5.78 ± 0.54	***	20		-1.87± 0.15	K_{stem} Ψ_{88}	-4.96 ± 0.59	***	17

π_{tlp}	-	K_{root} Ψ_{50}	-	-	3	π_{tlp}	**-2.03± 0.19**	***K*root Ψ50**	**-1.35 ± 0.21**	*	**6**
	-2.00± 0.13	g_S Ψ_{95}	-2.83 ± 0.25	***	27		**-1.84± 0.14**	**g_S Ψ95**	**-2.54 ± 0.39**	**0.06**	**13**
	-2.39± 0.08	Ψ_{min}	-2.17 ± 0.16	0.13	84		-1.97± 0.08	Ψ_{min}	-2.07 ± 0.17	0.47	42
	-2.30± 0.09	K_{stem} Ψ_{50}	-3.38 ± 0.22	***	74		-1.94± 0.07	K_{stem} Ψ_{50}	-2.88 ± 0.22	***	53
	-2.22± 0.10	K_{stem} Ψ_{88}	-5.30 ± 0.33	***	53		-1.94± 0.07	K_{stem} Ψ_{88}	-4.42 ± 0.32	***	47
	-1.48± 0.08	plant Ψ_{lethal}	-5.69 ± 0.44	***	15		-	plant Ψ_{lethal}	-	-	0
Ψ_{min}	-4.82± 0.83	K_{root} Ψ_{50}	-2.75 ± 0.80	*	7	Ψ_{min}	**-2.08± 0.72**	***K*root Ψ50**	**-1.40 ± 0.23**	**0.37**	**6**
	-3.69± 0.52	g_S Ψ_{95}	-3.34 ± 0.35	0.31	15		-2.27± 0.17	g_S Ψ_{95}	-2.54 ± 0.41	0.45	10
	-2.90± 0.25	K_{stem} Ψ_{50}	-3.54 ± 0.24	***	63		-2.38± 0.19	K_{stem} Ψ_{50}	-3.05 ± 0.20	**	44
	-3.03± 0.27	K_{stem} Ψ_{88}	-5.81 ± 0.35	***	50		-2.28± 0.19	K_{stem} Ψ_{88}	-4.61 ± 0.37	***	44
g_S Ψ_{95}	-3.08 ± 0.42	K_{stem} Ψ_{12}	-2.88 ± 0.53	0.74	8	g_S Ψ_{95}	-2.19 ± 0.26	K_{stem} Ψ_{12}	-1.50 ± 0.30	0.24	7
	-3.61 ± 0.62	K_{stem} Ψ_{50}	-3.88 ± 0.65	0.54	12		-2.17 ± 0.23	K_{stem} Ψ_{50}	-2.85 ± 0.31	0.06	8
	-2.96 ± 0.52	K_{stem} Ψ_{88}	-4.88 ± 0.98	*	9		-2.28 ± 0.29	K_{stem} Ψ_{88}	-3.74 ± 0.42	*	6
K_{stem} Ψ_{50}	-5.40 ± 0.86	K_{root} Ψ_{50}	-2.93 ± 0.92	***	6	K_{stem} Ψ_{50}	-2.83 ± 0.45	K_{root} Ψ_{50}	-1.38 ± 0.20	**	7

Table S6.4. Paired t-tests showing that the angiosperm temporal sequence (Fig. 6.1B) is robust to differences in the shape of the stem vulnerability curves, but potentially influenced by the shape of the root vulnerability curves in this compiled dataset. Symbols follow Table 6.1 and Table S6.2. The stem and root hydraulic traits are interpolated from the relationship between K_{stem} and Ψ_{stem} in drying stems or K_{root} and Ψ_{root} in drying roots, and recent studies have suggested that non-sigmoidal relationships may be produced by a methodological artefact that overestimates stem and root vulnerability (Sperry et al. 2012). Analyzing the angiosperm species with sigmoidal stem vulnerability curves separately (n = 148) did not change the position of the stem hydraulic traits in the temporal sequence, as the paired t-tests showed the same results as for all curve shapes combined. Analyzing the species with sigmoidal root vulnerability curves separately (n = 15) did shift K_{root} Ψ_{50} to a more drought tolerant position in the sequence, as K_{root} Ψ_{50} was not significantly different from π_{tlp} for these species. Overall, the angiosperm temporal sequence appears to be largely robust to methodological differences in the compiled stem and root hydraulic trait data. However, the shift in K_{root} Ψ_{50} suggests that testing for potential effects of curve shape is important for meta-analyzing stem and root hydraulic trait data. All of the gymnosperm species had sigmoidal stem and root vulnerability curves. The vulnerability curve shape is provided for each species with stem and root hydraulic trait data in the supplementary dataset, file "SupplementaryData6.1.csv".

	Mean		Mean	P	N		Mean		Mean	P	N
All stem vulnerability curve shapes (n = 184)						**Only sigmoidal stem vulnerability curves (n = 148)**					
K_{stem} Ψ_{12}	-2.23 ± 0.36	g_S Ψ_{50}	-1.68± 0.19	0.15	15	K_{stem} Ψ_{12}	-2.23± 0.36	g_S Ψ_{50}	-1.68 ± 0.19	0.15	15
	-1.83± 0.26	K_{leaf} Ψ_{50}	-1.95 ± 0.10	0.65	52		-2.19± 0.30	K_{leaf} Ψ_{50}	-2.02 ± 0.11	0.58	41
	-1.36± 0.14	K_{root} Ψ_{50}	-1.36 ± 0.15	0.98	39		-1.80± 0.29	K_{root} Ψ_{50}	-1.78 ± 0.38	0.95	11
	-1.23± 0.12	π_{tlp}	-1.97 ± 0.05	***	148		-1.62± 0.16	π_{tlp}	-2.09 ± 0.07	***	99
	-2.23± 0.36	g_S Ψ_{95}	-2.67 ± 0.34	0.22	15		-2.24± 0.35	g_S Ψ_{95}	-2.67 ± 0.34	0.21	15
	-1.32± 0.11	Ψ_{min}	-2.56 ± 0.16	***	97		-1.46± 0.13	Ψ_{min}	-2.70 ± 0.18	***	82
K_{stem} Ψ_{50}	-2.92 ± 0.38	g_S Ψ_{50}	-1.90± 0.16	**	26	K_{stem} Ψ_{50}	-3.47± 0.42	g_S Ψ_{50}	-1.68 ± 0.19	***	20
	-3.17 ± 0.23	K_{leaf} Ψ_{50}	-1.85± 0.09	**	68		-3.59± 0.27	K_{leaf} Ψ_{50}	-1.91 ± 0.09	***	53
	-3.07 ± 0.25	K_{root} Ψ_{50}	-1.51 ± 0.18	***	47		-3.28± 0.33	K_{root} Ψ_{50}	-1.55 ± 0.25	***	27
	-2.73 ± 0.12	π_{tlp}	-2.06± 0.05	***	198		-3.17± 0.16	π_{tlp}	-2.15 ± 0.06	***	127
	-2.92 ± 0.38	g_S Ψ_{95}	-3.23 ± 0.33	0.38	26		-3.47± 0.42	g_S Ψ_{95}	-3.04 ± 0.41	0.14	20
	-3.00 ± 0.14	Ψ_{min}	-2.61± 0.15	*	133		-3.33 ± 0.16	Ψ_{min}	-2.69± 0.17	***	107
K_{stem} Ψ_{88}	-4.43 ± 0.62	g_S Ψ_{50}	-1.72± 0.18	**	15	K_{stem} Ψ_{88}	-4.42± 0.62	g_S Ψ_{50}	-1.72 ± 0.18	***	15
	-5.07 ± 0.36	K_{leaf} Ψ_{50}	-1.91± 0.11	***	45		-5.40± 0.41	K_{leaf} Ψ_{50}	-1.99 ± 0.11	***	37
	-5.07 ± 0.43	K_{root} Ψ_{50}	-1.45 ± 0.18	***	43		-4.99± 0.53	K_{root} Ψ_{50}	-1.58 ± 0.27	***	25
	-4.62 ± 0.18	π_{tlp}	-1.97± 0.05	**	147		-4.89 ± 0.24	π_{tlp}	-2.09 ± 0.07	***	100
	-4.43 ± 0.62	g_S Ψ_{95}	-2.68 ± 0.34	**	15		-4.43± 0.62	g_S Ψ_{95}	-2.68 ± 0.34	***	15
	-5.25 ± 0.26	Ψ_{min}	-2.68± 0.17	***	94		-5.49± 0.28	Ψ_{min}	-2.76± 0.19	***	82
All root vulnerability curve shapes (n = 49)						**Only sigmoidal root vulnerability curves (n = 15)**					
K_{root} Ψ_{50}	-1.36 ± 0.15	K_{stem} Ψ_{12}	-1.36 ± 0.14	0.98	39	K_{root} Ψ_{50}	-1.66 ± 0.34	K_{stem} Ψ_{12}	-1.65± 0.27	0.99	13
	-1.51 ± 0.18	K_{stem} Ψ_{50}	-3.07 ± 0.25	***	47		-1.95 ± 0.43	K_{stem} Ψ_{50}	-3.79 ± 0.53	***	15
	-1.45 ± 0.18	K_{stem} Ψ_{88}	-5.07 ± 0.43	***	43		-1.98 ± 0.46	K_{stem} Ψ_{88}	-5.67 ± 0.82	***	14
	-1.35 ± 0.22	**π_{tlp}**	**-2.24 ± 0.10**	**	**22**		-1.80 ± 0.46	π_{tlp}	-2.17 ± 0.19	0.42	9
	-1.68 ± 0.30	Ψ_{min}	-3.19 ± 0.22	***	39		-2.13 ± 0.47	Ψ_{min}	-3.56 ± 0.66	*	13

Table S6.5. Univariate standardized major axis (SMA) correlations between each pair of traits measured for at least 5 species. These are the trait correlations shown in Fig. 6.3. In each cell, the top number is the r value, and the bottom numbers are the p-value (the p-value number is shown for $p > 0.05$, and for significant correlations, * indicates $p < 0.05$, ** indicates $p < 0.01$, and *** indicates $p < 0.001$) and the number of species (in parentheses). Significant correlations are bolded. All correlations remained significant after correction for multiple tests. The cell colors indicate the strength of the significant correlations, with dark red indicating $r \geq 0.75$, medium red indicating $r \geq 0.50$, pink indicating $r \geq 0.25$, and no color indicating $r \leq 0.25$.

	K_{root} Ψ_{50}	K_{stem} Ψ_{12}	K_{leaf} Ψ_{50}	π_{tlp}	g_S Ψ_{95}	Ψ_{min}	K_{stem} Ψ_{50}	K_{stem} Ψ_{88}	Ψ lethal
g_S Ψ_{50}	-	0.21 0.4 (17)	**0.60** *** (12)**	**0.73** ***** (40)**	**0.87** ***** (49)**	**0.87** ***** (40)**	**0.65** *** (23)**	**0.55** *** (17)**	-
K_{root} Ψ_{50}		**0.85** ***** (29)**	**0.63** *** (9)**	**0.77** ***** (20)**	-	**0.42** *** (24)**	**0.88** ***** (42)**	**0.85** ***** (24)**	-
K_{stem} Ψ_{12}			**0.38** **** (54)**	**0.39** ***** (119)**	**0.52** *** (17)**	**0.29** ***** (98)**	**0.84** ***** (147)**	**0.51** ***** (133)**	-
K_{leaf} Ψ_{50}				**0.66** ***** (105)**	0.50 0.1 (12)	**0.47** ***** (71)**	**0.54** ***** (70)**	0.35 0.2 (50)	-
π_{tlp}					**0.62** ***** (40)**	**0.57** ***** (140)**	**0.50** ***** (151)**	**0.43** ***** (118)**	**0.56** ***** **(15)**
g_S Ψ_{95}						**0.87** ***** (27)**	**0.77** ***** (29)**	**0.77** ***** (17)**	-
Ψ_{min}							**0.54** ***** (128)**	**0.58** ***** (98)**	-
K_{stem} Ψ_{50}								**0.90** ***** (144)**	-

Table S6.6. The univariate standardized major axis (SMA) correlations between each pair of traits measured for at least 5 species, including the stem and root hydraulic trait values interpolated from non-sigmoidally shaped vulnerability curves. Symbols follow Table S6.5. The only correlation that is changed by the inclusion of this data is that between K_{leaf} Ψ_{50} and K_{stem} Ψ_{88}, which is significant for this larger dataset, indicating that the correlations across species are largely robust to the methodological differences in this compiled dataset.

	K_{root} Ψ_{50}	K_{stem} Ψ_{12}	K_{leaf} Ψ_{50}	π_{tlp}	g_S Ψ_{95}	Ψ_{min}	K_{stem} Ψ_{50}	K_{stem} Ψ_{88}	Ψ lethal
g_S Ψ_{50}	-	0.21 0.4 (17)	**0.60** * **(12)**	**0.73** *** **(40)**	**0.87** *** **(49)**	**0.87** *** **(40)**	**0.47** * **(29)**	**0.55** * **(17)**	-
K_{root} Ψ_{50}		**0.86** *** **(57)**	**0.79** ** **(11)**	**0.67** *** **(33)**	-	**0.42** ** **(50)**	**0.88** *** **(76)**	**0.79** *** **(55)**	-
K_{stem} Ψ_{12}			**0.38** ** **(58)**	**0.44** *** **(168)**	**0.52** * **(17)**	**0.35** *** **(113)**	**0.83** *** **(209)**	**0.55** *** **(192)**	-
K_{leaf} Ψ_{50}				**0.66** *** **(105)**	0.51 0.1 (12)	**0.47** *** **(71)**	**0.53** *** **(85)**	**0.29** * **(58)**	-
π_{tlp}					**0.62** *** **(40)**	**0.57** *** **(140)**	**0.49** *** **(222)**	**0.42** *** **(165)**	**0.56** * **(15)**
g_S Ψ_{95}						**0.87** *** **(27)**	**0.50** *** **(29)**	**0.77** *** **(17)**	-
Ψ_{min}							**0.53** *** **(154)**	**0.58** *** **(110)**	-
K_{stem} Ψ_{50}								**0.89** *** **(204)**	-

Table S6.7. The r^2, Aikake Information Criterion corrected for small sample size (AICc) values, and sample size (N) for models predicting each trait as a function of 1) one other trait, Ψ_{min} (minimum seasonal water potential, a measure of maximum environmental water stress), and where relevant, phylogeny, and 2) a nested model excluding the trait predictor variable. This table shows the results plotted in Fig. 6.2. P() indicates a phylogenetic predictor, and the number in the parentheses shows the number of phylogenetic eigenvectors supported by the best-fit model. Comparing the AICc values of these models determines whether two traits are more correlated than expected from concerted convergence with the environment and, where relevant, relatedness. The model containing the trait predictor was supported if **Δ**AICc (AICc of the nested model – AICc of the full model) ≥ 2. The supported model is shown in bold. For the models with more than one best-fit predictor, we calculated the independent effects of these predictors on variance in the response variables. Incorporating π_{tlp} improved prediction of K_{leaf} Ψ_{50}, as expected, and π_{tlp} accounted for 76% of the variation in K_{leaf} Ψ_{50}. Contrary to prediction, accounting for K_{root} Ψ_{50} improved prediction of the stem hydraulic traits and vice versa, and the trait predictors accounted for 72– 96% of variation in these response variables. Accounting for K_{leaf} Ψ_{50} also improved prediction of K_{stem} Ψ_{12} and Ψ_{50}, with trait predictors accounting for 55 – 78% of variation in the response variables. Prediction of K_{stem} Ψ_{12} and Ψ_{50} was also improved by accounting for π_{tlp}, and vice versa, but the trait predictors accounted for a minority of the variation in the response variables (29 – 37%), suggesting that this coordination is driven by the confounding coordination of each trait with K_{leaf} Ψ_{50}. Consistent with this, including π_{tlp} did not improve the relationship between K_{stem} Ψ_{12} and Ψ_{50} and K_{leaf} Ψ_{50}, and K_{leaf} Ψ_{50} was a stronger predictor of K_{stem} Ψ_{50} than π_{tlp} and vice versa, although K_{leaf} Ψ_{50} and π_{tlp} were equally supported predictors of K_{stem} Ψ_{12}. The drivers of the correlations between π_{tlp} and K_{root} Ψ_{50} and K_{stem} Ψ_{88} could not be resolved, since the role of trait coordination depended on the response variable. There was insufficient data to test the hypotheses for a mechanistic linkage between K_{leaf} Ψ_{50} and the stomatal traits and leaf Ψ_{lethal}, and between the stem and root hydraulic traits and plant Ψ_{lethal}. As predicted, none of the other trait correlations showed stronger coordination between traits than expected from co-selection with Ψ_{min} and shared ancestry.

Response	**Predictors: full model**	**r^2**	**Predictors : w/o trait**	**ΔAICc**	**r^2**	**N**	**Trait Effect**	**Ψ_{min} Effect**	**Phylo. Effect**
π_{tlp}	g_S Ψ_{50}, Ψ_{min}	0.63	**Ψ_{min}**	0.1	**0.55**	19			
π_{tlp}	**K_{leaf} Ψ_{50}, Ψ_{min}, P(1)**	**0.54**	Ψ_{min}, P(1)	33.8	0.22	68	74%	18%	8%
π_{tlp}	g_S Ψ_{95}, Ψ_{min}	0.53	**Ψ_{min}**	-4.6	**0.55**	19			
π_{tlp}	**K_{stem} Ψ_{12}, Ψ_{min}, P(1)**	**0.42**	Ψ_{min}, P(1)	8.8	0.34	82	31%	64%	5%
π_{tlp}	**K_{stem} Ψ_{50}, Ψ_{min}, P(1)**	**0.44**	Ψ_{min}, P(1)	12.6	0.36	103	37%	55%	8%
π_{tlp}	K_{stem} Ψ_{88}, Ψ_{min}, P(1)	0.38	**Ψ_{min}, P(1)**	1.4	**0.36**	80		88%	12%
π_{tlp}	**K_{root} Ψ_{50}, Ψ_{min}**	**0.57**	Ψ_{min}	11.9	0.26	16	76%	24%	
g_S Ψ_{50}	π_{tlp}, Ψ_{min}	0.80	**Ψ_{min}**	0.1	**0.76**	19			
g_S Ψ_{50}	K_{stem} Ψ_{12}, Ψ_{min}, P(1)	0.62	**Ψ_{min}, P(1)**	-4.6	**0.63**	13		95%	5%
g_S Ψ_{50}	K_{stem} Ψ_{50}, Ψ_{min}	0.78	**Ψ_{min}**	-1.4	**0.76**	17			

g_S Ψ_{50}	K_{stem} Ψ_{88}, Ψ_{min}, P(1)	0.55	**Ψ_{min}, P(1)**	-6.0	**0.59**	12		93%	7%
g_S Ψ_{95}	π_{tlp}, Ψ_{min}	0.67	**Ψ_{min}**	-4.6	**0.69**	19			
g_S Ψ_{95}	K_{stem} Ψ_{12}, Ψ_{min}	0.77	**Ψ_{min}**	-4.6	**0.75**	13			
g_S Ψ_{95}	K_{stem} Ψ_{50}, Ψ_{min}	0.89	**Ψ_{min}**	-2.4	**0.86**	17			
g_S Ψ_{95}	K_{stem} Ψ_{88}, Ψ_{min}	0.78	**Ψ_{min}**	-1.9	**0.75**	12			
K_{leaf} Ψ_{50}	**π_{tlp}, Ψ_{min}**	**0.52**	Ψ_{min}	30.3	0.23	68	76%	24%	
K_{leaf} Ψ_{50}	**K_{stem} Ψ_{12}, Ψ_{min}**	**0.23**	Ψ_{min}	2.5	0.13	34	56%	43%	
K_{leaf} Ψ_{50}	**K_{stem} Ψ_{50}, Ψ_{min}**	**0.40**	Ψ_{min}	10.2	0.21	45	69%	31%	
K_{leaf} Ψ_{50}	K_{stem} Ψ_{88}, Ψ_{min}	0.07	**Ψ_{min}**	-2.4	**0.09**	30			
K_{stem} Ψ_{12}	g_S Ψ_{50}, Ψ_{min}	0	**Ψ_{min}**	-6.7	**0.08**	13			
K_{stem} Ψ_{12}	**K_{leaf} Ψ_{50}, Ψ_{min}**	**0.16**	Ψ_{min}	2.5	0.05	34	78%	22%	
K_{stem} Ψ_{12}	**π_{tlp}, Ψ_{min}, P(2)**	**0.37**	Ψ_{min}, P(2)	6.4	0.31	82	31%	12%	57%
K_{stem} Ψ_{12}	g_S Ψ_{95}, Ψ_{min}	0.15	**Ψ_{min}**	-4.6	**0.08**	13			
K_{stem} Ψ_{12}	**K_{root} Ψ_{50}, Ψ_{min}**	**0.85**	Ψ_{min}	28.4	0.09	17	96%	4%	
K_{stem} Ψ_{50}	g_S Ψ_{50}, Ψ_{min}	0.47	**Ψ_{min}**	-1.4	**0.44**	17			
K_{stem} Ψ_{50}	**K_{leaf} Ψ_{50}, Ψ_{min}, P(1)**	**0.48**	Ψ_{min}, P(1)	4.1	0.42	45	55%	32%	13%
K_{stem} Ψ_{50}	**π_{tlp}, Ψ_{min}, P(4)**	**0.51**	Ψ_{min}, P(4)	16.8	0.42	103	32%	23%	55%
K_{stem} Ψ_{50}	g_S Ψ_{95}, Ψ_{min}	0.57	**Ψ_{min}**	-2.4	**0.44**	17			
K_{stem} Ψ_{50}	**K_{root} Ψ_{50}, Ψ_{min}**	**0.86**	Ψ_{min}	32.9	0.30	22	81%	19%	
K_{stem} Ψ_{88}	g_S Ψ_{50}, Ψ_{min}	0.40	**Ψ_{min}**	-4.5	**0.45**	12			
K_{stem} Ψ_{88}	K_{leaf} Ψ_{50}, Ψ_{min}	0	**Ψ_{min}**	-3.0	**0**	32			
K_{stem} Ψ_{88}	**π_{tlp}, Ψ_{min}, P(1)**	**0.37**	Ψ_{min}, P(1)	3.0	0.33	80	29%	44%	26%
K_{stem} Ψ_{88}	g_S Ψ_{95}, Ψ_{min}	0.52	**Ψ_{min}**	-1.9	**0.45**	12			
K_{stem} Ψ_{88}	**K_{root} Ψ_{50}, Ψ_{min}**	**0.80**	Ψ_{min}	15.4	0.37	16	72%	28%	
K_{root} Ψ_{50}	π_{tlp}, Ψ_{min}, P(1)	0.56	**Ψ_{min}, P(1)**	-13.5	**0.24**	16		43%	57%
K_{root} Ψ_{50}	**K_{stem} Ψ_{12}, Ψ_{min}**	**0.85**	Ψ_{min}	28.4	0.09	17	93%	7%	
K_{root} Ψ_{50}	**K_{stem} Ψ_{50}, Ψ_{min}**	**0.82**	Ψ_{min}	32.9	0.14	22	91%	9%	
K_{root} Ψ_{50}	**K_{stem} Ψ_{88}, Ψ_{min}**	**0.72**	Ψ_{min}	19.4	0.14	16	87%	13%	
π_{tlp}	K_{stem} Ψ_{12}, Ψ_{min}, K_{leaf} Ψ_{50}	0.51	**Ψ_{min}, K_{leaf} Ψ_{50}**	-2.0	0.50	32			
π_{tlp}	K_{stem} Ψ_{12}, Ψ_{min}	0.25	**Ψ_{min}, K_{leaf} Ψ_{50}**	-12.7	0.50	32			
π_{tlp}	K_{stem} Ψ_{50}, Ψ_{min}, K_{leaf} Ψ_{50}	0.43	**Ψ_{min}, K_{leaf} Ψ_{50}**	-4.1	0.44	42			
π_{tlp}	K_{stem} Ψ_{50}, Ψ_{min}	0.28	**Ψ_{min}, K_{leaf} Ψ_{50}**	-15.8	0.44	42			
K_{stem} Ψ_{12}	π_{tlp}, Ψ_{min}, K_{leaf} Ψ_{50}	0.20	**Ψ_{min}, K_{leaf} Ψ_{50}**	-2.0	0.17	32			
K_{stem} Ψ_{12}	π_{tlp}, Ψ_{min}	0.22	Ψ_{min}, K_{leaf} Ψ_{50}	1.7	0.17	32			
K_{stem} Ψ_{50}	π_{tlp}, Ψ_{min}, K_{leaf} Ψ_{50}	0.43	**Ψ_{min}, K_{leaf} Ψ_{50}**	-3.1	0.44	42			
K_{stem} Ψ_{50}	π_{tlp}, Ψ_{min}	0.35	**Ψ_{min}, K_{leaf} Ψ_{50}**	-5.6	0.46	42			

Table S6.8. The analyses for the drivers of the trait correlations from Table S6.7, repeated for the dataset including stem and root hydraulic trait values interpolated from non-sigmoidally shaped vulnerability curves. Symbols follow Table S6.7. As in the smaller dataset tested in Table S6.7, π_{tlp} and K_{leaf} Ψ_{50}, and K_{root} Ψ_{50} and K_{stem} Ψ_{12} and Ψ_{88} were more strongly coordinated than expected from concerted convergence and phylogenetic relatedness, with trait predictors accounting for 55 – 94% of explained variation in the response variables. However, the coordination of K_{stem} Ψ_{12} and Ψ_{50} with π_{tlp} and K_{leaf} Ψ_{50} observed in the smaller dataset was not found here, indicating a need to account for the methodology of constructing stem vulnerability curves in resolving the functional coordination among these traits.

Response	**Predictors: full model**	**r^2**	**Predictors: trait removed**	**ΔAICc**	**r^2**	**N**	**Trait Effect**	**Ψ_{min} Effect**	**Phylo. Effect**
π_{tlp}	g_S Ψ_{50}, Ψ_{min}	0.63	**Ψ_{min}**	0.1	**0.55**	19			
π_{tlp}	**K_{leaf} Ψ_{50}, Ψ_{min}**	**0.50**	Ψ_{min}	30.3	0.21	68	78%	22%	
π_{tlp}	g_S Ψ_{95}, Ψ_{min}	0.53	**Ψ_{min}**	-4.6	**0.55**	19			
π_{tlp}	K_{stem} Ψ_{12}, Ψ_{min}, P(2)	0.38	**Ψ_{min}, P(2)**	-3.6	**0.42**	93		90%	10%
π_{tlp}	K_{stem} Ψ_{50}, Ψ_{min}, P(1)	0.40	**Ψ_{min}, P(1)**	-3.2	**0.43**	120		96%	4%
π_{tlp}	K_{stem} Ψ_{88}, Ψ_{min}	0.36	**Ψ_{min}**	1.7	**0.34**	88			
π_{tlp}	**K_{root} Ψ_{50}, Ψ_{min}**	**0.57**	Ψ_{min}	11.9	0.26	27	76%	24%	
g_S Ψ_{50}	π_{tlp}, Ψ_{min}	0.80	**Ψ_{min}**	0.1	**0.76**	19			
g_S Ψ_{50}	K_{stem} Ψ_{12}, Ψ_{min}	0.62	**Ψ_{min}**	-6.8	**0.59**	13			
g_S Ψ_{50}	K_{stem} Ψ_{50}, Ψ_{min}	0.74	**Ψ_{min}**	-2.9	**0.74**	23			
g_S Ψ_{50}	K_{stem} Ψ_{88}, Ψ_{min}	0.51	**Ψ_{min}**	-7.5	**0.56**	12			
g_S Ψ_{95}	π_{tlp}, Ψ_{min}	0.67	**Ψ_{min}**	-4.6	**0.69**	19			
g_S Ψ_{95}	K_{stem} Ψ_{12}, Ψ_{min}	0.77	**Ψ_{min}**	-4.6	**0.75**	13			
g_S Ψ_{95}	K_{stem} Ψ_{50}, Ψ_{min}	0.81	**Ψ_{min}**	-4.9	**0.82**	23			
g_S Ψ_{95}	K_{stem} Ψ_{88}, Ψ_{min}	0.78	**Ψ_{min}**	-1.5	**0.75**	12			
K_{leaf} Ψ_{50}	**π_{tlp}, Ψ_{min}**	**0.52**	Ψ_{min}	30.3	0.23	68	76%	24%	
K_{leaf} Ψ_{50}	K_{stem} Ψ_{12}, Ψ_{min}	0.24	**Ψ_{min}**	1.5	**0.17**	39			
K_{leaf} Ψ_{50}	K_{stem} Ψ_{50}, Ψ_{min}, P(1)	0.36	**Ψ_{min}, P(1)**	-4.9	**0.43**	53		76%	14%
K_{leaf} Ψ_{50}	K_{stem} Ψ_{88}, Ψ_{min}	0.14	**Ψ_{min}**	-3.0	**0.15**	32			
K_{stem} Ψ_{12}	g_S Ψ_{50}, Ψ_{min}	0	**Ψ_{min}**	-6.7	**0.08**	13			
K_{stem} Ψ_{12}	K_{leaf} Ψ_{50}, Ψ_{min}	0.17	**Ψ_{min}**	1.5	**0.09**	39			
K_{stem} Ψ_{12}	π_{tlp}, Ψ_{min}, P(2)	0.19	**Ψ_{min}, P(2)**	-31.7	**0.43**	93		21%	79%
K_{stem} Ψ_{12}	g_S Ψ_{95}, Ψ_{min}	0.15	**Ψ_{min}**	-4.6	**0.08**	13			
K_{stem} Ψ_{12}	**K_{root} Ψ_{50}, Ψ_{min}**	**0.76**	Ψ_{min}	51.2	0.09	39	94%	6%	

K_{stem} Ψ_{50}	g_S Ψ_{50}, Ψ_{min}	0.23	**Ψ_{min}**	-2.8	**0.22**	23			
K_{stem} Ψ_{50}	K_{leaf} Ψ_{50}, Ψ_{min}	0.38	**Ψ_{min}, P(1)**	-15.6	**0.55**	53		80%	20%
K_{stem} Ψ_{50}	π_{tlp}, Ψ_{min}, P(1)	0.29	**Ψ_{min}, P(1)**	-8.5	**0.23**	106		43%	57%
K_{stem} Ψ_{50}	g_S Ψ_{95}, Ψ_{min}	0.19	**Ψ_{min}**	-3.8	**0.22**	23			
K_{stem} Ψ_{50}	K_{root} Ψ_{50}, Ψ_{min}, P(1)	0.83	**Ψ_{min}, P(1)**	2.4	**0.84**	49		79%	21%
K_{stem} Ψ_{88}	g_S Ψ_{50}, Ψ_{min}	0.53	**Ψ_{min}**	-8.8	**0.57**	10			
K_{stem} Ψ_{88}	K_{leaf} Ψ_{50}, Ψ_{min}	0	**Ψ_{min}**	-3.0	**0**	32			
K_{stem} Ψ_{88}	π_{tlp}, Ψ_{min}	0.24	**Ψ_{min}**	1.7	**0.21**	88			
K_{stem} Ψ_{88}	g_S Ψ_{95}, Ψ_{min}	0.52	**Ψ_{min}**	-4.9	**0.45**	12			
K_{stem} Ψ_{88}	**K_{root} Ψ_{50}, Ψ_{min}**	**0.76**	Ψ_{min}	26.2	0.24	40	83%	17%	
K_{root} Ψ_{50}	π_{tlp}, Ψ_{min}, P(1)	0.56	**Ψ_{min}, P(1)**	-13.5	**0.24**	27		43%	57%
K_{root} Ψ_{50}	**K_{stem} Ψ_{12}, Ψ_{min}**	**0.77**	Ψ_{min}	51.6	0.10	39	94%	6%	
K_{root} Ψ_{50}	K_{stem} Ψ_{50}, Ψ_{min}, P(1)	0.77	**Ψ_{min}, P(1)**	1.5	**0.76**	49		76%	14%
K_{root} Ψ_{50}	**K_{stem} Ψ_{88}, Ψ_{min}**	**0.60**	Ψ_{min}	26.6	0.19	40	55%	45%	

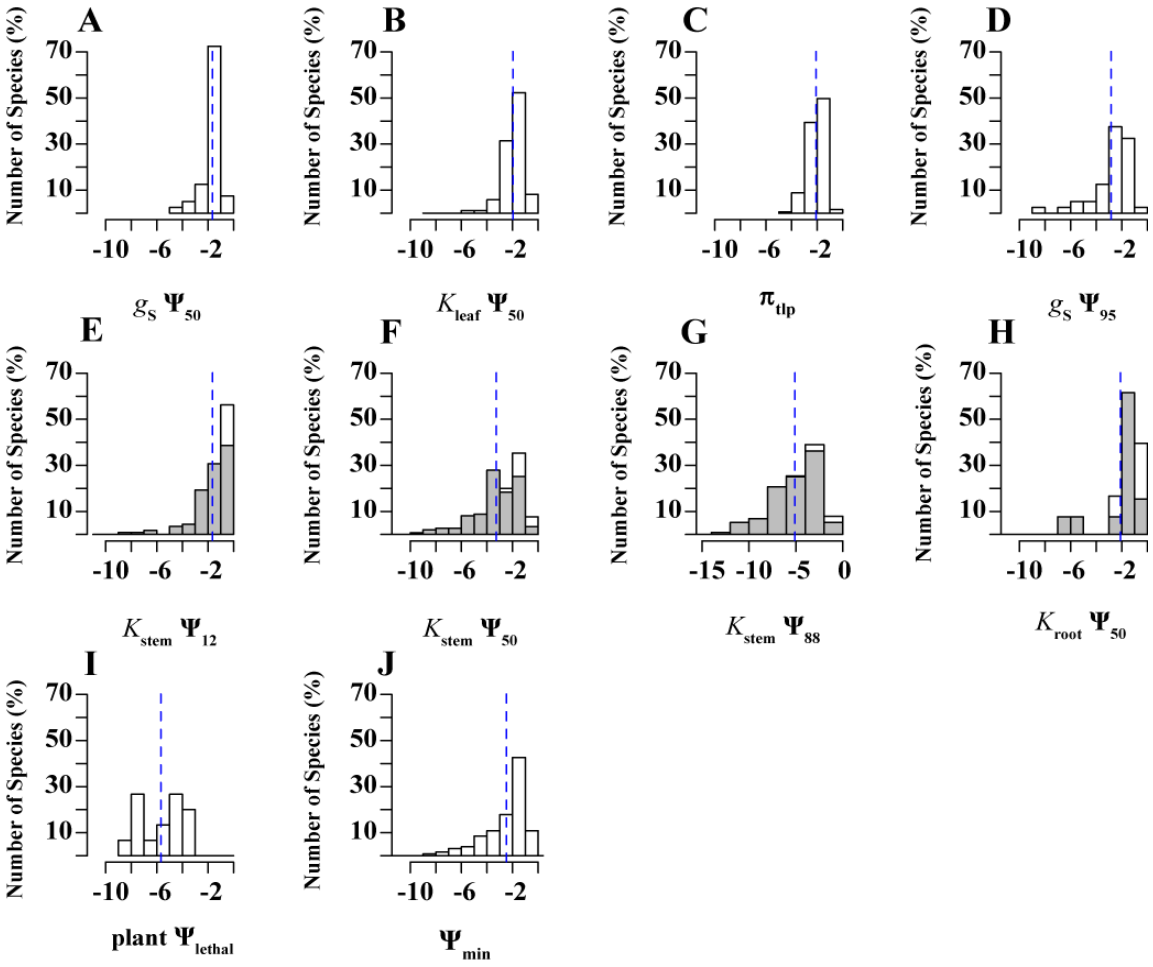
A
B
C
D
E
F
G
H
I
J
Number of Species (%)
70
50
30
10
-10
-6
-2
-15
-5
0
g_S Ψ_{50}
K_{leaf} Ψ_{50}
π_{tlp}
g_S Ψ_{95}
K_{stem} Ψ_{12}
K_{stem} Ψ_{50}
K_{stem} Ψ_{88}
K_{root} Ψ_{50}
plant Ψ_{lethal}
Ψ_{min}

Figure S6.1.

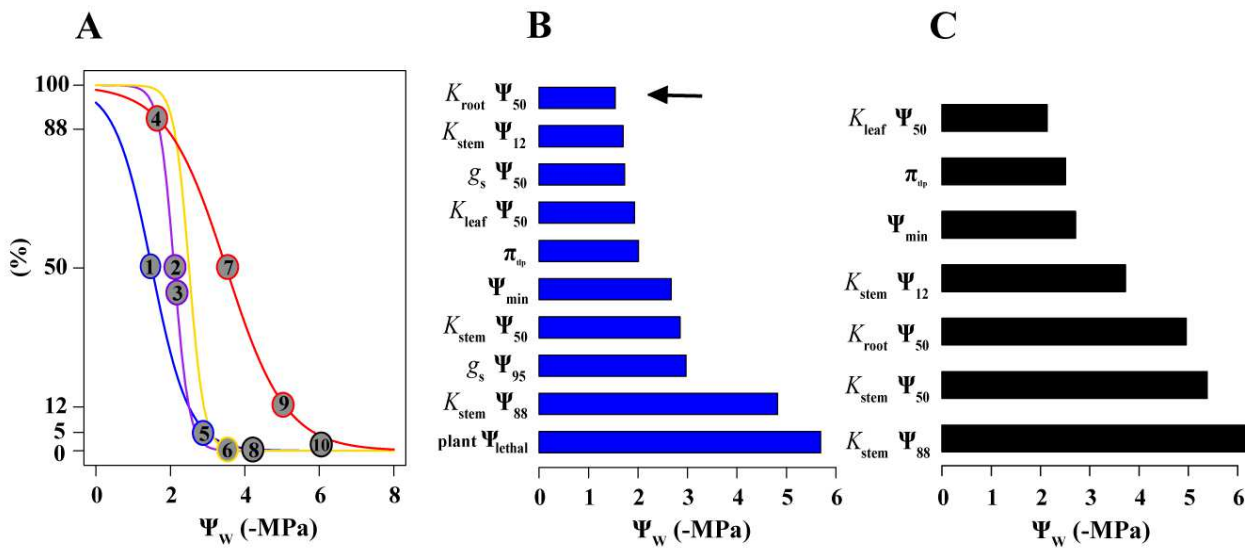
A
B
C
100
88
50
12
5
0
(%)
0
2
4
6
8
Ψ_W (-MPa)
K_root Ψ_50
K_stem Ψ_12
g_s Ψ_50
K_leaf Ψ_50
π_tlp
Ψ_min
K_stem Ψ_50
g_s Ψ_95
K_stem Ψ_88
plant Ψ_lethal
0
1
2
3
4
5
6
Ψ_W (-MPa)
K_leaf Ψ_50
π_tlp
Ψ_min
K_stem Ψ_12
K_root Ψ_50
K_stem Ψ_50
K_stem Ψ_88
0
1
2
3
4
5
6
Ψ_W (-MPa)

Figure S6.2.

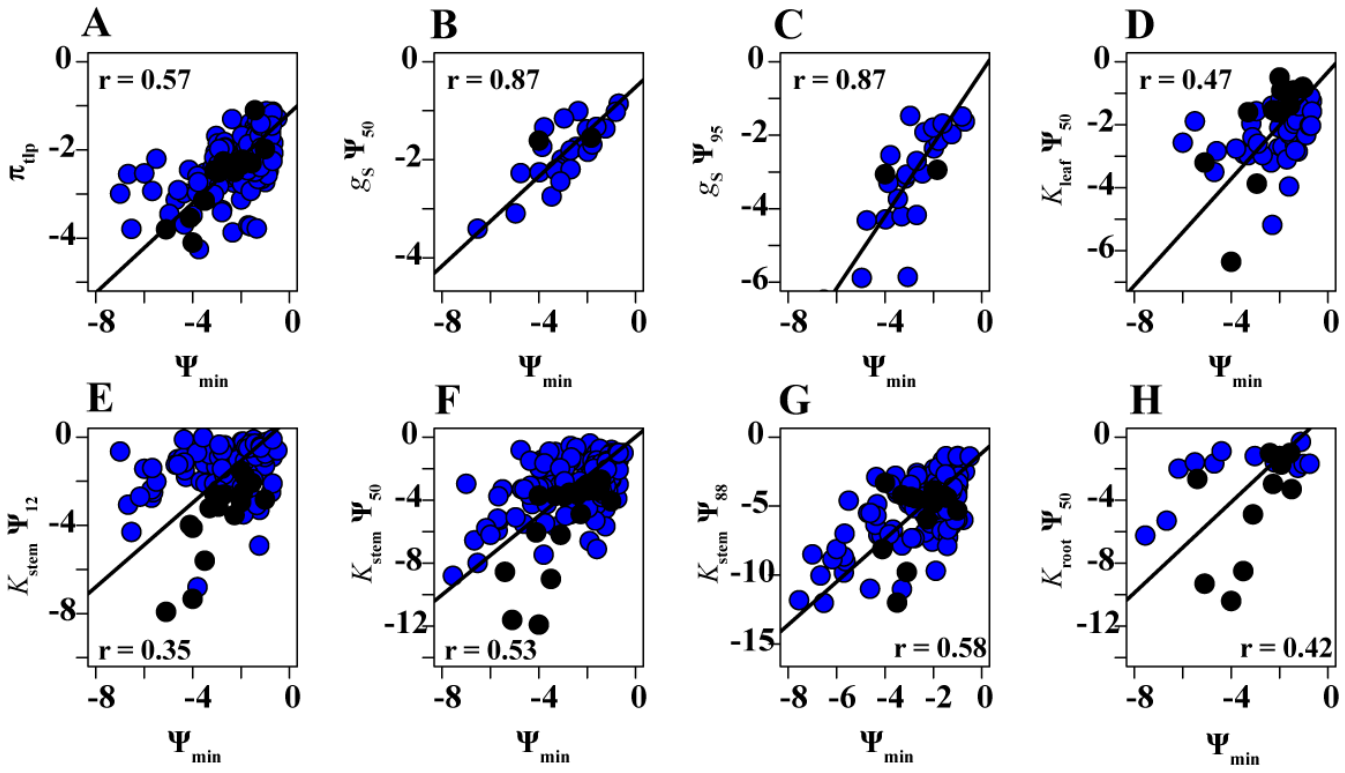
A
r = 0.57
π_{tlp}
Ψ_{min}
B
r = 0.87
$g_S \Psi_{50}$
Ψ_{min}
C
r = 0.87
$g_S \Psi_{95}$
Ψ_{min}
D
r = 0.47
$K_{leaf} \Psi_{50}$
Ψ_{min}
E
r = 0.35
$K_{stem} \Psi_{12}$
Ψ_{min}
F
r = 0.53
$K_{stem} \Psi_{50}$
Ψ_{min}
G
r = 0.58
$K_{stem} \Psi_{88}$
Ψ_{min}
H
r = 0.42
$K_{root} \Psi_{50}$
Ψ_{min}

Figure S6.3.

REFERENCES

META-ANALYSIS DATA REFERENCES*

1. Cheung YNS, Tyree MT, & Dainty J (1975) Water relations parameters on single leaves obtained in a pressure bomb and some ecological interpretations. *Can. J. Bot.* 53:1342-1346.
2. Melcher PJ*, et al.* (2012) Measurements of stem xylem hydraulic conductivity in the laboratory and field. *Methods Eco. Evol.* 3:685-694.
3. Sack L & Scoffoni C (2012) Measurement of leaf hydraulic conductance and stomatal conductance and their responses to irradiance and dehydration using the Evaporative Flux Method (EFM). *J Vis Exo* (70).
4. Brodribb T, Holbrook NM, Edwards EJ, & Gutierrez MV (2003) Relations between stomatal closure, leaf turgor and xylem vulnerability in eight tropical dry forest trees. *Plant Cell Environ.* 26:443-450.
5. Burnham KP & Anderson DR (2010) *Model selection and multi-model inference: a practical information-theoretic approach* (Springer) 2nd Ed p 488.
6. Guyot G, Scoffoni C, & Sack L (2012) Combined impacts of irradiance and dehydration on leaf hydraulic conductance: insights into vulnerability and stomatal control. *Plant Cell Environ* 35(5):857-871.
7. Baltzer JL, Davies SJ, Bunyavejchewin S, & Noor NSM (2008) The role of desiccation tolerance in determining tree species distributions along the Malay–Thai Peninsula. *Funct. Ecol.* 22(2):221-231.
8. Nilsen ET, Sharifi MR, & Rundel PW (1984) Comparative water relations of phreatophytes in the Sonoran Desert of California. *Ecology* 65(3):767-778.

9. Pockman WT & Sperry JS (2000) Vulnerability to xylem cavitation and the distribution of Sonoran Desert vegetation. *Am. J. Bot.* 87(9):1287-1299.

10. Nardini A, Peda G, & La Rocca N (2012) Trade-offs between leaf hydraulic capacity and drought vulnerability: morpho-anatomical bases, carbon costs and ecological consequences. *New Phytol.* 196:788-798.

11. Tissier J, Lambs L, Peltier J-P, & Marigo G (2004) Relationships between hydraulic traits and habitat preference for six Acer species occurring in the French Alps. *Ann. For. Sci.* 61:81-86.

12. Alder NN, Sperry JS, & Pockman WT (1996) Root and stem xylem embolism, stomatal conductance, and leaf turgor in *Acer grandidentatum* populations along a soil moisture gradient. *Oecologia* 105:293-301.

13. Martinez-Vilalta J, Prat E, Oliveras I, & Pinol J (2002) Xylem hydraulic properties of roots and stems of nine Mediterranean woody species. *Oecologia* 133:19-29.

14. Kubiske ME & Abrams MD (1994) Ecophysiological analysis of woody species in contrasting temperate communities during wet and dry years. *Oecologia* 98(3-4):303-312.

15. Pratt RB & Black RA (2006) Do invasive trees have a hydraulic advantage over native trees? *Biol Invasions* 8(6):1331-1341.

16. Hacke UG, Stiller V, Sperry JS, Pittermann J, & McCulloh KA (2001) Cavitation fatigue. embolism and refilling cycles can weaken the cavitation resistance of xylem. *Plant Physiol.* 125:779-786.

17. Johnson DM, McCulloh KA, Meinzer FC, Woodruff DR, & Eissenstat DM (2011) Hydraulic patterns and safety margins, from stem to stomata, in three eastern U.S. tree species. *Tree Physiol* 31(6):659-668.

18. Maherali H, Moura CF, Caldeira MC, Willson CJ, & Jackson RB (2006) Functional coordination between leaf gas exchange and vulnerability to xylem cavitation in temperate forest trees. *Plant Cell Environ.* 29(4):571-583.

19. Yang S & Tyree MT (1993) Hydraulic resistance in *Acer saccharum* shoots and its influence on leaf water potential and transpiration. *Tree Physiol.* 12:231-242.

20. Melcher PJ, Zwieniecki MA, & Holbrook NM (2003) Vulnerability of xylem vessels to cavitation in sugar maple. Scaling from individual vessels to whole branches. *Plant Physiol* 131(4):1775-1780.

21. Tyree MT & Dixon MA (1986) Water stress induced cavitation and embolism in some woody plants. *Physiol. Plantarum* 66(3):397-405.

22. Sperry JS & Hacke UG (2004) Analysis of circular bordered pit function I. Angiosperm vessels with homogenous pit membranes. *Am. J. Bot.* 91(3):369-385.

23. Tsuda M & Tyree MT (1997) Whole-plant hydraulic resistance and vulnerability segmentation in *Acer saccharinum*. *Tree Physiol.* 17:351-357.

24. Zhu SD, Song JJ, Li RH, & Ye Q (2013) Plant hydraulics and photosynthesis of 34 woody species from different successional stages of subtropical forests. *Plant Cell Environ* 36(4):879-891.

25. Chapotin SM, Razanameharizaka JH, & Holbrook NM (2006) Water relations of baobab trees (Adansonia spp. L.) during the rainy season: does stem water buffer daily water deficits? *Plant Cell Environ.* 29(6):1021-1032.

26. Davis SD & Mooney HA (1986) Tissue water relations of four co-occurring chaparral shrubs. *Oecologia* 70:527-535.

27. Jacobsen AL, Ewers FW, Pratt RB, Paddock WA, 3rd, & Davis SD (2005) Do xylem fibers affect vessel cavitation resistance? *Plant Physiol* 139(1):546-556.

28. Bucci SJ*, et al.* (2013) The stem xylem of Patagonian shrubs operates far from the point of catastrophic dysfunction and is additionally protected from drought-induced embolism by leaves and roots. *Plant Cell Environ* 36(12):2163-2174.

29. Scholz FG, Bucci SJ, Arias N, Meinzer FC, & Goldstein G (2012) Osmotic and elastic adjustments in cold desert shrubs differing in rooting depth: coping with drought and subzero temperatures. *Oecologia*.

30. Hao GY*, et al.* (2008) Stem and leaf hydraulics of congeneric tree species from adjacent tropical savanna and forest ecosystems. *Oecologia* 155(3):405-415.

31. Scoffoni C, Rawls M, McKown A, Cochard H, & Sack L (2011) Decline of leaf hydraulic conductance with dehydration: relationship to leaf size and venation architecture. *Plant Physiol* 156(2):832-843.

32. Chen J-W, Zhang Q, & Cao K-F (2008) Inter-species variation of photosynthetic and xylem hydraulic traits in the deciduous and evergreen Euphorbiaceae tree species from a seasonally tropical forest in south-western China. *Ecol. Res.* 24(1):65-73.

33. Lo Gullo MA, Nardini A, Trifilo P, & Salleo S (2005) Diurnal and seasonal variations in leaf hydraulic conductance in evergreen and deciduous trees. *Tree Physiol.* 25.

34. Mitchell PJ, Veneklaas EJ, Lambers H, & Burgess SSO (2008) Leaf water relations during summer water deficit: differential responses in turgor maintenance and variation

in leaf structure among different plant communities in south-western Australia. *Plant Cell Environ.* 31(12):1791-1802.

35. Hacke UG & Sauter JJ (1996) Drought-lnduced xylem dysfunction in petioles, branches, and roots of *Populus balsamifera* L. and *Alnus glutinosa* (L.) Gaertn. *Plant Physiol.* 111:413-417.

36. Sperry JS, Nichols KL, Sullivan JEM, & Eastlack SE (1994) Xylem embolism in ring-porous, diffuse-porous, and coniferous trees of northern Utah and interior Alaska. *Ecology* 75(6):1736-1752.

37. Fu PL*, et al.* (2012) Stem hydraulic traits and leaf water-stress tolerance are co-ordinated with the leaf phenology of angiosperm trees in an Asian tropical dry karst forest. *Ann Bot* 110(1):189-199.

38. Feild TS, Chatelet DS, & Brodribb T (2009) Ancestral xerophobia: a hypothesis on the whole plant ecophysiology of early angiosperms. *Geobiology* 7:237-264.

39. Hacke UG*, et al.* (2007) Water transport in vesselless angiosperms: conducting efficiency and cavitation safety. *Int. J. Plant Sci.* 168(8):1113-1126.

40. Johnson DM, Domec JC, Woodruff DR, McCulloh KA, & Meinzer FC (2013) Contrasting hydraulic strategies in two tropical lianas and their host trees. *Am J Bot* 100(2):374-383.

41. Johnson DM, Woodruff DR, McCulloh KA, & Meinzer FC (2009) Leaf hydraulic conductance, measured in situ, declines and recovers daily: leaf hydraulics, water potential and stomatal conductance in four temperate and three tropical tree species. *Tree Physiol* 29(7):879-887.

42. Castell C & Terradas J (1995) Water relations, gas exchange and growth of dominant and suppressed shoots of *Arbutus unedo* L. *Tree Physiol.* 15(6):405-409.

43. Jacobsen AL, Pratt RB, Davis SD, & Ewers FW (2008) Comparative community physiology: nonconvergence in water relations among three semi-arid shrub communities. *New Phytol* 180(1):100-113.

44. Bowman WD & Roberts SW (1985) Seasonal and diurnal water relations adjustments in three evergreen chaparral shrubs. *Ecology* 66(3):738-742.

45. Sperry JS, Hacke UG, Feild TS, Sano Y, & Sikkema EH (2007) Hydraulic consequences of vessel evolution in angiosperms. *Int. J. Plant Sci.* 168(8):1127-1139.

46. Blackman CJ, Brodribb TJ, & Jordan GJ (2009) Leaf hydraulics and drought stress: response, recovery and survivorship in four woody temperate plant species. *Plant Cell Environ* 32(11):1584-1595.

47. Blackman CJ, Brodribb TJ, & Jordan GJ (2010) Leaf hydraulic vulnerability is related to conduit dimensions and drought resistance across a diverse range of woody angiosperms. *New Phytol.* 188(4):1113-1123.

48. Hacke UG, Sperry JS, & Pittermann J (2000) Drought experience and cavitation resistance in six shrubs from the Great Basin, Utah. *Basic Appl Ecol* 1(1):31-41.

49. Sperry JS & Hacke UG (2002) Desert shrub water relations with respect to soil characteristics and plant functional type. *Funct. Ecol.* 16:367-378.

50. Zhu S-D & Cao K-F (2009) Hydraulic properties and photosynthetic rates in co-occurring lianas and trees in a seasonal tropical rainforest in southwestern China. *Plant Ecol.* 204(2):295-304.

51. Villagra M, Campanello PI, Bucci SJ, & Goldstein G (2013) Functional relationships between leaf hydraulics and leaf economic traits in response to nutrient addition in subtropical tree species. *Tree Physiol* 33(12):1308-1318.

52. Villagra M, Campanello PI, Montti L, & Goldstein G (2013) Removal of nutrient limitations in forest gaps enhances growth rate and resistance to cavitation in subtropical canopy tree species differing in shade tolerance. *Tree Physiol* 33(3):285-296.

53. Carter JL, Veneklaas EJ, Colmer TD, Eastham J, & Hatton TJ (2006) Contrasting water relations of three coastal tree species with different exposure to salinity. *Physiol. Plantarum* 127:360-373.

54. Froend RH & Drake PL (2006) Defining phreatophyte response to reduced water availability: preliminary investigations on the use of xylem cavitation vulnerability in *Banksia* woodland species. *Aust J Bot* 54(2):173.

55. Sperry JS & Saliendra NZ (1994) intra- and inter-plant variation in xyiem cavitation in *Betula occidentalis*. *Plant Cell Environ.* 17:1233-1241.

56. Alder NN, Pockman WT, Sperry JS, & Nusimer S (1997) Use of centrifugal force in the study of xylem cavitation. *J. Exp. Bot.* 48(308):665-674.

57. Pothier D & Margolis HA (1990) Changes in the water relations of balsam fir and white birch saplings after thinning. *Tree Physiol.* 6:371-380.

58. Chen JW, Zhang Q, Li XS, & Cao KF (2009) Independence of stem and leaf hydraulic traits in six Euphorbiaceae tree species with contrasting leaf phenology. *Planta* 230(3):459-468.

59. Bucci SJ*, et al.* (2006) Nutrient availability constrains the hydraulic architecture and water relations of savannah trees. *Plant Cell Environ* 29(12):2153-2167.

60. Domec JC*, et al.* (2006) Diurnal and seasonal variation in root xylem embolism in neotropical savanna woody species: impact on stomatal control of plant water status. *Plant Cell Environ.* 29:26-35.

61. Feild TS*, et al.* (2011) The ecophysiology of xylem hydraulic constraints by "basal" vessels in *Canella winterana* (Canellaceae). *Int. J. Plant Sci.* 172(7):879-888.

62. Litvak E, McCarthy HR, & Pataki DE (2012) Transpiration sensitivity of urban trees in a semi-arid climate is constrained by xylem vulnerability to cavitation. *Tree Physiol* 32(4):373-388.

63. Bhaskar R, Valiente-Banuet A, & Ackerly DD (2007) Evolution of hydraulic traits in closely related species pairs from Mediterranean and nonMediterranean environments of North America. *New Phytol* 176(3):718-726.

64. Pratt RB, Jacobsen AL, Ewers FW, & Davis SD (2007) Relationships among xylem transport, biomechanics and storage in stems and roots of nine Rhamnaceae species of the California chaparral. *New Phytol* 174(4):787-798.

65. Pratt RB*, et al.* (2007) Life history type and water stress tolerance in nine California chaparral species (Rhamnaceae). *Ecol Monogr* 77(2):239-253.

66. Pratt RB, Jacobsen AL, Mohla R, Ewers FW, & Davis SD (2008) Linkage between water stress tolerance and life history type in seedlings of nine chaparral species (Rhamnaceae). *J. Ecol.* 96(6):1252-1265.

67. Davis SD*, et al.* (2002) Shoot dieback during prolonged drought in Ceanothus (Rhamnaceae) chaparral of California: a possible case of hydraulic failure. *Am. J. Bot.* 89(5):820-828.

68. Lo Gullo MA, Nardini A, Trifilo P, & Salleo S (2003) Changes in leaf hydraulics and stomatal conductance following drought stress and irrigation in *Ceratonia siliqua* (Carob tree). *Physiol. Plantarum* 117:186-194.

69. Choat B*, et al.* (2012) Global convergence in the vulnerability of forests to drought. *Nature* 491:752-755.

70. Nardini A, Salleo S, & Raimondo F (2003) Changes in leaf hydraulic conductance correlate with leaf vein embolism in *Cercis siliquastrum* L. *Trees- Struct Func* 17(6):529-534.

71. Jacobsen AL, Pratt RB, Davis SD, & Ewers FW (2007) Cavitation resistance and seasonal hydraulics differ among three arid Californian plant communities. *Plant Cell Environ.* 30(12):1599-1609.

72. Choat B, Sack L, & Holbrook NM (2007) Diversity of hydraulic traits in nine *Cordia* species growing in tropical forests with contrasting precipitation. *New Phytol.* 175(4):686-698.

73. Roberts SW, Strain BR, & Knoerr KR (1980) Seasonal patterns of leaf water relations in four co-occurring forest tree species: parameters from pressure-volume curves. *Oecologia* 46:330-337.

74. Domec JC, Schafer K, Oren R, Kim HS, & McCarthy HR (2010) Variable conductivity and embolism in roots and branches of four contrasting tree species and their impacts on whole-plant hydraulic performance under future atmospheric CO(2) concentration. *Tree Physiol* 30(8):1001-1015.

75. Johnson DM, McCulloh KA, Woodruff DR, & Meinzer FC (2012) Evidence for xylem embolism as a primary factor in dehydration-induced declines in leaf hydraulic conductance. *Plant Cell Environ* 35(4):760-769.

76. Poot P & Veneklaas EJ (2012) Species distribution and crown decline are associated with contrasting water relations in four common sympatric eucalypt species in southwestern Australia. *Plant Soil* 364(1-2):409-423.

77. Brodribb TJ & Holbrook NM (2006) Declining hydraulic efficiency as transpiring leaves desiccate: two types of response. *Plant Cell Environ* 29(12):2205-2215.

78. Sobrado MA (1996) Embolism vulnerability of an evergreen tree. *Biol. Plantarum* 38(2):297-301.

79. Nolf M*, et al.* (2015) Stem and leaf hydraulic properties are finely coordinated in three tropical rain forest tree species. *Plant Cell Environ* 38(12):2652-2661.

80. Zolfaghar S, Villalobos-Vega R, Cleverly J, & Eamus D (2015) Co-ordination among leaf water relations and xylem vulnerability to embolism of Eucalyptus trees growing along a depth-to-groundwater gradient. *Tree Physiol* 35(7):732-743.

81. Martorell S*, et al.* (2014) Plasticity of vulnerability to leaf hydraulic dysfunction during acclimation to drought in grapevines: an osmotic-mediated process. *Physiol Plant*.

82. Arndt SK*, et al.* (2015) Vulnerability of native savanna trees and exotic Khaya senegalensis to seasonal drought. *Tree Physiol* 35(7):783-791.

83. Aranda I, Gil L, & Pardos J (1996) Seasonal water relations of three broadleaved species (*Fagus sylvatica* L., *Quercus petraea* (Mattuschka) Liebl. and *Quercus pyrenaica* Willd.) in a mixed stand in the centre of the Iberian Peninsula. *Forest Ecol. Manag.* 84(1-3):219-229.

84. Hacke UG & Sauter JJ (1995) Vulnerability of xylem to embolism in relation to leaf water potential and stomatal conductance in *Fagus sylvatica* f. purpurea and *Populus balsamifera*. *J. Exp. Bot.* 46(290):1177-1183.

85. Cochard H*, et al.* (2005) Evaluation of a new centrifuge technique for rapid generation of xylem vulnerability curves. *Physiol. Plantarum* 124(4):410-418.

86. Cochard H, Lemoine D, & Dreyer E (1999) The effects of acclimation to sunlight on the xylem vulnerability to embolism in *Fagus sylvatica* L. *Plant Cell Environ.* 22:101-108.

87. Rewald B (2008) Impact of climate change-induced drought on tree root hydraulic properties and competition belowground. PhD (Georg-August-Universität, Göttingen, Germany).

88. Hao G-Y, Sack L, Wang A-Y, Cao K-F, & Goldstein G (2010) Differentiation of leaf water flux and drought tolerance traits in hemiepiphytic and non-hemiepiphytic Ficus tree species. *Funct. Ecol.* 24(4):731-740.

89. Choat B, Jansen S, Zwieniecki MA, Smets E, & Holbrook NM (2004) Changes in pit membrane porosity due to deflection and stretching: the role of vestured pits. *J Exp Bot* 55(402):1569-1575.

90. Tognetti R, Longobusso A, & Raschi A (1999) Seasonal embolism and xylem vulnerability in deciduous and evergreen Mediterranean trees influenced by proximity to a carbon dioxide spring. *Tree Physiol.* 19:271-277.

91. Brodribb TJ & Holbrook NM (2003) Stomatal closure during leaf dehydration, correlation with other leaf physiological traits. *Plant Physiol.* 132(4):2166-2173.

92. Jarbeau JA, Ewers FW, & Davis SD (1995) The mechanism of water-stress-induced embolism in two species of chaparral shrubs. *Plant Cell Environ.* 18(2):189-196.

93. Tobin M, Lopez OR, & Kursar TA (1999) Responses of tropical understory plants to a severe drought: tolerance and avoidance of water stress. *Biotropica* 31(4):570-578.

94. Lopez OR, Kursar TA, Cochard H, & Tyree MT (2005) Interspecific variation in xylem vulnerability to cavitation among tropical tree and shrub species. *Tree Physiol.* 25:1553-1562.

95. Kikuta SB, Lo Gullo MA, Nardini A, Richter H, & Salleo S (1997) Ultrasound acoustic emissions from dehydrating leaves of deciduous and evergreen trees. *Plant Cell Environ.* 20:1361-1390.

96. Cochard H, Coll L, Le Roux X, & Ameglio T (2002) Unraveling the effects of plant hydraulics on stomatal closure during water stress in walnut. *Plant Physiol.* 128(1):282-290.

97. Bucci SJ*, et al.* (2008) Water relations and hydraulic architecture in Cerrado trees: adjustments to seasonal changes in water availability and evaporative demand. *Brazil J Plant Physiol* 20(3):233-245.

98. Roberts SW & Knoerr KR (1977) Components of water potential estimated from xylem pressure measurements in five tree species. *Oecologia* 28:191-202.

99. Gibbons JM & Newberry DM (2002) Drought avoidance and the effect of local topography on trees in the understorey of Bornean lowland rain forest. *Plant Ecol.* 164:1-18.

100. Tyree MT, Patino S, & Becker P (1998) Vulnerability to drought-induced embolism of Bornean heath and dipterocarp forest trees. *Tree Physiol.* 18:583-588.

101. Bucci SJ*, et al.* (2012) Hydraulic differences along the water transport system of South American Nothofagus species: do leaves protect the stem functionality? *Tree Physiol* 32(7):880-893.

102. Machado JL & Tyree MT (1994) Patterns of hydraulic architecture and water relations of two tropical canopy trees with contrasting leaf phenologies: *Ochroma pyramidale* and *Psuedobombax septenatum*. *Tree Physiol.* 14:219-240.

103. Duhme F & Hinckley TM (1992) Daily and seasonal variation in water relations of macchia shrubs and trees in France (Montpellier) and Turkey (Antalya). *Vegetatio* 99-100:185-198.

104. Trifilò P, Lo Gullo MA, Nardini A, Pernice F, & Salleo S (2007) Rootstock effects on xylem conduit dimensions and vulnerability to cavitation of Olea europaea L. *Trees* 21(5):549-556.

105. Serrano L, Penuelas J, Ogaya R, & Save R (2005) Tissue-water relations of two co-occurring evergreen Mediterranean species in response to seasonal and experimental drought conditions. *J Plant Res* 118(4):263-269.

106. Blackman CJ*, et al.* (2014) Leaf hydraulic vulnerability to drought is linked to site water availability across a broad range of species and climates. *Ann Bot* 114(3):435-440.

107. Gries D*, et al.* (2003) Growth and water relations of *Tamarix ramosissima* and *Populus euphratica* on Taklamakan desert dunes in relation to depth to a permanent water table. *Plant Cell Environ.* 26:725-736.

108. Thomas FM*, et al.* (2008) Regulation of the water status in three co-occurring phreatophytes at the southern fringe of the Taklamakan Desert. *J Plant Ecol* 5(4):227-235.

109. Pezeshki SR & Hinckley TM (1998) Water relations characteristics of *Alnus rubra* and *Populus trichocarpa*: responses to field drought *Can. J. For. Res.* 18:1159-1166.

110. Pita P, Canas I, Soria F, Ruiz F, & Toval G (2005) Use of physiological traits in tree breeding for improved yield in drought-prone environments. The case of *Eucalyptus globulus*. *Forest Syst.* 14(3):383-393.

111. Hukin D, Cochard H, Dreyer E, Le Thiec D, & Bogeat-Triboulot MB (2005) Cavitation vulnerability in roots and shoots: does Populus euphratica Oliv., a poplar from arid areas of Central Asia, differ from other poplar species? *J Exp Bot* 56(418):2003-2010.

112. Hultine KR*, et al.* (2006) Influence of soil texture on hydraulic properties and water relations of a dominant warm-desert phreatophyte. *Tree Physiol.* 26:313-323.

113. Meinzer FC*, et al.* (2008) Coordination of leaf and stem water transport properties in tropical forest trees. *Oecologia* 156(1):31-41.

114. Torrecillas A, Galego R, Pérez-Pastor A, & Ruiz-Sánchez MC (1999) Gas exchange and water relations of young apricot plants under drought conditions. *J. Ag. Sci.* 132(4):445-452.

115. Cochard H, Barigah TS, Kleinhentz M, & Eshel A (2008) Is xylem cavitation resistance a relevant criterion for screening drought resistance among *Prunus* species? *J Plant Phys* 165:976-982.

116. Wright SJ, Machado JL, Mulkey SS, & Smith AP (1992) Drought acclimation among tropical forest shrubs (*Psychotria*, Rubiaceae). *Oecologia* 89:457-463.

117. Iovi K, Kolovou C, & Kyparissis A (2009) An ecophysiological approach of hydraulic performance for nine Mediterranean species. *Tree Physiol* 29(7):889-900.

118. Bahari ZA, Pallardy SG, & Parker WC (1985) Photosynthesis, water relations, and drought adaptation in six woody species of oak-hickory forests in central Missouri. *Forest Sci* 31(3):557-569.

119. McElrone AJ, Pockman WT, Martinez-Vilalta J, & Jackson RB (2004) Variation in xylem structure and function in stems and roots of trees to 20 m depth. *New Phytol.* 163(3):507-517.

120. Sala A & Tenhunen JD (1994) Site-specific water relations and stomatal response of *Quercus ilex* in a Mediterranean watershed. *Tree Physiol.* 14:601-617.

121. Tognetti R, Longobusso A, & Raschi A (1998) Vulnerability of xylem to embolism in relation to plant hydraulic resistance in *Quercus pubescens* and *Quercus ilex* co-occurring in a Mediterranean coppice stand in central Italy. *New Phytol.* 139:437-447.

122. Limousin JM, Longepierre D, Huc R, & Rambal S (2010) Change in hydraulic traits of Mediterranean Quercus ilex subjected to long-term throughfall exclusion. *Tree Physiol* 30(8):1026-1036.

123. Cochard H, Breda N, & Granier A (1996) Whole tree hydraulic conductance and water loss regulation in Quercus during drought: evidence for stomatal control of embolism? *Ann For Sci* 53:197-206.

124. Cochard H, Breda N, Granier A, & Aussenac G (1992) Vulnerability to air embolism of three European oak species (*Quercus petraea* (Matt) Liebl, *Q pubescens* Willd, *Q robur* L). *Annuals of Forest Science* 49:225-233.

125. Glatzel G (1983) Mineral nutrition and water relations of hemiparasitic mistletoes: a question of partitioning. Experiments with *Loranthus europaeus* on *Quercus petraea* and *Quercus robur*. *Oecologia* 56:193-201.

126. Cochard H & Tyree MT (1990) Xylem dysfunction in *Quercus*: vessel sizes, tyloses, cavitation and seasonal changes in embolism. *Tree Physiol.* 6:393-407.

127. Matzner SL, Rice KJ, & Richards JH (2001) Intra-specific variation in xylem cavitation in interior live oak (*Quercus wislizenii* A. DC.). *J. Exp. Bot.* 52(357):783-789.

128. Cordero RA & Nilsen ET (2002) Effects of summer drought and winter freezing on stem hydraulic conductivity of *Rhododendron* species from contrasting climates. *Tree Physiol.* 22:919-928.

129. Pratt RB*, et al.* (2005) Mechanisms for tolerating freeze-thaw stress of two evergreen chaparral species: *Rhus ovata* and *Malosma laurina* (Anacardiaceae). *Am. J. Bot.* 92(7):1102-1113.

130. Stratton L, Goldstein G, & Meinzer FC (2000) Stem water storage capacity and efficiency of water transport: their functional significance in a Hawaiian dry forest. *Plant Cell Environ.* 23:99-106.

131. Zhu S-D, Chen Y-J, Cao K-F, & Ye Q (2015) Interspecific variation in branch and leaf traits among three Syzygium tree species from different successional tropical forests. *Funct Plant Biol* 42(4):423.

132. Ayup M, Hao X, Chen Y, Li W, & Su R (2012) Changes of xylem hydraulic efficiency and native embolism of Tamarix ramosissima Ledeb. seedlings under different drought stress conditions and after rewatering. *S Afr J Bot* 78:75-82.

133. Ganthaler A & Mayr S (2015) Dwarf shrub hydraulics: two vaccinium species (*Vaccinium myrtillus, Vaccinium vitis-idaea*) of the European Alps compared. *Physiol Plant*.

134. Nardini A & Salleo S (2000) Limitation of stomatal conductance by hydraulic traits: sensing or preventing xylem cavitation? *Trees* 15(1):14-24.

135. Wheeler JK, Sperry JS, Hacke UG, & Hoang N (2005) Inter-vessel pitting and cavitation in woody Rosaceae and other vesselled plants: a basis for a safety versus efficiency trade-off in xylem transport. *Plant Cell Environ.* 28:800-812.

136. Tombesi S, Nardini A, Farinelli D, & Palliotti A (2014) Relationships between stomatal behavior, xylem vulnerability to cavitation and leaf water relations in two cultivars of Vitis vinifera. *Physiol Plant* 152(3):453-464.

137. Klein T (2014) The variability of stomatal sensitivity to leaf water potential across tree species indicates a continuum between isohydric and anisohydric behaviours. *Funct. Ecol.* 28(6):1313-1320.

138. Cochard H (2006) Cavitation in trees. *Comptes Rendus Physique* 7(9-10):1018-1026.

139. Hacke UG & Jansen S (2009) Embolism resistance of three boreal conifer species varies with pit structure. *New Phytol* 182(3):675-686.

140. Brodribb TJ, McAdam SA, Jordan GJ, & Martins SC (2014) Conifer species adapt to low-rainfall climates by following one of two divergent pathways. *Proc Natl Acad Sci U S A* 111(40):14489-14493.

141. Yoder BJ (1983) Comparative water relations of *Abies grandis*, *Abies concolor* and their hybrids. Master of Science (Oregon State University).

142. Sperry JS & Ikeda T (1997) Xylem cavitation in roots and stems of Douglas-fir and white fir. *Tree Physiol.* 17:275-280.

143. Bouche PS*, et al.* (2014) A broad survey of hydraulic and mechanical safety in the xylem of conifers. *J Exp Bot* 65(15):4419-4431.

144. Hacke UG, Sperry JS, & Pittermann J (2004) Analysis of circular bordered pit function II. Gymnosperm tracheids with torus-margo pit membrances. *Am. J. Bot.* 91(3):386-400.

145. Piñol J & Sala A (2000) Ecological Implications of Xylem Cavitation for Several Pinaceae in the Pacific Northern USA. *Funct. Ecol.* 14(5):538-545.

146. Scholz FG, Bucci SJ, & Goldstein G (2014) Strong hydraulic segmentation and leaf senescence due to dehydration may trigger die-back in Nothofagus dombeyi under severe droughts: a comparison with the co-occurring Austrocedrus chilensis. *Trees* 28(5):1475-1487.

147. Willson CJ, Manos PS, & Jackson RB (2008) Hydraulic traits are influenced by phylogenetic history in the drought-resistance, invasive genus *Juniperus* (Cupressaceae). *Am. J. Bot.* 95(3):299-314.

148. Tognetti R, Raschi A, & Jones MB (2000) Seasonal patterns of tissue water relations in three Mediterranean shrubs co-occurring at a natural CO2 spring. *Plant Cell Environ.* 23(12):1341-1351.

149. Beikircher B & Mayr S (2008) The hydraulic architecture of *Juniperus communis* L. ssp. communis: shrubs and trees compared. *Plant Cell Environ* 31(11):1545-1556.

150. Mayr S, Hacke UG, Schmid P, Schwienbacher F, & Gruber A (2006) Frost drought in conifers at the alpine timberline: xylem dysfunction and adaptations. *Ecology* 87(12):3175-3185.

151. Ogle K, Barber JJ, Willson C, & Thompson B (2009) Hierarchical statistical modeling of xylem vulnerability to cavitation. *New Phytol* 182(2):541-554.

152. Woodruff DR*, et al.* (2015) Linking nonstructural carbohydrate dynamics to gas exchange and leaf hydraulic behavior in Pinus edulis and Juniperus monosperma. *New Phytol* 206(1):411-421.

153. Meinzer FC, Woodruff DR, Marias DE, McCulloh KA, & Sevanto S (2014) Dynamics of leaf water relations components in co-occurring iso- and anisohydric conifer species. *Plant Cell Environ* 37(11):2577-2586.

154. Miller RF & Shultz LM (1987) Water relations and leaf morphology of *Juniperus occidentalis* in the Northern Great Basin. *Forest Sci* 33(3):690-706.

155. Nowak RS, Moore DJ, & Tausch RJ (1999) Ecophysiological patterns of pinyon and juniper. *USDA Forest Service Proceedings* RMRS-P-9:35-46.

156. Badalotti A, Anfodillo T, & Grace J (2000) Evidence of osmoregulation in *Larix decidua* at Alpine treeline and comparative responses to water availability of two co-occurring evergreen species. *Ann. For. Sci.* 57(7):623-633.

157. Gross K & Koch W (1991) Water relations of *Picea abies*. I. Comparison of water relations parameters of spruce shoots examined at the end of the vegetation period and in winter. *Physiol. Plantarum* 83:290-295.

158. Mayr S, Wolfschwenger M, & Bauer H (2002) Winter-drought induced embolism in Norway spruce (*Picea abies*) at the Alpine timberline. *Physiol. Plantarum* 115:74-80.

159. Mayr S, Rothart B, & Damon B (2003) Hydraulic efficiency and safety of leader shoots and twigs in Norway spruce growing at the alpine timberline. *J. Exp. Bot.* 54(392):2563-2568.

160. Mayr S, Schwienbacher F, & Bauer H (2003) Winter at the alpine timberline. Why does embolism occur in norway spruce but not in stone pine? *Plant Physiol* 131(2):780-792.

161. Lu P, Biron P, Granier A, & Cochard H (1996) Water relations of adult Norway spruce (*Picea abies* (L) Karst) under soil drought in the Vosges mountains: whole-tree hydraulic conductance, xylem embolism and water loss regulation. *Ann For Sci* 53:113-121.

162. Major JE & Johnsen KH (1999) Shoot water relations of mature black spruce families displaying a genotype x environment interaction in growth rate. II. Temporal trends and response to varying soil water conditions. *Tree Physiol.* 19(6):375-382.

163. Andersen CP & McLaughlin SB (1991) Seasonal changes in shoot water relations of *Picea rubens* at two high elevation sites in the Smoky Mountains. *Tree Physiol.* 8:11-21.

164. Sperry JS & Tyree MT (1990) Water-stress-induced xylem embolism in three species of conifers. *Plant Cell Environ.* 13:427-436.

165. Linton MJ, Sperry JS, & Williams DG (1998) Limits to water transport in *Juniperus osteosperma* and *Pinus edulis*: implications for drought tolerance and regulation of transpiration. *Funct. Ecol.* 12:905-911.

166. Gonzalez-Benecke CA, Martin TA, & Peter GF (2010) Hydraulic architecture and tracheid allometry in mature *Pinus palustris* and *Pinus elliottii* trees. *Tree Physiol* 30(3):361-375.

167. Oliveras I*, et al.* (2003) Hydraulic properties of *Pinus halepensis*, *Pinus pinea* and *Tetraclinis articulata* in a dune ecosystem of Eastern Spain. *Plant Ecol.* 169:131-141.

168. Johnson DM, Meinzer FC, Woodruff DR, & McCulloh KA (2009) Leaf xylem embolism, detected acoustically and by cryo-SEM, corresponds to decreases in leaf hydraulic conductance in four evergreen species. *Plant Cell Environ* 32(7):828-836.

169. Charra-Vaskou K*, et al.* (2012) Hydraulic efficiency and safety of vascular and non-vascular components in Pinus pinaster leaves. *Tree Physiol* 32(9):1161-1170.

170. Stout D & Sala A (2003) Xylem vulnerability to cavitation in *Pseudotsuga menziesii* and *Pinus ponderosa* from contrasting habitats. *Tree Physiol.* 23:43-50.

171. Maherali H & DeLucia EH (2000) Xylem conductivity and vulnerability to cavitation of ponderosa pine growing in contrasting climates. *Tree Physiol.* 20:859-867.

172. Domec JC, Warren JM, Meinzer FC, Brooks JR, & Coulombe R (2004) Native root xylem embolism and stomatal closure in stands of Douglas-fir and ponderosa pine: mitigation by hydraulic redistribution. *Oecologia* 141(1):7-16.

173. Poyatos R*, et al.* (2007) Plasticity in hydraulic architecture of Scots pine across Eurasia. *Oecologia* 153(2):245-259.

174. Domec JC*, et al.* (2009) Acclimation of leaf hydraulic conductance and stomatal conductance of *Pinus taeda* (loblolly pine) to long-term growth in elevated CO(2) (free-air CO(2) enrichment) and N-fertilization. *Plant Cell Environ* 32(11):1500-1512.

175. Andrews SF, Flanagan LB, Sharp EJ, & Cai T (2012) Variation in water potential, hydraulic characteristics and water source use in montane Douglas-fir and lodgepole pine trees in southwestern Alberta and consequences for seasonal changes in photosynthetic capacity. *Tree Physiol* 32(2):146-160.

176. Woodruff DR, Meinzer FC, & Lachenbruch B (2008) Height-related trends in leaf xylem anatomy and shoot hydraulic characteristics in a tall conifer: safety versus efficiency in water transport. *New Phytol* 180(1):90-99.

177. Domec JC & Gartner BL (2012) Age- and position-related changes in hydraulic versus mechanical dysfunction of xylem: inferring the design criteria for Douglas-fir wood structure. *Tree Physiol.* 22:91-104.

178. Ishii HR, Azuma W, Kuroda K, Sillett SC, & Watling J (2014) Pushing the limits to tree height: could foliar water storage compensate for hydraulic constraints in *Sequoia sempervirens*? *Funct. Ecol.* 28(5):1087-1093.

179. Ambrose AR, Sillett SC, & Dawson TE (2009) Effects of tree height on branch hydraulics, leaf structure and gas exchange in California redwoods. *Plant Cell Environ* 32(7):743-757.

180. Zhang YJ, Rockwell FE, Wheeler JK, & Holbrook NM (2014) Reversible deformation of transfusion tracheids in *Taxus baccata* Is associated with a reversible decrease in leaf hydraulic conductance. *Plant Physiol* 165(4):1557-1565.

181. Collier DE & Boyer MG (1989) The water relations of *Thuja occidentalis* L. from two sites of contrasting moisture availability. *Bot. Gaz.* 150(4):445-448.

182. Benjamini Y & Hochberg Y (1995) Controlling the false discovery rate: a practical and powerful approach to multiple testing. *J R Stat Soc B* 57(1):289-300.

183. Bartlett MK, Scoffoni C, & Sack L (2012) The determinants of leaf turgor loss point and prediction of drought tolerance of species and biomes: a global meta-analysis. *Ecol. Lett.* 15:393-405.

184. Maherali H, Pockman WT, & Jackson RB (2004) Adaptive variation in the vulnerability of woody plants to xylem cavitation. *Ecology* 85(8):2184-2199.

185. Sperry JS, Christman MA, Torres-Ruiz JM, Taneda H, & Smith DD (2012) Vulnerability curves by centrifugation: is there an open vessel artefact, and are 'r' shaped curves necessarily invalid? *Plant Cell Environ* 35(3):601-610.

[*] = The meta-analysis references are presented in the numbered *Proceedings of the National Academy of Sciences* format so that the supplementary data can be clearly and concisely shown in Table S6.1.

TEXT REFERENCES

Baltzer, J. L., S. J. Davies, S. Bunyavejchewin, and N. S. M. Noor. 2008. The role of desiccation tolerance in determining tree species distributions along the Malay–Thai Peninsula. Functional Ecology **22**:221-231.

Bartlett, M. K., C. Scoffoni, R. Ardy, Y. Zhang, S. Sun, K. Cao, and L. Sack. 2012a. Rapid determination of comparative drought tolerance traits: using an osmometer to predict turgor loss point. Methods in Ecology and Evolution **3**:880-888.

Bartlett, M. K., C. Scoffoni, and L. Sack. 2012b. The determinants of leaf turgor loss point and prediction of drought tolerance of species and biomes: a global meta-analysis. Ecology Letters **15**:393-405.

Benjamini, Y., and Y. Hochberg. 1995. Controlling the false discovery rate: a practical and powerful approach to multiple testing. Journal of the Royal Statistical Society B **57**:289-300.

Bhaskar, R., and D. D. Ackerly. 2006. Ecological relevance of minimum seasonal water potentials. Physiologia Plantarum **127**:353-359.

Bivand, R., and G. Piras. 2015. Comparing implementations of estimation methods for spatial econometrics. Journal of Statistical Software **63**:1-36.

Blackman, C. J., T. J. Brodribb, and G. J. Jordan. 2009. Leaf hydraulics and drought stress: response, recovery and survivorship in four woody temperate plant species. Plant Cell Environ **32**:1584-1595.

Blackman, C. J., T. J. Brodribb, and G. J. Jordan. 2012. Leaf hydraulic vulnerability influences species' bioclimatic limits in a diverse group of woody angiosperms. Oecologia **168**:1-10.

Brodribb, T., N. M. Holbrook, E. J. Edwards, and M. V. Gutierrez. 2003. Relations between stomatal closure, leaf turgor and xylem vulnerability in eight tropical dry forest trees. Plant Cell Environ **26**:443-450.

Brodribb, T. J., and N. M. Holbrook. 2003. Stomatal closure during leaf dehydration, correlation with other leaf physiological traits. Plant Physiology **132**:2166-2173.

Brodribb, T. J., and N. M. Holbrook. 2004. Stomatal protection against hydraulic failure: a comparison of coexisting ferns and angiosperms. New Phytologist **162**:663-670.

Bucci, S. J., F. G. Scholz, P. I. Campanello, L. Montti, M. Jimenez-Castillo, F. A. Rockwell, L. L. Manna, P. Guerra, P. L. Bernal, O. Troncoso, J. Enricci, M. N. Holbrook, and G. Goldstein. 2012. Hydraulic differences along the water transport system of South American Nothofagus species: do leaves protect the stem functionality? Tree Physiol **32**:880-893.

Buckley, T. N. 2005. The control of stomata by water balance. New Phytol **168**:275-292.

Buckley, T. N. 2015. The contributions of apoplastic, symplastic and gas phase pathways for water transport outside the bundle sheath in leaves. Plant Cell Environ **38**:7-22.

Buckley, T. N., and K. A. Mott. 2002. Dynamics of stomatal water relations during the humidity response: implications of two hypothetical mechanisms. Plant Cell Environ **25**:407-419.

Choat, B., C. R. Brodersen, and A. J. McElrone. 2015. Synchrotron X-ray microtomography of xylem embolism in *Sequoia sempervirens* saplings during cycles of drought and recovery. New Phytologist **205**:1095 - 1105.

Choat, B., S. Jansen, T. Brodribb, H. Cochard, S. Delzon, R. Bhaskar, S. J. Bucci, T. S. Feild, S. M. Gleason, U. G. Hacke, A. L. Jacobsen, F. Lens, H. Maherali, J. Martinez-Vilalta, S. Mayr, M. Mencuccini, P. J. Mitchell, A. Nardini, J. Pittermann, R. B. Pratt, J. S. Sperry, M. Westoby, I. J. Wright, and A. E. Zanne. 2012. Global convergence in the vulnerability of forests to drought. Nature **491**:752-755.

Cochard, H., L. Coll, X. Le Roux, and T. Ameglio. 2002. Unraveling the effects of plant hydraulics on stomatal closure during water stress in walnut. Plant Physiology **128**:282-290.

Cochard, H., and S. Delzon. 2013. Hydraulic failure and repair are not routine in trees. Annals of Forest Science **70**:659-661.

Delzon, S., and H. Cochard. 2014. Recent advances in tree hydraulics highlight the ecological significance of the hydraulic safety margin. New Phytologist **203**:355-358.

Guyot, G., C. Scoffoni, and L. Sack. 2012. Combined impacts of irradiance and dehydration on leaf hydraulic conductance: insights into vulnerability and stomatal control. Plant Cell Environ **35**:857-871.

Jackson, R. B., J. S. Sperry, and T. E. Dawson. 2000. Root water uptake and transport: using physiological processes in global predictions. Trends in Plant Science **5**:1360-1385.

Johnson, D. M., K. A. McCulloh, D. R. Woodruff, and F. C. Meinzer. 2012. Hydraulic safety margins and embolism reversal in stems and leaves: why are conifers and angiosperms so different? Plant Sci **195**:48-53.

Johnson, D. M., D. R. Woodruff, K. A. McCulloh, and F. C. Meinzer. 2009. Leaf hydraulic conductance, measured in situ, declines and recovers daily: leaf hydraulics, water potential and stomatal conductance in four temperate and three tropical tree species. Tree Physiol **29**:879-887.

Klein, T. 2014. The variability of stomatal sensitivity to leaf water potential across tree species indicates a continuum between isohydric and anisohydric behaviours. Functional Ecology **28**:1313-1320.

Klein, T., D. Yakir, N. Buchmann, and J. M. Grunzweig. 2014. Towards an advanced assessment of the hydrological vulnerability of forests to climate change-induced drought. New Phytologist **201**:712-716.

Li, S., M. Feifel, Z. Karimi, B. Schuldt, B. Choat, and S. Jansen. 2015. Leaf gas exchange performance and the lethal water potential of five European species during drought. Tree Physiol.

Lo Gullo, M. A., A. Nardini, P. Trifilo, and S. Salleo. 2003. Changes in leaf hydraulics and stomatal conductance following drought stress and irrigation in *Ceratonia siliqua* (Carob tree). Physiologia Plantarum **117**:186-194.

Maherali, H., C. F. Moura, M. C. Caldeira, C. J. Willson, and R. B. Jackson. 2006. Functional coordination between leaf gas exchange and vulnerability to xylem cavitation in temperate forest trees. Plant, Cell and Environment **29**:571-583.

Maherali, H., W. T. Pockman, and R. B. Jackson. 2004. Adaptive variation in the vulnerability of woody plants to xylem cavitation. Ecology **85**:2184-2199.

McDowell, N. G., R. A. Fisher, C. Xu, J. C. Domec, T. Holtta, D. S. Mackay, J. S. Sperry, A. Boutz, L. Dickman, N. Gehres, J. M. Limousin, A. Macalady, J. Martinez-Vilalta, M.

Mencuccini, J. A. Plaut, J. Ogee, R. E. Pangle, D. P. Rasse, M. G. Ryan, S. Sevanto, R. H. Waring, A. P. Williams, E. A. Yepez, and W. T. Pockman. 2013. Evaluating theories of drought-induced vegetation mortality using a multimodel-experiment framework. New Phytol **200**:304-321.

Morris, H., L. Plavcova, P. Cvecko, E. Fichtler, M. A. F. Gillingham, H. I. Martinez-Cavrera, D. J. McGlinn, E. Wheeler, J. Zheng, K. Zieminska, and S. Jansen. 2016. A global analysis of parenchyma tissue fractions in secondary xylem of seed plants. New Phytologist **209**:1553-1565.

Murray, K., and M. M. Conner. 2009. Methods to quantify variable importance: implications for the analysis of noisy ecological data. Ecology **90**:348-355.

Nardini, A., and J. Luglio. 2014. Leaf hydraulic capacity and drought vulnerability: possible trade-offs and correlations with climate across three major biomes. Functional Ecology **28**:810-818.

Patterson, T. B., and T. J. Givnish. 2002. Phylogeny, concerted convergence, and phylogenetic niche conservatism in the core Liliales: insights from rbcL and ndhF sequence data. Evolution **56**:233-252.

Sack, L., and N. M. Holbrook. 2006. Leaf hydraulics. Annual Review of Plant Biology **57**:361-381.

Salleo, S., A. Nardini, F. Pitt, and M. A. Lo Gullo. 2000. Xylem cavitation and hydraulic control of stomatal conductance in laurel (*Laurus nobilis* L.). Plant Cell Environ **23**:71-79.

Scoffoni, C., C. Vuong, S. Diep, H. Cochard, and L. Sack. 2014. Leaf shrinkage with dehydration: coordination with hydraulic vulnerability and drought tolerance. Plant Physiol **164**:1772-1788.

Sheffield, J., and E. F. Wood. 2007. Characteristics of global and regional drought, 1950–2000: Analysis of soil moisture data from off-line simulation of the terrestrial hydrologic cycle. Journal of Geophysical Research **112**.

Skelton, R. P., A. G. West, and T. E. Dawson. 2015. Predicting plant vulnerability to drought in biodiverse regions using functional traits. Proc Natl Acad Sci U S A.

Sperry, J. S., M. A. Christman, J. M. Torres-Ruiz, H. Taneda, and D. D. Smith. 2012. Vulnerability curves by centrifugation: is there an open vessel artefact, and are 'r' shaped curves necessarily invalid? Plant Cell Environ **35**:601-610.

Tyree, M. T., and F. W. Ewers. 1991. The hydraulic architecture of trees and other woody plants. New Phytologist **119**:345-360.

Urli, M., A. J. Porte, H. Cochard, Y. Guengant, R. Burlett, and S. Delzon. 2013. Xylem embolism threshold for catastrophic hydraulic failure in angiosperm trees. Tree Physiol **33**:672-683.

Walsh, C., and R. Mac Nally. 2013. hier.part: Hierarchical Partitioning. R package version 1.0-4. http://CRAN.R-project.org/package=hier.part.

Warton, D. I., R. A. Duursma, D. S. Falster, and S. Taskinen. 2012. smatr 3- an R package for estimation and inference about allometric lines. Methods in Ecology and Evolution **3**:257-259.

Webb, C. O., D. D. Ackerly, and S. W. Kembel. 2008. Phylocom: software for the analysis of phylogenetic community structure and trait evolution. Bioinformatics **24**:2098-2100.

CHAPTER 7

CONCLUSIONS AND FUTURE DIRECTIONS

Climate change is expected to exacerbate drought for many plants, making drought tolerance a key driver of species and ecosystem responses. However, predicting these responses from organ-level drought tolerance requires a greater understanding of how plant physiological processes impact ecology. My thesis seeks to address several fundamental gaps in this understanding by characterizing the ecological impacts of interspecific and intraspecific variation in leaf drought tolerance.

My first chapter compares the predictive ability of several leaf physiology and functional traits for ecological drought tolerance and applies sensitivity analyses and meta-analyses to identify the cellular drivers of these traits. The leaf water potential at turgor loss point, or wilting (π_{tlp}), was significantly correlated with species' habitat water supply; indeed, more strongly so than the functional trait leaf mass per unit area (*LMA*), which is often used as a proxy for stress tolerance. The relative water content at turgor loss point (RWC_{tlp}) was not correlated with species distributions, and appears to be fairly similar across species. The cellular composition trait the osmotic potential at full hydration (π_o), or the solute concentration of a hydrated leaf cell, is the main driver of π_{tlp}, indicating that plants achieve greater leaf drought tolerance (a more negative π_{tlp} value) by accumulating solutes in the leaf cells. Contrary to prediction, the anatomy trait cell wall modulus of elasticity, or cell wall stiffness (ε), played no direct role in driving leaf drought tolerance, but instead a stiffer cell wall helped to maintain a greater RWC_{tlp}, and contributed to a tougher, sclerophyllous leaf phenotype that protects against nutrient, mechanical, and herbivory stresses independent of drought tolerance. These findings clarify biogeographic trends and the underlying basis of drought tolerance parameters, resolving decades of controversy in the plant

ecophysiology literature.

The role of π_o in driving π_{tlp} allowed me to develop a new method to rapidly estimate π_{tlp} from measurements of π_o. The π_{tlp} is typically interpolated from the leaf pressure-volume relationship, wherein drying leaves are repeatedly assessed for leaf water potential and leaf water content. Constructing these curves for 5-6 leaves, which is typically sufficient replication for reliable determination of a species mean, requires 1-2 days, which generally prohibits sampling large species sets. In Chapter 3, I optimized existing methods for measurements of π_o using vapor-pressure osmometry of freeze-thawed leaf discs from 30 species, and developed the first regression relationships to accurately estimate pressure–volume curve values of both π_o and π_{tlp} from osmometer values (r^2 = 0.80 and 0.85, respectively). This method enables accurate measurements of drought tolerance 30x faster than the pressure-volume curve method. This 95% reduction in effort leads me to expect it to have wide application for predicting species responses to climate variability and for assessing ecological and evolutionary variation in drought tolerance.

Plasticity in plant traits has been predicted to strongly influence species' drought responses, but broad patterns in plasticity had not been previously examined for drought tolerance traits. In Chapter 4, I conducted the first global analysis of plasticity in π_{tlp} for 283 wild and crop species in ecosystems worldwide. Plasticity in π_{tlp} ($\Delta\pi_{tlp}$) was widely prevalent across species but moderate (-0.44 MPa), accounting for 16% of dry season π_{tlp} values. The π_{tlp} values in the wet season were a considerably stronger predictor of π_{tlp} values under water stress across species of wild plants, while $\Delta\pi_{tlp}$ accounted for major differences in post-drought π_{tlp} for cultivars of certain crops. Climate was correlated with pre- and post-drought π_{tlp}, but not $\Delta\pi_{tlp}$. Thus, despite the wide prevalence of plasticity in this trait, π_{tlp} measured in one season can

reliably characterize most species' drought tolerances and distributions relative to water supply.

Chapters 2 and 4 showed π_{tlp} is an important driver of species distributions at a global scale. However, drought tolerance traits are also expected to significantly impact species distributions within ecosystems, through their effects on species' water requirements and competitive interactions. In Chapter 5, I tested hypotheses about the trait and environmental drivers of several key community assembly processes by identifying the strongest correlates of their characteristic spatial patterns in trait variation. For 43 evergreen tree species in a 20-ha seasonal tropical rainforest plot in Xishuangbanna, China, I compared the ability of drought-tolerance traits, hydraulic condutivity, and commonly measured leaf functional traits to predict the spatial patterns expected from the assembly processes of habitat associations, niche-overlap-based competition, and hierarchical competition. I distinguished the neighborhood-scale (0–20 m) patterns expected from competition from larger-scale habitat associations with a wavelet method. Species' drought tolerance and habitat variables related to soil water supply were strong drivers of habitat associations, and drought tolerance showed a significant spatial signal for influencing competition. Overall, the traits most strongly associated with habitat, as quantified using multivariate models, were leaf density, π_{tlp}, and stem hydraulic conductivity. At neighborhood scales, species spatial associations were positively correlated with similarity in π_{tlp}, consistent with hierarchical competition, wherein 'superior' drought tolerant species would outcompete drought sensitive species. Although the correlation between π_{tlp} and interspecific spatial associations was weak ($r^2 < 0.01$), this showed a persistent influence of drought tolerance on neighborhood interactions and community assembly. Quantifying the full impact of traits on competitive interactions in forests may require incorporating plasticity among individuals within species, especially among specific life stages, and moving beyond individual traits to integrate

the impact of multiple traits on whole-plant performance and resource demand.

Indeed, plant drought tolerance and water usage is determined by multiple traits, but the relationships among drought tolerance traits, either within individual plants or across species, have not been evaluated for general patterns across plant diversity. In Chapter 6, I meta-analyzed the available data for stomatal closure, wilting, declines in hydraulic conductivity in the leaves, stems, and roots, and plant mortality for 300 woody angiosperm and 49 gymnosperm species. These analyses resolved the general temporal sequence of drought responses within plants under increasing water stress, and the drivers of correlations among traits across species. The sequence addresses several key debates in the literature, showing that, for the angiosperms, 95% stomatal closure generally occurs after wilting and at similar water potentials to 50% loss of stem hydraulic conductivity. The root and stem hydraulic vulnerability traits occur at more drought tolerant positions along the gymnosperm sequence. Across species, the analyses show functional coordination among the hydraulic traits and the wilting point, or turgor loss point, beyond that expected from shared ancestry and co-selection with environmental water stress. These correlations provide a framework for hypothesizing plant responses to a wide range of water stress from one or two sampled traits, increasing the ability to rapidly characterize drought tolerance across diverse species. This resolution of the relationships among the drought tolerance traits also provides crucial, empirically-supported insight into representing variation in multiple traits in models of plant and ecosystem responses to drought.

These findings provide insight into the effects of inter- and intra-specific variation in leaf drought tolerance on ecology, including species distributions relative to water availability at global and within-ecosystem scales, competitive interactions among co-occurring species, and co-selection among functionally similar traits. However, accurately predicting ecosystem

responses to future climate scenarios is likely to require mechanistic models that scale up from these organ-level traits to plant-level gas exchange, then to species-level growth and survival rates, and then to species interactions and compositional changes at the ecosystem level (McDowell et al. 2013; Sperry & Love 2015). At this time, the decline in stem hydraulic conductivity with decreasing stem water potential is the only drought tolerance trait that has been explicitly incorporated into plant performance models (McDowell et al. 2013). While these models produced reasonable predictions of tree mortality rates under water stress, other studies have shown that more realistic representations of stomatal behavior are also needed to reduce uncertainty in model predictions (Powell et al. 2013; Rowland et al. 2015). Linking drought tolerance to species' population growth and survival rates is currently mainly limited by a lack of understanding as to how drought causes mortality (McDowell et al. 2008). However, both modeling and empirical approaches are making considerable progress in resolving the drought tolerance traits, environmental conditions, and biotic pressures that induce given mechanisms for plant death (Skelton et al. 2015; Mencuccini et al. 2015; Anderegg et al. 2016), as well as the capacity of different plant species to recover instead of die from severe drought stress (Urli et al. 2013; Trifilo et al. 2015; Li et al. 2016). At the ecosystem level, there is currently no detailed understanding of how drought tolerance traits will impact species interactions or community species composition. However, a promising approach to this problem has recently emerged in Farrior et al. 2015, which predicts the effects of competition for water on ecosystem carbon storage under varying precipitation regimes. Incorporating drought tolerance traits into this competition framework has strong potential to improve predictions of species interactions under climate change. Overall, predicting species and ecosystem responses to drought is a critical challenge that requires ideas from across science, from the biophysics of an air bubble forming in

a single xylem vessel to the long-term ecological dynamics governing the slow disappearance over decades of drought sensitive species from drying forests.

REFERENCES

Anderegg, W. R. L., Klein, T., Bartlett, M. K., Sack, L., Pellegrini, A. F. A., Choat, B. & Jansen, S. (2016). Meta-analysis reveals that hydraulic traits explain cross-species patterns of drought-induced tree mortality across the globe. *PNAS,* 113(18), 5024-5029.

Farrior, C. E., Rodriguez-Iturbe, I., Dybzinski, R., Levin, S. A. & Pacala, S. W. (2015). Decreased water limitation under elevated CO2 amplifies potential for forest carbon sinks. *PNAS.,* 112(23), 7213-7218.

Li, S., Feifel, M., Karimi, Z., Schuldt, B., Choat, B. & Jansen, S. (2016). Leaf gas exchange performance and the lethal water potential of five European species during drought. *Tree Physiol.,* 36(2), 179-192.

McDowell, N. G., *et al.* (2008). Mechanisms of plant survival and mortality during drought: why do some plants survive while others succumb to drought? *New Phytol.,* 178, 719-739.

McDowell, N. G., *et al.* (2013). Evaluating theories of drought-induced vegetation mortality using a multimodel–experiment framework. *New Phytol*., 200, 304-321.

Mencuccini, M., Minunno, F., Salmon, Y., Martinez-Vilalta, J. & Holtta, T. (2015). Coordination of physiological traits involved in drought-induced mortality of woody plants. *New Phytol.,* 208, 396-409.

Powell, T. L. *et al.* (2013). Confronting model predictions of carbon fluxes with measurements of Amazon forests subjected to experimental drought. *New Phytol.*, 200, 350-365.

Rowland, L. *et al.* (2015). Modelling climate change responses in tropical forests: similar productivity estimates across five models, but different mechanisms and responses. *Geosci. Model Dev.,*8, 1097-1110.

Skelton, R. P., West, A. G. & Dawson, T. E. (2015). Predicting plant vulnerability to drought in

biodiverse regions using functional traits. *PNAS,* 112, 5744-5749.

Sperry, J. S. & Love, D. M. (2015). What plant hydraulics can tell us about responses to climate-change droughts. *New Phytol.,* 207, 14-27.

Trifilo, P., Nardini, A., Lo Gullo, M. A., Barbera, P. M., Savi, T. & Raimondo, F. (2015). Diurnal changes in embolism rate in nine dry forest trees: relationships with species-specific xylem vulnerability, hydraulic strategy and wood traits. *Tree Physiol.,* 35(7), 694-705.

Urli, M., Porte, A. J., Cochard, H., Guengant, Y., Burlett, R. & Delzon, S. (2013). Xylem embolism threshold for catastrophic hydraulic failure in angiosperm trees. *Tree Physiol.,* 33, 672-683.

APPENDICES

SUPPLEMENTAL METHODS 2.1

Derivation and verification of new fundamental equations

Eqns 1 and 2 are new analytical solutions of the well-known pressure-volume curve equations, which characterize the relationship between total leaf water potential (Ψ_{leaf}) and cellular water volume in a leaf undergoing dehydration (Fig. 2.1A, B). In a pressure-volume curve, Ψ_{leaf} declines with relative water content (*RWC*; an easily measured proxy for relative water volume) as dehydration reduces both components of Ψ_{leaf}: the turgor potential supporting the cell walls (Ψ_P) and the solute potential of the cell contents (Ψ_S; Tyree & Hammel 1972; Richter 1978). As *RWC* decreases, the Ψ_P becomes inadequate to support the cell walls, and beyond the point of zero turgor, Ψ_S continues to become more negative with increasing symplastic osmotic concentration, in inverse proportion to *RWC*. When the *RWC* declines to the apoplastic fraction (a_f), the Ψ_S and Ψ_{leaf} tend to negative infinity.

In pressure-volume curve plots, *RWC* is conventionally expressed as *R*, or 100 – *RWC* (units %) to emphasize the drying process, and water potential is plotted as $1/\Psi$ to enable determination of turgor loss point (π_{tlp}) as the inflection point at which the Ψ_S curve becomes linear, and extrapolation of that section of the curve to the *y*-axis to determine the osmotic potential at full turgor (π_o) (Richter 1978). By definition, ε is the slope of Ψ_P against symplastic $RWC = (RWC - a_f)/(100\text{-}a_f)$. While some have reported a nonlinear decline of Ψ_P with *RWC* (Robichaux 1984), and thus a variable ε, the linear approximation between full turgor and π_{tlp} is often used (Koide *et al.* 2000), and we also used this simple linear approximation of ε to ensure agreement with a substantial majority of the literature; however, non-linearity in the interval between full and zero turgor would not affect our equation for the prediction of π_{tlp} (see caption

of Fig. 2.3). The π_{tlp} is the point at which the $1/\Psi$ plot becomes linear, because $\Psi_P = 0$ and $1/\Psi_S$ decreases linearly with relative water content, reflecting the linear increase in solute concentration as the leaf cells lose water, by the Van't Hoff equation ($\Psi_S = -\frac{R_j T n_s}{V}$, wherein R_j is the ideal gas constant, T is temperature, n_s is the number of solute particles, and V is cell volume; Nobel 2009). The π_o can be determined as the inverse of the *y*-intercept of the relationship between $-1/\Psi_S$ and R, i.e., the value of $-1/\Psi_S$ at full hydration. Notably, $100-a_f$ is the *x*-intercept of this relationship, because it is the R value where $-1/\Psi_S = 0$ or $\Psi_S = -\infty$ as symplastic volume declines and the solute concentration becomes infinitely high (Turner 1988; Koide *et al.* 2000). Given the graphical relationships in Fig. 2.1, Ψ_P and Ψ_{leaf} can be expressed as

$$\Psi_p = -\pi_o - \varepsilon(100\text{-}RWC_s) = -\pi_o - \varepsilon R_s \qquad \text{Eqn S2.1}$$

$$\Psi_{leaf} = \Psi_S + \Psi_p \qquad \text{Eqn S2.2}$$

Where RWC_s is the symplastic relative water content, i.e., $(RWC - a_f)/(100-a_f)$, and R_s is $100-RWC_s$.

At turgor loss point (π_{tlp}), where $\Psi_p = 0$ by definition, from Eqn S2.1

$$R_s = \frac{-\pi_o}{\varepsilon} \qquad \text{Eqn S2.3}$$

Using the inverse plot of the p-v curve gives the equation

$$-\frac{1}{\Psi_S} = -\frac{1}{\pi_o} + \frac{1}{\pi_o(100-a_f)}R = -\frac{1}{\pi_o} + \frac{1}{\pi_o}R_s \qquad \text{Eqn S2.4}$$

When $\Psi_S = \pi_{tlp}$, then R_s = 100 – symplastic relative water content at turgor loss point (RWC_{tlp}), and

$$RWC_{tlp} = \frac{\pi_o}{\pi_{tlp}} \qquad \text{Eqn S2.5}$$

By Eqn S2.3, when $\Psi_S = \pi_{tlp}$, $-\pi_o/\varepsilon$ can be substituted for R_s in Eqn S2.4, which after inversion and simplification gives the novel solutions:

$$\pi_{tlp} = \frac{\pi_o \varepsilon}{\pi_o + \varepsilon} \quad \text{Eqn 2.1}$$

$$RWC_{tlp} = \frac{\pi_o + \varepsilon}{\varepsilon} \quad \text{Eqn 2.2}$$

The eqns 2.1 and 2.2 are analytical solutions. To verify that the equations are accurate despite normal measurement error in reported parameters, we used data from the subset of the compiled studies that included all four of π_{tlp} or RWC_{tlp}, π_o, ε, and a_f, and that passed a test for rigorous p-v curve analysis. We independently calculated RWC_{tlp} for each species from the pressure-volume curve eqn S2.3 and rejected data with > 10% discrepancy, resulting in a dataset of n = 89 species from 22 studies. The π_{tlp} and RWC_{tlp} were calculated for each species using eqns 2.1 and 2.2 and compared to observed values with least-squares regression fitted through the origin to determine the robustness of the equations to reasonable measurement uncertainty in the original studies (R, version 2.12.0). The calculated π_{tlp} values were exceedingly well correlated with observed values ($r^2 = 0.99$; slope = 0.986 ± 0.012; Fig. S2.4A). The calculated RWC_{tlp} values showed a relatively weaker correlation with observed values ($r^2 = 0.57$; slope = 1.03 ± 0.008; Fig. S2.4B), apparently due to the RWC_{tlp} exhibiting less variation than π_{tlp} across the range of species, and its sensitivity to parameter ε (see "*Resolution of controversy (4)*"), which is estimated in the literature several different ways, and tends to involve greater measurement error than π_o and π_{tlp} (Sack *et al.* 2003; Scoffoni *et al.* 2011). Therefore, although both eqns 2.1 and 2.2 are analytical solutions, the relationship of π_{tlp} to its underlying parameters is especially robust to different techniques and measurement error.

SUPPLEMENTAL RESULTS AND DISCUSSION 2.1

Alternative formulation of ε and the impact of apoplastic fraction

We also determined alternative formulations of eqns 2.1 and 2.2, because some studies calculated modulus of elasticity as the slope of Ψ_P against *total* leaf relative water content rather than symplastic water content (e. g., Sack *et al.* 2003; Lenz *et al.* 2006; Baltzer *et al.* 2008): $\varepsilon^* = \frac{\varepsilon}{(100\text{-}a_f)}$. The solutions for π_{tlp} and symplastic RWC_{tlp} become:

$$\pi_{tlp} = \frac{\pi_o \varepsilon^*}{\frac{\pi_o}{100\text{-}a_f} + \varepsilon^*} \qquad \text{Eqn 2.1a}$$

$$RWC_{tlp} = \frac{\frac{\pi_o}{100\text{-}a_f} + \varepsilon^*}{\varepsilon^*} \qquad \text{Eqn 2.2a}$$

Because these alternative models allow examination of the a_f as an independent p-v parameter in affecting drought tolerance, we repeated all analyses with these alternative formulations, after converting the ε values in our global dataset to ε^*. These analyses re-affirmed the importance of osmotic potential at full turgor (π_o) as the main driver of turgor loss point (π_{tlp}), with minimal influence of ε* and a_f.

We found that eqn 1a was an excellent predictor of observed π_{tlp} as was eqn 1 (Fig. S2.5A; $\widehat{\pi}_{tlp} = 0.986\pi_{tlp}$, with standard error = 0.029, $r^2 = 0.99$, $p < 2 \times 10^{-16}$; compare with Fig. 2.3A). Eqn 2a allowed a weaker prediction of observed RWC_{tlp} than eqn 2 (Fig. S2.5B; $\widehat{RWC}_{tlp} = 0.992\pi_{tlp}$, with standard error = 0.011, $r^2 = 0.35$, $p < 2 \times 10^{-16}$; compare with Fig. 2.4B), possibly due to the additional error introduced by the inclusion of a_f,, which is determined in the p-v curve by extrapolating across a wide range of RWC values from a small slope value, and is therefore subject to considerable estimation error (Andersen *et al.* 1991).

To test eqn 2.1a for the sensitivity of π_{tlp} to other p-v parameters, we simulated π_{tlp} for a range of values of ε* at two constant values of the other parameters (Fig. S2.6A, B). As in the analysis of

eqn 2.1, π_{tlp} declined strongly as π_o became more negative across the range of values of π_o regardless of the other parameter values (not shown; as in Fig. 2.6A), and the π_{tlp} was sensitive to ε^* only within a narrow range of low ε^* values (Fig. S2.6A, B), and depending on π_o. The π_o defines the possible range of covariation in π_{tlp} and ε: the π_o sets not only the highest π_{tlp} attainable, but also the lowest ε^* attainable, because the relationship of π_{tlp} to ε^* is asymptotic, and biologically infeasible values of π_{tlp} occur when $\varepsilon^* \leq -\frac{\pi_o}{100-a_f}$ (denominator becomes zero or π_{tlp} becomes positive in eqn 2.2a). Thus, the range of ε^* which has an impact on π_{tlp} depends on π_o: a more negative value of π_o results in sensitivity of π_{tlp} to ε^* over a greater range of ε^* values (Fig. S2.6A). Increases in a_f, when all other parameters were held constant, shifted the π_{tlp} and ε^* relationship slightly to the right by increasing the value of ε^* at which the vertical asymptote occurs. This had a relatively small impact on π_{tlp} at a given value of ε^* (Fig. S2.6B). In summary, shifts in π_o will always have an impact on π_{tlp}, but the importance of variation in ε^* and a_f on π_{tlp} depends on both the original value of ε^* and the value of π_o, with little influence on π_{tlp} under most conditions.

In our meta-analysis of the impact on π_{tlp} for plants of given species of shifting p-v parameters during drought, we confirmed the dominance of osmotic adjustment, with no role of adjustment of ε^* during drought and only a minimal effect of a_f (Fig. S2.7). For taxa that decreased ε^* in response to drought, this adjustment only reduced π_{tlp} by 0.004 MPa on average, and shifts in a_f reduced π_{tlp} by 0.05 MPa on average.

Across species, as in the sensitivity analysis for eqns 2.1 and 2.2, the mean value for $\delta\pi_{tlp}/\delta\pi_o$ was again nearly 30-fold greater than that of $\delta\pi_{tlp}/\delta\varepsilon^*$, and twice as large as that of $\delta\pi_{tlp}/\delta a_f$ ($p < 2 \times 10^{-16}$, paired t-tests). Notably, π_{tlp} was correlated with a_f in the opposite direction than that representing the direct causal influence of a_f, similarly to the finding for ε (see main text).

Mechanistically, a higher a_f should drive more negative π_{tlp} (Fig. 2.2D), but species with higher a_f tended to have higher π_{tlp}. A positive correlation of a_f and π_o drove this pattern. Thus there was no evidence for differences in a_f driving functional species variation in π_{tlp}.

We used Eqn 2.2a to determine the sensitivity of symplastic RWC_{tlp} to a_f within and across species. Parameter simulations for Eqn 2.2a demonstrated similar parameter relationships as for π_{tlp}, with RWC_{tlp} increasing asymptotically with ε*, the curve shifting right to a lower value as π_o was more negative and as a_f increased (Fig. S2.6C, D). However, RWC_{tlp} appeared intrinsically more responsive to a_f than π_{tlp} was.

Within species, droughted plants shifted in their RWC_{tlp} values due to all three parameters. On average, shifts in π_o induced a 4.6% decline in RWC_{tlp} values, shifts in a_f a 3.4% decline, and shifts in ε* a 4.7% increase.

Analyses of the determinants of RWC_{tlp} across species using partial derivatives showed that π_o was more important than ε* but that a_f was more important than ε*. The $\delta RWC_{tlp}/\delta\pi_o$ was nearly 6-fold greater on average than $\delta RWC_{tlp}/\delta\varepsilon$*, while $\delta RWC_{tlp}/\delta a_f$ was 2.5-fold greater on average than $\delta RWC_{tlp}/\delta\pi_o$ ($p < 2 \times 10^{-16}$, paired t-tests).

In summary, the alternative model formulation confirmed the importance of π_o as the main driver of π_{tlp} within and among species, with minimal influence of other p-v parameters. The drivers of RWC_{tlp} included π_o, ε*, and a_f, supporting the role of shifts in wall investment and in the distribution between apoplast and symplast for maintaining cell hydration when π_o is shifted downward to increase drought tolerance.

SUPPLEMENTAL RESULTS AND DISCUSSION 2.2

The role of capacitance and elasticity in drought survival

In our analysis of drought tolerance we focused on the advantage of a low turgor loss point to maintain stomatal opening and gas exchange and growth despite drying soil. Thus, we did not focus on capacitance ($C = \Delta R/\Delta\Psi_{leaf}$), which confers drought tolerance of different types: (1) the ability to buffer transient changes in transpiration driven by atmospheric drought, and especially (2) water storage *to extend survival after stomata close* (Sack *et al.* 2003; Hao *et al.* 2010). Capacitance is also expressible as a function of the other parameters that predict π_{tlp}. Thus, these parameters also can importantly influence the ability to survive drought as shown in the following derivation.

In the p-v plot, C changes with leaf water potential, and one may approximate two capacitances, that between full turgor and turgor loss point (C_{ft}) and that between turgor loss point and the water potential Ψ_{lethal} at which the leaf tissue dies (C_{tlp}), using linear regression of *RWC* against bulk Ψ_{leaf} within these intervals. This assumption does not affect the further derivations. The C_{ft}, which may play a functional role in buffering Ψ_{leaf} during fluctuations in transpiration (Sack *et al.* 2003), depends on the π_o ε and a_f:

$$C_{ft} = \frac{(100\text{-total RWC}_{tlp})}{0\text{-}\pi_{tlp}} \qquad \text{Eqn S2.6}$$

Combined with eqns 2.1, 2.2 and 2.3:

$$C_{ft} = \frac{(100\text{-}a_f)(\pi_o + \varepsilon)}{\varepsilon^2} \qquad \text{Eqn S2.7}$$

The C_{tlp}, which contributes to water storage after stomata close, also depends on the π_o ε and a_f:

$$C_{tlp} = \frac{\Delta R}{\Delta \Psi_s} = \frac{(\text{total RWC}_{tlp}\text{- total RWC}_{lethal})}{(\pi_{tlp}\text{-}\Psi_{lethal})} \qquad \text{Eqn S2.8}$$

Combined with eqns 2.1, 2.2, 2.3 and S2.4:

$$C_{tlp} = \frac{(100\text{-}a_f)\left(\frac{\pi_o}{\Psi_{lethal}} - \frac{\pi_o+\varepsilon}{\varepsilon}\right)}{\Psi_{lethal} - \frac{\pi_o \varepsilon}{\pi_o+\varepsilon}} \qquad \text{Eqn S2.9}$$

C_{tlp} is important when stomata close in the dehydrated leaf, as it is a factor determining the storage water content per area that can be lost before lethal desiccation ($WC_{storage}$):

$$WC_{storage} = \left(\Psi_{lethal} - \pi_{tlp}\right) \cdot C_{tlp} \cdot RWC_{tlp} \cdot SWC \cdot LMA \qquad \text{Eqn S2.10}$$

where *SWC* is the saturated water content (i.e., the mass of water in fully hydrated leaf per dry leaf mass), and *LMA* is the leaf mass per area. Notably, the higher the $WC_{storage}$, the longer the leaf can survive after stomatal closure. At that stage, the epidermal transpiration rate is determined by the vapor pressure deficit and epidermal properties including cuticle and leakage from closed stomata. By eqn S2.10, C_{tlp} contributes to leaf survival time under given environmental conditions. Such leaf survival is important in many shrubs and trees of Mediterranean and semi-arid systems, and expressed most significantly among plants with tissue water storage (Ogburn & Edwards 2010; Pasquet-Kok *et al.* 2010). Notably, a low ε can contribute to water storage and survival time, by increasing C_{tlp} (eqn S2.8; a higher ε leads to a higher RWC_{tlp}; Fig. 2.3D). Additionally, a high *LMA* or *SWC* could also contribute to survival time, all else being equal. That would be the case in plants where water storage tissue accounts for a substantial fraction of the leaf thickness; however, in plants lacking specialized water storage tissue, a high *LMA* is typically associated with low *SWC* (i.e., the two are negatively correlated; Garnier & Laurent 1994; Roderick *et al.* 1999; Vendramini *et al.* 2002) which would nullify the benefit of high *LMA* or *SWC* for $WC_{storage}$. Enhancing survival by increasing $WC_{storage}$ is a type of drought avoidance, and a totally distinct mode of drought tolerance from the lowering of turgor loss point. Outside of specialist plants such as succulents, high water content does not tend to reflect adaptation for drought as does a low π_{tlp} (Vendramini *et al.* 2002).

SUPPLEMENTAL REFERENCES FOR CHAPTER 2

Andersen M.N., Jensen C.R. & Losch R. (1991). Derivation of pressure-volume curves by a non-linear regression procedure and determination of apoplastic water. *J. Exp. Bot.*, 42, 159-165.

Baltzer J.L., Davies S.J., Bunyavejchewin S. & Noor N.S.M. (2008). The role of desiccation tolerance in determining tree species distributions along the Malay-Thai Peninsula. *Funct. Ecol.*, 22, 221-231.

Baltzer J.L., Gregoire D.M., Bunyavejchewin S., Noor N.S.M. & Davies S.J. (2009). Coordination of foliar and wood anatomical traits contributes to tropical tree distributions and productivity along the Malay-Thai peninsula. *Am. J. Bot.*, 96, 2214-2223.

Blackman C.J., Brodribb T.J. & Jordan G.J. (2010). Leaf hydraulic vulnerability is related to conduit dimensions and drought resistance across a diverse range of woody angiosperms. *New Phytol.*, 188, 1113-1123.

Engelbrecht B.M.J. & Kursar T.A. (2003). Comparative drought-resistance of seedlings of 28 species of co-occurring tropical woody plants. *Oecologia*, 136, 383-393.

Garnier E. & Laurent G. (1994). Leaf anatomy, specific mass and water content in congeneric annual and perennial grass species. *New Phytol.*, 128, 725-736.

Grubb P.J. (1989). The role of mineral nutrients in the tropics: a plant ecologist's view. In: *Mineral Nutrients in Tropical Forest and Savanna Ecosystems* (ed. Proctor J). Blackwell Scientific Publications Oxford, pp. 417-439.

Hallik L., Niinemets U. & Wright I.J. (2009). Are species shade and drought tolerance reflected in leaf-level structural and functional differentiation in Northern Hemisphere temperate woody flora? *New Phytol.*, 184, 257-274.

Hao G.Y., Sack L., Wang A.Y., Cao K.F. & Goldstein G. (2010). Differentiation of leaf water flux and drought tolerance traits in hemiepiphytic and non-hemiepiphytic *Ficus* tree species. *Funct. Ecol.*, 24, 731-740.

Koide R.T., Robichaux R.H., Morse S.R. & Smith C.M. (2000). Plant water status, hydraulic resistance and capacitance. In: *Plant Physiological Ecology: Field Methods and Instrumentation* (eds. Pearcy RW, Ehleringer JR, Mooney HA & Rundel PW). Kluwer Dordrecht, the Netherlands, pp. 161-183.

Lenz T.I., Wright I.J. & Westoby M. (2006). Interrelations among pressure-volume curve traits across species and water availability gradients. *Physiol. Plant.*, 127, 423-433.

Niinemets U. & Valladares F. (2006). Tolerance to shade, drought, and waterlogging of temperate Northern Hemisphere trees and shrubs. *Ecol. Monogr.*, 76, 521-547.

Nobel P.S. (2009). *Physicochemical and Environmental Plant Physiology, 5th edition*. Academic Press, San Diego.

Ogburn R.M. & Edwards E.J. (2010). The ecological water-use strategies of succulent plants. In: *Advances in Botanical Research, Vol 55* (ed. Kader JCDM), pp. 179-225.

Pasquet-Kok J., Creese C. & Sack L. (2010). Turning over a new "leaf": multiple functional significances of leaves versus phyllodes in Hawaiian *Acacia koa*. *Plant, Cell & Environment*, 33, 2084-2100.

Poorter H., Niinemets U., Poorter L., Wright I.J. & Villar R. (2009). Causes and consequences of variation in leaf mass per area (LMA): a meta-analysis. *New Phytol.*, 182, 565-588.

Poorter L. & Markesteijn L. (2008). Seedling traits determine drought tolerance of tropical tree species. *Biotropica*, 40, 321-331.

Prior L.D., Eamus D. & Bowman D. (2003). Leaf attributes in the seasonally dry tropics: a comparison of four habitats in northern Australia. *Funct. Ecol.*, 17, 504-515.

Richter H. (1978). Diagram for description of water relations in plant cells and organs. *J. Exp. Bot.*, 29, 1197-1203.

Robichaux R.H. (1984). Variation in the tissue water relations of two sympatric Hawaiian *Dubautia* species and their natural hybrid. . *Oecologia*, 65, 75-81.

Roderick M.L., Berry S.L., Noble I.R. & Farquhar G.D. (1999). A theoretical approach to linking the composition and morphology with the function of leaves. *Funct. Ecol.*, 13, 683-695.

Sack L., Cowan P.D., Jaikumar N. & Holbrook N.M. (2003). The 'hydrology' of leaves: co-ordination of structure and function in temperate woody species. *Plant, Cell and Environment*, 26, 1343-1356.

Scoffoni C., Rawls M., McKown A., Cochard H. & Sack L. (2011). Decline of leaf hydraulic conductance with dehydration: relationship to leaf size and venation architecture. *Plant Physiol.*, 156, 832-843.

Turner N.C. (1988). Measurement of plant water status by the pressure chamber technique. *Irrig. Sci.*, 9, 289-308.

Tyree M.T. & Hammel H.T. (1972). Measurement of turgor pressure and water relations of plants by pressure bomb technique. *J. Exp. Bot.*, 23, 267-282.

Vendramini F., Diaz S., Gurvich D.E., Wilson P.J., Thompson K. & Hodgson J.G. (2002). Leaf traits as indicators of resource-use strategy in floras with succulent species. *New Phytol.*, 154, 147-157.

Wright S.J., Kitajima K., Kraft N.J.B., Reich P.B., Wright I.J., D.E. B., Condit R., Dalling J.W., Davies S.J., Diaz S., Engelbrecht B.M.J., Harms K.E., Hubbell S.P., Marks C.O., Ruiz-Jaen M.C., Salvador C.M. & Zanne A.E. (2010). Functional traits and the growth-mortality trade-off in tropical trees. *Ecology*, 91, 3664-3674.

SUPPLEMENTAL METHODS 4.1

Osmometer measurements

We measured osmotic adjustment ($\Delta\pi_o$) and plasticity in turgor loss point ($\Delta\pi_{tlp}$) for 13 evergreen tree species at the Xishuangbanna Tropical Botanical Garden (XTBG) forest plot in Yunnan, China (101°34'26"-47"E and 21°36'42"-58"N) (Lan *et al.* 2011) using a rapid osmometer method (Bartlett *et al.* 2012). XTBG is a seasonally dry tropical forest with a mean annual temperature of 21.0°C and mean annual precipitation of 1608 mm, with 80% of annual precipitation occurring during the May-October wet season (Lan *et al.* 2011). All trees $\geq$ 1 cm in diameter have been censused according to standard Center for Tropical Forest Science protocols (Condit 1998). To capture seasonal variation, we assessed π_o and π_{tlp} in July during the wet season and in March during the dry season.

We collected one branch per individual from 3-6 saplings per species, which we re-cut underwater at least 2 nodes distal to the original cut and rehydrated overnight in humidified, opaque plastic bags in cool and dark conditions. After rehydration, three mature leaves per branch were collected, double-bagged in humidified Whirlpak bags, and stored in an opaque plastic bag in a refrigerator for up to one week prior to measurement. To conduct the osmometer measurements, each leaf was quickly cleaned and a disc was collected from the middle of the leaf with a 8mm diameter cork borer, avoiding the secondary veins. The disc was wrapped in a foil envelope, frozen for at least 2 minutes in liquid nitrogen to break cell walls and mix symplastic contents, then punctured 10-15 times with sharp-tipped forceps to increase evaporation in the osmometer (Vapro 5520 & 5600, Wescor, Logan, Utah, USA). The disc was then immediately sealed in the osmometer chamber and solute concentration measurements were taken repeatedly until the sample reached equilibrium, or the difference between measurements

was less than 5 mmol kg^{-1}. The leaf and leaf disc were exposed to air for less than 40 seconds for all steps after the leaf was taken out of the Whirlpak bag to limit evaporation. We then measured leaf thickness and fresh area, and oven-dried the leaves for 72 hours at 70°C, to assess leaf density ($\rho = \frac{\text{thickness} \times \text{area}}{\text{dry mass}}$; g cm^{-3}). We converted the solute concentrations to osmometer solute potentials (π_{osm}) with the Van't Hoff equation ($\pi_{osm} = \frac{-2.5}{1000} \times$ concentration; MPa), and used published regression relationships between π_{osm} and π_{tlp} ($r^2 = 0.86$, range of π_{osm} = -0.64 to -3.03 MPa, range of π_{tlp} = -1.37 to -3.00 MPa, n = 30 species) and π_{osm}, leaf density, and π_o (r^2 = 0.85, range of π_o = -0.92 to -2.31 MPa, n = 30 species) to calculate the pressure-volume curve parameters (Sack *et al.* 2011; Bartlett *et al.* 2012). The regression equations are:

$$\pi_{tlp} = 0.832\pi_{osm} - 0.631 \qquad \text{Eqn S4.1}$$

$$\pi_{tlp} = 0.466\,\pi_{osm} - 9.31 \times 10^{-5}\pi_{osm}\rho - 9.26 \times 10^{-4}\rho - 0.455 \qquad \text{Eqn S4.2}$$

SUPPLEMENTAL METHODS 4.2

Uncertainty measurements

To determine whether the uncertainty of these π_{tlp} values was within the range of the uncertainty for the π_{tlp} values estimated from pressure-volume curves, we calculated the standard error (SE) of π_{tlp} for each species we assessed with the osmometer from the calibration regression, following (Zar 1998):

$$SE = \sqrt{s^2_{yx}\left(\frac{1}{m} + \frac{1}{n} + \frac{(x_i - \bar{x})^2}{\sum x^2}\right)} \qquad \text{Eqn S4.3}$$

where *m* is the sample size for the focal species for which SE is being calculated (*m* ranges from 3 to 6 for these species), *n* is the number of species in the regression (n = 30), x_i is the mean π_{osm} for the focal species, $\bar{x}$ is the mean π_{osm} across the 30 species in the regression, x is the π_{osm} for each of the 30 species in the regression, and s^2_{yx} is the residual mean square for the regression between π_{osm} and π_{tlp}. The standard errors varied from 7 to 18% of the species means for wet and dry season π_{tlp}, well within the range for the species that were assessed with pressure-volume curves (standard error = 0 - 40% of the species mean for pre- and post-drought π_{tlp}, with the mean across species = 5%).

SUPPLEMENTAL METHODS 4.3

Comparing the results of precision-weighted and unweighted effect sizes

Traditional meta-analytic methods analyze trends in effect sizes weighted by precision, such that each effect size contributes to the overall effect size proportionally to the strength of its statistical support (Gurevitch & Hedges 1999; Rosenberg *et al.* 2004). Measures of within-species variation (i.e., the standard errors of the mean values) for π_{tlp} were only available for 85 wild species and 18 crop species in our compiled dataset. Therefore, we first analyzed trends in unweighted effect sizes from the full dataset we compiled from the literature. Next, to assess the sensitivity of our findings to species-level precision, we repeated our analyses from the main text for precision-weighted and unweighted effect sizes for 1) the subset of species for which intraspecific variation was reported, and for 2) the full dataset of species with the maximum standard deviation reported in the subset assigned to the species with an unknown intraspecific variation (0.98 for the pre-drought π_{tlp} and 1.06 for the post-drought π_{tlp}, 0.97 for pre-drought π_o and 0.77 for post-drought π_o); this last analysis effectively tested the influence of considering precision to be very low for those studies that did not report within-species variation. If the studies in the full dataset reported a range of sample sizes instead of exact sample sizes for each species (i.e. 4-6 leaves of each species were assessed for π_{tlp}), then we used the smallest number given as the sample size. These manipulations weight the species with known precision more highly than the species with the unknown precision in the full dataset to test whether reducing the relative influence of the potentially less precise values would significantly change our findings.

For each species, we calculated precision-weighted effect size as the Hedges' d metric of standardized mean difference, following (Hedges & Olkin 1985), where N is the sample size and σ is the standard deviation:

$$d = \frac{\Delta\pi_{tlp}}{S} J \qquad \text{Eqn S4.4}$$

$$S = \sqrt{\frac{\left(N_{pre\text{-}drought}\right)\left(\sigma^2_{pre\text{-}drought}\right) + \left(N_{post\text{-}drought}\right)\left(\sigma^2_{post\text{-}drought}\right)}{N_{pre\text{-}drought} + N_{post\text{-}drought} - 2}} \qquad \text{Eqn S4.5}$$

$$J = 1 - \frac{3}{4\left(N_{pre\text{-}drought} + N_{post\text{-}drought} - 2\right) - 1} \qquad \text{Eqn S4.6}$$

The variance in Hedges' d, which is used to weight species effect sizes in analyses across species, was calculated for each species as:

$$v = \frac{N_{pre\text{-}drought} + N_{post\text{-}drought}}{N_{pre\text{-}drought} N_{post\text{-}drought}} - \frac{d^2}{2\left(N_{pre\text{-}drought} + N_{post\text{-}drought}\right)} \qquad \text{Eqn S4.7}$$

To test for significant seasonal plasticity in π_{tlp}, we determined mean effect size across species while modeling the study as a random effect variable, using the model structure in Eqn 4.1 in the main text. We also repeated the analyses using the model structure in Eqn 4.4 to test for significant differences among biomes and correlations between effect size and climate. Significance was assessed with a mixed-effects model that weighted species-level effect sizes by 1/v (Rosenberg *et al.* 2004). We used parametric tests to determine the significance of the weighted effect sizes, as the results from weighted effect sizes are considered to be robust to non-normality (Rosenberg *et al.* 1999).

To test whether plasticity in π_{tlp} or pre-drought π_{tlp} is a more important contributor to post-drought π_{tlp}, we calculated the relative rate of pre-drought to post-drought π_{tlp} and the variance of the relative rate for each species as:

$$RR = \ln\left(\frac{\pi_{pre\text{-}drought}}{\pi_{post\text{-}drought}}\right) \qquad \text{Eqn S4.8}$$

$$v_{\ln(RR)} = \frac{1 - \pi_{pre\text{-}drought}}{N_{pre\text{-}drought}\pi_{pre\text{-}drought}} + \frac{1 - \pi_{post\text{-}drought}}{N_{post\text{-}drought}\pi_{post\text{-}drought}} \qquad \text{Eqn S4.9}$$

We then fitted the model in Eqn 4.1 to the relative rates. If the mean relative rate across species was significantly greater than 0.5, then pre-drought π_{tlp} is a more important contributor to post-drought π_{tlp} than $\Delta\pi_{tlp}$.

Some of our analyses from the main text were not applicable to the weighted effect sizes. Mixed effects models are highly sensitive to small numbers of higher-level groups, with 10 groups considered to be the minimum for robust parameter estimates (Maas & Hox 2005). Thus, there was insufficient replication to analyze weighted effect sizes for ΔRWC_{tlp} in wild species (n = 8 studies) or for the plasticity of any variable for crop species (n = 9 studies for $\Delta\pi_{tlp}$ and 3 for ΔRWC_{tlp}). There are also no weighted effect size equivalents for pre- and post-drought π_{tlp} to compare correlations with climate, since weighted effect sizes inherently measure differences between treatments (which are seasons here).

The Hedges' d and relative rate effect sizes were calculated with the MetaWin 2.0 software (Rosenberg *et al.* 1999), and all model fitting was conducted with the *metafor* package in R (Viechtbauer 2010). We repeated the analyses described in the main text for the unweighted effect sizes for the subset of species with precision reported to compare trends for precision-weighted and unweighted effect sizes for the same species.

SUPPLEMENTAL METHODS 4.4

Phylogenetic relatedness

The influence of phylogenetic relatedness on species variation in drought trait plasticity was not a main focus of our study, especially because the previous literature did not focus on ideal designs for such a question (e.g., sampling many species within given lineages for which phylogenies are highly resolved, or within lineages that have diversified across moisture gradients). In this study, we were particularly focused on broad variation across diverse species and biomes in drought plasticity without examining its underlying phylogenetic patterning. However, within these constraints, we sought to determine how much variance in drought tolerance plasticity might be explained by the phylogenetic relationships among species. Theoretically, we could test for this effect by fitting species as an additional random effect, and specifying a phylogenetic variance-covariance matrix as the error structure for the species variable. We found that our dataset could not be robustly analyzed with the computational tools currently available for these analyses. The plasticity and plasticity contribution data were significantly non-normal, even after square root and log transformation (Shapiro test, maximum $p = 0.0002$). One software that can incorporate relatedness into mixed-effects models is the *MCMCglmm* package in R, which fits mixed-effects models with Markov chain Monte Carlo techniques (Hadfield 2010). Although *MCMCglmm* can fit a number of distributions besides normal, our dataset was in fact significantly better fitted by a normal distribution than any other distribution that *MCMCglmm* is capable of fitting, based on AIC model comparisons calculated by the *fitdistrplus* package in R. Further, none of the currently available nonparametric tests that we are aware of can correctly account for the complex error structure created by the phylogenetic variance-covariance matrix. Thus, we would expect our parameter estimates for this model to be

strongly skewed. Attempting to fit this model with *MCMCglmm* yielded a relatively small signal for relatedness, accounting for about 10% of the total variance of $\Delta\pi_{tlp}$, while the distributions for the parameter estimates are strongly skewed, as expected from non-normal data. Thus, the importance of relatedness to variation in drought tolerance plasticity remains an open and important question. Further research to robustly determine phylogenetic patterns in drought tolerance plasticity may determine turgor loss points within given lineages that diversified across moisture gradients, and the variation across species within highly diverse communities, for which certain families are represented by many species, to be examined using explicit community phylogenetic analyses.

SUPPLEMENTAL RESULTS AND DISCUSSION 4.1

The findings of our analyses for weighted effect sizes were the same as our findings for unweighted effect sizes, in almost all cases. Both unweighted and weighted effect sizes showed significant seasonal adjustment in π_{tlp} across species. The mean precision-weighted effect size for $\Delta\pi_{tlp}$ across wild species was significantly less than zero for both the subset of species with intraspecific variation reported (mean = -1.18, n = 85 species) and the full dataset with assigned standard deviations (mean = -0.55, n = 246 species, both $p < 0.01$). (Here, as in the main text, "mean" refers to the intercept of the mixed effects model described in Eqn 4.1, which estimates the mean plasticity across species after accounting for the non-independence of species nested within the same study). The mean unweighted effect size (i. e., species means for $\Delta\pi_{tlp}$) was also significantly less than zero for the subset of species with precision reported (mean [95% confidence intervals] = -0.43 MPa [-0.34 to –0.51 MPa], n = 85 species). Thus, our analyses detected significant seasonal plasticity in drought tolerance across species both with and without considering intraspecific variation.

We also found that pre-drought π_{tlp} was a stronger contributor to post-drought π_{tlp} than plasticity using both weighted and unweighted effect sizes. The contribution of pre-drought π_{tlp} to post-drought π_{tlp} was significantly greater than 0.5 for the precision-weighted effect sizes for both datasets, with a mean unlogged relative rate [95% CI] equal to 86% [82 to 91%] for the subset and 85% [82 to 88%] for the full dataset. We found the same results for unweighted effect sizes for the subset (mean contribution [95% CI] equal to 84% [81 to 87%]. Therefore, both traditional meta-analyses and analyses of species means were able to identify pre-drought π_{tlp} as a more important contributor to post-drought π_{tlp} than $\Delta\pi_{tlp}$, across species.

We also found the same findings for weighted and unweighted effect sizes for correlations between traits and climate. $\Delta\pi_{tlp}$ and $\Delta\pi_o$ were not significantly correlated with any of the climate variables for precision-weighted effect sizes for the subset of species with precision measures ($p > 0.2$), unweighted effect sizes for the species subset ($p > 0.08$), or weighted effect sizes for the full dataset, with the minimum precision assigned to the species without precision reported ($p > 0.06$).

The one analysis which yielded a different result when using weighted versus unweighted effect sizes was the test for differences across biomes in $\Delta\pi_{tlp.}$ In this case, we found significant biome differences when using precision-weighted effect sizes for the subset of species with reported precision ($p < 0.01$, n = 85 species), but not when using unweighted effect sizes for the subset ($p = 0.4$, n = 85 species), or when using either unweighted or weighted effect sizes for the full dataset ($p = 0.9$ and 0.4, respectively, n = 240 species). However, for the analysis with significant biome differences, these differences did not correspond with ecosystem water availability, as the temperate conifers, a wet biome, showed the most negative effect size (i. e., the most negative shift in π_{tlp}). There were no significant biome differences for unweighted or weighted effect sizes for $\Delta\pi_o$ in the full dataset or the subset (all $p > 0.3$). Thus, estimates for biome differences in $\Delta\pi_{tlp}$ will be improved as data for species means and intraspecific variation become available for a wider range of species diversity.

SUPPLEMENTAL REFERENCES FOR CHAPTER 4

Bartlett M.K., Scoffoni C., Ardy R., Zhang Y., Sun S., Cao K., et al. (2012). Rapid determination of comparative drought tolerance traits: using an osmometer to predict turgor loss point. *Methods Eco. Evol.*, 3, 880-888.

Condit R. (1998). *Tropical Forest Census Plots*. Springer, Georgetown, Texas.

Gurevitch J. & Hedges L.V. (1999). Statistical issues in ecological meta-analyses. *Ecology*, 80, 1142-1149.

Hadfield J.D. (2010). MCMC Methods for multi-response generalized linear mixed models: MCMCglmm. *Journal of Statistical Software*, 33, 1-22.

Hedges L.V. & Olkin I. (1985). *Statistical methods for meta-analysis*. Academic Press, New York.

Hijmans R.J., Cameron S.E., Parra J.L., Jones P.G. & Jarvis A. (2005). Very high resolution interpolated climate surfaces for global land areas. *Int. J. Climatol.*, 25, 1965-1978.

Lan G., Zhu H. & Cao M. (2011). Tree species diversity of a 20-ha plot in a tropical seasonal rainforest in Xishuangbanna, southwest China. *J. For. Res.-Jpn.*, 17, 432-439.

Maas C.J.M. & Hox J.J. (2005). Sufficient sample sizes for multi-level modeling. *Methodology*, 1, 86-92.

MetaWin: Statistical software for meta-analysis. (1999). Sinauer Associates, Sunderland, Massachusetts.

Rosenberg M.S., Garrett K.A., Su Z. & Bowden R.L. (2004). Meta-analysis in plant pathology: Synthesizing research results. *Phytopathology*, 94, 1013-1017.

Sack L., Pasquet-Kok J. & PrometheusWiki Contributors (2011). Leaf pressure-volume curve parameters. URL http://prometheuswiki.publish.csiro.au/tiki-citation.php?page=Leaf pressure-volume curve parameters

Viechtbauer W. (2010). Conducting meta-analyses in R with the metafor package. *Journal of Statistical Software*, 36, 1-48.

Wright I.J., Reich P.B., Westoby M., Ackerly D.D., Baruch Z., Bongers F., et al. (2004). The worldwide leaf economics spectrum. *Nature*, 428, 821-827.

Zar J.H. (1998). *Biostatistical Analysis*. 4th edn. Prentice Hall.

SUPPLEMENTAL METHODS 5.1

Trait measurements

One branch per individual was collected from trees immediately surrounding the plot to avoid biasing growth censuses. The individuals were identified to the species level by staff botanists. The collected branches were re-cut underwater at least 2 nodes distal to the original cut, and rehydrated overnight in a humidified, opaque plastic bag in cool and dark conditions.

We measured turgor loss point (π_{tlp}; MPa) for 3 leaves per individual from 5 - 6 individuals per species with an osmometer method (Bartlett et al. 2012). We then assessed each leaf for thickness (averaged for the top, middle, and bottom of the leaf), fresh mass, fresh area (measured with a LI-COR 3100 leaf area meter (Lincoln, Nebraska, USA)) and dry mass after oven drying at 70°C for 72 hours. We used these measurements to calculate leaf mass per unit area (*LMA* = dry mass/fresh area; g m^{-2}), leaf density (ρ = *LMA*/thickness; g cm^{-3}) and leaf dry matter content (*LDMC* = dry mass/fresh mass; g g^{-1}). Leaf nitrogen concentration (N_{mass}; g g^{-1}) was measured for 2 leaves from 3 - 6 trees per species. Leaves were initially oven-dried at 70°C for 72 hours, then stored in ambient conditions and oven-dried again for 24 hours before sample preparation. The leaves were then ground with a mechanical grinder and homogenized, then measured for nitrogen concentration with an elemental analyzer (PDZ Europa ANCA-GSL analyzer, Northwich, UK). One rehydrated branch each from 5 - 10 individuals per species was assessed for the water transport traits sapwood area-based and leaf area-based stem hydraulic conductance (K_S and K_L, respectively; kg s^{-1} m^{-1} MPa^{-1}) according to the standard low-pressure steady-state flowmeter method (Sack et al. 2011, Melcher et al. 2012).

We measured the traits known to exhibit seasonal plasticity during the dry season for π_{tlp}, *LMA*, *LDMC* and ρ and the wet season for N_{mass} (Bahari et al. 1985, Ishida et al. 2006). These

sampling times capture species values when these traits are most important to plant function, since leaf drought tolerance is most important to plant performance during drought (Bahari et al. 1985), carbon assimilation is most responsive to leaf nutrient investment when photosynthesis is not primarily limited by water stress (Grassi and Magnani 2005), and increased investment in leaf longevity is especially useful in more resource-limited conditions when leaves are more difficult to replace (Wright et al. 2004). We tested whether seasonal plasticity is likely to considerably change our findings by comparing wet and dry season values for a subset of 18 species for *LMA* and *LDMC* and 14 species for ρ and π_{tlp}. While paired t-tests indicated these traits exhibited significant seasonal plasticity in the directions expected (all $p < 0.04$), the wet and dry season values for each trait were significantly correlated for all traits ($r^2 = 0.35 – 0.89$, $p < 0.03$) except ρ ($r^2 = 0.26$, $p = 0.09$). Thus, despite seasonal plasticity, species' relative leaf structural investment and drought tolerance appear to be maintained across seasons, suggesting that the season in which traits were measured is not likely to strongly impact our results. We assessed K_S and K_L throughout the wet and dry seasons, as these traits have been shown not to exhibit seasonal plasticity in stems that are flushed to remove embolisms (Jacobsen et al. 2007).

We verified that these traits reliably capture species differences by using a one-way ANOVA to test for differences among species and partition variance within and across species for each trait. Trait values were logged prior to analysis. All traits were significantly different across species (all $p < 0.0001$). The proportion of variation explained by species differences was smallest for the conductivity traits K_S (24%) and K_L (25%) and largest for π_{tlp} (77%). Variation across species accounted for over half of the total variation in all traits except K_S and K_L. Thus, these traits adequately capture species differences, despite variation within species.

SUPPLEMENTAL METHODS 5.2

Habitat variables

We used the 10m-resolution elevation map of the plot to calculate the topographic variables convexity, aspect, slope, and topographic wetness index (*TWI*), and the light variables average daily overall, direct, and diffuse radiation in the wet and dry seasons. We converted the circular aspect variable into the linear components northness (cos(aspect)) and eastness (sin(aspect)) (Clark et al. 1999). *TWI* was calculated as the ratio of all area upslope of each quadrat to quadrat slope (Pathak 2010, Kanagaraj et al. 2011). Solar radiation was estimated on every day from May 1, 2012 – October 31, 2012 for the wet season and November 1, 2012 - April 30, 2013 for the dry season using the ArcGIS 9.3 standard overcast sky model, which estimates solar radiation as a function of latitude, date, and topography.

Species mean topographic variables were calculated as both uncorrected and corrected means for 10 × 10m quadrat density. Correcting for quadrat density weights habitat means for quadrats where a species is disproportionately overrepresented. Habitat means were density-corrected according to the following formula:

$$\mathrm{ENV_{j,WA}} = \frac{\sum_{i=1}^{2000} \mathrm{ENV_i} \frac{\mathrm{Density_{ij}}}{\mathrm{Abundance_j}} \frac{\mathrm{Density_{total}}}{\mathrm{Density_i}}}{\sum_{i=1}^{2000} \frac{\mathrm{Density_{ij}}}{\mathrm{Abundance_j}} \frac{\mathrm{Density_{total}}}{\mathrm{Density_i}}} \qquad \text{Eqn S5.1}$$

where $ENV_{j,WA}$ is the density-corrected mean of an environmental variable for species j, ENV_i is the value of that environmental variable in 10m × 10m quadrat i, $Density_i$ is the number of individuals in quadrat i, 2000 is the number of quadrats, $Density_{ij}$ is the number of individuals of species j in quadrat i, $Density_{total}$ is the total tree density in the plot, and $Abundance_j$ is the total abundance of species j. The uncorrected mean, in contrast, represents what quadrats the species occurs in regardless of specialization. Uncorrected means were calculated as:

$$ENV_j = \sum_{i=1}^{2000} \frac{ENV_i \, Density_{ij}}{Density_{total}}$$ Eqn S5.2

As another axis of habitat variation, we characterized neighborhood crowding for each species by averaging neighborhood tree density, neighboring tree basal area, total neighborhood basal area, and scaled neighborhood basal area for 20m radius circular neighborhoods around each individual. Scaled neighborhood basal area is the sum of the ratio of the basal areas of all 1 through *M* neighboring trees to the basal area of focal tree *k*, averaged for all 1 through *K* individuals of species *j*:

$$\text{Scaled Neighborhood } BA_j = \frac{1}{K}\sum_{k=1}^{K}\sum_{m=1}^{M}\frac{\pi\left(\frac{DBH_m}{2}\right)^2}{\pi\left(\frac{DBH_k}{2}\right)^2}$$ Eqn S5.3

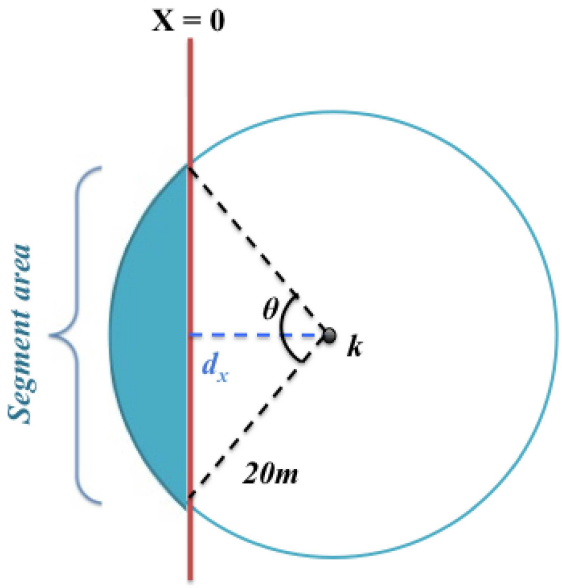

For focal trees that occurred less than 20m from the edge of the plot, we estimated density, basal area, and scaled basal area for a complete circular neighborhood by treating the edge of the plot as a chord intersecting the circular neighborhood, and dividing the neighborhood variable calculated from the partial neighborhood by the percent area that the partial neighborhood occupies of the whole. For example, for a focal tree *k* that is d_x meters from the X = 0 plot boundary and d_y meters from the Y = 0 and Y = 500 plot boundaries, and $d_x < 20 < d_y$, the neighborhood basal area (BA) can be approximated as:

$$\theta = 2\cos^{-1}\left(\frac{d_x}{20}\right)$$ Eqn S5.4

$$\text{Segment area} = \frac{20^2}{2}(\theta - \sin\theta)$$ Eqn S5.5

$$BA_{corrected} = \frac{BA_{partial}}{1 - \frac{\text{Segment area}}{400\pi}}$$ Eqn S5.6

In the four corner quadrats where the focal trees are less than 20m from both boundaries, this approximation method can be adapted for a circle intersected by two chords:

$$\theta_1 = 2\cos^{-1}\left(\frac{d_x}{20}\right) \qquad \text{Eqn S5.7}$$

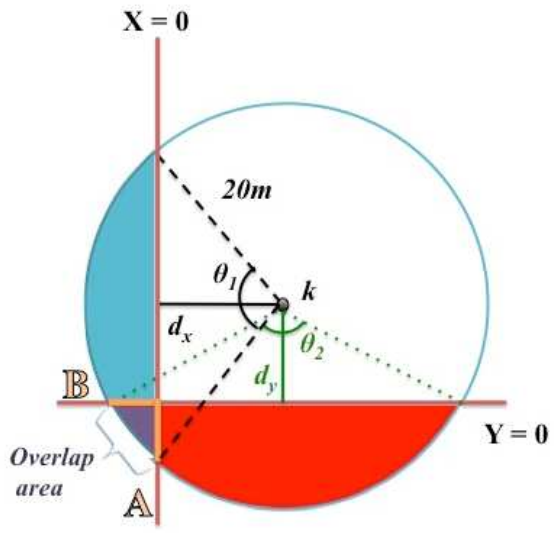

$$\theta_2 = 2\cos^{-1}\left(\frac{d_y}{20}\right) \qquad \text{Eqn S5.8}$$

$$A = \sqrt{400\text{-}d_x^{\,2}}\text{-}\, d_y \qquad \text{Eqn S5.9}$$

$$B = \sqrt{400\text{-}d_y^{\,2}}\text{-}\, d_x \qquad \text{Eqn S5.10}$$

$$\text{Overlap area} = \frac{1}{2}AB \qquad \text{Eqn S5.11}$$

$$\text{Segment 1} = \frac{20^2}{2}\left(\theta_1\text{-}\ \sin\theta_1\right) \qquad \text{Eqn S5.12}$$

$$\text{Segment 2} = \frac{20^2}{2}\left(\theta_2\text{-}\ \sin\theta_2\right) \qquad \text{Eqn S5.13}$$

$$BA_{corrected} = \frac{BA_{partial}}{1\text{-}\frac{\text{Segment 1+Segment 2-Overlap area}}{400\pi}} \qquad \text{Eqn S5.14}$$

Computational methods

We determined the best-fit multivariate models for predicting trait means from habitat variables with the *likelihood* package for R software v. 3.1.0 (Murphy 2012, R Core Team 2014), and we calculated spatial associations between species pairs using the the *wavelet.bivariate* function in the *CTFSR* package for R software (Detto and Brenes 2014). We used the *geiger* package to calculate Pagel's λ statistic for each trait and habitat variable (Harmon et al. 2008), and *caper* to apply phylogenetic least-squared regression tests to the univariate and best-fit multivariate models relating traits to habitat (Orme et al. 2012).

SUPPLEMENTAL METHODS 5.3

Weighting spatial associations by tree size

Inferring competition processes from spatial patterns is complicated by the dependence of competitive impact on tree size. Larger trees are expected to have greater resource demand and uptake, and thus, to have a stronger exclusionary impact on neighbors, while conventional spatial analyses weight co-occurrence between small and large trees equally. Weighting tree density by size may enhance the ability of the wavelet method to detect signatures for competitive interactions.

To test the hypothesis that spatial signatures for competitive interactions are stronger among large trees (hypothesis 4 in Table 5.1), we conducted a novel analysis using the wavelet method to calculate spatial association for tree density weighted by basal area, so that the influence of individual trees on overall spatial association scaled with size. With this weighting, spatial patterns among large adult trees become the most influential to the overall spatial association, associations among large trees and saplings are intermediate, and associations among saplings are the least influential. If the spatial association between two species is driven by patterns in large trees, then the size-weighted associations will be more positive than the unweighted, density-based associations if the large trees are clustered, or more negative if the large trees are segregated. If the spatial pattern in the unweighted, density-based association is largely driven by the small trees and the large trees are more randomly associated, than the weighted associations will be closer to zero, which indicates random association.

Because the size-weighted analysis is new in this study, we included here several simulations to demonstrate what this weighted analysis measures. We conducted these simulations using the *lansing* forest plot dataset from the *spatstat* package in R because it is

readily available and thus easily reproducible for further exploration by interested readers. The *lansing* dataset provides the x and y coordinates for 514 maple trees and 346 red oak trees in a 924m × 924m forest plot in Lansing Woods, Michigan, USA (Gerrard 1969, Baddeley and Turner 2005). For our first simulation, we used the wavelet method to calculate the unweighted, density-based spatial association for these species by supplying tree density data to the *wavelet.bivariate* function in the *CTFSR* package in R (Fig. S5.7A) (Detto and Brenes 2014). To show how weighing tree density by size affected the spatial association metric, we simulated three different relationships between tree size and spatial patterns: 1) tree size scaled positively with proximity to interspecific neighbors, so that the large adult trees of each species were more clustered; 2) tree size scaled negatively with proximity to neighbors, so that the small trees of each species were more clustered; and 3) tree size varied randomly with proximity to neighbors.

To produce these relationships, since tree size data is not included in the *lansing* dataset, we first calculated nearest neighbor distance between each tree and the closest member of the other species using the *nncross* function in the *spatstat* package. We assumed that trees with a smaller nearest neighbor distance were more closely associated with the other species and simulated a tree size that scaled positively, negatively, or randomly with this distance. To simulate greater association among large trees, we estimated tree size according to the function:

$$\text{DBH} = 1 + \frac{0.05}{\text{Nearest neighbor distance}} \qquad \text{Eqn S5.15}$$

The two trees with identical x-y coordinates were assigned the maximum DBH of 20 cm. This estimation produced a positively-skewed size distribution, with a large number of small trees, relatively few large trees, and a minimum DBH of 1 cm and a maximum DBH of 20 cm, which is consistent with size distributions observed for the XTBG study species.

We then repeated this simulation assuming that smaller trees were more closely spaced, according to the formula:

$$\mathrm{DBH} = 1 + 100\mathrm{Nearest\ neighbor\ distance} \qquad \text{Eqn S5.16}$$

which produces a similar size distribution as Eqn S5.16 (Fig. S5.7C). Again, the two trees with identical x-y coordinates were assigned the maximum DBH of 20 cm.

We then simulated tree size being randomly associated with proximity to interspecific neighbors by randomly sampling numbers from a gamma distribution with a shape parameter = 1.5 and scale parameter = 2 and adding 1 to these numbers to simulate DBHs, which produced a similar size distribution as Eqn. S5.15 and S5.16. We repeated this simulation 500 times and calculated 95% confidence intervals for the spatial association to demonstrate that random patterns in tree size produce a spatial association metric that is not significantly different from the unweighted, density-based associations.

We then calculated spatial association for each simulated dataset of tree sizes by supplying the tree diameters instead of densities to the *wavelet.bivariate* function.

Spatial association calculated from the unweighted tree density showed that the two species were randomly associated (Fig. S5.7A, black line). The first simulation, where larger trees were assumed to be more closely spaced to interspecific neighbors, showed significant clustering between the two species at distances less than 60m apart (Fig. S5.7A, red line). This result indicates that the presence of one species has little impact on the distribution of saplings for the second species, but over time, the large adult trees fail to competitively exclude each other and persist in the same neighborhood for long periods of time. This finding supports the interpretation of negligible or extremely weak competition between the two species. The second simulation, where larger trees are assumed to be more distant from interspecific neighbors,

showed significant spatial *segregation* at distances about 50m apart (Fig. S5.7A, blue line). This result suggests that the two species are unable to persist together over time, and supports the interpretation of strong competition. The third simulation, with tree sizes randomly distributed across the landscape, shows that weighting by size does not produce significantly different spatial association measures than tree density alone when the influence of different trees to overall association varies randomly with proximity (Fig. S5.7A, gray band).

There are several additional points about these analyses that are important to consider when interpreting differences in spatial association across species pairs. The density-based spatial association between two species is normalized by their abundance, so that spatial associations are independent of total abundance. Analogously, size-weighted associations are normalized by the total tree basal area of the two species. Therefore, this method does not weight an individual tree by its absolute size, but instead by the ratio of that tree's size to the total tree area for that species pair. This normalization has two important implications for comparing associations across species pairs. First, differences in size alone do not impact the weighted spatial associations. For example, if the maximum DBH of the *lansing* species is increased to 200cm and the previous simulations repeated, the spatial associations remain the same (data not shown). Thus, species differences in size alone, and not the relationships between proximity and size, will not substantially impact size-weighted associations. Second, the influence of a given tree size will vary across species pairs. For example, a 20cm tree will be more influential for a species pair with mostly small saplings than for a species pair with mostly large trees. Allowing this influence to vary across species pairs produces a more realistic relationship between tree size and age across species, because giving each DBH the same influence across species would assume that all trees of the same size have persisted for approximately the same amount of time

and are approximately the same age, despite the large variation in growth rates observed among tropical tree species (Condit et al. 2006). Making a large tree more influential for a species with many small saplings and few other large trees assumes that tree has been growing longer, and has experienced neighborhood competition for a longer period of time, than a tree of the same size from a species with many other large trees and few small saplings. Indeed, previous studies of tropical tree size distributions have found that growth rate correlates with size distributions, such that species with many small saplings and few large trees have slower growth rates than species with many large trees and relatively few small saplings (Wright et al. 2003).

To ensure the relationships between size-weighted spatial associations and traits were not driven by species differences in size distributions, we tested trait correlations with the minimum adult diameter, which is the 95th percentile of all diameters within 10% of the largest diameter (King et al. 2006), and the skew of the size distribution (g_1), calculated as (Wright et al. 2003):

$$g_1 = \frac{n \sum_i (x_i - \bar{x})^3}{(n-1)(n-2)s^3} \qquad \text{Eqn S5.17}$$

where n is the number of individuals, x_i is the logged DBH of individual i, $\bar{x}$ is the mean logged DBH of all individuals, and s is the standard deviation of the logged DBHs. We verified that all trait values were independent of adult size and the skew of the size distribution ($r^2 = 0.002$-0.09; $p = 0.07$-0.93).

SUPPLEMENTAL REFERENCES FOR CHAPTER 5

Baddeley, A. and R. Turner. 2005. Spatstat: an R package for analyzing spatial point patterns. Journal of Statistical Software **12**:1-42.

Bahari, Z. A., S. G. Pallardy, and W. C. Parker. 1985. Photosynthesis, water relations, and drought adaptation in six woody species of oak-hickory forests in central Missouri. Forest Science **31**:557-569.

Bartlett, M. K., C. Scoffoni, and L. Sack. 2012. The determinants of leaf turgor loss point and prediction of drought tolerance of species and biomes: a global meta-analysis. Ecology Letters **15**:393-405.

Bartlett, M. K., et al. 2012. Rapid determination of comparative drought tolerance traits: using an osmometer to predict turgor loss point. Methods in Ecology and Evolution **3**:880-888.

Brodribb, T. J. and T. S. Feild. 2000. Stem hydraulic supply is linked to leaf photosynthetic capacity: evidence from New Caledonian and Tasmanian rainforests. Plant, Cell & Environment **23**:1381-1388.

Clark, D. B., M. W. Palmer, and D. A. Clark. 1999. Edaphic factors and landscape-scale distrbutions of tropical rain forest trees. Ecology **80**:2662-2675.

Condit, R., et al. 2006. The importance of demographic niches to tree diversity. Science **313**:98-101.

Detto, M. and T. Brenes. 2014. Function: Wavelet.bivariate. *In CTFS R package.* R. Condit editor., http://ctfs.arnarb.harvard.edu/Public/CTFSRPackage.

Gerrard, D. J. 1969. Competition quotient: a new measure of the competition affecting individual forest trees. Research Bulletin, Agricultural Experimental Station, Michigan State University **20**.

Grassi, G. and F. Magnani. 2005. Stomatal, mesophyll conductance and biochemical limitations to photosynthesis as affected by drought and leaf ontogeny in ash and oak trees. Plant, Cell & Environment **28**:834-849.

Harmon, L. J., J. T. Weir, C. D. Brock, R. E. Glor, and W. Challenger. 2008. GEIGER: Investigating evolutionary radiations. Bioinformatics **24**:129-131.

Ishida, A., et al. 2006. Contrasting seasonal leaf habits of canopy trees between tropical dry-deciduous and evergreen forests in Thailand. Tree physiology **26**:643-656.

Jacobsen, A. L., R. B. Pratt, S. D. Davis, and F. W. Ewers. 2007. Cavitation resistance and seasonal hydraulics differ among three arid Californian plant communities. Plant, Cell & Environment **30**:1599-1609.

Kanagaraj, R., T. Wiegand, L. S. Comita, and A. Huth. 2011. Tropical tree species assemblages in topographical habitats change in time and with life stage. Journal of Ecology **99**:1441-1452.

King, D. A., S. J. Davies, and N. S. M. Noor. 2006. Growth and mortality are related to adult tree size in Malaysian mixed dipterocarp forest. Forest Ecology & Management **223**:152-158.

Malhi, Y., et al. 1998. Carbon dioxide transfer over a Central Amazonian rain forest. Journal of Geophysical Research **103**:31593.

Melcher, P. J., et al. 2012. Measurements of stem xylem hydraulic conductivity in the laboratory and field. Methods in Ecology and Evolution **3**:685-694.

Mercado, L. M., et al. 2009. Impact of changes in diffuse radiation on the global land carbon sink. Nature **458**:1014-1017.

Murphy, L. 2012. Likelihood: methods for maximum likelihood estimation. R package v. 1.5.

Niinemets, U. 2001. Global-scale climatic controls of leaf dry mass per area, density, and thickness in trees and shrubs. Ecology **82**:453-469.

Orme, D., et al. 2012. caper: Comparative Analyses of Phylogenetics and Evolution in R. R package version 0.5.

Pathak, P. 2010. TWI. ArcScripts: http://arcscripts.esri.com/details.asp?dbid=16750.

R Core Team. 2014. R: A language and environment for statistical computing. R Foundation for Statistical Computing, Vienna, Austria.

Sack, L., M. K. Bartlett, C. Creese, G. Guyot, C. Scoffoni, and PrometheusWiki Contributors. 2011. Constructing and operating a hydraulic flow meter. PrometheusWiki.

Wright, I. J., et al. 2004. The worldwide leaf economics spectrum. Nature **428**:821-827.

Wright, S. J., H. C. Muller-Landau, R. Condit, and S. P. Hubbell. 2003. Gap-dependent recruitment, realized vital rates, and size distributions of tropical trees. Ecology **84**:3174-3185.

SUPPLEMENTAL METHODS 6.1

The compiled drought tolerance traits were measured according to standard methods. The turgor loss point (π_{tlp}) was interpolated from pressure-volume curves, which relate the relative water content, a measure of cell volume, to the leaf water potential (Ψ_L) in a dehydrating leaf (Cheung et al. 1975). This value is a bulk leaf trait, representing the volume-weighted average π_{tlp} of all of the leaf cells. The water potential thresholds for 50% declines in leaf, stem, and root hydraulic conductivity (K_{leaf}, K_{stem}, and K_{root} Ψ_{50}), and for 12% and 88% declines in stem conductivity (K_{stem} Ψ_{12} and Ψ_{88}) were interpolated from curves relating the percent loss of hydraulic conductivity to the water potential of dehydrating leaves, stems, or roots (Melcher et al. 2012, Sack and Scoffoni 2012). The water potential thresholds for 50% and 95% declines in g_S (g_S Ψ_{50} and Ψ_{95}) were interpolated from curves relating g_S to Ψ_L for a dehydrating plant or excised branch (Brodribb et al. 2003). Because more studies report g_S Ψ_{50} than g_S Ψ_{95}, from each study, we extracted data from plots of the g_S - Ψ_L curve with ImageJ software. We then compared Aikake Information Criteria values corrected for small sample sizes (AICc) for exponential, sigmoidal, logistic, and linear models for each curve with the *optim* function in R software (v. 3.1.0) (Burnham and Anderson 2010, Guyot et al. 2012), and interpolated g_S Ψ_{50} and Ψ_{95} from the best-fit model for each curve. The water potential at plant death (plant Ψ_{lethal}) was measured as the Ψ_L of a plant dehydrated to the point of all leaves showing at least some tissue damage (Baltzer et al. 2008).

SUPPLEMENTAL REFERENCES FOR CHAPTER 6

Baltzer, J. L., S. J. Davies, S. Bunyavejchewin, and N. S. M. Noor. 2008. The role of desiccation tolerance in determining tree species distributions along the Malay–Thai Peninsula. Functional Ecology **22**:221-231.

Brodribb, T., N. M. Holbrook, E. J. Edwards, and M. V. Gutierrez. 2003. Relations between stomatal closure, leaf turgor and xylem vulnerability in eight tropical dry forest trees. Plant Cell Environ **26**:443-450.

Burnham, K. P., and D. R. Anderson. 2010. Model selection and multi-model inference: a practical information-theoretic approach. 2nd edition. Springer.

Cheung, Y. N. S., M. T. Tyree, and J. Dainty. 1975. Water relations parameters on single leaves obtained in a pressure bomb and some ecological interpretations. Canadian Journal of Botany **53**:1342-1346.

Guyot, G., C. Scoffoni, and L. Sack. 2012. Combined impacts of irradiance and dehydration on leaf hydraulic conductance: insights into vulnerability and stomatal control. Plant Cell Environ **35**:857-871.

Melcher, P. J., N. M. Holbrook, M. J. Burns, M. A. Zwieniecki, A. R. Cobb, T. J. Brodribb, B. Choat, and L. Sack. 2012. Measurements of stem xylem hydraulic conductivity in the laboratory and field. Methods in Ecology and Evolution **3**:685-694.

Sack, L., and C. Scoffoni. 2012. Measurement of leaf hydraulic conductance and stomatal conductance and their responses to irradiance and dehydration using the Evaporative Flux Method (EFM). Journal of Visualized Experiments.